Queen Mary
University of London

Scattering Amplitudes from Rational Maps and Correlators in AdS/CFT

SHUN-QING ZHANG

Supervisor

DR CONGKAO WEN

March 9, 2023

Centre for Theoretical Physics
Department of Physics and Astronomy
Queen Mary University of London

Declaration

I, Shun-Qing Zhang, confirm that the research included within this thesis is my own work or that where it has been carried out in collaboration with, or supported by others, that this is duly acknowledged below and my contribution indicated. Previously published material is also acknowledged below.

I attest that I have exercised reasonable care to ensure that the work is original, and does not to the best of my knowledge break any UK law, infringe any third party's copyright or other Intellectual Property Right, or contain any confidential material.

I accept that the College has the right to use plagiarism detection software to check the electronic version of the thesis.

I confirm that this thesis has not been previously submitted for the award of a degree by this or any other university.

The copyright of this thesis rests with the author and no quotation from it or information derived from it may be published without the prior written consent of the author.

Signature:
Date: March 9, 2023

Details of collaboration and publications:

This thesis describes research carried out with my supervisor and collaborators, which are published in [1–5]. It also contains some unpublished material. Where other sources have been used, they are cited in the bibliography.

Abstract

This thesis focuses on novel techniques of computing scattering amplitudes and correlation functions in quantum field theories. We begin with the twistor formulation of amplitudes in six dimensions (6D), which compute tree-level n-point scattering amplitudes in (2,0) M5-brane (as well as (1,1) D5-brane), (1,1) super Yang-Mills (SYM), (2,2) supergravity (SUGRA), and (2,0) SUGRA theories. We also obtain loop amplitudes in lower dimensions, 4D for instance, by performing dimensional reduction and taking the forward limit of the aforementioned 6D theories. Next, we study reformulating S-matrices in terms of the positive geometry, amplituhedron, which was first introduced to describe scattering in the 4D $\mathcal{N} = 4$ SYM theory. Similarly, We propose a positive geometry, called orthogonal momentum amplituhedron, to describe the tree-level scattering amplitudes of the 3D Chern-Simons matter theory (often termed ABJM theory). We study the co-dimension one boundaries and construct the canonical forms in this space of positive geometry.

Recently, the integrated correlators of four BPS operators in the $\mathcal{N} = 4$ SYM theory were computed by the supersymmetric localisation. We show that in the perturbative regime, the integrated correlators are given by linear combinations of periods of certain conformal Feynman graphs. The periods involving multiple zeta values are of great interest in the study of mathematical physics and number theory. Finally, we study the four-point tree-level holographic correlators of arbitrary weights in the (2,0) supergravity theory on $AdS_3 \times S^3$, with two operators in tensor multiplet and the other two in gravity multiplet. We utilise the hidden 6D conformal symmetry, analogous to 10D symmetry for $AdS_5 \times S^5$, to arrive compact formulae in Mellin space. In the limits of maximally R-symmetry violating (MRV) limit and flat space, the formulae agree with results in other AdS backgrounds and the flat-space 6D amplitudes, respectively.

Acknowledgements

Contents

7

Chapter 1

Introduction

The S-matrix of a Quantum Field Theory (QFT) is arguably the most fundamental physical observable. Directly related to measurements in particle scattering experiments, the study of an S-matrix is of both theoretical and experimental importance. In recent years, rich mathematical structures have been discovered in field theory scattering amplitudes with the use of new formalisms that dramatically simplify calculations. Here we give a concrete example of this simplification; in order to calculate the n-gluon tree-level MHV (Maximal Helicity Violating) amplitude of the Yang-Mills theory, which contains two negative helicity gluons and $n-2$ positive helicity gluons, the number of Feynman diagrams to be summed over is given by the following

n	4	5	6	7	8	9	10	...
# of diagrams	4	25	220	2,485	34,300	559,405	10,525,900	...

As n increases, the number of Feynman diagrams drastically increases, rendering the calculation in the traditional way intractable. However, if the focus is instead put on only on-shell variables and novel S-matrix methods are applied, the MHV amplitude can be easily obtained and put in a simple form [6]:

$$A_n(\cdots i^- \cdots j^- \cdots) = \frac{\langle ij \rangle^4}{\langle 12 \rangle \langle 23 \rangle \cdots \langle n1 \rangle} \, . \tag{1.0.1}$$

The angle brackets are products of four-dimensional (4D) on-shell variables that solve the $p^2 = 0$ on-shell condition, which states a 4D momentum is product of two spinors, λ^α and $\tilde{\lambda}^{\dot\alpha}$:

$$p_i^{\alpha\dot\alpha} \;=\; \lambda_i^\alpha \tilde{\lambda}_i^{\dot\alpha} \, , \tag{1.0.2}$$

and angle brackets are contraction of spinors with the Levi-Civita tensor. This remarkably simple result (1.0.1) can be derived by the Britto-Cachazo-Feng-Witten (BCFW) recursion relation that makes use of the analytic properties of S-matrix to glue the fundamental three-point amplitudes to form a higher-point one [7], whilst the three-point

vertex is completely fixed by Lorentz invariance. The BCFW recursion also extends to the next-to-MHV (NMHV) amplitudes; furthermore, the work by Witten provides a nice description of higher degree N^{k-2}MHV amplitude in terms of a world-sheet twistor string theory [8].

The 4D twistor formula has led to similar formulation for the amplitudes of super-symmetric theories in 6D, especially the the probe M5-brane theory, where the traditional Lagrangian description was known to be subtle. Two major twistor-like formula in 6D, rational maps [1, 9, 10] and polarised scattering equation [11], both have world-sheet origins (see Fig.1.1), were introduced to describe amplitudes of a wide range of theories, including the aforementioned single probe M5-brane theory, D-brane theories, $\mathcal{N} = (1, 1)$ super Yang-Mills, (2,2) supergravity, (2,0) supergravity, theories and so on. The analogous twistor formula has also been extend to ten and eleven dimensions [12].
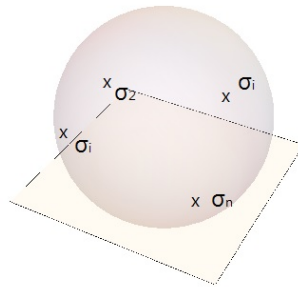
Figure 1.1: The worldsheet Riemann sphere for tree-level scattering amplitudes with punctures σ_i

The worldsheet descriptions of amplitudes has also been extended to loop level [13, 14]. In particular, for constructing a n-point one-loop amplitudes in lower dimensions, one begins with a $(n + 2)$-point tree-level amplitudes in the corresponding theory in the higher dimensions, and sets n of the external momenta in the lower dimensions. The remaining two momenta are taken to be forward and stay in the higher dimensions that play the role of the loop momenta in the theory in the lower dimensions. This construction has been applied to obtain one-loop SYM and SUGRA amplitude [15, 16]. Analogous construction also applies for the two-loop amplitudes [17–19].

The study of scattering amplitudes also provides new insights to other research fields in the high energy physics, such as holographic correlation functions in the context of AdS/CFT correspondence [20]. These amplitude-inspired approaches have been applied to compute the correlators in different holographic backgrounds, such as $AdS_5 \times S^5$, $AdS_5 3 \times S^3$, *etc.* The techniques including boostrap [21], Mellin space approach [22], hidden 10d/6d conformal symmetry [23–25], and so on, which bypass the traditional Witten diagrams and directly arrive at the final simple results.
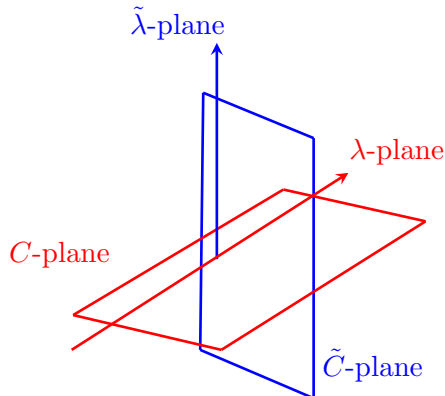
Figure 1.2: In the Grassmannian language, the 4D momentum conservation is guaranteed by the orthogonality of the C- and $\tilde{C}$-plane, which contain the 4D spinor λ^α and $\tilde{\lambda}^{\dot\alpha}$, respectively.

Moreover, the simplicity the final results of on-shell observables often suggests deeper *mathematical structures* in the theory. For instance, the amplitudes of $\mathcal{N} = 4$ SYM theory has a beautiful description in terms of integral over the Grassmannian manifold $G(k, n)$, which is a k-plane in n dimensions [26]. In this language, the usual 4D momentum conservation

$$\sum_{i=1}^{n} \lambda_i^\alpha \tilde{\lambda}_i^{\dot\alpha} = 0 \,, \tag{1.0.3}$$

becomes a statement of the orthogonality of the C- and $\tilde{C}$-plane, which contain the 4D spinor λ^α and $\tilde{\lambda}^{\dot\alpha}$, respectively, as shown in Fig.1.2

The Grassmannian formalism of 4D $\mathcal{N} = 4$ SYM was later generalised to a positive geometry, called amplituhedron [27]. In this amplituhedron description, the quantum mechnical properties of amplitudes, locality and unitarity, become emergent properties of a more underlying mathematical principle, positivity. Similarly, the grassmannian structures also appear in the 3D Chern-Simons theory (often termed ABJM theory), positive orthogonal grassmannian OG_+ [28–30], and it leads to the amplituhedron description for the theory [3,31]. In addition, the 6D superamplitude have structure of symplectic grassmannian (or Lagrangian Grassmannian LG), which provides a bigger picture that unifies different 6D twistor formulations [32]. Finally, there are many other physical observables in various theories that has nice geometric descriptions, such as the ABHY associahedron for the bi-joint ϕ^3 theory (without any supersymmetry) [33], EFT-Hedron for the effective field theories [34], Correlahedron for the correlation function [35], and Amplituhedron-like geometries for the "squared amplitude" [36], *etc.*

In the study of integrated correlated correlators of BPS operators in the $\mathcal{N} = 4$ SYM theory [37–39], many multi-zeta valued numbers appear in the perturbative expansion, which is related to the periods of certain conformal graphs [4]. It is very interesting to investigate how those periods (multi-zeta values), usually studied in the mathematical

physics as well as number theory, also make appearance in many QFTs [40].

In the thesis, we review these on-shell methods as well as the mathematical aspects of the amplitudes, see also the reviews articles [41–47]. Some keywords are:

- spinor helicity formalism

- Grassmannian formalism, positive geometry, amplituhedron

- twistor formulae, rational maps, polarised scattering equations

- soft theorems and symmetries

- AdS/CFT correspondence, Mellin amplitudes

- integrated correlator in $\mathcal{N} = 4$ SYM, BPS operators

and so on.

The thesis is organised as follows:

In chapter 2, we briefly review background materials of scattering amplitudes such as spinor-helicity formalism, Grassmannian, twistor formulation, soft theorems, *etc*, which will be useful for chapter 3,4, and 5

Chapter 3, which is based on [1], considers the twistor formulation of scattering amplitudes in six dimensions. The 6D (2,0) supersymmetric theory has a long lasting issues with the traditional Lagrangian formulation. The issue can be circumvented by directly focusing on the on-shell degrees of freedom. Twistor formulation gives closed form formulae of tree-level n-point scattering amplitudes of various 6D theories, including 6D $(2,0)$ M5-brane, $(1,1)$ D5-brane, $(1,1)$ SYM, $(2,2)$ SUGRA, and $(2,0)$ SUGRA. The twistor formula expresses S-matrix as an integral localised on the scattering equations. The dynamic part of the theory are encoded in the integrands. We utilise the formula to obtain the complete tree-level S matrix of 6D $(2,0)$ supergravity coupled to 21 abelian tensor multiplets. By studying its soft limits, we are able to explore the local moduli space of this theory, $\frac{SO(5,21)}{SO(5) \times SO(21)}$. By dimensional reduction, we also obtain a new formula for the tree-level S matrix of 4D $\mathcal{N} = 4$ Einstein-Maxwell theory.

In chapter 4, which is based on [2], we study the loop corrections of the world-volume D3-brane theory in 4D, which is obtained by taking forward limit as well as dimensional reduction of tree-level amplitudes of the world-volume M5/D5-brane theory in 6D. The tree-level amplitudes of M5-brane theory will be presented by the twistor formula introduced in the previous chapter 3. We show the MHV amplitudes in the D3-brane theory at one loop order are purely rational terms (except for the four-point amplitude). Upon performing a supersymmetry reduction on the M5-brane tree-level amplitudes, we also

construct one-loop corrections to the non-supersymmetric D3-brane amplitudes, which agree with the known results in the literature. The above results are verified by the generalised unitarity cuts method.

In chapter 5, which is based on [3], we introduce the positive geometry that describes scattering amplitudes in the 3D ABJM theory, called the orthogonal momentum amplituhedron. The scattering amplitude can be identified as the canonical form on the space defined by the product of positive orthogonal Grassmannian and the moment curve. The co-dimension one boundaries of the amplituhedron are given by the odd-particle planar Mandelstam variables. After reviewing the momentum amplituhedron for the 4D $\mathcal{N} = 4$ sYM theory, we apply similar construction for the 3D ABJM theory, which can be viewed as the kinematic projection of the 4D case. The Grassmannian formalism for the ABJM theory with reduced $\mathcal{N} = 4$ supersymmetry will follow. In such formalism, the canonical form can be naturally lifted to the volume form for the amplituhedron, from which we extract the volume function that projects to scattering amplitudes. We provide evidence that the BCFW triangulation of the amplitude tiles the amplituhedron by proving it in an explicit 8 point case.

In chapter 6, we review the background materials of correlation functions in conformal theories, such as Mellin space approach, hidden conformal symmetry, integrated correlator, *etc*, which will be useful for chapter 7 and 8.

In chapter 7, which is based on [4], we study the integrated correlators of four stress-tensor operators in the well-known $\mathcal{N} = 4$ SYM theory, and show in the perturbative regime they can be interpreted as periods of conformal graphs. The integrated correlators are computed by supersymmetric localisation techniques, which gives results that are finite in the Yang-Mills couplings τ and the rank of gauge group N. The results allow us obtain arbitrary order in g_{YM}, which matches the explicit computation of Feynman integral with specific measure in that corresponding loop order. By observing the aforementioned integral are periods of certain conformal graphs, we utilise the programming packages `HyperInt` [48] and `HyperlogProcedure` [49] to systematically evaluate integrals up to 4 loops in the planar limit. The results agree with the prediction from supersymmetric localisation, and it further predicts a period of a certain six-loop integral.

Chapter 8 , which is based on [5], focuses on four-point tree-level holographic correlators of chiral primary operators of arbitrary conformal weights in the (2, 0) supergravity on $AdS_3 \times S^3$. Due to the fact the supergravity on $AdS_3 \times S^3$ has half supersymmetry, it contains two super multiplet: gravity multiplet and tensor multiplet. We show that correlator with all four operator in tensor multiplet as well as the correlator with two in tensor and two in gravity multiplet have simple expressions in the Mellin space. This

is achieved by exploiting a hidden six-dimensional conformal symmetry, analogous to the ten-dimensional one for $AdS_5 \times S^5$, that packages a AdS_3 correlator with arbirary weights as a handful of corraltors in 6D flat space. Furtheremore, the AdS_3 correlators are shown to agree with 6D (2, 0) supergravity amplitudes when taking the flat-space limit.

Finally, we summarise the results and point out several interesting future directions in chapter 9. Some details of computations are relegated to the appendices, App.A and App.B.

Chapter 2

Review on Scattering Amplitudes

This chapter reviews several background materials of scattering amplitudes, including spinor-helicity formalisms in 3,4, and 6 dimensions, Grassmannian formalism and amplituhedron for 4D $\mathcal{N} = 4$ SYM and 3D ABJM theory, twistor formulation for 6D amplitudes, and soft theorems.

2.1   Spinor-helicity formalism

We introduce the power spinor-helicty formalism which solves the on-shell conditions, $p^2 = 0$, in various dimensions.

- **4D**: We start with the most familiar case, $D = 4$, where a four-component vector can be mapped to a two by two matrix by dotting into Pauli matrices, $\sigma^\mu = (1, \vec{\sigma})$, as follows

$$p_{\alpha\dot\alpha} = p_\mu \sigma^\mu_{\alpha\dot\alpha} = \begin{pmatrix} -p_0 + p_3 & p_1 - ip_2 \\ p_1 + ip_2 & -p_0 - p_3 \end{pmatrix}, \qquad (2.1.1)$$

and then on-shell condition reads as

$$\det(p) = -p^\mu p_\mu = 0 \,. \qquad (2.1.2)$$

The vanishing determinant of $p_{\alpha\dot\alpha}$ suggests a 4D massless vector can be decomposed into an outer product of two spinors λ_i^α and $\tilde\lambda_i^{\dot\alpha}$

$$p_i^{\alpha\dot\alpha} \;=\; \lambda_i^\alpha \tilde\lambda_i^{\dot\alpha} \,, \qquad (2.1.3)$$

where indices $\alpha = 1, 2$ and $\dot\alpha = 1, 2$ are the $SL(2, \mathbb{C}) \times SL(2, \mathbb{C})$ Lorentz indices. Lorentz invariant products, which we call angle and square brackets, are defined

by contracting the spinors using Levi-Civita tensor,

$$\begin{aligned}
\langle ij \rangle &= \lambda_{i\alpha}\lambda_{j\beta}\epsilon^{\alpha\beta} \\
[ij] &= \tilde{\lambda}_{i\dot{\alpha}}\tilde{\lambda}_{j\dot{\beta}}\epsilon^{\dot{\alpha}\dot{\beta}} \,,
\end{aligned} \tag{2.1.4}$$

and the Mandelstam variables are given by

$$s_{ij} = -(p_i + p_j)^2 = -2p_i \cdot p_j = \langle ij \rangle [ji] \,. \tag{2.1.5}$$

The little group that leaves momentum invariant in 4D is $U(1)$, which transforms the spinors as

$$\lambda_i \to t_i \lambda_i \qquad \text{and} \qquad \tilde{\lambda}_i \to t_i^{-1}\tilde{\lambda}_i \,, \tag{2.1.6}$$

and the scattering amplitude transforms covariantly as

$$A(1^{h_1} \cdots n^{h_n}) \to \prod_i t_i^{-2h_i} A(1^{h_1} \cdots n^{h_n}) \,, \tag{2.1.7}$$

where h_i's are the helicities of the external particles. A maximal helicity violating (MHV) that has two negative glouns and the rest positive are given by the famous Parke-Taylor formula,

$$A_n(\cdots i^- \cdots j^- \cdots) = \frac{\langle ij \rangle^4}{\langle 12 \rangle \langle 23 \rangle \cdots \langle n1 \rangle} \,, \tag{2.1.8}$$

which has a surprising simple form that is not obvious from the Feynman diagram's perspective.

- **3D**: The 3D case is similar to 4D, where we consider (2.1.1) with $p_2 = 0$ since we are in one dimension lower, so that $p_i^{\alpha\beta}$ is now a symmetric matrix

$$p_{\alpha\beta} = \begin{pmatrix} -p_0 + p_3 & p_1 \\ p_1 & -p_0 - p_3 \end{pmatrix} \,, \tag{2.1.9}$$

which again has a vanishing determinant ($p^2 = 0$) that allows us to write it as a product of two spinors

$$p_i^{\alpha\beta} = \lambda_i^\alpha \lambda_i^\beta \,, \tag{2.1.10}$$

where the index $\alpha = 1, 2$ denotes a $SL(2, \mathbb{R})$ Lorentz index in 3D. The Lorentz invariant products is simply the angle bracket

$$\langle ij \rangle = \lambda_{i\alpha}\lambda_{j\beta}\epsilon^{\alpha\beta} \,, \tag{2.1.11}$$

and the Mandelstam variable is given by

$$s_{ij} = -\langle ij \rangle^2. \tag{2.1.12}$$

- **6D**: A 6D null momentum can be parametrised using the spinor-helicity variables [50],

$$p_i^{AB} = \lambda_{i,a}^A \lambda_{i,b}^B \epsilon^{ab} := \langle \lambda_i^A \, \lambda_i^B \rangle, \tag{2.1.13}$$

where $A, B = 1, 2, 3, 4$ being the spinor index of the $Spin(5,1)$ Lorentz group, and $a = 1, 2$ is a left-handed index of the $SU(2)_L \times SU(2)_R$ massless little group. We can also express the momenta in terms of right-handed index:

$$p_{i,AB} = \epsilon_{ABCD} \, p_i^{CD} = \tilde{\lambda}_{i,A,\hat{a}} \tilde{\lambda}_{i,B,\hat{b}} \, \epsilon^{\hat{a}\hat{b}} := [\tilde{\lambda}_{i,A} \, \tilde{\lambda}_{i,B}]. \tag{2.1.14}$$

Also, the Lorentz invariant product are given by

$$\langle 1_{a_1} 2_{a_2} 3_{a_3} 4_{a_4} \rangle = \epsilon_{ABCD} \lambda_{1,a_1}^A \lambda_{2,a_2}^B \lambda_{3,a_3}^C \lambda_{4,a_4}^D \tag{2.1.15}$$

$$[1_{\hat{a}_1} 2_{\hat{a}_2} 3_{\hat{a}_3} 4_{\hat{a}_4}] = \epsilon_{ABCD} \tilde{\lambda}_{1\hat{a}_1}^A \tilde{\lambda}_{2\hat{a}_2}^B \tilde{\lambda}_{3\hat{a}_3}^C \tilde{\lambda}_{4\hat{a}_4}^D \tag{2.1.16}$$

$$\langle \lambda_i^a | \tilde{\lambda}_{j,\hat{b}}] = \lambda_i^{A,a} \tilde{\lambda}_{j,A,\hat{b}} = [\tilde{\lambda}_{j,\hat{b}} | \lambda_i^a \rangle. \tag{2.1.17}$$

2.2 Review on Grassmannian formalism

Scattering amplitudes of 4D $\mathcal{N} = 4$ SYM theory has a beautiful description in terms of a contour integral, denoted by $\mathcal{L}_{k,n}$, over a Grassmannian manifold, $G(k,n)$, which is a k-plane in n dimensions. Similar construction is extended to the 3D ABJM theory, of which the S-matrices for $n = 2k$ particles are described by the orthogonal Grassmannian $OG(k, 2k)$. We will review both formalisms in this section.

2.2.1 Grassmannian formalism for $\mathcal{N} = 4$ SYM theory: $\mathcal{L}_{k,n}$

We first review the Grassmannian formalism for the 4D $\mathcal{N} = 4$ SYM theory. We package all the helicity states into a single Grassmann coherent state labeled by Grassmann parameters $\tilde{\eta}^I$ with $I = 1, \ldots, 4$ as follows

$$\Omega \equiv |{+}1\rangle + \tilde{\eta}^I \left| {+}\tfrac{1}{2} \right\rangle_I + \frac{1}{2!} \tilde{\eta}^I \tilde{\eta}^J |0\rangle_{IJ} + \frac{1}{3!} \epsilon_{IJKL} \tilde{\eta}^I \tilde{\eta}^J \tilde{\eta}^K \left| {-}\tfrac{1}{2} \right\rangle^L + \frac{1}{4!} \epsilon_{IJKL} \tilde{\eta}^I \tilde{\eta}^J \tilde{\eta}^K \tilde{\eta}^L |{-}1\rangle. \tag{2.2.1}$$

We denote the complete amplitude as $\mathcal{A}_n(\lambda_a, \widetilde{\lambda}_a, \widetilde{\eta}_a)$, which is now a polynomial in the $\widetilde{\eta}$'s. It is convenient to expand this according to,

$$\mathcal{A}_n(\lambda_a, \widetilde{\lambda}_a, \widetilde{\eta}_a) = \sum_k \mathcal{A}_n^{(k)}(\lambda_a, \widetilde{\lambda}_a, \widetilde{\eta}_a), \qquad (2.2.2)$$

where $\mathcal{A}_n^{(k)}$ is a polynomial of $\widetilde{\eta}$'s with the degree $4k$, and it is often called an $\mathrm{N}^{(k-2)}\mathrm{MHV}$ amplitude. One can extract any amplitude A_n from the superamplitude $\mathcal{A}_n$ by projecting out the desired external states, *i.e.* perform a Grassmann integral, for example

$$A_n(1^+ \ldots i^- \ldots j^- \ldots n^+) = \left(\prod_{A=1}^4 \frac{\partial}{\partial \widetilde{\eta}_{iA}} \right) \left(\prod_{B=1}^4 \frac{\partial}{\partial \widetilde{\eta}_{jB}} \right) \mathcal{A}_n(\Omega_1, \ldots, \Omega_n) \bigg|_{\eta_{kC}=0} . \quad (2.2.3)$$

The Grassmannian formula for n-point $\mathrm{N}^{k-2}\mathrm{MHV}$ tree-level scattering amplitudes reads

$$\begin{aligned}
&\mathcal{L}_{k,n} \\
&= \int \frac{d^{k \times n} C}{\mathrm{Vol}(GL(k))} \frac{1}{(12\cdots k)\ldots(n1\cdots k-1)} \delta^{(n-k)\times 2}(\tilde{C} \cdot \lambda) \delta^{k\times 2}(C \cdot \tilde{\lambda}) \delta^{(n-k)\times 4}(\tilde{C} \cdot \tilde{\eta}),
\end{aligned}$$
$$(2.2.4)$$

where $\tilde{C}$ is the orthogonal complement of the Grassmannian C that satisfies $C\tilde{C}^T = 0$, and $(1\ldots k)$ is a consecutive minor of columns from 1 to k. The bosonic delta functions in (2.2.4) in general do not fully localise the integral. The leftover free c-variables need to be performed contour integrals, and the number is given by the following counting. There are $n \times k$ c's in the Grassmannian C, with k^2 of them being gauge fixed. There are $2k + 2(n-k)$ bosonic delta functions, where 4 of them are redundant due to 4D momentum conservation. So the counting of c-variables to be integrated is

$$n_\tau = n \times k - k^2 - 2k - 2(n-k) + 4 = (k-2)(n-k-2). \qquad (2.2.5)$$

The formula (2.2.4) can also be expressed in terms of on-shell diagram variables, α_i (e.g. BCFW-bridge) coordinates,

$$\int_{C_\sigma} \frac{d\alpha_1}{\alpha_1} \wedge \cdots \wedge \frac{d\alpha_d}{\alpha_d} \, \delta^{(n-k)\times 2}\big(C_\sigma^T \cdot \lambda\big) \delta^{k\times 2}\big(C_\sigma \cdot \widetilde{\lambda}\big) \delta^{k\times 4}\big(C_\sigma \cdot \widetilde{\eta}\big). \qquad (2.2.6)$$

where the boundary measurement in C_σ (subscript σ denotes certain configuration) can be determined by the left-right path in the on-shell diagram [26]. Since the on-shell condition has been solved, the bosonic delta-functions fully localises the $d = (2n-4)$ degrees of freedom of the cell.

2.2.2 Grassmannian for 3D ABJM: $\mathcal{L}_{k,2k}$

The 3D example that also has a Grassmannian description is the $\mathcal{N} = 6$ Chern-Simons matter theory (ABJM theory) [51], which has the following on-shell degrees of freedom

$$
\begin{aligned}
\Phi &= X_4 + \eta_A\,\psi^A - \frac{1}{2}\epsilon^{ABC}\,\eta_A\eta_B\,X_C - \eta_1\eta_2\eta_3\,\psi^4\,, \\
\bar{\Psi} &= \bar{\psi}_4 + \eta_A\bar{X}^A - \frac{1}{2}\epsilon^{ABC}\,\eta_A\eta_B\,\bar{\psi}_C - \eta_1\eta_2\eta_3\,\bar{X}^4\,,
\end{aligned}
\tag{2.2.7}
$$

which contains 4 complex scalars X^A, and 4 complex fermions $\psi_{A\alpha}$, as well as their conjugate $\bar{X}^{\mathsf{A}}$, $\bar{\psi}_{\mathsf{A}\alpha}$. The tree-level ABJM amplitudes can be compactly written as:

$$
\mathcal{A}_n^{\text{tree}} = \delta^3(\sum_{i=1}^n p_i)\delta^6(\sum_{i=1}^n q_i)F_n(\lambda_i,\eta_i)
\tag{2.2.8}
$$

where p_i, q_i are the on-shell momentum, super-momentum for each external leg,

$$
p_i{}^{\alpha\beta} = \lambda_i^\alpha\lambda_i^\beta\,, \quad q_i{}^{\alpha\mathsf{A}} = \lambda_i^\alpha\eta_i^{\mathsf{A}}\,,
\tag{2.2.9}
$$

and $F_n(\lambda_i,\eta_i)$ is a rational function of Lorentz invariants $\lambda_i^\alpha\lambda_{j\alpha} = \langle ij\rangle$ and fermionic variables η_i^{A}. We note that for 3D ABJM theory, only the even-multiplicity amplitudes, *i.e.* $n - 2k$ with $k = 2,3,4\cdots$, are non-vanishing. This is because for odd number of external states, there always exist at least one Chern-Simons gauge field, which doesn't have any physical degree of freedom; hence, the S-matrix vanishes.

The Grassmannian representation of scattering amplitudes of the ABJM theory is based on a so-called orthogonal Grassmannian $C \in OG(k,2k)$. The orthogonal Grassmannian can be viewed as a $k \times 2k$ matrix C_{mi} satisfying

$$
(CC^T)_{mp} = \sum_{i=1}^{2k} C_{mi}C_{pi} = 0\,.
\tag{2.2.10}
$$

The tree-level $n\ (= 2k)$-point scattering amplitudes of the ABJM theory can be written as the following Grassmannian integral [28]

$$
\mathcal{L}_{k,2k} = \int \frac{d^{k\times 2k}C}{\text{Vol}(GL(k))}\frac{1}{M_1 M_2\ldots M_k}\delta^{\frac{k(k+1)}{2}}(C\cdot C^T)\prod_{a=1}^k \delta^{2|3}(C_a\cdot\Lambda)\,,
\tag{2.2.11}
$$

where M_i is a minor involving the k consecutive columns from j to $j + k - 1$ and we have grouped the on-shell variables into a $2|3$ spinor $\Lambda_i = (\lambda_i^\alpha, \eta_i^A)$. The above integral is $GL(k)$ invariant, where $d^{k\times 2k}C$, $\delta^{\frac{k(k+1)}{2}}(C\cdot C^T)$, $\delta^{2|3}(C_a\cdot\Lambda)$, have $GL(k)$ weight $2k^2$, $-k(k+1)$, k, respectively. Each minor has weight k, in total the integral has weight $2k^2 - k(k+1) + k - k^2 = 0$. Similar to the case of Grassmannian formalism in 4D

SYM, the bosonic delta functions do not fully localise the dC-integral for higher k, in general, there are

$$n_\tau = 2k^2 - k^2 - 2k - \frac{k(k+1)}{2} + 3 = \frac{(k-2)(k-3)}{2} \tag{2.2.12}$$

contour integral to be performed, which are determined by the vanishing of certain minor(s). For $k = 2, 3$ case, that is 4- and 6-point, the Grassmannians are top cells. The above integral for ABJM (2.2.11) also has another representation using the variables of on-shell diagram [30, 52], which have already solved the orthogonal conditions and have been localised in certain BCFW cells. It is given by

$$\mathcal{L}_{k,2k} = \sum_{\{\alpha\}} \int \left[\prod_{i=1}^{n_v} d\log\left(\tan\theta_i\right) \right] \mathcal{J} \prod_{a=1}^{k} \delta^{2|3} \left(C_a(\theta_i, \alpha_i) \cdot \Lambda \right), \tag{2.2.13}$$

where $\alpha_i = \pm 1$ parametrises positive/negative branch, and θ_i are the vertices in the on-shell diagram. The number of vertices, n_v, is determined from the free variables in C subtracted the orthogonal conditions and the conditions for vanishing minors,

$$n_v = 2k^2 - k^2 - \frac{k(k+1)}{2} - n_\tau = 2k - 3. \tag{2.2.14}$$

Finally, $\mathcal{J}$ is the Jacobian corresponding to the closed loop in the on-shell diagram, which arises from the $\mathcal{N} = 6$ SUSY. Here we give a set of simple rules of $\mathcal{J}$, which can be decomposed into several contributions depending the configuration of these loops, *e.g.* sharing a vertex or an edge and so on. Explicitly,

$$\mathcal{J} = 1 + \mathcal{J}_1 + \mathcal{J}_2 + \mathcal{J}_3 + \mathcal{J}_{13} + \mathcal{J}_{23}, \tag{2.2.15}$$

where for the purpose of the thesis we only encounter $\mathcal{J}_1$ and $\mathcal{J}_2$, which are given by

- $\mathcal{J}_1$ contains contributions from all single closed loops J_i, products of disjoint pairs of closed loops $J_i J_j$, disjoint triples of closed loops $J_i J_j J_k$ and so on.

$$\mathcal{J}_1 = \sum_{\text{single}} J_i + \sum_{\text{disjoint pairs}} J_i J_j + \sum_{\text{disjoint triples}} J_i J_j J_k + \dots .$$

  Every face forms a oriented closed loop, which contributes as the follows: if the loop is closed anti-clockwise, it gives a product of c's, otherwise it gives a product of s's.

- $\mathcal{J}_2$ takes into account the contributions for closed loops that share a single vertex. This contribution is given by products of c's ($cos(\theta)$'s) or s's ($sin(\theta)$'s) of the corresponding loops with that of the shared vertex removed.
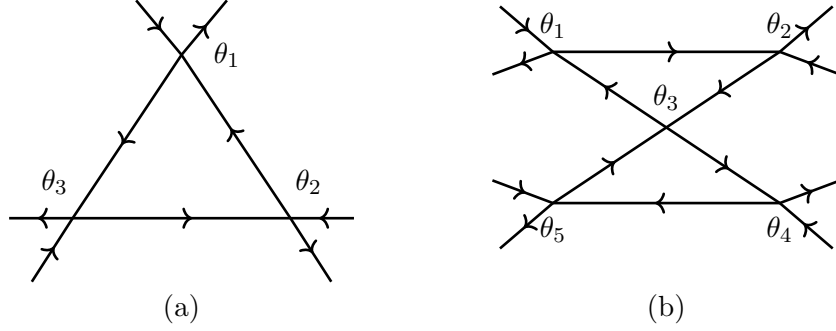
Figure 2.1: The on-diagrams for 6- and 8-pt ABJM theory with 3 and 5 internal vertices, restively. Their Jacobi are given in (2.2.16) according to the rule.

Let us apply the above rule to obtain Jacobian of the following 6- and 8-pt diagrams shown in Fig.2.1, denoted by $\mathcal{J}_a$ and $\mathcal{J}_b$, respectively. The rule gives the following:

$$
\begin{aligned}
\mathcal{J}_a &= 1 + \mathcal{J}_{a,1} = 1 + c_1 c_2 c_3\,, \\
\mathcal{J}_b &= 1 + \mathcal{J}_{b,1} + \mathcal{J}_{b,2} = 1 + s_1 s_2 s_3 + s_3 s_4 s_5 + s_1 s_2 s_4 s_5\,.
\end{aligned}
\tag{2.2.16}
$$

We have used blue/red colour to indicate the Jacobian is built from the first/second rule listed above.

2.2.3 Positive geometry: Amplituhedron

We review the geometric descriptions of scattering amplitudes in 4D SYM and 3D ABJM theories. The idea in [53] is to introduce a positive geometry Y by taking product of the positive grassmannian C and the positive external data Z as

$$
Y = C \cdot Z\,.
\tag{2.2.17}
$$

Here, the dot product simply means summing the particle indices,and the positivity is assured by all consecutive minors of C and Z being positive, which also guarantees the positivity of Y. The canonical form of the Y-space, which can be obtained using BCFW-triangulation, gives the scattering amplitudes. The original formulation for SYM theory relies on the momentum twistor variables. For the purpose of generalising to 3D, the momentum amplituhedron proposed recently [54], which also describes SYM scattering, will be adapted. The momentum amplituhedron, $\mathcal{M}_{n,k}$, for n-particle N^{k-2}MHV scattering is defined as a image of positive Grassmannian $G_+(k,n)$ through the map

$$
\Phi_{(\Lambda,\tilde{\Lambda})}\colon G_+(k,n) \to G(k,k+2) \times G(n-k,n-k+2)\,.
\tag{2.2.18}
$$

The pair of Grassmannian elements: $(\tilde{Y}, Y) \in G(k, k+2) \times G(n-k, n-k+2)$ is given by:

$$\tilde{Y}_{\dot{a}}^{\dot{A}} = \sum_{i=1}^{n} c_{\dot{a}i}\tilde{\Lambda}_i^{\dot{A}}, \quad Y_a^A = \sum_{i=1}^{n} c_{ai}^{\perp}\Lambda_i^A . \tag{2.2.19}$$

One can quickly figure out the dimension of $(\tilde{Y}, Y)$ is given as

$$\dim(G(k, k+2)) + \dim(G(n-k, n-k+2)) = 2k + 2(n-k) - 4 = 2n - 4 , \tag{2.2.20}$$

where the (-4) comes from the 4D momentum conservation

$$P^{\alpha\dot{\alpha}} = \sum_{i=1}^{n} \left(Y^{\perp} \cdot \Lambda^T\right)_i^{\alpha} \left(\tilde{Y}^{\perp} \cdot \tilde{\Lambda}^T\right)_i^{\dot{\alpha}} = 0. \tag{2.2.21}$$

The dimension $2n - 4$ exactly matches the degrees of freedom in the SYM Grassmannian formalism using on-shell diagram variables in (2.2.6). Let us illustrate how to obtain scattering amplitudes from the positive geometry with a simple 4-point MHV example.

- We first parametrise the 4-point positive grassmannian, $G_+(2, 4)$, as the following matrix

$$C = \begin{pmatrix} 1 & \alpha_2 & 0 & -\alpha_3 \\ 0 & \alpha_1 & 1 & \alpha_4 \end{pmatrix} , \quad \alpha_i \geq 0 . \tag{2.2.22}$$

- Then we use the relation $Y = C \cdot \Lambda$ to write the boundary measurement α_i's in terms of Y-brackets

$$\alpha_1 = \frac{\langle Y12 \rangle}{\langle Y13 \rangle}, \alpha_2 = \frac{\langle Y23 \rangle}{\langle Y13 \rangle}, \alpha_3 = \frac{\langle Y34 \rangle}{\langle Y13 \rangle}, \alpha_4 = \frac{\langle Y14 \rangle}{\langle Y13 \rangle} . \tag{2.2.23}$$

- The volume form is simply given by wedging the dlog's as

$$\boldsymbol{\Omega}_{4,2} = \bigwedge_{j=1}^{4} \mathrm{dlog}\alpha_j = \mathrm{dlog}\frac{\langle Y12 \rangle}{\langle Y13 \rangle} \wedge \mathrm{dlog}\frac{\langle Y23 \rangle}{\langle Y13 \rangle} \wedge \mathrm{dlog}\frac{\langle Y34 \rangle}{\langle Y13 \rangle} \wedge \mathrm{dlog}\frac{\langle Y14 \rangle}{\langle Y13 \rangle}$$

$$= \frac{\langle 1234 \rangle^2}{\langle Y12 \rangle \langle Y23 \rangle \langle Y41 \rangle \langle Y23 \rangle} \langle Y d^2 Y_1 \rangle \langle Y d^2 Y_2 \rangle . \tag{2.2.24}$$

- From the equation above, we read off the volume function:

$$\Omega_{4,2} = \frac{\langle 1234 \rangle^2}{\langle Y12 \rangle \langle Y23 \rangle \langle Y41 \rangle \langle Y23 \rangle}$$

$$= \frac{\langle 1234 \rangle^2 [1234]^2}{\langle Y12 \rangle \langle Y23 \rangle [\tilde{Y}12][\tilde{Y}23]} \,, \qquad (2.2.25)$$

  where the two expressions above are equivalent due to momentum conservation.

- Finally, we project $(Y, \tilde{Y})$ to $(Y^*, \tilde{Y}^*)$, given as

$$Y^* = \begin{pmatrix} \mathbb{0}_{2 \times (n-k)} \\ \mathbb{1}_{(n-k) \times (n-k)} \end{pmatrix}, \quad \tilde{Y}^* = \begin{pmatrix} \mathbb{0}_{2 \times (k)} \\ \mathbb{1}_{(k) \times (k)} \end{pmatrix}, \qquad (2.2.26)$$

  to obtain the 4-point MHV amplitude

$$\mathcal{A}_{4,2}^{\text{tree}} = \delta^4(p) \frac{\delta^4(q) \delta^4(\tilde{q})}{\langle 12 \rangle \langle 23 \rangle [12][23]} \,. \qquad (2.2.27)$$

To describe the 3D ABJM scattering amplitudes, which only involves middle sectors, *i.e.* $n = 2k$, we introduce the orthogonal momentum amplituhedron, $\mathcal{O}_k$, which is an image of positive Grassmannian $G_+(k, 2k)$ through the map

$$\Phi_\Lambda \colon G_+(k, 2k) \to G(k, k+2) \,. \qquad (2.2.28)$$

The Grassmannian element Y is defined as:

$$Y_a^A = \sum_{i=1}^{n=2k} C_{ai} \Lambda_i^A \,, \qquad (2.2.29)$$

which has the dimension $2k - 3$ due the 3D momentum conservation

$$0 = \sum_{i=1}^{n} P_i^{\alpha\beta} = \sum_{i=1}^{n} (-1)^i \left(Y^\perp \cdot \Lambda^T \right)_i^\alpha \left(Y^\perp \cdot \Lambda^T \right)_i^\beta \,,$$

Let us again illustrate this formalism with the simplest 4-point example

- We first paramerise the 4-point orthogonal Grassmannian, $OG_+(2, 4)$, as

$$C = \begin{pmatrix} 1 & \cos\theta & 0 & -\sin\theta \\ 0 & \sin\theta & 1 & \cos\theta \end{pmatrix}, \qquad 0 \leq \theta \leq \frac{\pi}{2} \,. \qquad (2.2.30)$$

- Using $Y = C \cdot \Lambda$, we write the trignometric functions in $OG_+(2, 4)$ in terms of Y-brackets, and volume form is the $d\log\tan(\theta)$'(the Jacobian is 1 for 4-pt) as

the following

$$\mathbf{\Omega}_{4,2}^{3d} = d \log \frac{\langle Y12 \rangle}{\langle Y23 \rangle} . \tag{2.2.31}$$

- Plugging the volume form above into the relation

$$\mathbf{\Omega}_{2k,k}^{3d} \wedge d^3 P \, \delta^3(P) = \prod_{a=1}^{k} \langle Y_1 \dots Y_k d^2 Y_a \rangle \delta^3(P) \, \Omega_{2k,k}^{3d} ,$$

gives volume function

$$\Omega_{4,2}^{3d} = \langle 1234 \rangle^2 \frac{\langle Y13 \rangle}{\langle Y12 \rangle \langle Y23 \rangle} ,$$

- Projecting Y to Y^* and integrating $d^2\phi$, we arrives at the 4-point amplitude

$$\mathcal{A}_4^{3d} = \delta^4(\sum_i q_i) \frac{\langle 13 \rangle}{\langle 12 \rangle \langle 23 \rangle} , \qquad q_i^{\alpha I} = \lambda_i^{\alpha} \eta_i^I .$$

The more involved 6-point case will be covered in the chapter 5, where we will have more detailed discussions on the boundaries of orthogonal momentum amplituhedron, which corresponds to the factorisation and soft limits of the ABJM theory. The BCFW triagulation and the tiling of the amplituhedron space will also be studied with an 8-point example.

2.3 Twistor formulation for 6D amplitudes

We review the twistor-like formulation of the tree-level amplitudes for various 6D supersymmetric theories, including 6D $(2,0)$ M5-brane, $(1,1)$ D5-brane, $(1,1)$ SYM, $(2,2)$ SUGRA, and $(2,0)$ SUGRA. In this section, we focus on the world-volume M5-brane theory in 11D Minkowski spacetime background with $(2,0)$ supersymmetry, which describes interactions of one self-dual tensor B^{ab}, five scalars, and four spinors. The on-shell superfield is given by

$$\Phi^{\text{M5-brane}}(\eta) = \phi + \eta_a^I \psi_I^a + \epsilon_{IJ} \eta_a^I \eta_b^J B^{ab} + \eta_a^I \eta^{J,a} \phi_{IJ} + (\eta^3)_a^I \bar{\psi}_I^a + (\eta)^4 \bar{\phi} , \tag{2.3.1}$$

where $I, J = 1, 2$, $(\eta^3)_a^I = \epsilon_{JK} \eta^{Ib} \eta^{Jb} \eta_a^K$ and $(\eta^4) = \epsilon_{IJ} \epsilon_{KL} \eta_a^I \eta_b^J \eta^{Ka} \eta^{Lb}$. The on-shell degrees of freedom are represented as

$$\phi^{IJ} : (\mathbf{1}, \mathbf{1}; \mathbf{3}, \mathbf{1}) \quad B^{ab} : (\mathbf{3}, \mathbf{1}; \mathbf{1}, \mathbf{1}) \quad \psi^{aI} : (\mathbf{2}, \mathbf{1}; \mathbf{2}, \mathbf{1}) . \tag{2.3.2}$$

The sixteen supercharges are given by

$$q^{AI} = \lambda_a^A \eta^{Ia} \qquad \text{and} \qquad \bar{q}^{AI} = \lambda_a^A \frac{\partial}{\partial \eta^{Ia}} \, . \tag{2.3.3}$$

The four-point super amplitude takes the following simple form

$$A_4^{\text{M5-brane}} = \delta^6 \left(\sum_{i=1}^4 p_i^{AB} \right) \delta^8 \left(\sum_{i=1}^4 q_i^{AI} \right) . \tag{2.3.4}$$

2.3.1 Connected formula

The formulation is to write an n-point tree amplitude as an integral over an n-punctured Riemann sphere

$$A_n^{6D} = \int d\mu_n^{6D} \, \mathcal{I}_L \, \mathcal{I}_R \, , \tag{2.3.5}$$

where $d\mu_n^{6D}$ is the theory independent measure that imposes the scattering equations [55] that completely localises the integral,

$$\sum_{i \neq j} \frac{p_i \cdot p_j}{\sigma_{ij}} = 0 \, , \quad \text{for all} \ \ j \, , \tag{2.3.6}$$

where $\sigma_{ij} := \sigma_i - \sigma_j$. The information of the theory is specified by the integrands $\mathcal{I}_L \, \mathcal{I}_R$. The integral is invariant under the $SL(2, \mathbb{C})$ transformation

$$\sigma_i \to \frac{\beta \sigma_i + \gamma}{\alpha \sigma_i + \delta} \, , \quad \text{with} \ \ \beta \delta - \alpha \gamma = 1 \, , \tag{2.3.7}$$

and the measure $d\mu_n^{6D}$ carries $SL(2, \mathbb{C})$ weight -4, that is

$$d\mu_n^{6D} \to \prod_{i=1}^n (\alpha \sigma_i + \delta)^{-4} \, d\mu_n^{6D} \, , \tag{2.3.8}$$

which constraints the half integrands, $\mathcal{I}_{L/R}$, to have weight 2. There are two different types of the twistor formuation. One is the polarised scattering equations proposed by Geyer and Mason [11], and the other is based on the rational maps formalism [1, 9, 10]. The two seemly different formulations are shown to be equivalent by introducing a symplectic Grassmannian.

2.3.2 Rational maps

Let us begin with the scattering map in 4D, which maps a point on the moduli space (the Riemann sphere, $\mathbb{CP}^1$) to a null light cone

$$\sigma \to \rho_\alpha(\sigma) \, \tilde{\rho}_{\dot{\alpha}}(\sigma) \, , \tag{2.3.9}$$

where $\rho_\alpha(\sigma)$ and $\tilde{\rho}_{\dot{\alpha}}(\sigma)$ are polynomials of degree d and $\bar{d}$ respectively, subject to the condition $d + \bar{d} = n - 2$. Through the use of scattering maps in 4D, the Witten-RSV formula for amplitudes in $\mathcal{N} = 4$ Super Yang-Mills theory can be obtained [56]. The polynomial degree d is related to the degree of classifying sectors; hence, the formula allows for a natural extension beyond the MHV case. The scattering maps given in (2.3.9) rely on 4D spinor-helicity formalism. In order to extend this formalism to study six-dimensional (6D) scattering amplitudes, the 6D scattering maps

$$\sigma \to \rho_a^A(\sigma)\,\rho_b^B(\sigma)\,\epsilon^{a\,b} \tag{2.3.10}$$

are introduced. Here the polynomial degree of $\rho_a^A(\sigma)$ is $m = \frac{n}{2} - 1$ (we focus on even n in this section), such that the total degree is $n - 2$. The expansion is explicitly given as

$$\rho_a^A(\sigma) = \sum_{k=0}^m \rho_{a,k}^A\,\sigma^k\,, \tag{2.3.11}$$

The bosonic measure is defined as

$$d\mu_n^{6D} = \frac{\prod_{i=1}^n d\sigma_i \prod_{k=0}^m d^8\rho_k}{\text{vol}\,(SL(2,\mathbb{C})_\sigma \times SL(2,\mathbb{C})_\rho)} \frac{1}{V_n^2} \prod_{i=1}^n E_i^{6D}\,. \tag{2.3.12}$$

The coordinates σ_i label the n punctures, and the Vandermonde factor is given as $V_n = \prod_{i<j} \sigma_{ij}$. The volume of $SL(2,\mathbb{C})$ gauge groups are mod out in a standard way (i.e. gauge fixing 3 of σ_i's). The 6D scattering equations are given by

$$E_i^{6D} = \delta^6\left(p_i^{AB} - \frac{\langle \rho_a^A(\sigma_i)\,\rho^{B\,a}(\sigma_i)\rangle}{\prod_{j\neq i}\sigma_{ij}}\right)\,. \tag{2.3.13}$$

Having introduced the bosonic measure, it is natural to define a fermionic measure, which serves as a half integrand for the supersymmetric theories. For the $(2,0)$ SUSY, it is given by

$$\int d\Omega_F^{(2,0)} = V_n \int \prod_{k=0}^m d^4\chi_k^{I\,a} \prod_{i=1}^n \delta^8\left(q_i^{A\,I} - \frac{\langle \rho_a^A(\sigma_i)\,\chi^{I\,a}(\sigma_i)\rangle}{\prod_{j\neq i}\sigma_{ij}}\right)\,, \tag{2.3.14}$$

where the supercharge is simply given by $q_i^{A\,I} = \langle \lambda_i^A \eta_i^I \rangle$, and the fermionic rational map is defined as

$$\chi^{I\,a}(\sigma) = \sum_{k=0}^m \chi_k^{I\,a}\,\sigma^k\,. \tag{2.3.15}$$

Another half integrand of the M5 (and D5)-brane theorie is the reduced Pfaffian

$$\mathcal{I}_L^{\text{M5}} = \left(\text{Pf}' S_n\right)^2 , \qquad \mathcal{I}_R^{\text{M5}} = \left(\text{Pf}' S_n\right) \int d\Omega_F^{(2,0)} , \qquad (2.3.16)$$

where S_n is an antisymmetric n by n matrix whose entries are explicitly given by:

$$[S_n]_{ij} = \begin{cases} \dfrac{p_i \cdot p_j}{\sigma_i - \sigma_j} & \text{if} \quad i \neq j, \\ 0 & \text{if} \quad i = j, \end{cases} \qquad \text{for} \qquad i, j = 1, 2, \ldots, n . \qquad (2.3.17)$$

The reduced Pfaffian of S_n, $\text{Pf}' S_n$, that has appeared in CHY formula for EFTs, such as non-linear sigma model, Born-Infeld, and special Galileon theories [57] is defined as

$$\text{Pf}' S_n = \frac{(-1)^{k+l}}{\sigma_{kl}} \text{Pf}(S_n)_{kl}^{kl} , \qquad (2.3.18)$$

where $(S_n)_{kl}^{kl}$ is an $(n-2) \times (n-2)$ matrix with the k-th and l-th rows and columns of S_n removed, and the result is independent of the choice of k, l.

Now we give the connected formula for the n-point tree-level scattering amplitude of the M5-brane theory

$$\mathcal{A}_n^{\text{M5-brane}} = \int d\mu_n^{6D} \left(\left(\text{Pf}' S_n\right)^3 \int d\Omega_F^{(2,0)} \right) . \qquad (2.3.19)$$

The connected formula (2.3.19) gives the following four-point amplitude

$$A_4^{\text{M5-brane}} = \delta^6 \left(\sum_{i=1}^4 p_i^{AB} \right) \delta^8 \left(\sum_{i=1}^4 q_i^{AI} \right) , \qquad (2.3.20)$$

and the higher-point amplitudes for $n = 6, 8$ are checked in [9].

2.3.3 Polarised scattering equation

The polarised scattering equations was introduced by Geyer and Mason [11], which expresses 6D amplitudes as an integral (2.3.5). The measure takes the following form

$$d\mu_n^{6D} = \frac{\prod_{i=1}^n d\sigma_i \, d^2 v_i \, d^2 u_i}{\text{vol}(SL(2,\mathbb{C})_\sigma \times SL(2,\mathbb{C})_u)} \prod_{i=1}^n \delta\left(\langle v_i \, \epsilon_i \rangle - 1\right) \delta^4 \left(\langle v_i \lambda_i^A \rangle - \langle u_i \lambda^A(\sigma_i) \rangle \right) , \qquad (2.3.21)$$

where the $SL(2,\mathbb{C})$ symmetries of world-sheet coordinates σ_i and the coordinates u_i are mod out. The rational functions $\lambda^{Aa}(\sigma)$ are given as

$$\lambda^{Aa}(\sigma) = \sum_{j=1}^{n} \frac{u_j^a \langle \epsilon_j \lambda_j^A \rangle}{\sigma - \sigma_j} \,. \tag{2.3.22}$$

Here λ_j^{Ab} are the 6D helicity spinors, and the delta function constraints in the measure implies the momentum conservation, i.e. $\sum_{i=1}^{n} \langle \lambda_i^A \lambda_i^B \rangle = 0$. It is worth noticing the measure can be recast into a matrix form,

$$d\mu_n^{6D} = \frac{\prod_{i=1}^{n} d\sigma_i \, d^2 v_i \, d^2 u_i}{\mathrm{vol}(SL(2,\mathbb{C})_\sigma \times SL(2,\mathbb{C})_u)} \prod_{i=1}^{n} \delta(\langle v_i \, \epsilon_i \rangle - 1) \delta^4(V \cdot \Omega \cdot \Lambda^A) \,, \tag{2.3.23}$$

where the external helicity spinors are arranged as a $2n$-dimensional vector

$$\Lambda^A := \{\lambda_{1,1}^A, \lambda_{2,1}^A, \ldots, \lambda_{n,1}^A, \lambda_{1,2}^A, \lambda_{2,2}^A, \ldots, \lambda_{n,2}^A\} \,. \tag{2.3.24}$$

and V is a $n \times 2n$ matrix

$$V_{i;j,a} = \begin{cases} v_{i,a} & \text{if} \quad i = j \\ -\frac{\langle u_i u_j \rangle}{\sigma_{ij}} \epsilon_{j,a} & \text{if} \quad i \neq j, \end{cases} \tag{2.3.25}$$

with $\sigma_{ij} := \sigma_i - \sigma_j$, and Ω is the symplectic metric

$$\Omega = \begin{pmatrix} 0 & \mathbb{I}_n \\ -\mathbb{I}_n & 0 \end{pmatrix} \,. \tag{2.3.26}$$

Under the condition $\langle v_i \, \epsilon_i \rangle = 1$, the matrix V obeys the symplectic condition,

$$V \cdot \Omega \cdot V^T = 0 \,. \tag{2.3.27}$$

Similarly, the fermionic part, *i.e.* the integrands, can be written in the matrix form; for example, the half integrand of (1,1) SYM is given by

$$\mathcal{I}^{(1,1)} = \delta^n(V \cdot \Omega \cdot \eta) \, \delta^n(\widetilde{V} \cdot \widetilde{\Omega} \cdot \tilde{\eta}) \det{}' H_n \,, \tag{2.3.28}$$

with $\eta, \tilde{\eta}$ being the Grassmann version of Λ^A,

$$\eta = \{\eta_{1,1}, \eta_{2,1}, \ldots, \eta_{n,1}, \eta_{1,2}, \eta_{2,2}, \ldots, \eta_{n,2}\} \,, \tag{2.3.29}$$

$$\tilde{\eta} = \{\tilde{\eta}_{1,\hat{1}}, \tilde{\eta}_{2,\hat{1}}, \ldots, \tilde{\eta}_{n,\hat{1}}, \tilde{\eta}_{1,\hat{2}}, \tilde{\eta}_{2,\hat{2}}, \ldots, \tilde{\eta}_{n,\hat{2}}\} \,. \tag{2.3.30}$$

The $n \times n$ matrix H_n has the following entries [11]

$$H_{ij} = \frac{\langle \epsilon_i \lambda_i^A \rangle [\tilde{\epsilon}_j \tilde{\lambda}_{A,j}]}{\sigma_{ij}} \quad \text{for} \quad i \neq j \,, \qquad u_{i,a} H_{ii} = -\lambda_a^A(\sigma_i)[\tilde{\epsilon}_i \tilde{\lambda}_{A,i}] \,, \qquad (2.3.31)$$

and the reduced determinant $\det' H$ is defined as

$$\det' H = \frac{\det H_{[kl]}^{[ij]}}{\langle u_i u_j \rangle [\tilde{u}_k \tilde{u}_l]} \,. \qquad (2.3.32)$$

Here we list the integrands that corresponds to specific 6D supersymmetric theories:

6D Theory (Tree)	$\mathcal{I}_L$	$\mathcal{I}_R$
$\mathcal{N}{=}(1,1)$ SYM	$\mathrm{PT}(\alpha)$	$\mathcal{I}^{(1,1)}$
$\mathcal{N}{=}(2,2)$ SUGRA	$\mathcal{I}^{(1,1)}$	$\mathcal{I}^{(1,1)}$
M5	$(\mathrm{Pf}' A_n)^2$	$\mathcal{I}^{(2,0)}$
D5	$(\mathrm{Pf}' A_n)^2$	$\mathcal{I}^{(1,1)}$
$\vdots$	$\vdots$	$\vdots$

In order to compare with the rational map formalism, we can recast (2.3.12) into a Veronese form by integrating out the moduli $\rho_{a,k}^A$ as following [10]

$$d\mu_n^{\mathrm{6D}} = \frac{d^n \sigma d^{3n} W}{\mathrm{vol}\,(SL(2,\mathbb{C})_\sigma \times SL(2,\mathbb{C})_W)} \delta^{4 \times n}(C \cdot \Omega \cdot \Lambda^A) \qquad (2.3.33)$$

where we have introduced n additional 2×2 matrices $(W_i)_a^b$ satisfying $|W_i| = \det W_i = \frac{1}{\prod_{j \neq i} \sigma_{ij}}$, and the matrix C is explicitly given by

$$C_{k,b;i,a} = (W_i)_a^b \, \sigma_i^k \,, \qquad (2.3.34)$$

which also satisfies the symplectic condition:

$$C \cdot \Omega \cdot C^T = 0 \,, \qquad (2.3.35)$$

Therefore C is a symplectic Grassmannian. In [32], it was shown the 6D measure for the polarised scattering equation (2.3.23) and for the rational maps (2.3.12) are equivalent as the following

$$\int d\mu_n^{\mathrm{6D}} = \int \frac{d^n \sigma d^{3n} W}{\mathrm{vol}\,(SL(2,\mathbb{C})_\sigma \times SL(2,\mathbb{C})_W)} \delta^{4 \times n}(C \cdot \Omega \cdot \Lambda^A) \qquad (2.3.36)$$

$$= \int \frac{d^n \sigma d^n v d^{2n} u}{\mathrm{vol}\,(SL(2,\mathbb{C})_\sigma \times SL(2,\mathbb{C})_u)} \delta^{4 \times n}(V \cdot \Omega \cdot \Lambda^A) \,.$$

The two expressions above are related by

$$C_{\mathrm{GL}(n)} \cdot C = V \,, \tag{2.3.37}$$

which is a $\mathrm{GL}(n)$ transformation.

2.4 Loop from tree amplitudes

Having introduced the twistor formulae for 6D tree superamplitudes, we now show the loop 4D amplitudes can be obtained by taking the forward limit as well as dimensional reduction from the 6D tree ones, which are described by the worldsheet formula

$$A_n^{6D} = \int d\mu_n^{6D} \, \mathcal{I}_L \, \mathcal{I}_R \,. \tag{2.4.1}$$

This approach has been applied to loop amplitudes using CHY formalisam [13, 14], or twistor formulae in many theories, *e.g.* one-loop SYM and SUGRA amplitudes [15, 16], as well as two-loop amplitudes [17–19]. The idea is to introduce two extra particles staying in higher dimension (6D in our case) in forward limit (see Fig.2.2), which will serve as loop momentum ℓ,

$$\lambda_{n+1,a}^A = \begin{pmatrix} \lambda_1^\alpha & \lambda_2^\alpha \\ \tilde{\lambda}_1^{\dot\alpha} & \tilde{\lambda}_2^{\dot\alpha} \end{pmatrix}, \quad \lambda_{n+2,a}^A = \begin{pmatrix} \lambda_1^\alpha & -\lambda_2^\alpha \\ \tilde{\lambda}_1^{\dot\alpha} & -\tilde{\lambda}_2^{\dot\alpha} \end{pmatrix}, \tag{2.4.2}$$

while other particles have lower dimensional kinematics (4D in our case):

$$\lambda_{i,a}^A = \begin{pmatrix} 0 & \lambda_i^\alpha \\ \tilde{\lambda}_i^{\dot\alpha} & 0 \end{pmatrix}, \quad \text{for } i = 1, ..., n \,. \tag{2.4.3}$$

With this setting we obtain the one-loop 4D amplitude:

$$
\begin{aligned}
\mathcal{A}_{n,\mathrm{4D}}^{(1)} &= \int \frac{d^4\ell}{\ell^2} \int d^{2\mathcal{N}}\eta_{n+1} d^{2\widetilde{\mathcal{N}}}\tilde\eta_{n+1} \, \mathcal{A}_{n+2,\mathrm{6D}}^{(0)}\big|_{\mathrm{F.L.}} \\
&= \int \frac{d^4\ell}{\ell^2} \int d\mu_{n+2}^{6\mathrm{D}} \, d^{2\mathcal{N}}\eta_{n+1} d^{2\widetilde{\mathcal{N}}}\tilde\eta_{n+1} \, \mathcal{I}_L \mathcal{I}_R \big|_{\mathrm{F.L.}} \,.
\end{aligned}
\tag{2.4.4}
$$

In chapter 4, we will apply this approach (2.4.4) to obtain a one-loop 6-point D3-brane amplitude from an 8-point tree-level M5-brane (or D5-brane) amplitude, which are purely rational terms. The result is further confirmed by generalised unitarity methods. Also, by performing a supersymmetric reduction on the M5-brane tree-level superamplitudes, we obtain one-loop corrections to the non-supersymmetric D3-brane amplitudes, which agree with the known results in the literature [58].
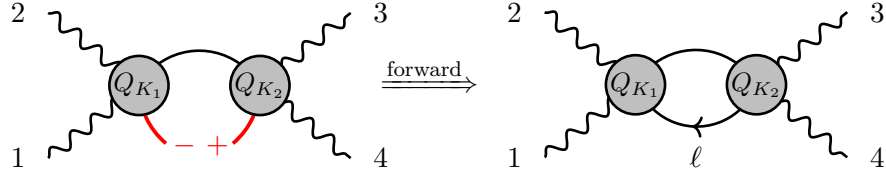
Figure 2.2: The figure shows a 6-point tree amplitude reducing to a 4-point loop amplitude. The curvy lines denote 4D particles, the solid lines denote 6D particles, and the red line are forward limit particles (6D).

2.5 Soft theorems

Soft theorem arising from the spontaneous symmetry breaking states that an amplitude with one (or more) soft Goldstone boson(s) will universally reduce to a lower point one, which is due to the fact that the theory has degenerate vacuum. The vacuums are related to each other by $|\theta\rangle = e^{i\,\theta\cdot T}|0\rangle$, where T^a is the broken generator and θ_a is the vacuum expectation value (vev) of the scalar. The amplitude evaluated at the $|\theta\rangle$ vacuum can be perturbatively expanded as

$$|\theta\rangle = e^{i\,\theta\cdot T}|0\rangle = |0\rangle + \theta_a|\pi^a\rangle + \frac{1}{2}\theta_a\theta_b|\pi^a\pi^b\rangle \cdots, \tag{2.5.1}$$

where $|\pi^a\rangle$ and $|\pi^a\pi^b\rangle$ are vacuums with one and two soft scalar(s), respectively. The amplitude must be the same at either $|0\rangle$ or $|\theta\rangle$ vacuum, that is

$$\langle\theta|n\rangle = \langle 0|n\rangle, \tag{2.5.2}$$

where $|n\rangle$ is an n-particle state with all momenta finite. We plug in the the state $|\theta\rangle$ in (2.5.1) to (2.5.2) and look at each order expansion in θ. The zeroth order expansion of $\langle\theta|n\rangle$ already gives $\langle 0|n\rangle$, which means all higher order expansion in θ must be zero. In the first order expansion, there is only one term, $\langle\pi^a|n\rangle$, which is an (n+1)-point amplitude with one soft scalar. According to our earlier statement, $A_{n+1}(\pi^a, \cdots)$ must vanish, which is known as the "Adler's zero" [59]. The second order expansion has two terms, which means they need to cancel each other. These two terms are given by

$$\langle\pi^a\pi^b|n\rangle + \frac{1}{2}\sum_{i=1}^{n}\frac{p_i\cdot(p_1-p_2)}{p_i\cdot(p_1+p_2)}\langle 0|\pi_1,\pi_2,\cdots,[T^a,T^b]\pi_i,\cdots,\pi_n\rangle, \tag{2.5.3}$$

We conclude that amplitude with two soft scalars, $A_{n+2}(\pi^a, \pi^b\cdots)$, behaves as

$$A_{n+2}(\pi^a,\pi^b,\ldots) \to \frac{1}{2}\sum_{i=1}^{n}\frac{p_i\cdot(p_1-p_2)}{p_i\cdot(p_1+p_2)}f^{abc}H_{i,c}A_n, \tag{2.5.4}$$

where f^{abc} is the structure constant of the relation $[T^a, T^b] = f^{abc} H^c$, which encodes the information of the coset structure G/H. The probing of a theory's global symmetry with the double soft theorem has been applied to the $\mathcal{N} = 8$ SUGRA theory [60], where the 70 scalars are elements in the coset space $E_7/SU(8)$. Similarly, we can study the double limit of type IIB string theory compactified on K3, which has a well studied moduli space described by the coset [61],

$$\mathcal{M}_{(2,0)} = SO(5, 21; \mathbb{Z}) \backslash SO(5, 21)/(SO(5) \times SO(21)). \tag{2.5.5}$$

The discrete group is invisible in the supergravity approximation, so we concern ourselves with the local form of the moduli space of supergravity theory, namely $\frac{SO(5,21)}{SO(5) \times SO(21)}$. It has dimension of 105, which corresponds precisely to the 105 scalars in the 21 tensor multiplets. These scalars are Goldstone bosons of the breaking of $SO(5, 21)$ to $SO(5) \times SO(21)$, which are the R-symmetry and flavor symmetry, respectively. Therefore, the scalars obey soft theorems, which are the tools to explore the structure of the moduli space directly from the S matrix [60].

We find that the amplitudes behave like pion amplitudes with "Adler's zero" in the single soft limit. For $p_1 \to 0$, we find,

$$A_n(\phi_1^{f_1}, 2, \ldots, n) \to \mathcal{O}(p_1), \tag{2.5.6}$$

and the same for other scalars in the tensor multiplets. As we mentioned earlier, The commutator algebra of the coset space may be explored by considering double soft limits for scalars. Begin with the flavor symmetry, we find for $p_1, p_2 \to 0$ simultaneously

$$A_n(\phi_1^{f_1}, \bar{\phi}_2^{f_2}, \ldots) \to \frac{1}{2} \sum_{i=3}^{n} \frac{p_i \cdot (p_1 - p_2)}{p_i \cdot (p_1 + p_2)} R_i^{f_1 f_2} A_{n-2}, \tag{2.5.7}$$

where f_i's are flavor indices, and $R_i^{f_1 f_2}$ is a generator of the unbroken $SO(21)$, which may be viewed as the result of the commutator of two broken generators. $R_i^{f_1 f_2}$ acts on superfields as

$$\begin{aligned} R_i^{f_1 f_2} \Phi_i^{f_2} &= \Phi_i^{f_1}, & R_i^{f_1 f_2} \Phi_i^{f_1} &= -\Phi_i^{f_2}, \\ R_i^{f_1 f_2} \Phi_i^{f_3} &= 0, & R_i^{f_1 f_2} \Phi_{i, \hat{a}\hat{b}} &= 0, \end{aligned} \tag{2.5.8}$$

where $f_3 \neq f_1, f_2$. Therefore, the generator exchanges tensor multiplets of flavor f_1 with ones of f_2, and sends all others and the graviton multiplet to 0.

To study the $SO(5)$ R-symmetry generators we take soft limits of two scalars which

do not form a R-symmetry singlet. For instance

$$A_n(\bar{\phi}_1, \phi_2^{IJ}, \ldots) \to \frac{1}{2} \sum_{i=3}^{n} \frac{p_i \cdot (p_1 - p_2)}{p_i \cdot (p_1 + p_2)} R_i^{IJ} A_{n-2} \,, \tag{2.5.9}$$

with $R_i^{IJ} = \eta_{i,a}^I \eta_i^{J,a}$. Similarly, other choices of soft scalars lead to the remaining R-symmetry generators:

$$R_{i,IJ} = \frac{\partial}{\partial \eta_{i,a}^I} \frac{\partial}{\partial \eta_i^{J,a}}, \quad R_{i,J}^I = \eta_{i,a}^I \frac{\partial}{\partial \eta_{i,a}^J}. \tag{2.5.10}$$

Finally, we consider the cases where soft scalars carry different flavors and do not form an R-symmetry singlet. This leads to new soft theorems:

$$\boxed{A_n(\bar{\phi}_1^{f_1}, \phi_2^{f_2,IJ}, \ldots) \to \sum_{i=3}^{n} \frac{p_1 \cdot p_2}{p_i \cdot (p_1 + p_2)} R_i^{f_1 f_2} R_i^{IJ} A_{n-2}} \tag{2.5.11}$$

and similarly for other R-symmetry generators. The results of the soft limits now take account of both flavor and R-symmetry generators, reflecting the direct product structure in $\frac{SO(5,21)}{SO(5) \times SO(21)}$. This is a new phenomenon that is not present in pure $(2,0)$ supergravity [60, 62].

Having introduced the background materials, we are ready to use them to study many interesting topics of scattering amplitudes and on-sell methods in the following chapter 3, 4, and 5.

Chapter 3

6D Scattering Amplitudes from Rational Maps

3.1 Introduction

To describe scattering amplitudes of supersymmetric theories in higher dimensions, [9, 10] introduced a six-dimensional rational map formalism in the spirit of [8, 56, 63]. Using this formalism, extremely compact formulas were found for tree-level amplitudes of a wide range of interesting theories, including maximally supersymmetric gauge theories and supergravity in diverse dimensions, as well as the world-volume theories of probe D-branes and the M5-brane in flat space. In the case of the M5-brane [9], which contains a chiral tensor field, the formalism circumvents a common difficulty in formulating a covariant action principle due to the self-duality constraint.

In this thesis, we continue to explore the utility of the 6D rational maps and spinor-helicity formalism and present the tree-level S matrix for the theory of 6D $(2,0)$ supergravity. This chiral theory arises as the low-energy limit of Type IIB string theory compactified on a K3 surface [64] and is particularly interesting because it describes the interaction of self-dual tensors and gravitons.

To describe massless scattering in 6D, it is convenient to introduce spinor-helicity variables [50],

$$p_i^{AB} = \lambda_{i,a}^A \lambda_{i,b}^B \epsilon^{ab} := \langle \lambda_i^A \, \lambda_i^B \rangle. \tag{3.1.1}$$

Here, and throughout, $i = 1, \ldots, n$ labels the n particles, $A = 1, 2, 3, 4$ is a spinor index of the $Spin(5,1)$ Lorentz group, and $a = 1, 2$ is a left-handed index of the $SU(2)_L \times SU(2)_R$ massless little group. This is the only non-trivial little-group information that enters for chiral $(2,0)$ supersymmetry–the $(2,0)$ supergravity multiplet and a number of $(2,0)$ tensor multiplets, which contain a chiral tensor. The tensor multiplets transform

as singlets of $SU(2)_R$, whereas the gravity multiplet is a triplet; later we will introduce the doublet index $\hat{a}$ for $SU(2)_R$.

We also introduce a flavor index f_i with $i = 1, \ldots, 21$ to label the 21 tensor multiplets; this is the number that arises in 6D from compactification of the NS and R fields of Type IIB superstring theory on a K3 surface. It is also the unique number for which the gravitational anomalies cancel. The anomaly cancellation has also been studied from the amplitude point of view where one uses four-point amplitudes and unitarity, see [65]. We assume that we are at generic points of the moduli space, where perturbative amplitudes are well-defined. The string-theory moduli space has singularities at fixed points of its $SO(5, 21; \mathbb{Z})$ duality group. At such points one or more tensor multiplets are replaced by non-Lagrangian $(2, 0)$ CFTs, and a perturbative analysis is no longer possible. Therefore, the amplitudes presented in this article are applicable at generic points in the moduli space where we can treat the tensor multiplets as abelian. Interestingly one can explore the moduli space of the theory from the S matrix by studying soft limits [60]. Indeed, we derive new soft theorems from the formula we construct, which describe precisely the moduli space of 6D $(2, 0)$ supergravity: $\frac{SO(5,21)}{SO(5) \times SO(21)}$.

In the rational-map formulation, amplitudes for n particles are expressed as integrals over the moduli space of rational maps from the n-punctured Riemann sphere to the space of spinor-helicity variables. In general, the amplitudes take the following form [9, 10, 55],

$$A_n^{6D} = \int d\mu_n^{6D} \, \mathcal{I}_L \, \mathcal{I}_R \,, \tag{3.1.2}$$

where $d\mu_n^{6D}$ is the measure encoding the 6D kinematics and the product $\mathcal{I}_L \, \mathcal{I}_R$ is the integrand that contains the dynamical information of the theories, including supersymmetry. The measure is given by

$$d\mu_n^{6D} = \frac{\prod_{i=1}^n d\sigma_i \prod_{k=0}^m d^8\rho_k}{\mathrm{vol}\, (SL(2, \mathbb{C})_\sigma \times SL(2, \mathbb{C})_\rho)} \frac{1}{V_n^2} \prod_{i=1}^n E_i^{6D}, \tag{3.1.3}$$

and $n = 2m + 2$ (we will discuss $n = 2m + 1$ later). The coordinates σ_i label the n punctures, and $V_n = \prod_{i<j} \sigma_{ij}$, with $\sigma_{ij} = \sigma_i - \sigma_j$. They are determined up to an overall $SL(2, \mathbb{C})_\sigma$ Möbius group transformation, whose "volume" is divided out in a standard way. The 6D scattering equations are given by

$$E_i^{6D} = \delta^6 \left(p_i^{AB} - \frac{\langle \rho^A(\sigma_i) \, \rho^B(\sigma_i) \rangle}{\prod_{j \neq i} \sigma_{ij}} \right). \tag{3.1.4}$$

These maps are given by degree-m polynomials $\rho_a^A(\sigma) = \sum_{k=0}^m \rho_{a,k}^A \sigma^k$, which are determined up to an overall $SL(2, \mathbb{C})_\rho$ transformation, whose volume is divided out. This

group is a complexification of $SU(2)_L$.

It is straightforward to see that (3.1.4) implies the on-shell conditions $p_i^2 = 0$ and momentum conservation. Furthermore as shown in [9,10], this construction implies that the integrals are completely localized on the $(n-3)!$ solutions, which are equivalent to those of the general dimensional scattering equations [55],

$$\sum_{i \neq j} \frac{p_i \cdot p_j}{\sigma_{ij}} = 0, \quad \text{for all} \quad j. \tag{3.1.5}$$

As we will see shortly that, unlike the general-dimensional scattering equations, the use of the spinor-helicity coordinates and 6D scattering equations allows us to make supersymmetry manifest.

Now consider $n = 2m + 1$, for which we have [10],

$$d\mu_n^{6D} = \frac{\left(\prod_{i=1}^{n} d\sigma_i \prod_{k=0}^{m-1} d^8 \rho_k\right) d^4 \omega \langle \xi d\xi \rangle}{\text{vol}\left(SL(2,\mathbb{C})_\sigma, SL(2,\mathbb{C})_\rho, T\right)} \frac{1}{V_n^2} \prod_{i=1}^{n} E_i^{6D}. \tag{3.1.6}$$

The polynomials $\rho_a^A(\sigma)$ now are given by

$$\rho_a^A(\sigma) = \sum_{k=0}^{m-1} \rho_{a,k}^A \sigma^k + \omega^A \xi_a \sigma^m, \tag{3.1.7}$$

and there is a shift symmetry $T(\alpha)$ acting on ω^A: $\omega^A \to \omega^A + \alpha \langle \xi \rho_{m-1}^A \rangle$, which we also have to mod out.

Here we review the integrand factors for 6D $(2,2)$ supergravity, since they will be relevant. For $(2,2)$ supergravity, we have,

$$\mathcal{I}_L = \text{det}' S_n, \quad \mathcal{I}_R = \Omega_F^{(2,2)}, \tag{3.1.8}$$

where S_n is a $n \times n$ anti-symmetric matrix, with entries: $[S_n]_{ij} = \frac{p_i \cdot p_j}{\sigma_{ij}}$. This matrix has rank $(n-2)$, and the reduced Pfaffian and determinant are defined as

$$\text{Pf}' S_n = \frac{(-1)^{i+j}}{\sigma_{ij}} \text{Pf} S_{ij}^{ij}, \quad \text{det}' S_n = \left(\text{Pf}' S_n\right)^2. \tag{3.1.9}$$

Here S_{ij}^{ij} means that the i-th and j-th rows and columns of S_n are removed, and the result is i, j independent [57]. $\Omega_F^{(2,2)}$ is a fermionic function of Grassmann coordinates $\eta_i^{Ia}, \tilde{\eta}_i^{\hat{I}\hat{a}}$, which we use to package the supermultiplet of on-shell states into a 'superfield',

$$\Phi^{(2,2)}(\eta, \tilde{\eta}) = \phi' + \cdots + \eta_a^I \eta_{I,b} B^{ab} + \tilde{\eta}^{\hat{I},\hat{a}} \tilde{\eta}_{\hat{I}}^{\hat{b}} B_{\hat{a}\hat{b}} \tag{3.1.10}$$
$$+ \cdots + \eta_a^I \eta_{I,b} \tilde{\eta}_{\hat{a}}^{\hat{I}} \tilde{\eta}_{\hat{I},\hat{b}} G^{ab\hat{a}\hat{b}} + \cdots + (\eta)^4 (\tilde{\eta})^4 \bar{\phi}',$$

where B^{ab} and $B_{\hat{a}\hat{b}}$ are self-dual and anti self-dual two forms, and $G^{ab\hat{a}\hat{b}}$ is the graviton. Here $I, \hat{I} = 1, 2$ are the R-symmetry indices corresponding to a $SU(2) \times SU(2)$ subgroup of the full $USp(4) \times USp(4)$ R-symmetry. The fermionic function $\Omega_F^{(2,2)}$ imposes the conservation of supercharge, which may be viewed as a double copy: $\Omega_F^{(2,2)} = \Omega_F^{(2,0)} \Omega_F^{(0,2)}$, and $\Omega_F^{(2,0)}$ is given by

$$\Omega_F^{(2,0)} = V_n \prod_{k=0}^{m} \delta^4 \left(\sum_{i=1}^{n} C_{a,k;i,b}\, \eta_i^{Ib} \right). \tag{3.1.11}$$

The $n \times 2n$ matrices $C_{a,k;i,b} = (W_i)_a^b \sigma_i^k$ and $(W_i)_a^b$ can be expressed in terms of $\rho_a^A(\sigma_i)$ via

$$p_i^{AB} W_{i,b}^a = \frac{\rho^{[A,a}(\sigma_i)\, \lambda_{i,b}^{B]}}{\prod_{j \neq i} \sigma_{ij}}, \tag{3.1.12}$$

which is independent of A, B, and satisfies $\det W_i = \prod_{j \neq i} \sigma_{ij}^{-1}$. The matrix $C_{a,k;i,b}$ is a symplectic Grassmannian which was used in [10] as an alternative way to impose the 6D scattering equations in a Veronese form. $\Omega_F^{(0,2)}$ is the conjugate of $\Omega_F^{(2,0)}$, and the definition is identical, with the understanding that we use the right-handed variables, such as $\tilde{\eta}_{\hat{a}}^{\hat{I}}, \tilde{\lambda}_{\hat{A}\hat{a}}, \tilde{\rho}_{\hat{A}\hat{a}}, \tilde{\xi}_{\hat{a}}, (\tilde{W}_i)_{\hat{a}}^{\hat{b}}$, etc. Explicitly, we have

$$\Omega_F^{(0,2)} = V_n \prod_{k=0}^{m} \delta^4 \left(\sum_{i=1}^{n} \tilde{C}_{\hat{a},k;i,\hat{b}}\, \tilde{\eta}_i^{\hat{I}\hat{b}} \right), \tag{3.1.13}$$

where $\tilde{C}_{\hat{a},k;i,\hat{b}} = (\tilde{W}_i)_{\hat{a}}^{\hat{b}} \sigma_i^k$ and $\tilde{W}_{i,b}^a$ can be expressed in term of

$$p_{i,AB} \tilde{W}_{i,\hat{b}}^{\hat{a}} = \frac{\tilde{\rho}_{[A}^{\hat{a}}(\sigma_i)\, \tilde{\lambda}_{B],i,\hat{b}}}{\prod_{j \neq i} \sigma_{ij}}, \tag{3.1.14}$$

with the condition $\det \tilde{W}_i = \prod_{j \neq i} \sigma_{ij}^{-1}$ and the maps are given by $\tilde{\rho}_a^{\hat{A}}(\sigma) = \sum_{k=0}^{m} \tilde{\rho}_{\hat{a},k}^A \sigma^k$ that satisfy that following equation

$$p_{i,AB} - \frac{[\tilde{\rho}_A(\sigma_i)\, \tilde{\rho}_B(\sigma_i)]}{\prod_{j \neq i} \sigma_{ij}} = 0. \tag{3.1.15}$$

For $n = 2m + 1$, the integrands take a slightly different form. For the fermionic part, we have

$$\begin{aligned}\Omega_F^{(2,0)} &= V_n \prod_{k=0}^{m-1} \delta^4 \left(\sum_{i=1}^{n} C_{a,k;i,b}\, \eta_i^{Ib} \right) \\ &\quad \times \delta^2 \left(\sum_{i=1}^{n} \xi^a C_{a,m;i,b}\, \eta_i^{Ib} \right).\end{aligned} \tag{3.1.16}$$

whereas the $n \times n$ matrix S_n is modified to an $(n+1) \times (n+1)$ matrix, which we

denote $\hat{S}$. $\hat{S}_n$ is defined in the same way as S_n, but with $i, j = 1, \ldots, n, \star$. Here $\sigma_\star$ is a reference puncture, and $p_\star$ is given by

$$p_\star^{AB} = \frac{2\, q^{[A} p^{B]C}(\sigma_\star)\tilde{q}_C}{q^D[\tilde{\rho}_D(\sigma_\star)\,\tilde{\xi}]\langle\rho^E(\sigma_\star)\,\xi\rangle\tilde{q}_E}, \tag{3.1.17}$$

where q and $\tilde{q}$ are arbitrary spinors.

3.2 6D $(2,0)$ Supergravity

The 6D $(2,0)$ supergravity theory contains 21 tensor multiplets and the graviton multiplet. The superfield of the tensor multiplet is a singlet of the little group,

$$\Phi(\eta) = \phi + \cdots + \eta_a^I \eta_{I,b} B^{ab} + \cdots + (\eta)^4 \bar{\phi}, \tag{3.2.1}$$

where $a, b = 1, 2$ are the $SU(2)_L$ little-group indices. The graviton multiplet transforms as a $(\mathbf{1}, \mathbf{3})$ of the little group, so the superfield carries explicit $SU(2)_R$ indices,

$$\Phi_{\hat{a}\hat{b}}(\eta) = B_{\hat{a}\hat{b}} + \ldots + \eta_a^I \eta_{I,b} G_{\hat{a}\hat{b}}^{ab} + \ldots + (\eta)^4 \bar{B}_{\hat{a}\hat{b}}, \tag{3.2.2}$$

and $\Phi_{\hat{a}\hat{b}}(\eta) = \Phi_{\hat{b}\hat{a}}(\eta)$. We see that both the tensor multiplet and graviton multiplet can be obtained from the 6D $(2,2)$ superfield in $(3.1.10)$ via SUSY reductions [66][*],

$$\begin{aligned}
\Phi(\eta) &= \int d\tilde{\eta}_{\hat{a}}^{\hat{I}} d\tilde{\eta}_{\hat{I}}^{\hat{a}}\, \Phi^{(2,2)}(\eta, \tilde{\eta})\big|_{\tilde{\eta}\to 0}\,, \\
\Phi_{\hat{a}\hat{b}}(\eta) &= \int d\tilde{\eta}_{\hat{a}}^{\hat{I}} d\tilde{\eta}_{\hat{I}\hat{b}}\, \Phi^{(2,2)}(\eta, \tilde{\eta})\big|_{\tilde{\eta}\to 0}\,.
\end{aligned} \tag{3.2.3}$$

These integrals have the effect of projecting onto the right-handed $USp(4)$ R-symmetry singlet sector, which reduces $(2,2) \to (2,0)$. Using the reduction, the amplitudes of $(2,0)$ supergravity with n_1 supergravity multiplets and n_2 tensor multiplets of the same flavor $(n_1 + n_2 = n)$ can be obtained from the $(2,2)$ supergravity amplitude via

$$A_{n_1,n_2}^{(2,0)} = \int \prod_{i\in n_1} d\tilde{\eta}_{i,\hat{a}_i}^{\hat{I}} d\tilde{\eta}_{i,\hat{I}\hat{b}_i} \prod_{j\in n_2} d\tilde{\eta}_{j,\hat{a}_j}^{\hat{J}} d\tilde{\eta}_{j,\hat{J}}^{\hat{a}_j} A_n^{(2,2)}(\eta, \tilde{\eta}).$$

Note $A_n^{(2,2)}(\eta, \tilde{\eta}) \sim \eta^{2n}\tilde{\eta}^{2n}$, so the integration removes all $\tilde{\eta}$'s. The fermionic integral can be performed using $(3.1.8)$, and $(3.1.11)$ (or $(3.1.16)$ for odd n), and we obtain

$$A_{n_1,n_2}^{(2,0)} = \int d\mu_n^{6\text{D}} \tilde{M}_{\hat{a}\hat{b},n_1 n_2}\, V_n \det{}' S_n\, \Omega_F^{(2,0)}, \tag{3.2.4}$$

---

[*]For the superfield of the tensor, $\Phi(\eta)$, one may choose different I, J; however, only the case of $I = 1, J = 2$ leads to non-vanishing results when we integrate away $\tilde{\eta}$'s from the amplitudes of $(2,2)$ supergravity.

where $\tilde{M}_{\hat{a}\hat{b},n_1n_2}$, which we will define shortly, is obtained by integrating out $\Omega_F^{(0,2)}$.

We begin with n even, as the odd-n case works in a similar fashion. Introducing the $n \times n$ matrix

$$\tilde{M}_{\hat{a}_1\cdots\hat{a}_n} = \begin{pmatrix} \tilde{C}_{\hat{1},0;1,\hat{a}_1} & \tilde{C}_{\hat{1},0;2,\hat{a}_2} & \cdots & \tilde{C}_{\hat{1},0;n,\hat{a}_n} \\ \vdots & \vdots & \cdots & \vdots \\ \tilde{C}_{\hat{1},m;1,\hat{a}_1} & \tilde{C}_{\hat{1},m;2,\hat{a}_2} & \cdots & \tilde{C}_{\hat{1},m;n,\hat{a}_n} \\ \tilde{C}_{\hat{2},0;1,\hat{a}_1} & \tilde{C}_{\hat{2},0;2,\hat{a}_2} & \cdots & \tilde{C}_{\hat{2},0;n,\hat{a}_n} \\ \vdots & \vdots & \cdots & \vdots \\ \tilde{C}_{\hat{2},m;1,\hat{a}_1} & \tilde{C}_{\hat{2},m;2,\hat{a}_2} & \cdots & \tilde{C}_{\hat{2},m;n,\hat{a}_n} \end{pmatrix}, \tag{3.2.5}$$

then $\tilde{M}_{\hat{a}\hat{b},n_1n_2}$ is given by

$$\tilde{M}_{\hat{a}\hat{b},n_1n_2} = \det \tilde{M}_{\hat{a}_1\cdots\hat{a}_n} \det \tilde{M}_{\hat{b}_1\cdots\hat{b}_n}. \tag{3.2.6}$$

Note that here $\hat{a}$ and $\hat{b}$ denote sets of indices. The indices $\hat{a}_i, \hat{b}_i$ are contracted if $i \in n_2$, whereas for $j \in n_1$ we symmetrize $\hat{a}_j, \hat{b}_j$. This corresponds to constructing little-group singlets for tensor multiplets and triplets for graviton multiplets. After the contraction and symmetrization, the result of (3.2.6) simplifies drastically [*]

$$\tilde{M}_{\hat{a}\hat{b},n_1n_2} \to \frac{\mathrm{Pf}X_{n_2}}{V_{n_2}} \tilde{M}_{\hat{a}\hat{b},n_10}, \tag{3.2.7}$$

where X_{n_2} is a $n_2 \times n_2$ anti-symmetric matrix given by

$$[X_{n_2}]_{ij} = \begin{cases} \frac{1}{\sigma_{ij}} & \text{if} \quad i \neq j \\ 0 & \text{if} \quad i = j, \end{cases} \tag{3.2.8}$$

and $\tilde{M}_{\hat{a}\hat{b},n_10}$ contains only the graviton multiplets. Let's remark that the simplification (3.2.7) (especially the appearance of $\mathrm{Pf}X_{n_2}$) will be crucial for the generalization to amplitudes with multiple tensor flavors which is more interesting and relevant for type IIB on K3.

At this point in the analysis, we have obtained the tree-level amplitudes of 6D $(2,0)$ supergravity with a single flavor of tensor multiplets:

$$A_{n_1,n_2}^{(2,0)} = \int d\mu_n^{6\mathrm{D}} \frac{\mathrm{Pf}X_{n_2}}{V_{n_2}} \tilde{M}_{\hat{a}\hat{b},n_10} V_n \det' S_n \, \Omega_F^{(2,0)}. \tag{3.2.9}$$

The factor $\mathrm{Pf}X_{n_2}$ requires the non-vanishing amplitudes to contain an even number n_2

---

[*]The identity may be understood by studying the zeros and singularities on both sides of the equation (3.2.7), we have also checked it explicitly up to $n = 12$.

of tensor multiplets, as expected. For odd n, the matrix $\tilde{M}_{\hat{a}_1\cdots\hat{a}_n}$ is given by

$$\tilde{M}_{\hat{a}_1\cdots\hat{a}_n} = \begin{pmatrix} \tilde{\xi}^{\hat{b}}\tilde{C}_{\hat{b},m;1,\hat{a}_1} & \tilde{\xi}^{\hat{b}}\tilde{C}_{\hat{b},m;2,\hat{a}_2} & \cdots & \tilde{\xi}^{\hat{b}}\tilde{C}_{\hat{b},m;n,\hat{a}_n} \\ \tilde{C}_{\hat{1},0;1,\hat{a}_1} & \tilde{C}_{\hat{1},0;2,\hat{a}_2} & \cdots & \tilde{C}_{\hat{1},0;n,\hat{a}_n} \\ \vdots & \vdots & \cdots & \vdots \\ \tilde{C}_{\hat{1},m-1;1,\hat{a}_1} & \tilde{C}_{\hat{1},m-1;2,\hat{a}_2} & \cdots & \tilde{C}_{\hat{1},m-1;n,\hat{a}_n} \\ \tilde{C}_{\hat{2},0;1,\hat{a}_1} & \tilde{C}_{\hat{2},0;2,\hat{a}_2} & \cdots & \tilde{C}_{\hat{2},0;n,\hat{a}_n} \\ \vdots & \vdots & \cdots & \vdots \\ \tilde{C}_{\hat{2},m-1;1,\hat{a}_1} & \tilde{C}_{\hat{2},m-1;2,\hat{a}_2} & \cdots & \tilde{C}_{\hat{2},m-1;n,\hat{a}_n}, \end{pmatrix}$$

recall $\tilde{\xi}^{\hat{b}}$ is the right-hand version of ξ^b in (3.1.7). Then the amplitudes take the same form

$$A^{(2,0)}_{n_1,n_2} = \int d\mu_n^{6D} \frac{\mathrm{Pf}X_{n_2}}{V_{n_2}} \tilde{M}_{\hat{a}\hat{b},n_10} V_n \det' \hat{S}_n \, \Omega_F^{(2,0)}. \tag{3.2.10}$$

3.2.1   Multi-flavor tensor multiplets

As we have emphasized, the identity (3.2.7) is crucial for the generalization to multiple tensor flavors, which is required for the 6D $(2,0)$ supergravity. Indeed, the formula takes a form similar to that of a Einstein-Maxwell theory worked out by Cachazo, He and Yuan [57], especially the object $\mathrm{Pf}X_{n_2}$. In that case, in passing from single-$U(1)$ photons to multiple-$U(1)$ ones, one simply replaced the matrix X_n by $\mathcal{X}_n$ [57],

$$[\mathcal{X}_n]_{ij} = \begin{cases} \frac{\delta_{f_i f_j}}{\sigma_{ij}} & \text{if} \quad i \neq j \\ 0 & \text{if} \quad i = j \end{cases} \tag{3.2.11}$$

which allows the introduction of multiple distinct flavors: namely, f_i, f_j are flavor indices, and $\delta_{f_i f_j} = 1$ if particles i, j are of the same flavor, otherwise $\delta_{f_i f_j} = 0$. Inspired by this result, we are led to a proposal for the complete tree-level S matrix of 6D $(2,0)$ supergravity with multiple flavors of tensor multiplets:

$$\boxed{A^{(2,0)}_{n_1,n_2} = \int d\mu_n^{6D} \frac{\mathrm{Pf}\mathcal{X}_{n_2}}{V_{n_2}} \tilde{M}_{\hat{a}\hat{b},n_10} V_n \det' S_n \, \Omega_F^{(2,0)}.} \tag{3.2.12}$$

Again, the 6D scattering equations and integrands take different forms depending on whether n is even or odd. [*] . Since n_2 is necessarily even, this is equivalent to distinguishing whether n_1 is even or odd.

Equation (3.2.12) is our main result, which is a localized integral formula that de-

---

[*]It should be emphasized that the artificial difference between the formulas of even- and odd-point amplitudes is due to the peculiar property of 6D scattering equations in the rational map form, not specific to the chiral $(2,0)$ supergravity we consider in this thesis.

scribes all tree-level superamplitudes of abelian tensor multiplets (with multiple flavors) coupled to gravity multiplets. We can verify that it has all the correct properties. For instance, due to the fact that all the building blocks of the formula come from either 6D $(2,2)$ supergravity or Einstein-Maxwell theory, they all behave properly in the factorization limits, and transform correctly under the symmetries: $SL(2,\mathbb{C})_\sigma$, $SL(2,\mathbb{C})_\rho$, etc. Also, as we will show later, when reduced to 4D the proposed formula produces (supersymmetric) Einstein-Maxwell amplitudes, which is another consistency check. Finally, it is straightforward to check that the formula gives correct low-point amplitudes, e.g. [67]

$$
\begin{aligned}
A_{0,4}^{(2,0)} &= \delta^8(Q)\left(\frac{\delta^{f_1f_2}\delta^{f_3f_4}}{s_{12}} + \frac{\delta^{f_1f_3}\delta^{f_2f_4}}{s_{13}} + \frac{\delta^{f_2f_3}\delta^{f_1f_4}}{s_{23}}\right), \\
A_{2,2}^{(2,0)} &= \delta^{f_1f_2}\frac{\delta^8(Q)[1_{\hat{a}_1}2_{\hat{a}_2}3_{\hat{a}_3}4_{\hat{a}_4}][1^{\hat{a}_1}2^{\hat{a}_2}3_{\hat{b}_3}4_{\hat{b}_4}]}{s_{12}\,s_{23}\,s_{31}} + \text{sym}\,.
\end{aligned}
$$

$$(3.2.13)$$

We symmetrize $\hat{a}_3,\hat{b}_3$ and $\hat{a}_4,\hat{b}_4$ for the graviton multiplets, and $[1_{\hat{a}_1}2_{\hat{a}_2}3_{\hat{a}_3}4_{\hat{a}_4}] = \epsilon_{ABCD}\tilde{\lambda}_{1\hat{a}_1}^A\tilde{\lambda}_{2\hat{a}_2}^B\tilde{\lambda}_{3\hat{a}_3}^C\tilde{\lambda}_{4\hat{a}_4}^D$, and $\delta^8(Q) = \delta^8(\sum_{i=1}^4 \lambda_{i,a}^A\eta_i^{Ia})$.

3.3   The K3 Moduli Space from Soft Limits

Type IIB string theory compactified on K3 has a well studied moduli space described by the coset [61],

$$\mathcal{M}_{(2,0)} = SO(5,21;\mathbb{Z})\backslash SO(5,21)/(SO(5)\times SO(21)). \qquad (3.3.1)$$

The discrete group is invisible in the supergravity approximation, so we concern ourselves with the local form of the moduli space of supergravity theory, namely $\frac{SO(5,21)}{SO(5)\times SO(21)}$. It has dimension of 105, which corresponds precisely to the 105 scalars in the 21 tensor multiplets. These scalars are Goldstone bosons of the breaking of $SO(5,21)$ to $SO(5)\times SO(21)$, which are the R-symmetry and flavor symmetry, respectively. Therefore, the scalars obey soft theorems, which are the tools to explore the structure of the moduli space directly from the S matrix [60].

We find that the amplitudes behave like pion amplitudes with "Adler's zero" [59] in the single soft limit. Indeed for $p_1 \to 0$, we find,

$$A_n(\phi_1^{f_1}, 2, \ldots, n) \to \mathcal{O}(p_1)\,, \qquad (3.3.2)$$

and the same for other scalars in the tensor multiplets. The commutator algebra of the coset space may be explored by considering double-soft limits for scalars. Begin with

the flavor symmetry, we find for $p_1, p_2 \to 0$ simultaneously

$$A_n(\phi_1^{f_1}, \bar{\phi}_2^{f_2}, \ldots) \to \frac{1}{2} \sum_{i=3}^{n} \frac{p_i \cdot (p_1 - p_2)}{p_i \cdot (p_1 + p_2)} R_i^{f_1 f_2} A_{n-2} , \qquad (3.3.3)$$

where f_i's are flavor indices, and $R_i^{f_1 f_2}$ is a generator of the unbroken $SO(21)$, which may be viewed as the result of the commutator of two broken generators. $R_i^{f_1 f_2}$ acts on superfields as

$$\begin{aligned} R_i^{f_1 f_2} \Phi_i^{f_2} &= \Phi_i^{f_1}, \quad R_i^{f_1 f_2} \Phi_i^{f_1} = -\Phi_i^{f_2}, \\ R_i^{f_1 f_2} \Phi_i^{f_3} &= 0, \quad R_i^{f_1 f_2} \Phi_{i,\hat{a}\hat{b}} = 0, \end{aligned} \qquad (3.3.4)$$

where $f_3 \neq f_1, f_2$. Therefore, the generator exchanges tensor multiplets of flavor f_1 with ones of f_2, and sends all others and the graviton multiplet to 0.

To study the $SO(5)$ R-symmetry generators we take soft limits of two scalars which do not form a R-symmetry singlet. For instance

$$A_n(\bar{\phi}_1, \phi_2^{IJ}, \ldots) \to \frac{1}{2} \sum_{i=3}^{n} \frac{p_i \cdot (p_1 - p_2)}{p_i \cdot (p_1 + p_2)} R_i^{IJ} A_{n-2} , \qquad (3.3.5)$$

with $R_i^{IJ} = \eta_{i,a}^I \eta_i^{J,a}$. Similarly, other choices of soft scalars lead to the remaining R-symmetry generators:

$$R_{i,IJ} = \frac{\partial}{\partial \eta_{i,a}^I} \frac{\partial}{\partial \eta_i^{J,a}}, \quad R_{i,J}^I = \eta_{i,a}^I \frac{\partial}{\partial \eta_{i,a}^J} . \qquad (3.3.6)$$

Finally, we consider the cases where soft scalars carry different flavors and do not form an R-symmetry singlet. This actually leads to new soft theorems:

$$\boxed{A_n(\bar{\phi}_1^{f_1}, \phi_2^{f_2,IJ}, \ldots) \to \sum_{i=3}^{n} \frac{p_1 \cdot p_2}{p_i \cdot (p_1 + p_2)} R_i^{f_1 f_2} R_i^{IJ} A_{n-2}} \qquad (3.3.7)$$

and similarly for other R-symmetry generators. The results of the soft limits now contain both flavor and R-symmetry generators, reflecting the direct product structure in $\frac{SO(5,21)}{SO(5) \times SO(21)}$. This is a new phenomenon that is not present in pure $(2,0)$ supergravity [60, 62].

The above soft theorems may be obtained by analyzing how the integrand and the scattering equations behave in the limits. For instance, the vanishing of the amplitudes in the single-soft limits is due to

$$\int d\mu_n^{6D} \sim \mathcal{O}(p_1^{-1}), \quad \det'S_n \sim \mathcal{O}(p_1^2), \qquad (3.3.8)$$

and the rest remains finite. The double-soft theorems require more careful analysis along the lines of, e.g. [68]. The structures of double-soft theorems, however, are already indicated by knowing the four-point amplitudes given in (5.4.23), since important contributions are diagrams with a four-point amplitude on one side such that the propagator becomes singular in the limit. Note that when we study of the moduli space, the scalars we choose do not form a singlet, therefore the most singular diagrams with a three-point amplitude on one side are not allowed. If instead the two scalars do form a singlet, then such diagrams dominate and contain a propagating soft graviton. The soft theorem for such a pair of scalars is simply given by Weinberg's soft graviton theorem attached with the three-point amplitude, which we have also checked using our formula. Finally, we have also checked the soft theorems explicitly using our formula (3.2.12) to numerically compute the *left-hand side* of Eq.(3.3.7), and match to the known analytic expression of the *right-hand side* for various examples. We present one example of six-point amplitude in the double-soft limit in the following subsection.

3.3.1 An explicit example: A_6 double-soft limit

Let us consider the double-soft limit of the following six-point amplitude, which is numerically computed by (3.2.12) under double-soft kinematics ($p_1, p_2 \to 0$):

$$A_6(\bar{\phi}_1^{f_1}, \phi_2^{f_2,11}, \phi_3^{f_2,22}, \phi_4^{f_1}, \bar{\phi}_5^{f_1}, \phi_6^{f_1}), \tag{3.3.9}$$

where $\phi_2^{f,11}$ and $\phi_2^{f,22}$ are conjugate of each other, and we choose leg-2 and leg-3 to be in flavor f_1 and others in flavor f_2. Under the double-soft limit, according to (3.3.7), it should reduce to the form:

$$\int d^2\eta_{3,2} d^4\eta_5 \sum_{i=3}^{6} \frac{p_1 \cdot p_2}{p_i \cdot (p_1 + p_2)} R_i^{f_1 f_2} R_i^{11} A_4(\Phi_3^{f_2}, \Phi_4^{f_1}, \Phi_5^{f_1}, \Phi_6^{f_1}). \tag{3.3.10}$$

where $d^2\eta_{3,2} = d\eta_{3,2}^a d\eta_{3,2,a}$ and $d^4\eta_5 = d\eta_{5,1}^1 d\eta_{5,1}^2 d\eta_{5,2}^1 d\eta_{5,2}^2$. Now we explicitly act $R_i^{f_1 f_2}$ and $R_i^{11} = \eta_{i,a}^1 \eta_i^{1,a}$ on each superfield and then extract the four-point amplitude, which is given by

$$\frac{p_1 \cdot p_2}{p_3 \cdot (p_1 + p_2)} A_4(\bar{\phi}_3^{f_1}, \phi_4^{f_1}, \bar{\phi}_5^{f_1}, \phi_6^{f_1}) - \frac{p_1 \cdot p_2}{p_4 \cdot (p_1 + p_2)} A_4(\phi_3^{f_2,22}, \phi_4^{f_2,11}, \bar{\phi}_5^{f_1}, \phi_6^{f_1})$$

$$- \frac{p_1 \cdot p_2}{p_5 \cdot (p_1 + p_2)} \times 0 - \frac{p_1 \cdot p_2}{p_6 \cdot (p_1 + p_2)} A_4(\phi_3^{f_2,22}, \phi_4^{f_1}, \bar{\phi}_5^{f_1}, \phi_6^{f_2,11}). \tag{3.3.11}$$

Here we have seen the effect of flavor rotation and $SO(5)$ scalar rotation. For example, leg-3 of the first term in the above expression $\phi_3^{f_2,22}$ becomes $\bar{\phi}_3^{f_1}$ due to $R_3^{f_1 f_2}$ and R_3^{11}. And the minus signs in some terms are due to the flavor rotation from f_1 to f_2. We can further extract the four-point component amplitudes according to (5.4.23)

while carefully select the channels according to the flavor configuration after the flavor rotation. Then we obtain

$$\frac{p_1 \cdot p_2}{p_3 \cdot (p_1 + p_2)} s_{35}^2 \left(\frac{1}{s_{45}} + \frac{1}{s_{46}} + \frac{1}{s_{56}} \right) - \frac{p_1 \cdot p_2}{p_4 \cdot (p_1 + p_2)} s_{35} s_{45} \frac{1}{s_{56}} - \frac{p_1 \cdot p_2}{p_6 \cdot (p_1 + p_2)} s_{35} s_{56} \frac{1}{s_{45}} .$$
(3.3.12)

We have numerically checked the double-soft limit of the chosen six-point amplitude agrees with the above expression.

3.4 4D $\mathcal{N} = 4$ Einstein-Maxwell Theory

One can dimensionally reduce 6D $(2,0)$ supergravity to obtain 4D $\mathcal{N} = 4$ Einstein-Maxwell theory. The tree-level amplitudes of this theory capture the leading low-energy behavior of Type IIB (or Type IIA) superstring theory on K3 $\times T^2$.

The reduction to 4D can be obtained by decomposing the 6D spinor as $A \to \alpha = 1, 2$, $\dot{\alpha} = 3, 4$. The compact momenta are $P_i^{\alpha\beta} = P_i^{\dot{\alpha}\dot{\beta}} = 0$; this is implemented by $\lambda_a^A \to \lambda_+^\alpha = 0$ and $\lambda_-^{\dot{\alpha}} = 0$.

The 6D tensor superfield becomes an $\mathcal{N} = 4$ vector multiplet in 4D, in a non-chiral form [9, 69],

$$\Phi(\eta_a) \to V_{\mathcal{N}=4}(\eta_+, \eta_-) = \phi + \eta_-^{\hat{I}} \psi_{\hat{I}}^- + \dots$$
$$+ (\eta_+)^2 A^+ + (\eta_-)^2 A^- + \dots + (\eta_+)^2 (\eta_-)^2 \bar{\phi}.$$
(3.4.1)

Dimensional reduction of $\Phi^{\hat{a}\hat{b}}(\eta)$ is analogous. It separates into 3 cases, where $\Phi^{\hat{+}\hat{-}} \to V_{\mathcal{N}=4}(\eta_+, \eta_-)$, and $\Phi^{\hat{+}\hat{+}}$, $\Phi^{\hat{-}\hat{-}}$ become a pair of positive and negative-helicity graviton multiplets

$$\Phi^{\hat{+}\hat{+}}(\eta_a) \to \mathcal{G}_{\mathcal{N}=4}^+(\eta_+, \eta_-) = A^+ + \eta_-^{\hat{I}} \psi_{\hat{I}}^{-+} + \dots$$
$$+ (\eta_+)^2 G^{++} + (\eta_-)^2 \phi + \dots + (\eta_+)^2 (\eta_-)^2 \bar{A}^+ ,$$
(3.4.2)
$$\Phi^{\hat{-}\hat{-}}(\eta_a) \to \mathcal{G}_{\mathcal{N}=4}^-(\eta_+, \eta_-) = \bar{A}^- + \eta_-^{\hat{I}} \Psi_{\hat{I}}^{--} + \dots$$
$$+ (\eta_-)^2 G^{--} + (\eta_+)^2 \bar{\phi} + \dots + (\eta_+)^2 (\eta_-)^2 A^- .$$
(3.4.3)

We see the on-shell spectrum of the 4D supergravity theory consists of the $\mathcal{G}^+$ and $\mathcal{G}^-$ superfields coupled to 22 $\mathcal{N} = 4$ Maxwell multiplets.

We are now ready to perform the dimensional reduction on (3.2.12). As discussed in [10], the reduction to 4D kinematics may be subtle in this formalism that only the middle sector of even n (or next to the middle sector of odd n) is straightforward. The strategy we adapt here is that once we obtain the formula for the middle (or next to the middle) sector, we then generalize them for other sectors, which is straightforward.

First, the 6D measure reduces to

$$d\mu^{\text{4D}} = \frac{\prod_{i=1}^{n} d\sigma_i \prod_{k=0}^{d} d^2\rho_k \prod_{k=0}^{\tilde{d}} d^2\tilde{\rho}_k}{\text{vol}\left(SL(2,\mathbb{C})_\sigma \times \text{GL}(1,\mathbb{C})\right)} \frac{1}{R(\rho)R(\tilde{\rho})} \prod_{i=1}^{n} E_i^{\text{4D}}$$

where $R(\rho)$, $R(\tilde{\rho})$ are the resultants of the polynomials

$$\rho^\alpha(\sigma) = \sum_{k=0}^{d} \rho_k^\alpha \, \sigma^k, \quad \tilde{\rho}^{\dot{\alpha}}(\sigma) = \sum_{k=0}^{\tilde{d}} \tilde{\rho}_k^{\dot{\alpha}} \, \sigma^k, \tag{3.4.4}$$

with $d + \tilde{d} = n - 2$, and the 4D scattering equations are given by

$$E_i^{\text{4D}} = \delta^4\left(p_i^{\alpha\dot{\alpha}} - \frac{\rho^\alpha(\sigma_i)\tilde{\rho}^{\dot{\alpha}}(\sigma_i)}{\prod_{j\neq i} \sigma_{ij}}\right). \tag{3.4.5}$$

The 2×2 matrix $(\tilde{W}_i)_{ab}$ reduces to

$$(\tilde{W}_i)_{\hat{+}\hat{+}} = (\tilde{W}_i)_{\hat{-}\hat{-}} = 0, \quad (\tilde{W}_i)_{\hat{+}\hat{-}} = t_i, \quad (\tilde{W}_i)_{\hat{-}\hat{+}} = \tilde{t}_i. \tag{3.4.6}$$

with $t_i = \frac{\lambda_i^\alpha}{\rho^\alpha(\sigma_i)}$, $\tilde{t}_i = \frac{\tilde{\lambda}_i^{\dot{\alpha}}}{\tilde{\rho}^{\dot{\alpha}}(\sigma_i)}$ (independent of $\alpha, \dot{\alpha}$), and $t_i\tilde{t}_i = \prod_{j\neq i} \frac{1}{\sigma_{ij}}$. As for the integrand, the parts that reduce to 4D non-trivially are

$$\tilde{M}_{\hat{a}\hat{b}}^{n_1} \to \tilde{T}_{\hat{a}\hat{b}}^{n_1}, \quad \det' S_n \to R^2(\rho)R^2(\tilde{\rho})V_n^{-2}. \tag{3.4.7}$$

Assume we have m_1 $\mathcal{G}^+$ superparticles and m_2 $\mathcal{G}^-$, with $m_1 + m_2 = n_1$ [*], we find $\tilde{T}^{n_1}$ is given by

$$\tilde{T}^{n_1} = T_+^{m_1} \, T_-^{m_2} = \left(V_{m_1}^2 \prod_{i\in m_1} t_i^2\right)\left(V_{m_2}^2 \prod_{j\in m_2} \tilde{t}_j^2\right), \tag{3.4.8}$$

where $V_{m_1} = \prod_{i<j} \sigma_{ij}$ for $i, j \in m_1$, and similarly for V_{m_2}. We therefore obtain a general formula for the amplitudes of 4D $\mathcal{N} = 4$ Einstein-Maxwell theory:

$$A_n^{\mathcal{N}=4} = \int d\mu^{\text{4D}} \frac{\text{Pf}\mathcal{X}_{n_2}}{V_{n_2}V_n} T_+^{m_1} T_-^{m_2} R^2(\rho)R^2(\tilde{\rho}) \, \Omega_F^{\mathcal{N}=4}, \tag{3.4.9}$$

where $\Omega_F^{\mathcal{N}=4}$ implements the 4D $\mathcal{N} = 4$ supersymmetry, arising as the reduction of

---

[*]We do not consider $\Phi^{\hat{+}\hat{-}}$ here since they are identical to the vector, for which we have already included, as shown in (3.4.2)

$\Omega_F^{(2,0)}$,

$$\Omega_F^{\mathcal{N}=4} = \prod_{k=0}^{d} \delta^2(\sum_{i=1}^{n} t_i \sigma_i^k \eta_{i+}^I) \prod_{k=0}^{\tilde{d}} \delta^2(\sum_{i=1}^{n} \tilde{t}_i \sigma_i^k \eta_{i-}^{\hat{I}}). \tag{3.4.10}$$

The formula should be understood as summing over $d, \tilde{d}$ obeying $d + \tilde{d} = n - 2$. However, it is clear from the superfields that we should require

$$d = \frac{n_2}{2} + m_1 - 1, \qquad \tilde{d} = \frac{n_2}{2} + m_2 - 1, \tag{3.4.11}$$

recall n_2 is even. Therefore, for a given number of photon and graviton multiplets, the summation over sectors becomes a sum over different m_1, m_2. We have checked (3.4.9) against many explicit amplitudes, and also verified that the integrand is identical to that of [57] for certain component amplitudes.

3.5   Conclusion

We have presented a formula for the tree-level S matrix of 6D $(2,0)$ supergravity. The formula for single-flavor tensor multiplets is constructed via a SUSY reduction of the one for $(2,2)$ supergravity. We observed important simplifications in deriving the formula, particularly the appearance of the object $\mathrm{Pf}\,X_n$, crucially for the generalization to 21 flavors required for $(2,0)$ supergravity. By studying soft limits of the formula, we were able to explore the moduli space of the theory. Via dimensional reduction, we also deduced a new formula for amplitudes of 4D $\mathcal{N} = 4$ Einstein-Maxwell. Since 6D $(2,0)$ supergravity has a UV completion as a string theory, it would be of interest to extend our formula to include α' corrections, perhaps along the lines of [70]. Also, a recent paper [11] introduces an alternative form of the scattering equations that treats even and odd points equally, but uses a different formalism for supersymmetry. It will be interesting to study our formula into this formalism.

Our results provide an S matrix confirmation of various properties of $(2,0)$ supergravity and the dimensionally reduced theory as predicted by string dualities. While the 10D theory has a dilaton that sets the coupling, in 6D this scalar is one of the 105 moduli fields, and appears equally with the other 104 scalars. If one considers the compactification on K3 $\times T^2$, standard U-dualities imply equivalence to the Type IIA superstring theory on the same geometry or the heterotic string theory compactified to 4D on a torus. The formulas discussed in this thesis apply to all these cases, at least at generic points of the moduli space.

Chapter 4

Loop From Tree Amplitudes

4.1 Introduction

The world-volume effective theories of probe branes play important roles in superstring theory and M-theory. This paper studies loop corrections to scattering amplitudes in the world-volume theory of a probe D3-brane of type IIB superstring theory in a 10D Minkowski-space background. The effective field theory is described by the Dirac-Born-Infeld theory with 4D $\mathcal{N} = 4$ supersymmetry [71–76], and we will refer it as the D3-brane theory. We will argue that the loop corrections to the scattering amplitudes in the D3-brane theory can be obtained from the tree-level amplitudes in theories in higher dimensions. In particular, the relevant higher-dimensional theories are the world-volume theories of a probe M5-brane (of M-theory) in an 11D Minkowski-space background or a probe D5-brane (of type IIB superstring theory) in a 10D Minkowski-space background. We will refer to these two 6D theories as the M5-brane theory and the D5-brane theory, respectively.

The tree-level superamplitudes in the M5-brane theory and D5-brane theory are described by twistor formulations either based on rational maps [1, 9, 10], or based on the polarised scattering equations [11, 77] * (see also [78] for a recent review on the M5-brane theory and the twistor formulations for the tree-level amplitudes in the theory). These different forms of twistor formulations were later unified in the picture of the Symplectic Grassmannian representation of the 6D superamplitudes [32]. The 6D formulae extend the well-known twistor formulation of the scattering amplitudes for 4D $\mathcal{N} = 4$ super Yang–Mills (SYM) [8, 56]. The twistor formulations have been applied to the tree-level superamplitudes in a variety of supersymmetric theories in 6D. Besides the M5-brane theory and D5-brane theory that we have been discussing, it also describes 6D maximal super Yang-Mills theory, as well as the supergravity theories

---

*The 6D polarised scattering equations have been extended to scattering amplitudes in 10D and 11D supersymmetric theories [12].

with $(2,2)$ and $(2,0)$ supersymmetries [1, 10].

The D3-brane theory, M5-brane theory, and the D5-brane theory are known to be closely related, as predicted by superstring theory and M-theory. Specifically, both of the 6D theories (the D5 and M5-brane theory) can be truncated (by a procedure of dimensional reduction) to give rise to the 4D theory (the D3-brane theory). The truncation reduces the M5-brane (or D5-brane) tree-level amplitudes in 6D to the D3-brane tree-level amplitudes in 4D [9]. The tree-level scattering amplitudes in the D3-brane theory have many interesting properties, just to name a few here: the only non-trivial tree-level amplitudes in the D3-brane theory are those with the same number of minus-helicity and plus-helicity photons, namely the helicity is conserved [79]; the amplitudes obey soft theorems, which are very strong constraints that allow to uniquely fix all the tree-level amplitudes in the theory [80–85]; furthermore, the D-brane tree-level amplitudes are an important part of the so-called unifying relations that relate tree amplitudes in a wide range of effective field theories [86].

It is not surprising that, when dimensionally reduced to 4D, these twistor formulations for 6D tree-level amplitudes reproduce the corresponding formulae for the 4D tree-level amplitudes [87]. This paper considers constructing loop corrections to the scattering amplitudes in the 4D theories from the tree-level amplitudes in 6D theories. In particular, we will construct loop corrections to the amplitudes in the D3-brane theory from the M5-brane (or D5-brane) tree-level amplitudes. As a warm up example, we will also consider loop corrections to the scattering amplitudes in 4D $\mathcal{N} = 4$ SYM and $\mathcal{N} = 8$ supergravity from the tree-level amplitudes in 6D SYM and supergravity, respectively. In the case of 4D $\mathcal{N} = 4$ SYM and $\mathcal{N} = 8$ supergravity, the construction reproduces known results in the literature.

With the help of CHY formulation [55, 88] of scattering amplitudes, and built on earlier works from ambi-twistor string theory [89, 90], it is known that the loop corrections in lower dimensions can be obtained from those in higher dimensions via a peculiar dimensional reduction [13–16] (see also [91]). In particular, for constructing a n-point one-loop amplitudes in lower dimensions, we begin with a $(n+2)$-point tree-level amplitudes in the corresponding theory in the higher dimensions, and set n of the external momenta in the lower dimensions whereas the remaining two momenta are taken to be forward and stay in the higher dimensions. The forward momenta play the role of the loop momenta of the one-loop amplitudes in the theory in the lower dimensions. Analogous constructions for the two-loop amplitudes have been pushed forward in [17–19], where two pairs of forward momenta become the loop momenta of the two-loop amplitudes. Instead of using the general dimensional CHY formulations, we will apply the 6D twistor formulations in [1,9–11,32,77] to construct loop corrections to amplitudes in 4D. The advantage of using the 6D twistor formulae is that they make the supersymmetry manifest, and allow us to conveniently utilise the spinor-helicity

formalism, which is a powerful tool for computing scattering amplitudes in 4D theories (see, for instance, [92, 93], for a review.)

The rest of this chapter is organised as follows. Section 4.2 reviews the 6D scattering equations, and their applications to the tree-level superamplitudes in various 6D supersymmetric theories. Section 4.3 discusses the construction of loop superamplitudes in 4D theories from the twistor formulae of 6D tree-level superamplitudes with appropriate forward limits. To illustrate the ideas, we take the one- and two-loop four-point amplitudes in $\mathcal{N} = 4$ SYM and $\mathcal{N} = 8$ supergravity as examples. In section 4.4, we apply the ideas to construct loop corrections to the D3-brane theory. In particular, we focus on the maximally-helicity-violating (MHV) amplitudes at one loop, which are given by contact rational terms. The same results are achieved using generalised unitarity methods. We compute explicitly the four- and six-point amplitudes, and also comment on the structure of the n-point MHV amplitude. In section 4.5, through a supersymmetric reduction of 6D tree-level superamplitudes in the M5-brane theory, we study one-loop corrections to the non-supersymmetric D3-brane amplitudes. We further show that our results are in agreement with those in the reference [58], which were obtained recently by Elvang, Hadjiantonis, Jones and Paranjape using generalised unitarity methods.

4.2 6D twistor formulations

In this section, we will briefly review the twistor formulations for tree-level superamplitudes in 6D theories following the references [1, 9–11, 32]. These twistor formulae of 6D tree-level amplitudes will provide the basis for constructing loop corrections to the amplitudes in 4D theories using forward limits.

4.2.1 6D scattering equations

The scattering amplitudes of massless particles in 6D are described in terms of the 6D spinor-helicity formalism [50], which expresses the 6D massless momentum as

$$p^{AB} = \langle \lambda^A \lambda^B \rangle = \frac{1}{2} \epsilon^{ABCD} [\tilde{\lambda}_C \tilde{\lambda}_D] \,, \tag{4.2.1}$$

where $A, B = 1, 2, 3, 4$ are spinor indices of Lorentz group $\mathrm{Spin}(1, 5)$. Here we have used the short-hand notations

$$\langle \lambda^A \lambda^B \rangle := \lambda_a^A \lambda_b^B \epsilon^{ab} \,, \quad [\tilde{\lambda}_A \tilde{\lambda}_B] := \tilde{\lambda}_{A,\hat{a}} \tilde{\lambda}_{B,\hat{b}} \epsilon^{\hat{a}\hat{b}} \,, \tag{4.2.2}$$

where a, b and $\hat{a}, \hat{b}$ are little-group indices. For a massless particle in 6D, the little group is $\mathrm{Spin}(4) \sim \mathrm{SU}(2)_L \times \mathrm{SU}(2)_R$, so a, b in the above equation are the indices of $\mathrm{SU}(2)_L$

with $a, b = 1, 2$, and $\hat{a}, \hat{b} = \hat{1}, \hat{2}$ refer to $SU(2)_R$.

The kinematics of massless particles in 6D can be nicely described by the 6D scattering equations, either via rational maps [1, 9, 10] or equivalently the polarised scattering equations [11]. We will utilise the polarised scattering equations in our discussions,[*] which take the following form

$$\int d\mu_n^{6D} = \int \frac{\prod_{i=1}^n d\sigma_i \, d^2 v_i \, d^2 u_i}{\mathrm{vol}(SL(2,\mathbb{C})_\sigma \times SL(2,\mathbb{C})_u)} \prod_{i=1}^n \delta\left(\langle v_i \, \epsilon_i \rangle - 1\right) \delta^4\left(\langle v_i \lambda_i^A \rangle - \langle u_i \lambda^A(\sigma_i) \rangle\right), \tag{4.2.3}$$

where we mod out the $SL(2,\mathbb{C})$ symmetries acting on world-sheet coordinates σ_i as well as on the coordinates u_i. The rational functions $\lambda^{Aa}(\sigma)$ are given by

$$\lambda^{Aa}(\sigma) = \sum_{j=1}^n \frac{u_j^a \langle \epsilon_j l_j^A \rangle}{\sigma - \sigma_j}. \tag{4.2.4}$$

Here l_j^{Ab} are the 6D helicity spinors that we introduced in (4.2.1), and the constraints in (4.2.3) implies the momentum conservation, i.e. $\sum_{i=1}^n \langle l_i^A l_i^B \rangle = 0$. It is convenient to choose the little-group spinors ϵ_i that enter in the constraints $\langle v_i \, \epsilon_i \rangle = 1$ to be $\epsilon_{i,a} = (0, 1)$. For such a choice, the delta-function constraints $\langle v_i \, \epsilon_i \rangle = 1$ are solved by $v_{i,a} = (1, v_i)$.

It is worth noticing that (4.2.3) can be recast into a matrix form,

$$\int d\mu_n^{6D} = \int \frac{\prod_{i=1}^n d\sigma_i \, d^2 v_i \, d^2 u_i}{\mathrm{vol}(SL(2,\mathbb{C})_\sigma \times SL(2,\mathbb{C})_u)} \prod_{i=1}^n \delta(\langle v_i \, \epsilon_i \rangle - 1) \delta^4(V \cdot \Omega \cdot \Lambda^A), \tag{4.2.5}$$

where Λ^A is a $2n$-dimensional vector encoding the external helicity spinors,

$$\Lambda^A := \{\lambda_{1,1}^A, \lambda_{2,1}^A, \ldots, \lambda_{n,1}^A, \lambda_{1,2}^A, \lambda_{2,2}^A, \ldots, \lambda_{n,2}^A\}. \tag{4.2.6}$$

and V is a $n \times 2n$ matrix that follows from (4.2.3)

$$V_{i;j,a} = \begin{cases} v_{i,a} & \text{if} \quad i = j \\ -\frac{\langle u_i u_j \rangle}{\sigma_{ij}} \epsilon_{j,a} & \text{if} \quad i \neq j, \end{cases} \tag{4.2.7}$$

with $\sigma_{ij} := \sigma_i - \sigma_j$, and Ω is the symplectic metric

$$\Omega = \begin{pmatrix} 0 & \mathbb{I}_n \\ -\mathbb{I}_n & 0 \end{pmatrix}. \tag{4.2.8}$$

---

[*]All the discussions also apply to the formalism based on rational maps, see the reference [32] for a detailed discussion of rational maps and their equivalence to the polarised scattering equations via a symplectic Grassmannian.

Importantly, under the condition $\langle v_i \, \epsilon_i \rangle = 1$, the matrix V obeys the following symplectic condition [32],

$$V \cdot \Omega \cdot V^T = 0 \,. \tag{4.2.9}$$

Therefore the space of the matrices V forms the symplectic Grassmannian [94, 95]. Finally, one may define a different set of 6D scattering equations with the helicity spinors $\tilde{\lambda}_{i,A}^{\hat{a}}$,

$$\int d\tilde{\mu}_n^{6D} = \int \frac{\prod_{i=1}^n d\sigma_i \, d^2\tilde{v}_i \, d^2\tilde{u}_i}{\mathrm{vol}(SL(2,\mathbb{C})_\sigma \times SL(2,\mathbb{C})_u)} \prod_{i=1}^n \delta([\tilde{v}_i \, \tilde{\epsilon}_i] - 1)\delta^4(\tilde{V} \cdot \Omega \cdot \tilde{\Lambda}_A) \,, \tag{4.2.10}$$

which is needed for determining $\tilde{v}_i, \tilde{u}_i$. The variables $\tilde{v}_i, \tilde{u}_i$ are required for constructing superamplitudes of the non-chiral theories such as 6D SYM, D5-brane theory and supergravity theories.

4.2.2 6D tree-level superamplitudes

To describe the on-shell supersymmetry in 6D, we further introduce Grassmann variables, $\eta_{i,a}^I$ and $\tilde{\eta}_{i,\hat{a}}^{\tilde{I}}$, with $I = 1, 2, \cdots, \mathcal{N}$ and $\tilde{I} = 1, 2, \cdots, \widetilde{\mathcal{N}}$ for a theory with $(\mathcal{N}, \widetilde{\mathcal{N}})$ supersymmetry, and i is the particle label. In particular, the supercharges are defined by

$$q_i^{A,I} = \langle \lambda_i^A \, \eta_i^I \rangle \,, \qquad \bar{q}_{I,i}^A = \lambda_{i,a}^A \frac{\partial}{\partial \eta_{i,a}^I} \,, \tag{4.2.11}$$

and similarly

$$\tilde{q}_{A,i}^{\tilde{I}} = [\tilde{\lambda}_{A,i} \, \tilde{\eta}_i^{\tilde{I}}] \,, \qquad \bar{\tilde{q}}_{A,i,\tilde{I}} = \tilde{\lambda}_{i,A,\hat{a}} \frac{\partial}{\partial \tilde{\eta}_{i,\hat{a}}^{\tilde{I}}} \,. \tag{4.2.12}$$

We note the supercharges obey the correct supersymmetry algebra, $\{q_i^{A,I}, \bar{q}_{J,i}^B\} = \delta_J^I \, p_i^{AB}$, and similar algebra relations for $\tilde{q}_{A,i}^{\tilde{I}}, \bar{\tilde{q}}_{A,i,\tilde{I}}$. The superamplitudes should be annihilated by the total supercharges, namely $Q_n^{A,I} = \sum_{i=1}^n q_i^{A,I}$, $\bar{Q}_n^{A,I} = \sum_{i=1}^n \bar{q}_i^{A,I}$. Therefore, the n-point superamplitude must be proportional to $\delta^{4\mathcal{N}}(Q_n) \, \delta^{4\widetilde{\mathcal{N}}}(\bar{Q}_n)$.

The on-shell spectrum of a supersymmetric theory can be packaged into an on-shell superfield with the help of the Grassmann variables, $\eta_{i,a}^I$ and $\tilde{\eta}_{i,\hat{a}}^{\tilde{I}}$, and the on-shell superamplitudes are functions of helicity spinors as well as the Grassmann variables. Let us begin with the 6D SYM with $(1,1)$ supersymmetry. The on-shell spectrum of the theory is given by

$$\Phi(\eta, \bar{\eta}) = \phi^{1\hat{1}} + \eta_a \psi^{a\hat{1}} + \tilde{\eta}_{\hat{a}} \psi^{1\hat{a}} + \eta_a \tilde{\eta}_{\hat{a}} A^{a\hat{a}} + \ldots + (\eta)^2(\tilde{\eta})^2 \phi^{2\hat{2}} \,, \tag{4.2.13}$$

where, for instance, $\phi^{1\hat{1}}$ is one of four scalars of the theory, and $A^{a\hat{a}}$ is the 6D gluon. Similar to the CHY construction of scattering amplitudes [55, 88], the tree-level amplitudes of a generic 6D theory take the following form in the twistor formulations

$$\mathcal{A}_n = \int d\mu_n^{\text{6D}} \mathcal{I}_L \mathcal{I}_R \,. \tag{4.2.14}$$

In the above formula, the measure $d\mu_n^{\text{6D}}$ imposes the 6D scattering equations which are given in (4.2.3) or (4.2.5), and $\mathcal{I}_L$ and $\mathcal{I}_R$ specify the dynamics of the theory, which will be called as left and right integrand. In the case of 6D $(1,1)$ SYM, the twistor formula of the tree-level superamplitudes is given as

$$\mathcal{A}_n^{\text{SYM}}(\alpha) = \int d\mu_n^{\text{6D}} \mathcal{I}_L^{(1,1)} \mathcal{I}_R^{(\alpha)} \,, \tag{4.2.15}$$

where the left and right integrands take the following form

$$\mathcal{I}_L^{(1,1)} = \delta^n(V \cdot \Omega \cdot \eta)\delta^n(\widetilde{V} \cdot \widetilde{\Omega} \cdot \tilde{\eta}) \det{}'H_n \,, \qquad \mathcal{I}_R^{(\alpha)} = \text{PT}(\alpha) \,. \tag{4.2.16}$$

Here $\eta, \tilde{\eta}$ are the Grassmann version of Λ^A in (4.2.6),

$$\begin{aligned}
\eta &= \{\eta_{1,1}, \eta_{2,1}, \ldots, \eta_{n,1}, \eta_{1,2}, \eta_{2,2}, \ldots, \eta_{n,2}\} \,, \\
\tilde{\eta} &= \{\tilde{\eta}_{1,\hat{1}}, \tilde{\eta}_{2,\hat{1}}, \ldots, \tilde{\eta}_{n,\hat{1}}, \tilde{\eta}_{1,\hat{2}}, \tilde{\eta}_{2,\hat{2}}, \ldots, \tilde{\eta}_{n,\hat{2}}\} \,,
\end{aligned} \tag{4.2.17}$$

and the Grassmann delta functions in $\mathcal{I}_L^{(1,1)}$ imply the conservation of supercharges of 6D $(1,1)$ supersymmetry.

Other building blocks of the integrands are defined as below. First, $\text{PT}(\alpha)$ is the Parke–Taylor factor, which encodes the colour structure of Yang–Mills amplitudes. The notation α represents a permutation of the external particles $\{1, 2, \ldots, n\}$. For instance, when α is the identity permutation,

$$\text{PT}(1, 2, \ldots, n) = \frac{1}{\sigma_{12}\sigma_{23}\cdots\sigma_{n-1\,n}\sigma_{n1}} \,. \tag{4.2.18}$$

The $n \times n$ matrix H_n has the following entries [11]

$$H_{ij} = \frac{\langle \epsilon_i \lambda_i^A \rangle [\tilde{\epsilon}_j \tilde{\lambda}_{A,j}]}{\sigma_{ij}} \quad \text{for} \quad i \neq j \,, \qquad u_{i,a} H_{ii} = -\lambda_a^A(\sigma_i)[\tilde{\epsilon}_i \tilde{\lambda}_{A,i}] \,. \tag{4.2.19}$$

Here, just as $\epsilon_{i,a}$, we can choose $\tilde{\epsilon}_{i,\hat{a}} = (0, 1)$. Note that H_{ii} is independent of the choice of little-group index a, namely it is a Lorentz scalar. The reduced determinant $\det'H$

in $\mathcal{I}_L^{(1,1)}$ is defined as

$$\det{}'H = \frac{\det H_{[kl]}^{[ij]}}{\langle u_i u_j \rangle [\tilde{u}_k \tilde{u}_l]} \,, \qquad (4.2.20)$$

where $H_{[kl]}^{[ij]}$ means that we remove the i-th and j-th columns as well as the k-th and l-th rows, and the result is independent of the choices of i, j and k, l. Note that the conjugate variables such as $\tilde{v}_i, \tilde{u}_i$ appeared in the integrands are determined by scattering equations in (4.2.10).

The tree-level superamplitudes in 6D supergravity with $(2,2)$ supersymmetry are obtained by the double copy of the $(1,1)$ SYM superamplitudes. We have,

$$\mathcal{M}_n^{(2,2)} = \int d\mu_n^{6\mathrm{D}} \delta^{2 \times n}(V \cdot \Omega \cdot \eta^I) \delta^{2 \times n}(\widetilde{V} \cdot \widetilde{\Omega} \cdot \tilde{\eta}^{\tilde{I}}) (\det{}'H_n)^2 \,, \qquad (4.2.21)$$

where $I = 1, 2$ and $\tilde{I} = \tilde{1}, \tilde{2}$ for the 6D $(2,2)$ supersymmetry.

Let us turn to the M5-brane theory and D5-brane theory. The D5-brane theory has $(1,1)$ supersymmetry and contains the same spectrum as SYM, that is given in (4.2.13). The M5-brane theory is a chiral theory with $(2,0)$ supersymmetry, and the on-shell superfield is a tensor multiplet, which is given as

$$\Phi(\eta) = \phi + \eta_I^a \psi_a^I + \eta_I^a \eta^{I,b} B_{ab} + \ldots + (\eta)^4 \bar{\phi} \,, \qquad (4.2.22)$$

with $I = 1, 2$, and B_{ab} is the on-shell 6D self-dual tensor. For the D5-brane theory and the M5-brane theory, only the even-multiplicity amplitudes are non-trivial, and the odd-multiplicity ones vanish identically. The left integrands for the M5-brane theory and the D5-brane theory of the twistor formulations are in fact the same,

$$\mathcal{I}_L^{\mathrm{M5}} = \mathcal{I}_L^{\mathrm{D5}} = (\mathrm{Pf}'S_n)^2 \,, \qquad (4.2.23)$$

where S_n, which is only defined for even n, is an $n \times n$ matrix with entries given as

$$[S_n]_{ij} = \frac{p_i \cdot p_j}{\sigma_{ij}} \,, \qquad (4.2.24)$$

with p_i, p_j being the 6D momenta. The reduced Pfaffian of S_n, $\mathrm{Pf}'S_n$, is defined as

$$\mathrm{Pf}'S_n = \frac{(-1)^{k+l}}{\sigma_{kl}} \mathrm{Pf}(S_n)_{kl}^{kl} \,, \qquad (4.2.25)$$

where $(S_n)_{kl}^{kl}$ is an $(n-2) \times (n-2)$ matrix with the k-th and l-th rows and columns of S_n removed, and the result is independent of the choice of k, l. The right integrand of

the D5-brane superamplitudes is given by

$$\mathcal{I}_R^{\mathrm{D5}} = \delta^n \left(V \cdot \Omega \cdot \eta\right) \delta^n \left(\tilde{V} \cdot \Omega \cdot \tilde{\eta}\right) (\mathrm{Pf}\, U_n)^{-\frac{1}{2}} (\mathrm{Pf}\, \tilde{U}_n)^{-\frac{1}{2}} \,\mathrm{Pf}'\, S_n \,, \tag{4.2.26}$$

whereas the right integrand of the M5-brane superamplitudes takes a simpler form,

$$\mathcal{I}_R^{\mathrm{M5}} = \delta^{2 \times n} \left(V \cdot \Omega \cdot \eta^I\right) (\mathrm{Pf}\, U_n)^{-1} \,\mathrm{Pf}'\, S_n \,. \tag{4.2.27}$$

The fermionic delta functions in $\mathcal{I}_R^{\mathrm{D5}}$ lead to the $(1,1)$ supersymmetry for the D5-brane theory, and the fermionic delta functions in $\mathcal{I}_R^{\mathrm{M5}}$ encode $(2,0)$ supersymmetry for the M5-brane theory. The object U_n that appears in the above formulae is an $n \times n$ anti-symmetric matrix with entries given by

$$U_{ij} = \frac{\langle u_i\, u_j \rangle^2}{\sigma_{ij}} \,, \tag{4.2.28}$$

and one may define the conjugate matrix $\tilde{U}_n$ in a similar fashion using $\tilde{u}_i$. Note that $\mathrm{Pf}'\, S_n$ is related to $\det' H_n$ through the following identity

$$(\mathrm{Pf}\, U_n)^{-\frac{1}{2}} (\mathrm{Pf}\, \tilde{U}_n)^{-\frac{1}{2}} \,\mathrm{Pf}'\, S_n = \det' H_n \,, \tag{4.2.29}$$

which is true under the support of 6D scattering equations. In summary, the tree-level superamplitudes in the M5-brane theory is given by

$$\mathcal{A}_n^{\mathrm{M5}} = \int d\mu_n^{\mathrm{6D}}\, \mathcal{I}_L^{\mathrm{M5}}\, \mathcal{I}_R^{\mathrm{M5}} \,, \tag{4.2.30}$$

with $\mathcal{I}_L^{\mathrm{M5}}$ and $\mathcal{I}_R^{\mathrm{M5}}$ given in (4.2.23) and (4.2.27), respectively. A similar formula can be written down for the D5-brane superamplitudes. From the twistor formulae, we can obtain explicit superamplitudes, for instance, the four-point amplitude of M5-brane theory is simply

$$\mathcal{A}_4^{\mathrm{M5}} = \delta^8(Q_4) \,, \tag{4.2.31}$$

where recalling that Q_4 is the supercharge, and it is defined as $Q_4^{A,I} = \sum_{i=1}^{4} \langle \lambda_i^A\, \eta_i^I \rangle$.

4.2.3 D3-brane massive tree-level amplitudes

After a dimensional reduction to 4D, the M5-brane superfield defined in (4.2.22) reduces to the D3-brane superfield, which is identical to the superfield of $\mathcal{N} = 4$ SYM, given as

(in the non-chiral form),

$$\Phi_{\mathcal{N}=4}(\eta_+, \eta_-) = \phi + \eta_+^{\tilde{I}}\psi_{\tilde{I}}^+ + \eta_-^I\psi_I^- + \cdots + (\eta_+)^2 A^+ + (\eta_-)^2 A^- + \cdots + (\eta_+)^2(\eta_-)^2 \bar{\phi},$$
(4.2.32)

where we have identified $\{\eta_1, \tilde{\eta}_{\hat{1}}\}$ of 6D $(1,1)$ supersymmetry as η_-^I with $I = 1, 2$, and $\{\eta_2, \tilde{\eta}_{\hat{2}}\}$ as $\eta_+^{\tilde{I}}$ with $\tilde{I} = 1, 2$. The supercharges are given by

$$Q_n^{\alpha, I} = \sum_{i=1}^n \lambda_i^\alpha \eta_{i,-}^I, \qquad \tilde{Q}_n^{\dot\alpha, \tilde{I}} = \sum_{i=1}^n \tilde{\lambda}_i^{\dot\alpha} \eta_{i,+}^{\tilde{I}}.$$
(4.2.33)

So $A^{1\hat{1}}$ is identified as the minus-helcity photon (or gluon, in the case of SYM) A^-, $A^{2\hat{2}}$ as the plus-helcity photon (or gluon) A^+ etc. The tree-level amplitudes in the D3-brane theory are obtained through a dimension reduction by setting all the external momenta of the M5-brane amplitudes in 4D [9]. The dimension reduction procedure leads to the twistor formulations for the tree-level superamplitudes in the D3-brane theory [87].

Here we are interested in tree-level superamplitudes in the D3-brane theory with massive states, since they are relevant for constructing loop corrections that we will consider in the section 4.4.2 using generalised unitarity methods. The massive tree-level amplitudes in the D3-brane theory can also be obtained from the M5-brane tree-level amplitudes by a careful dimension reduction. In particular, the masses may be viewed as extra dimensional momenta as Kaluza-Klein modes. The D3-brane superfield with massive sates is straightforwardly obtained from (4.2.22)

$$\Phi_{\text{massive}}(\eta) = \phi + \eta_I^a \psi_a^I + \eta_I^a \eta^{I,b} A_{ab} + \ldots + (\eta)^4 \bar{\phi},$$
(4.2.34)

where $a = 1, 2$ are the little group indices of massive particles in 4D, for instance A_{ab} is the 4D massive vector. The superamplitudes in the D3-brane theory with both massless and massive states are obtained from (4.2.30) by setting the 6D helicity spinors as

$$\lambda_{i,a}^A = \begin{pmatrix} 0 & \lambda_i^\alpha \\ \tilde{\lambda}_i^{\dot\alpha} & 0 \end{pmatrix},$$
(4.2.35)

for the massless states, and

$$\lambda_{j,a}^A = \begin{pmatrix} \lambda_{j,1}^\alpha & \lambda_{j,2}^\alpha \\ \tilde{\lambda}_{j,1}^{\dot\alpha} & \tilde{\lambda}_{j,2}^{\dot\alpha} \end{pmatrix},$$
(4.2.36)

for the massive states with complexified masses given by $\mu_j = \langle \lambda_j^1 \lambda_j^2 \rangle$ and $\tilde{\mu}_j = \langle \tilde{\lambda}_j^{\dot 1} \tilde{\lambda}_j^{\dot 2} \rangle$.[*]

---

[*]The same procedure has been applied to 6D SYM amplitudes to obtain massive amplitudes in 4D $\mathcal{N} = 4$ SYM on the Coulomb branch [10].

We will mostly consider the case with two massive states (say, they are particles i and j), in which case $\mu_i = -\mu_j = \mu$ and $\tilde{\mu}_i = -\tilde{\mu}_j = \tilde{\mu}$, because the extra dimensional momenta should be conserved. For instance, at four points, from (4.2.31), we find the superamplitude with two massive and two massless states is given by

$$
\begin{aligned}
\mathcal{A}_4 \quad &= \delta^4(\lambda_{1,a}^\alpha \eta_1^{Ia} + \lambda_{2,a}^\alpha \eta_2^{Ia} + \lambda_3^\alpha \eta_{3,-}^I + \lambda_4^\alpha \eta_{4,-}^I) \\
&\times \delta^4(\tilde{\lambda}_{1,a}^{\dot\alpha} \eta_1^{\tilde{I}a} + \tilde{\lambda}_{2,a}^{\dot\alpha} \eta_2^{\tilde{I}a} + \tilde{\lambda}_3^{\dot\alpha} \eta_{3,+}^{\tilde{I}} + \tilde{\lambda}_4^{\dot\alpha} \eta_{4,+}^{\tilde{I}}) \,,
\end{aligned}
\tag{4.2.37}
$$

where particles 1 and 2 are massive, and 3 and 4 are massless. From the superamplitude, we can also obtain component amplitudes, for instance,

$$
A_4(\phi_1, \bar{\phi}_2, 3^+, 4^+) = -\mu^2 [3\,4]^2 \,,
\tag{4.2.38}
$$

where $\phi_1, \bar{\phi}_2$ are massive scalars with mass μ.

For higher-point amplitudes, we can construct the superamplitude by writing down an ansatz consisting of factorisation terms, which are obtained from lower-point amplitudes, as well as some possible contact terms, and then compare the ansatz with the twistor formula (4.2.30) to determine any unfixed parameters. For instance, at six points, the factorisation terms of the tree-level amplitude with two massive states are shown in Fig.(4.1), where each diagram takes the form of

$$
\int d^4\eta_K \, \delta^8(Q_L) \frac{1}{P_K^2} \delta^8(Q_R) + \text{Perm} \,.
\tag{4.2.39}
$$

We have used the four-point superamplitude given in (4.2.31) with the understanding that kinematics are projected to 4D as described in the above paragraphs. The Grassmann integration is to sum over the intermediate states, and "Perm" represents summing over all the independent permutations (we will use the same notation in the later sections). It is straightforward to check that the factorisation terms as shown in Fig.(4.1) agree with (4.2.30), it therefore implies that no contact term exists at six points. This is consistent with the known fact that a six-point supersymmetric contact term with six derivatives is not allowed by $(2,0)$ (and $(1,0)$) supersymmetry [96]. This is also in agreement with what was found in [58] for the all-plus and single-minus amplitudes (with two additional massive scalars).[*]

Similar computation applies to higher-point amplitudes. In particular, consider the eight-point superamplitudes, for which the factorisation terms schematically take the

---

[*]We should be careful when discussing contact terms because one can always modify the factorisation terms such that the contact terms are changed accordingly. However, here we are talking about superamplitudes and the question whether one can write down a supersymmetric contact term is unambiguous.
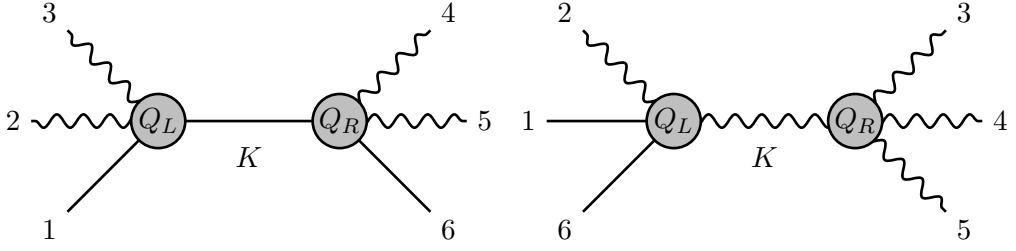
Figure 4.1: The vertices, Q_L and Q_R, represent four-point superamplitudes $\delta^8(Q_L)$ and $\delta^8(Q_R)$. They are glued together by an on-shell propagator K. The curvy lines denote massless particles in 4D, while the solid line indicates 4D massive particles. In the above diagram, we choose leg-1 and leg-6 to be massive states in 4D.

form of

$$\int d^4\eta_{P_{K_1}} \, d^4\eta_{P_{K_3}} \, \delta^8(Q_{K_1})\delta^8(Q_{K_2})\delta^8(Q_{K_3})\frac{1}{P_{K_1}^2 P_{K_3}^2} + \text{Perm}. \qquad (4.2.40)$$

We find in general contact terms are required to match with the twistor formula (4.2.30), except for the special cases with the helicity configurations being all-plus and single-minus photons (with two additional massive scalars), which agrees with the results of [58]. However, for more general helicity configurations, we do require contact terms. For instance, the amplitude of two-minus photons, with the factorisation terms given in (4.2.40) (after projecting to the corresponding component amplitude), we find the following contact term is required to match with twistor formula (4.2.30),

$$
\begin{aligned}
A_{\text{cont}}(1^-, 2^-, 3^+, 4^+, 5^+, 6^+, \phi_7, \bar{\phi}_8) &= -6\mu^2\langle 12\rangle^2([34]^2[56]^2 + \text{Perm}) \qquad (4.2.41) \\
&= -6\mu^2\langle 12\rangle^2([34]^2[56]^2 + [35]^2[46]^2 + [36]^2[45]^2)\,,
\end{aligned}
$$

where $\phi_7, \bar{\phi}_8$ are massive scalars with mass μ. We will come back to this term when we consider its contributions to loop corrections.

4.3 Loops from trees

This section will describe the general ingredients for constructing loop amplitudes from tree-level amplitudes in higher dimensions using the twistor formulations. We would like to emphasise that our construction makes the supersymmetry manifest, and utilises the powerful spinor helicity formalism. This is due to the fact that, instead of the general-dimensional CHY formulae, we will apply the 6D twistor formulations that we reviewed in the previous section, from which we will construct the loop corrections to 4D superamplitudes. To illustrate the idea, we will study the well-known one- and two-loop superamplitudes in $\mathcal{N} = 4$ SYM and $\mathcal{N} = 8$ supergravity using our construction.

The loop corrections to the D3-brane superamplitudes (as well as non-supersymmetric D3-brane amplitudes) will be studied in the following sections.

4.3.1 Loop corrections from higher-dimensional tree amplitudes

It was argued [13, 14] that with an appropriate forward limit, the CHY scattering equations for the tree-level amplitudes give rise to the one-loop scattering equations that were originally obtained from the ambi-twistor theory [89, 90]. To construct the loop corrections to n-point scattering amplitudes in lower-dimensional theories, we start with the $(n{+}2)$-point tree-level amplitudes in corresponding theory in the higher dimensions. We then set n of the external momenta in the lower dimensions of the loop amplitudes that we are interested in, whereas the remaining two momenta, which still stay in the higher dimensions, are taken to be forward. This pair of the forward momenta play the role of the loop momenta of the one-loop amplitudes in the lower dimensions. Analogously, with a careful analysis, the two-loop corrections to n-point amplitudes can be obtained from the $(n{+}4)$ tree-level in higher dimensions with two pairs of forward momenta that become the loop momenta of the loop amplitudes [17–19].

Explicitly, the forward limit procedure in our construction works in the following way: To compute an n-point one-loop amplitude in 4D, we set the kinematics (the spinor-helicity variables) of the $(n{+}2)$-point tree-level amplitude in 6D being parametrised as

$$\lambda_{i,a}^A = \begin{pmatrix} 0 & \lambda_i^\alpha \\ \tilde{\lambda}_i^{\dot\alpha} & 0 \end{pmatrix}, \quad \text{for } i = 1, ..., n\,, \tag{4.3.1}$$

which become the massless external kinematics of the one-loop amplitude in 4D. We also use $k_i^{\alpha\dot\alpha} = \lambda_i^\alpha \tilde{\lambda}_i^{\dot\alpha}$ to denote massless 4D momenta for external particles. As for the remaining two helicity spinors of the forward-limit particles, we set them to be

$$\lambda_{n+1,a}^A = \begin{pmatrix} \lambda_1^\alpha & \lambda_2^\alpha \\ \tilde{\lambda}_1^{\dot\alpha} & \tilde{\lambda}_2^{\dot\alpha} \end{pmatrix}, \quad \lambda_{n+2,a}^A = \begin{pmatrix} \lambda_1^\alpha & -\lambda_2^\alpha \\ \tilde{\lambda}_1^{\dot\alpha} & -\tilde{\lambda}_2^{\dot\alpha} \end{pmatrix}, \tag{4.3.2}$$

such that $\langle \lambda_{n+1}^A \lambda_{n+1}^B \rangle = -\langle \lambda_{n+2}^A \lambda_{n+2}^B \rangle$, namely the 6D momenta $p_{n+1}^{AB}, p_{n+2}^{AB}$ are forward and the 4D part is identified as the loop momentum ℓ with $\ell^2 \neq 0$. Furthermore, we should identify the Grassmann variables $\eta_i^I, \tilde{\eta}_i^{\tilde I}$ (for $i = 1, 2, \cdots, n$) with the Grassmann variables of lower-dimensional supersymmetric theories (as we will see explicitly in examples in the following sections). As for the forward-limit pair, we set

$$\eta_{n+2}^{I,1} = \eta_{n+1}^{I,1}, \quad \eta_{n+2}^{I,2} = -\eta_{n+1}^{I,2}, \quad \tilde{\eta}_{n+2}^{\tilde I,\hat 1} = \tilde{\eta}_{n+1}^{\tilde I,\hat 1}, \quad \tilde{\eta}_{n+2}^{\tilde I,\hat 2} = -\tilde{\eta}_{n+1}^{\tilde I,\hat 2}, \tag{4.3.3}$$

such that the supercharges $q_{n+1}^I = -q_{n+2}^I$ and $\tilde{q}_{n+1}^{\tilde I} = -\tilde{q}_{n+2}^{\tilde I}$. This is required for the conservation of supercharges of external particles, namely $\sum_{i=1}^n q_i^I = \sum_{i=1}^n \tilde{q}_i^{\tilde I} = 0$.

With this set up, we conjecture the twistor formulation for the one-loop amplitude is then given as

$$
\begin{aligned}
\mathcal{A}^{(1)}_{4\mathrm{D},n} &= \int \frac{d^4\ell}{\ell^2} \int d^{2\mathcal{N}}\eta_{n+1} d^{2\widetilde{\mathcal{N}}}\tilde{\eta}_{n+1}\, \mathcal{A}^{(0)}_{6\mathrm{D},n+2}\big|_{\mathrm{F.L.}} \\
&= \int \frac{d^4\ell}{\ell^2} \int d\mu^{6\mathrm{D}}_{n+2}\, d^{2\mathcal{N}}\eta_{n+1} d^{2\widetilde{\mathcal{N}}}\tilde{\eta}_{n+1}\, \mathcal{I}_L \mathcal{I}_R\big|_{\mathrm{F.L.}}\,,
\end{aligned}
\tag{4.3.4}
$$

where we have denoted the n-point one-loop amplitude in 4D as $\mathcal{A}^{(1)}_{4\mathrm{D},n}$. The object $\mathcal{A}^{(0)}_{6\mathrm{D},n+2}\big|_{\mathrm{F.L.}}$ denotes the 6D $(n+2)$-point tree-level amplitude with the special forward kinematics given in (4.3.1) and (4.3.2), as well as (4.3.3) for the Grassmann variables. The Grassmann integral is to sum over all the internal states for the pair of the particles that are taken to be forward. In the last step of (4.3.4), we have expressed the 6D tree-level amplitudes in the twistor formulations, with the measure $d\mu^{6\mathrm{D}}_{n+2}$ given in (4.2.5), and the precise form of the integrand $\mathcal{I}_L$ and $\mathcal{I}_R$ depends on the theory we are considering. As discovered in [15] (see also [97]), this formulation typically leads to loop integrands with linear propagators, and we will see more examples, *e.g.* one-loop SYM in (4.3.8) and one-loop SUGRA in (4.3.11), as numerical checks of (4.3.4) in the following sections.[*]

4.3.2 Loop corrections to SYM and supergravity superamplitudes

To illustrate the ideas, we consider the one- and two-loop amplitudes in 4D $\mathcal{N} = 4$ SYM and $\mathcal{N} = 8$ supergravity from our construction. Under the dimensional reduction, the 6D SYM superfield (4.2.13) reduces to the superfield of 4D $\mathcal{N} = 4$ SYM (in the non-chiral form) as shown in (4.2.32). For the pair of particles that we take to be forward (i.e. the particles $(n+1)$ and $(n+2)$), we set the Grassmann variables as

$$
\eta^1_{n+2} = \eta^1_{n+1}\,, \quad \eta^2_{n+2} = -\eta^2_{n+1}\,, \quad \tilde{\eta}^{\tilde{1}}_{n+2} = \tilde{\eta}^{\tilde{1}}_{n+1}\,, \quad \tilde{\eta}^{\tilde{2}}_{n+2} = -\tilde{\eta}^{\tilde{2}}_{n+1}\,.
\tag{4.3.5}
$$

According to the procedure discussed in the previous section, the one-loop superamplitudes in $\mathcal{N} = 4$ SYM are then given by

$$
\mathcal{A}^{(1)}_n(\alpha) = \int \frac{d^4\ell}{\ell^2} \int d\mu^{6\mathrm{D}}_{n+2} \int d^2\eta_{n+1} d^2\tilde{\eta}_{n+1}\, \mathcal{I}^{(1,1)}_L\, \mathcal{I}^{(n+1,\alpha,n+2)}_R\big|_{\mathrm{F.L.}}\,,
\tag{4.3.6}
$$

---

[*]For a proposal of obtaining loop integrands with standard quadratic Feynman propagators using CHY formulation, see [98–101].

with the left and right integrands given by

$$\mathcal{I}_L^{(1,1)} = \delta^{n+2}(V \cdot \Omega \cdot \eta)\delta^{n+2}(\widetilde{V} \cdot \widetilde{\Omega} \cdot \tilde{\eta})\det' H_{n+2} \,,$$
$$\mathcal{I}_R^{(n+1,\alpha,n+2)} = \sum_{\text{cyclic}} \text{PT}(n+1,\alpha,n+2)\,, \tag{4.3.7}$$

where the cyclic sum is to sum over all the cyclic permutation of α. Again, it should be understood that the kinematics in the above formula are taken to be: n of the helicity spinors are in 4D, and two remain in 6D and being forward, whereas the Grassmann variables are identified according to (4.2.32) and (4.3.5).

As an example, we construct the one-loop corrections to the four-point superamplitude in 4D $\mathcal{N} = 4$ SYM. Following the procedure discussed previously, we begin with the six-point tree-level superamplitude of 6D $(1,1)$ SYM, and dimensionally reduce four of the external kinematics (including the fermionic ones) to 4D $\mathcal{N} = 4$ SYM, whereas the remaining two of them are in 6D and are taken to be forward, as illustrated in Fig.(4.2). We find that the one-loop integrand of the four-point amplitude in 4D $\mathcal{N} = 4$ SYM is given by

$$\mathcal{A}_4^{(1)} = \delta^4(Q_4)\delta^4(\tilde{Q}_4) \times I_{\text{box}}(k_1,k_2,k_4)\,, \tag{4.3.8}$$

where the supercharges $Q_4, \tilde{Q}_4$ are defined in (4.2.33). The box integral $I_{\text{box}}(k_1,k_2,k_4)$ is defined as

$$I_{\text{box}}(k_1,k_2,k_4) = \int d^4\ell \, \frac{1}{\ell^2 \, (2\ell \cdot k_1) \, (2\ell \cdot (k_1 + k_2) + 2k_1 \cdot k_2) \, (-2\ell \cdot k_4)} + \text{cyclic}\,, \tag{4.3.9}$$

where the integral is in the linear propagator representation and we also sum over four cyclic permutations. The result is in agreement with (2.45) in [16] (with the overall normalisation being one). Importantly, as we show in Appendix B, the linear-propagator representation (4.3.9) is equivalent to the standard box integral with quadratic propagators, namely

$$\tilde{I}_{\text{box}}(k_1,k_2,k_4) = \int d^4\ell \, \frac{1}{\ell^2 \, (\ell + k_1)^2 \, (\ell + k_1 + k_2)^2 \, (\ell - k_4)^2}\,, \tag{4.3.10}$$

that appears in [102, 103].

Similar construction applies to the one-loop corrections to the four-point superamplitude in 4D $\mathcal{N} = 8$ supergravity. For the $\mathcal{N} = 8$ supergravity loop amplitudes, we begin with the six-point tree-level superamplitude of $(2,2)$ supergravity. The prescription then leads to the following result

$$\mathcal{M}_4^{(1)} = \delta^8(Q_4)\delta^8(\tilde{Q}_4)\left[I_{\text{box}}(k_1,k_2,k_4) + \text{Perm}\right]\,, \tag{4.3.11}$$
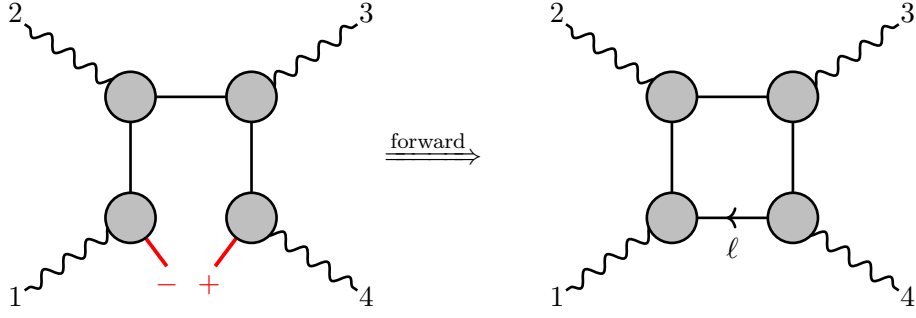
Figure 4.2: The curvy line means the particle momentum is restricted in 4D (as parametrised in (4.3.1)), while the particle with the solid line still remains in 6D kinematics. The red line represents the forward-limit particle pair with 6D kinematics, which is understood as loop momentum.

where $Q_4, \tilde{Q}_4$ are defined in (4.2.33), but now with $I = 1, 2, 3, 4$ and $\tilde{I} = 1, 2, 3, 4$ for the $\mathcal{N} = 8$ supersymmetry. We also sum over all the permutations due to the permutation symmetry of gravity amplitudes, and (4.3.11) indeed reproduces the known result in (2.46) of [16], which is equivalent to the original result in the quadratic propagator form [104].

The construction may be generalised to higher loops, especially the two-loop corrections [17–19]. For describing two-loop corrections, we will need $(n+4)$-point tree amplitudes as input, and set two pairs of particles in forward limit (p_{n+1}^{AB}, p_{n+2}^{AB} are forward, so as p_{n+3}^{AB}, p_{n+4}^{AB}), and require their supercharges to cancel among each other. To be explicit, the second pair of forward-limit particles $(n+3)$ and $(n+4)$ should obey the same relation in (4.3.2) and (4.3.3) as the first particle pair $(n+1)$ and $(n+2)$ do. With the similar setup as one-loop amplitude, we can write down the twistor formulation of two-loop amplitude as

$$
\begin{aligned}
\mathcal{A}_{\text{4D},n}^{(2)} &= \int \frac{d^4\ell_1}{\ell_1^2} \frac{d^4\ell_2}{\ell_2^2} \int \prod_{i=n+1,n+3} d^{2\mathcal{N}}\eta_i d^{2\tilde{\mathcal{N}}}\tilde{\eta}_i \, \mathcal{A}_{\text{6D},n+4}^{(0)}\big|_{\text{F.L.}} \\
&= \int \frac{d^4\ell_1}{\ell_1^2} \frac{d^4\ell_2}{\ell_2^2} \int \prod_{i=n+1,n+3} d^{2\mathcal{N}}\eta_i d^{2\tilde{\mathcal{N}}}\tilde{\eta}_i \int d\mu_{n+4}^{\text{6D}} \mathcal{I}_L \mathcal{I}_R\big|_{\text{F.L.}},
\end{aligned}
\tag{4.3.12}
$$

where ℓ_1 and ℓ_2 are the momenta of the two forward-limit particles, $(n+1)$ and $(n+3)$, which are identified as loop momenta with $\ell_1^2 \neq 0$ and $\ell_2^2 \neq 0$. We denote the two-loop n-point amplitude in 4D as $\mathcal{A}_{\text{4D},n}^{(2)}$. The internal states of all forward-limit particles are summed over by performing Grassmann integral.

Using the formula (4.3.12), we reproduce the well-known four-point two-loop SYM and supergravity amplitudes in [17, 19, 105, 106] [*]. The two-loop SYM can be obtained

---

[*]In the work of [19], the two-loop scattering equations have two different choices, $\alpha = \pm 1$ (here α refers to the parameter in their paper, not the colour ordering), which corresponds to our choice of

by using the 6D $\mathcal{N} = (1,1)$ SYM expressed in twistor formula

$$\mathcal{A}_n^{(2)}(\alpha) = \int d\mu_{n+4}^{\text{6D}} \int \prod_{i=n+1,n+3} d^2\eta_i d^2\tilde{\eta}_i \, \mathcal{I}_L^{(1,1)} \, \mathcal{I}_R^{(2\text{-loop},\alpha)}\big|_{\text{F.L.}}, \qquad (4.3.13)$$

where the left integrand with $(1,1)$ supersymmetry is

$$\mathcal{I}_L^{(1,1)} = \delta^{n+4}(V \cdot \Omega \cdot \eta)\delta^{n+4}(\widetilde{V} \cdot \widetilde{\Omega} \cdot \tilde{\eta}) \det' H_{n+4}, \qquad (4.3.14)$$

and the right integrand is a two-loop Parke-Taylor factor, which in general contains the planar and non-planar parts of the SYM amplitude. For example, the planar part is given by the following integrand

$$\begin{aligned}
\mathcal{I}_R^{(2\text{-loop},\alpha),\text{P}} &= c_\alpha^{\text{P}}(n+1,n+2,n+3,n+4) + c_\alpha^{\text{P}}(n+2,n+1,n+4,n+3) \\
&\quad + c_\alpha^{\text{P}}(n+3,n+4,n+1,n+2) + c_\alpha^{\text{P}}(n+4,n+3,n+2,n+1),
\end{aligned} \qquad (4.3.15)$$

where the superscript P denotes planar, and the factor $c_\alpha^{\text{P}}(a,b,c,d)$ is defined as

$$\begin{aligned}
c_\alpha^{\text{P}}(a,b,c,d) = \sum_{\text{cyclic } \alpha} &\Big(\text{PT}(a,b,d,c,\alpha_1,\alpha_2,\alpha_3,\alpha_4) + \text{PT}(a,b,\alpha_1,d,c,\alpha_2,\alpha_3,\alpha_4) \\
&+ \text{PT}(a,b,\alpha_1,\alpha_2,d,c,\alpha_3,\alpha_4) + \text{PT}(a,c,d,b,\alpha_1,\alpha_2,\alpha_3,\alpha_4) \Big).
\end{aligned}$$
$$(4.3.16)$$

We have numerically checked that (4.3.13) with planar integrand in (4.3.15) agree with the postulate (21) in [17], which is shown to be equal to

$$\mathcal{A}^{(2),\text{P}}(\alpha) = \delta^4(Q_4)\delta^4(\tilde{Q}_4)\Big(k_{\alpha_1} \cdot k_{\alpha_2} \, I_{\alpha_1\alpha_2,\alpha_3\alpha_4}^{\text{planar}} + k_{\alpha_4} \cdot k_{\alpha_1} \, I_{\alpha_4\alpha_1,\alpha_2\alpha_3}^{\text{planar}} \Big), \qquad (4.3.17)$$

where the planar two-loop boxes, $I_{\alpha_1\alpha_2,\alpha_3\alpha_4}^{\text{planar}}$ are defined in the Appendix.A of [17], see equation (A5). We have also checked the agreement between our formula and the known result for the non-planar sector. Similarly, the four-point two-loop superamplitude in 4D $\mathcal{N} = 8$ supergravity can be obtained by considering the eight-point tree-level amplitude of the 6D $(2,2)$ supergravity, which is expressed in the twistor formulation as given in (4.2.21). We have verified that the result of this construction is in the agreement with the known result [17, 106][*].

---

setting the momenta to be $2\,p_{n+1} \cdot p_{n+3} = \alpha\,(\ell_1 + \alpha\,\ell_2)^2$. Here we have chosen $\alpha = 1$, and we could have made the choice with $\alpha = -1$ to obtain the same result.

[*]For the two-loop $\mathcal{N} = 8$ supergravity integrand, we numerically checked the ratio of (4.2.21) with different helicities agrees with the ratio of the tree-level amplitude, for example, $\mathcal{M}_{1^-2^-3^+4^+}^{(2,2)}/\mathcal{M}_{1^-2^+3^-4^+}^{(2,2)} = \langle 12 \rangle^8/\langle 13 \rangle^8$.

4.4 Supersymmetric D3-brane amplitudes at one loop

In this section, we consider one-loop corrections to the superamplitudes in the D3-brane theory using forward limits of higher-dimensional tree-level amplitudes, following the general prescription of the previous sections. The results will be further confirmed using generalised unitarity methods. The higher-dimensional amplitudes that are relevant for constructing the loop corrections to D3-brane amplitudes are the tree-level amplitudes in the M5-brane theory[*]. Because the construction makes the supersymmetry manifest, the amplitudes with all-plus and single-minus helicity configurations manifestly vanish. So the first non-trivial helicity configurations are those with two minus photons, namely the MHV amplitudes.

It is known that the non-trivial tree-level amplitudes in the D3-brane theory are helicity conserving [79]. So the MHV amplitudes vanish at tree level (except for the four-point case), and they do not have non-trivial four-dimensional cuts at one-loop order. Therefore the one-loop MHV amplitudes (with more than four points) can only be rational terms. To extract the rational terms, it is necessary to consider the loop momenta in general d dimensions. We will treat the extra-dimensional loop momenta as masses, therefore, it is equivalent to consider 4D loop momenta with massive states running in the loop.

In our construction, this is set up by separating the massless 6D momenta (which will be taken to be forward) into ℓ_{4D} and two extra dimensions, such that when the loop momentum ℓ_{4D} is put on-shell, we have $\ell_{4D}^2 = -\mu^2$. With such convention, we write a 6D momentum as its 4D component ($\ell_{4D} := \ell$) with extra dimensions, that will be called as p_4 and p_5, which correspond to the components of the fifth and the sixth dimension, respectively. The 6D momentum is explicitly written as

$$\ell_{6D} = (\ell, p_4, p_5), \tag{4.4.1}$$

then the massless condition is

$$0 = \ell_{6D}^2 = \ell^2 + \mu\tilde{\mu}, \quad \text{with} \quad \mu = p_4 + ip_5, \quad \tilde{\mu} = p_4 - ip_5. \tag{4.4.2}$$

Since we have identified the momentum of a forward-limit particle as the loop momentum as shown in (4.3.2), μ and $\tilde{\mu}$ can also be expressed in terms of $\lambda_{n+1,a}^A$:

$$\mu = \langle \lambda_{n+1}^1 \, \lambda_{n+1}^2 \rangle, \qquad \tilde{\mu} = \langle \lambda_{n+1}^3 \, \lambda_{n+1}^4 \rangle. \tag{4.4.3}$$

---

[*]The same results can be obtained if we use the D5-brane tree amplitudes. The D5-brane theory has different supersymmetry from the M5-brane theory; however, such difference no longer exists after dimensional reduction to 4D. We have checked explicitly for a few examples that the lower-dimensional results are indeed independent of the choices. In practice, the twistor formula for M5-brane tree amplitudes is simpler, which involves only the "left-handed" variables since it is a chiral theory, as can be seen from (4.2.26) and (4.2.27).

We now have a massive particle in the loop with a loop momentum, $\tilde{\ell} = \ell + \mu$ with $\tilde{\ell}^2 = \ell^2 + \mu^2$. Also, the linear propagators are unchanged since μ is in the extra dimension, so we have

$$\tilde{\ell} \cdot k_i = (\ell + \mu) \cdot k_i = \ell \cdot k_i \, , \tag{4.4.4}$$

for a 4D external momentum k_i.

With this setup, the one-loop D3-brane amplitudes can be obtained from the tree-level M5-brane amplitude by a similar construction we outlined in previous sections,

$$\mathcal{A}_{\text{D3},\, n}^{(1)} = \int \frac{d^D \tilde{\ell}}{(2\pi)^D} \frac{1}{\tilde{\ell}^2} \int d^4 \eta_{n+1} \, \mathcal{A}_{\text{M5},\, n+2}^{(0)} \big|_{\text{F.L.}} \, , \tag{4.4.5}$$

where $d^4 \eta_{n+1} = d\eta_{n+1,1}^1 d\eta_{n+1,1}^2 d\eta_{n+1,2}^1 d\eta_{n+1,2}^2$, and Grassmann integration is to sum over the superstates of the forward-limit particles. Again in the above formula, it should be understood that it is the tree-level forward-limit amplitude on the right-hand side that gives the one-loop integrand. This tree-level M5-brane amplitude is expressed in the twistor formulation as

$$\mathcal{A}_{\text{M5},\, n+2}^{(0)} = \int d\mu_{n+2}^{\text{6D}} \, \mathcal{I}_L^{\text{M5}} \mathcal{I}_R^{\text{M5}} \, , \tag{4.4.6}$$

where the left and right integrands $\mathcal{I}_L^{\text{M5}}$ and $\mathcal{I}_R^{\text{M5}}$ are given in (4.2.23), and (4.2.27), respectively.

4.4.1 One-loop corrections to D3-brane superamplitudes

Let us begin with the one-loop correction to a four-point amplitude, which is very similar to the case of four-point one-loop amplitudes of $\mathcal{N} = 4$ SYM in the previous section. We will show that the one-loop amplitude receives correction from the bubble diagram in the Fig.(4.3). Using the general formula (4.4.5) and solving the scattering equations, we find that the one-loop correction to the four-point superamplitude in the D3-brane theory takes the following form

$$\mathcal{A}_{\text{D3},4}^{(1)} = \mathcal{A}_{\text{D3},4}^{(0)} \left(s_{12}^2 \, I_{\text{bubble}}(k_1, k_2) + \text{Perm} \right) \, , \tag{4.4.7}$$

where $\mathcal{A}_{\text{D3},4}^{(0)}$ is the tree-level amplitude of the D3-brane theory, and it is given by

$$\mathcal{A}_{\text{D3},4}^{(0)} = \delta^4 (\sum_{i=1}^4 \lambda_i^\alpha \eta_{i,-}^I) \delta^4 (\sum_{i=1}^4 \tilde{\lambda}_i^{\dot{\alpha}} \eta_{i,+}^{\tilde{I}}) \, . \tag{4.4.8}$$

Note that it is the supersymmetrisation of the higher-derivative term F^4. As we have seen in the previous section, in this construction the loop integrands are typically in the
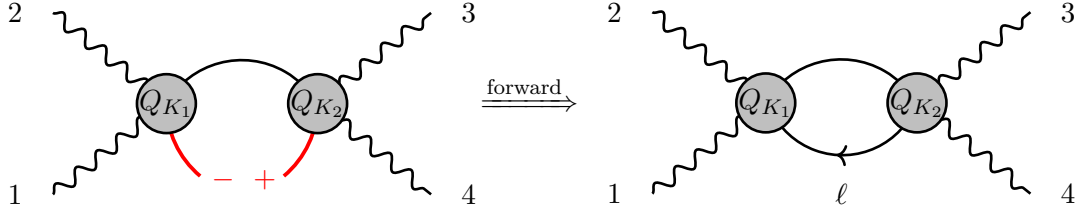
Figure 4.3: The bubble diagram comes from gluing the leg-$(n+1)$ and leg-$(n+2)$ (denoted by $-$ and $+$, respectively) of a six-point tree amplitude. The original $s_{1\,2\,n+1}$ channel becomes the linear propagator of the first term in (4.4.9).

linear propagator representation. For the four-point case we consider here, the bubble integral is defined by

$$I_{\text{bubble}}(k_1, k_2) = \int \frac{d^D \tilde{\ell}}{(2\pi)^D} \bigg[\frac{1}{\tilde{\ell}^2 \left(2\tilde{\ell} \cdot (k_1 + k_2) + 2k_1 \cdot k_2 \right)}$$
$$+ \frac{1}{\tilde{\ell}^2 \left(-2\tilde{\ell} \cdot (k_1 + k_2) + 2k_1 \cdot k_2 \right)} \bigg]. \qquad (4.4.9)$$

Recall $\tilde{\ell} = \ell + \mu$, so that $\tilde{\ell}^2 = \ell^2 + \mu^2$ and $\tilde{\ell} \cdot (k_1 + k_2) = \ell \cdot (k_1 + k_2)$. As shown in Appendix B, (4.4.9) is equivalent to the standard bubble integral with quadratic propagators

$$\tilde{I}_{\text{bubble}}(k_1, k_2) = \int \frac{d^D \tilde{\ell}}{(2\pi)^D} \bigg[\frac{1}{\tilde{\ell}^2 (\tilde{\ell} + k_1 + k_2)^2} \bigg]. \qquad (4.4.10)$$

The result (4.4.7) is in agreement with the result in the reference [107] that was originally obtained using unitarity cuts [108, 109], which is in the quadratic propagator form (4.4.10), and only massless loop propagators were considered. The bubble integral (4.4.9) or (4.4.10) is UV divergent in 4D, therefore the result (4.4.7) leads to a UV counter term for the D3-brane effective Lagrangian, which is of the form $d^4 F^4$ (and its supersymmetric completion), or equivalently in momentum space it is given as

$$(s_{12}^2 + s_{23}^2 + s_{13}^2) \, \delta^4 (\sum_{i=1}^4 \lambda_i^\alpha \eta_{i,-}^I) \delta^4 (\sum_{i=1}^4 \tilde{\lambda}_i^{\dot{\alpha}} \eta_{i,+}^{\tilde{I}}) \,. \qquad (4.4.11)$$

The above four-point superamplitude is expressed in a non-chiral form, where the superfield is given by (4.2.32). For describing the MHV superamplitudes at higher points which we will study shortly, it is more convenient to use the chiral version. The chiral version is obtained by a Grassmann Fourier transform. For instance, the chiral

superfield is obtained from non-chiral superfield given in (4.2.32) through,

$$V_{\mathcal{N}=4}(\eta_-,\xi) = \int d^2\eta_+ e^{\eta_+^{\tilde{I}}\xi_{\tilde{I}}} \Phi_{\mathcal{N}=4}(\eta_+,\eta_-)\,. \qquad (4.4.12)$$

After combining η_-^I and $\xi_{\tilde{I}}$ and denoting them as η^A with $A = 1,2,3,4$, which transform under $SU(4)$ R-symmetry, we obtain the superfield in a chiral form,

$$V_{\mathcal{N}=4}(\eta) = A^+ + \eta^A\psi_A^+ + \eta^A\eta^B\phi_{AB} + \frac{1}{3!}\varepsilon_{ABCD}\eta^A\eta^B\eta^C\psi^{D-} + \eta^1\eta^2\eta^3\eta^4 A^-\,, \quad (4.4.13)$$

and the supercharges take the form

$$q_i^{\alpha A} = l_i^\alpha \eta_i^A \quad \text{and} \quad q_{i,A}^{\dot\alpha} = \tilde{l}_i^{\dot\alpha}\frac{\partial}{\partial\eta_i^A}\,. \qquad (4.4.14)$$

In the chiral representation, the four-point tree-level D3-brane superamplitude is given by [96]

$$\mathcal{A}_{\mathrm{D3},4}^{(0)} = \left(\frac{[12]}{\langle 34\rangle}\right)^2 \delta^8\left(\sum_{i=1}^4 q_i^{\alpha I}\right), \qquad (4.4.15)$$

where $\left(\frac{[12]}{\langle 34\rangle}\right)^2$ is the Jacobian factor from the Grassmann Fourier transform, and importantly it is permutation invariant and $\langle 34\rangle^2$ in the denominator is not a pole. When expressed in the chiral form, the four-point D3-brane superamplitude at one loop takes the following form

$$\mathcal{A}_{\mathrm{D3},4}^{(1)} = \delta^8\left(Q_4\right)\left([12]^2[34]^2 \times I_{\mathrm{bubble}}(k_1,k_2) + \mathrm{Perm}\right), \qquad (4.4.16)$$

where we define $Q_n^{\alpha A} = \sum_{i=1}^n q_i^{\alpha A}$. We will continue to utilise the chiral representation for the discussion on higher-point D3-brane superamplitudes.

The one-loop corrections to higher-point superamplitudes can be obtained similarly from the general formula (4.4.5). To illustrate the idea, we will consider the six-point MHV amplitude. Using the formula (4.4.5) with $n = 6$, we find the MHV amplitude is proportional to an overall supercharge, $\delta^8(Q_6)$, as required by $\mathcal{N} = 4$ supersymmetry. Explicitly, the one-loop superamplitude is constructed by taking forward the eight-point tree-level superamplitude as shown in the Fig.(4.4). Note that the contact term of eight-point amplitude does not contribute. We find that the integrand for the one-loop six-point MHV amplitude takes a very similar form as the four-point result given in (4.4.16). It is given as

$$\mathcal{A}_{\mathrm{D3},6}^{(1),\mathrm{MHV}} = \delta^8(Q_6)\left(\mu^2\,[12]^2[34]^2[56]^2 \times I_{\mathrm{triangle}}(k_1,k_2;k_3,k_4;k_5,k_6) + \mathrm{Perm}\right). \qquad (4.4.17)$$
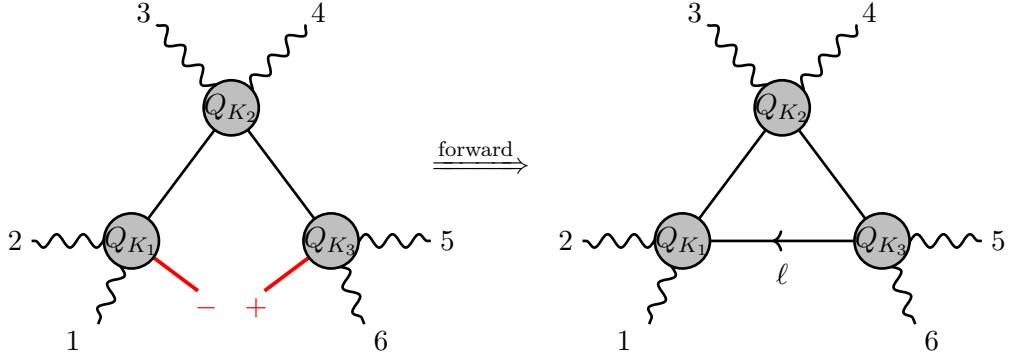
Figure 4.4: Triangle diagram arises from gluing an eight-point tree diagram, where the $s_{1\,2\,n+1}$ and $s_{5\,6\,n+2}$ channels give rise to the linear propagators in the first term of (4.4.17). The other two terms correspond to identifying the other two internal lines in the diagram with loop momentum.

The integral I_{triangle} is the scalar triangle integral in the linear propagator representation, which takes the following form

$$
I_{\text{triangle}}(k_1, k_2; k_3, k_4; k_5, k_6)
$$
$$
= -\int \frac{d^D \tilde{\ell}}{(2\pi)^D} \Big(\frac{1}{\tilde{\ell}^2 \left[2\tilde{\ell} \cdot (k_1 + k_2) + 2k_1 \cdot k_2\right] \left[-2\tilde{\ell} \cdot (k_5 + k_6) + 2k_5 \cdot k_6\right]}
$$
$$
+ \frac{1}{\tilde{\ell}^2 \left[2\tilde{\ell} \cdot (k_3 + k_4) + 2k_3 \cdot k_4\right] \left[-2\tilde{\ell} \cdot (k_1 + k_2) + 2k_1 \cdot k_2\right]}
$$
$$
+ \frac{1}{\tilde{\ell}^2 \left[2\tilde{\ell} \cdot (k_5 + k_6) + 2k_5 \cdot k_6\right] \left[-2\tilde{\ell} \cdot (k_3 + k_4) + 2k_3 \cdot k_4\right]} \Big). \tag{4.4.18}
$$

This result is verified by (4.4.5) for $n = 6$ by solving numerically the scattering equations in the formula with the forward kinematics. There are three terms with linear propagators in the above equation, each of them can be understood as assigning the forward pair of legs in different places; for example, the first term in (4.4.17) is shown in the Fig.(4.4). In principle, the one-loop corrections to higher-point amplitudes can be obtained in a similar fashion; however, solving scattering equations with higher-point kinematics becomes more and more difficult. We hope to develop better numerical and analytical methods to handle this issue, which we leave as a further research direction.

4.4.2 Generalised unitarity methods

In this section, we will construct the one-loop amplitudes through the d-dimensional generalised unitary methods [110]. The d-dimensional cuts are necessary to extract the rational terms of the loop amplitudes since the rational terms have vanishing four-dimensional cuts. As in the previous section, again the extra dimensional loop momenta will be viewed as the masses of the internal propagating particles in 4D. Therefore, ef-
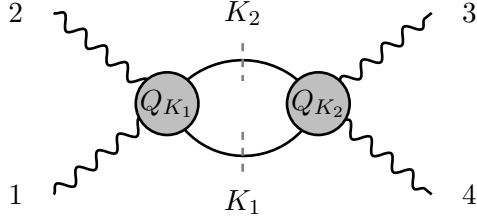
Figure 4.5: The four-point bubble diagram is formed by gluing two tree-level four-point superamplitudes. We identify K_1 as loop momentum ($K_1 = \ell$), then the on-shell conditions ($K_i^2 = 0$) can be read as $\ell^2 = 0$, and $(\ell + k_1 + k_2)^2 = 0$.

fectively we will perform four-dimensional cuts, but with massive loop momenta. We will find the results agree with those computed in the previous section using the twistor formulations. Of course, they are in different representations: one in the linear propagator representation, the other in the standard quadratic propagator representation.

Let us first begin with the four-point case. The one-loop amplitude only receives contribution from the bubble diagram, which can be formed by gluing two four-point superamplitudes as shown in the Fig.(4.5). Explicitly, it is given by

$$\int \frac{d^D\tilde{\ell}}{(2\pi)^D} \int \Big(\prod_{i=1}^{2} d^4\eta_{K_i}\Big)\Big(\prod_{i=1}^{2} \frac{1}{K_i^2}\Big)\, \delta^8(Q_{K_1})\delta^8(Q_{K_2})\,, \qquad (4.4.19)$$

where the explicit form of the four-point superamplitudes are given by

$$Q_{K_1} = \sum_{i=1,2,K_1,-K_2} \lambda_{i,a}^A \eta_i^{I,a}\,, \quad \text{and} \quad Q_{K_2} = \sum_{i=3,4,K_2,-K_1} \lambda_{i,a}^A \eta_i^{I,a}\,. \qquad (4.4.20)$$

Note for the external states, they are massless, therefore

$$\lambda_{i,a}^A = \begin{pmatrix} 0 & \lambda_i^\alpha \\ \tilde{\lambda}_i^{\dot\alpha} & 0 \end{pmatrix}\,, \quad \text{for} \ \ i = 1, ..., 4\,. \qquad (4.4.21)$$

From (4.4.19), we deduce that the one-loop correction to the MHV amplitude is given by

$$\delta^8(Q_4)\,[12]^2[34]^2 \int \frac{d^D\tilde{\ell}}{(2\pi)^D}\left(\frac{1}{\tilde{\ell}^2(\tilde{\ell} + k_1 + k_2)^2}\right) + \text{Perm}\,. \qquad (4.4.22)$$

In the above formula we have summed over the permutations, and after linearising the propagators as we show in Appendix B, the result agrees with the one obtained from the twistor formula given in (4.4.16).

We now consider the six-point amplitude. Due to the fact that there is no six-point contact term, for the MHV amplitude, only the triangle diagram is non-trivial, for
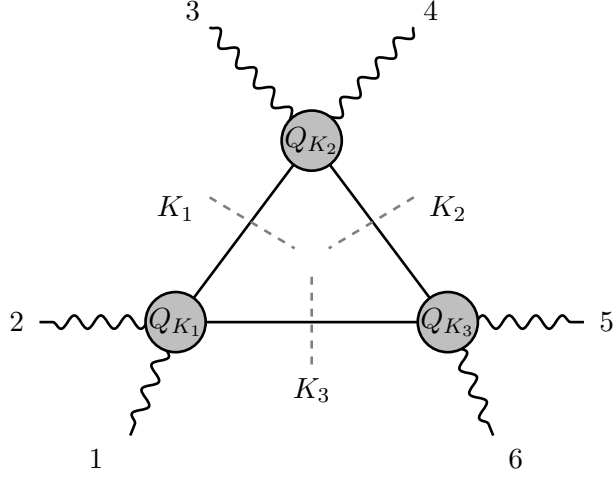
Figure 4.6: Legs-(1,2), (3,4), and (5,6) are glued in three different corners with on-shell propagators, K_1, K_2 and K_3. When K_3 is identified with the loop momentum, the diagram gives the contribution as (4.4.24).

which we glue three four-point superamplitudes as shown in the Fig.(4.6). We pair up external leg-$(1,2)$, $(3,4)$, and $(5,6)$ in three different corners, and the internal massive lines are denoted as K_1, K_2, and K_3. The suprsymmetric gluing result of four-point superamplitudes gives

$$\int \frac{d^D\tilde{\ell}}{(2\pi)^D} \int \Big(\prod_{i=1}^{3} d^4\eta_{K_i}\Big)\Big(\prod_{i=1}^{3}\frac{1}{K_i^2}\Big)\, \delta^8(Q_{K_1})\delta^8(Q_{K_2})\delta^8(Q_{K_3})\,. \tag{4.4.23}$$

Explicit numeric evaluation of the above formula leads to the following result for the one-loop correction to the six-point MHV amplitude

$$-\delta^8(Q_6)\,[12]^2[34]^2[56]^2 \int \frac{d^D\tilde{\ell}}{(2\pi)^D}\left(\frac{\mu^2}{\tilde{\ell}^2(\tilde{\ell}+k_1+k_2)^2\,(\tilde{\ell}-k_5-k_6)^2}\right) + \text{Perm}\,. \tag{4.4.24}$$

Here we have chosen the loop momentum to be K_3 $(K_3 = \tilde{\ell})$, and we have also summed over permutations to obtain the complete answer. Again, as explained in Appendix B, (4.4.24) is in agreement with (4.4.17), which we obtained from the twistor formulations.

As for a general n-point MHV amplitude, it is easy to see that it contains a $(n/2)$-gon integrand which takes the same form as the four- and six-point amplitudes we have computed, namely,

$$\delta^8(Q_n) \int \frac{d^D\tilde{\ell}}{(2\pi)^D}\Big[\frac{(-1)^{n/2}\mu^{2(\frac{n}{2}-2)}\,[12]^2[34]^2\cdots[n-1\,n]^2}{\tilde{\ell}^2\,(\tilde{\ell}+\sum_{i=1}^{2}k_i)^2(\tilde{\ell}+\sum_{i=1}^{4}k_i)^2\cdots(\tilde{\ell}+\sum_{i=1}^{n-2}k_i)^2} + \text{Perm}\Big]\,. \tag{4.4.25}$$

However, as we know that for general helicity configurations, the tree-level amplitudes (with two massive states) at higher points require contact terms, (e.g. (4.2.41) for the eight-point case), it implies that besides the $(n/2)$-gon topology, the one-loop amplitude in general also receives contributions from the integrands with lower-gon topologies. For instance, for the eight-point MHV amplitude, a bubble diagram will also contribute due to the contact term shown in (4.2.41) (as well as its supersymmetric completion). We leave the computation of the one-loop corrections to the n-point MHV amplitude as a future research direction.

4.4.3 Rational terms of MHV D3-brane amplitudes at one loop

In the previous sections, we obtained the one-loop integrand for the MHV amplitude of the D3-brane theory, either using the forward limit of the twistor formulations or the generalised unitary methods. The one-loop integral can be performed explicitly using the dimension shifting formula [111], see for instance the Appendix C of [58]. Explicitly, for a m-gon scalar integral, we have

$$\int \frac{d^D\tilde{\ell}}{(2\pi)^D} \frac{\mu^{2(m-2)}}{\prod_{i=1}^m (\tilde{\ell} + \sum_{j=1}^i K_j)^2} = -\frac{i(-1)^m}{(4\pi)^2} \frac{\Gamma(m-2)}{\Gamma(m)} + \mathcal{O}(\epsilon)\,, \qquad (4.4.26)$$

where we have taken $D = 4 - 2\epsilon$ and considered the small ϵ limit. We therefore obtain the one-loop correction to the six-point MHV amplitude of the D3-brane theory, which is given by a contact rational term,

$$\mathcal{A}_6^{\mathrm{MHV}} = -\frac{i}{32\pi^2} \delta^8(Q_6) \left([12]^2[34]^2[56]^2 + \mathrm{Perm}\right)\,. \qquad (4.4.27)$$

It is straightforward to see that the above result is the unique answer that has the right power counting and correct little-group scaling, and further require the answer do not possess poles. Indeed, we do not allow MHV amplitudes to have poles since the theory has no three-point amplitudes. Similarly, at n points, the unique answer that is consistent with the power counting and little-group scaling takes the following form

$$-\frac{i}{32\pi^2} \delta^8(Q_n) \left([12]^2[34]^2 \cdots [n{-}1\,n]^2 + \mathrm{Perm}\right)\,. \qquad (4.4.28)$$

The above result is also in agreement with (4.4.25) after performing the integral using (4.4.26). However, as we commented that the $(n/2)$-gon integral (4.4.25) is only a part of the full answer for $n > 6$, therefore the overall coefficient of (4.4.28) has to be determined by explicit computations after including all the lower-topology integrands.

We would like to comment that the presence of the above rational term for the MHV helicity configuration violates the $U(1)$ symmetry of the tree-level D3-brane amplitudes, which would only allow helicity conserved amplitudes as we commented previously.

However, since the rational terms we obtained are purely contact without any poles, they can be simply cancelled by adding local counter terms. [*]

Finally, due to the fact that the scalars of D3-brane theory are Goldstone bosons of spontaneously breaking of translation and Lorentz rotation, the corresponding amplitudes with these scalars should obey enhanced soft behaviour [80, 83],

$$A(k_1, k_2, \cdots, k_n)\big|_{k_1 \to 0} \sim \mathcal{O}(k_1^2), \tag{4.4.29}$$

where k_1 is the momentum of one of the scalars. The enhanced soft behaviour was further argued to be valid when the loop corrections are taken into account [112]. To study the soft behaviour of the scalar fields, we consider the rational term with the helicity configuration $(\phi_1, \bar{\phi}_2, 3^-, 4^+, \cdots, n^+)$, where $\phi_1, \bar{\phi}_2$ are scalars. From (4.4.27), we see that the rational term is then proportional to

$$\langle 13 \rangle^2 \langle 23 \rangle^2 \left([12]^2[34]^2 \cdots [n{-}1\,n]^2 + \text{Perm}\right). \tag{4.4.30}$$

It is easy to see that each term in the permutation goes as $\mathcal{O}(k_1^2)$ (or $\mathcal{O}(k_2^2)$) in the soft limit $k_1 \to 0$ (or $k_2 \to 0$), which is consistent with the enhanced soft behaviour of the D3-brane theory.

4.5 Non-supersymmetric D3-brane amplitudes at one loop

The loop corrections to scattering amplitudes in 4D lower-supersymmetric theories or non-supersymmetric theories can be obtained by a supersymmetry reduction on 6D tree-level superamplitudes such that only relevant states (instead of the full super multiplets) run in the loops. Using this idea, we will study loop corrections to the amplitudes in the non-supersymmetric Born-Infeld (BI) theory. In particular, for the BI theory, we project the external states to be photons and the internal particles to be a pair of massive vectors.

In the following sections, we will consider one-loop amplitudes with all-plus external photons (the Self-Dual sector) and single-minus external photons (the Next-to-Self-Dual sector). They vanish identically in the supersymmetric theory, and for the non-supersymmetric theory, they are purely rational terms at one-loop order. Therefore, just as in the case of one-loop MHV amplitudes in the supersymmetric theory, to extract the rational terms we require the internal particles propagating in the loop to be massive. We find that the results from the forward-limit construction agrees with those in [58], which were computed originally using the generalised unitarity methods [108, 109].

---

[*]See similar discussion for the non-supersymmetric BI theory [58].

4.5.1 Self-Dual sector

We begin with the amplitudes in the Self-Dual (SD) sector, namely the amplitudes with all-plus helicity configuration. We perform a supersymmetric reduction by choosing all external legs to be plus-helicity photons and the forward-limit particles to be a pair of massive vectors or massive scalars[*]. With such construction, the one-loop n-point amplitude in the SD sector is given by

$$A_{\text{SD},n}^{(1)} = \int \frac{d^D \tilde{\ell}}{(2\pi)^D} \frac{1}{\tilde{\ell}^2} \int (\prod_{i=1}^{n} d^2 \eta_{i,2}) \, d^4 \eta_{n+1} \, \mathcal{A}_{\text{M5},n+2}^{(0)}\big|_{\text{F.L.}} \, , \tag{4.5.1}$$

where $d^2 \eta_{i,a} = \frac{1}{2} \epsilon_{IJ} d\eta_{i,a}^I d\eta_{i,a}^J$. This choice of Grassmann variables integration projects all the external legs (i.e. particles 1 to n) to be plus-helicity photons, and it also sets the internal particles $n+1$ and $n+2$ to be scalars. In the following discussions, we provide the numeric checks of (4.5.1), as well as (4.5.6) for the Next-to-Self-Dual sector, for $n = 4, 6$ cases.

In the case of $n = 4$, carrying out the Grassmann integral in (4.5.1) and solving the scattering equations, we find that the one-loop correction to the four-point amplitude in the SD sector is given by

$$A_{\text{SD},4}^{(1)} = (\mu^2)^2 [12]^2 [34]^2 \, I_{\text{bubble}}(k_1, k_2) + \text{Perm} \, , \tag{4.5.2}$$

where the bubble integral $I_{\text{bubble}}(k_1, k_2)$ is given in (4.4.9). The above expression agrees with the loop integrand in (4.1) of [58], except for the propagators being linearised. Note that, with our notation Perm, (4.5.1) has three independent terms, *i.e* $I_{\text{bubble}}(k_1, k_2)$, $I_{\text{bubble}}(k_1, k_3)$, and $I_{\text{bubble}}(k_1, k_4)$, which agrees with the notation in [58], *e.g.* (4.1) in their paper also has three terms under $\mathcal{P}(2, 3, 4)$ permutation with a $\frac{1}{2}$ pre-factor. The result after integration using (C.17) of [58] is given by

$$A_{\text{SD},4}^{(1)} = \frac{i}{960\pi^2} \left([12]^2 [34]^2 s_{12}^2 + [13]^2 [24]^2 s_{13}^2 + [14]^2 [23]^2 s_{14}^2 \right) + \mathcal{O}(\epsilon). \tag{4.5.3}$$

Similar computation applies to higher-point cases. Let us consider the six-point case

---

[*]For the all-plus and single-minus helicity configurations, one can in fact replace the internal massive vectors by massive scalars to simplify the computation, see, for instance, [58] for the argument. We have checked that the same results are obtained by choosing the internal states being either massive vectors or massive scalars.

here, that is given by (4.5.1) with $n = 6$, from which we find

$$
\begin{aligned}
A_{\mathrm{SD},\,6}^{(1)} = -\int &\frac{d^D\tilde{\ell}}{(2\pi)^D}(\mu^2)^3\Big[[12]^2[34]^2[56]^2 \\
&\times\Big(\frac{1}{\tilde{\ell}^2\left[2\tilde{\ell}\cdot(k_1+k_2)+2k_1\cdot k_2\right]\left[-2\tilde{\ell}\cdot(k_5+k_6)+2k_5\cdot k_6\right]} \\
&+\frac{1}{\tilde{\ell}^2\left[2\tilde{\ell}\cdot(k_3+k_4)+2k_3\cdot k_4\right]\left[-2\tilde{\ell}\cdot(k_1+k_2)+2k_1\cdot k_2\right]} \\
&+\frac{1}{\tilde{\ell}^2\left[2\tilde{\ell}\cdot(k_5+k_6)+2k_5\cdot k_6\right]\left[-2\tilde{\ell}\cdot(k_3+k_4)+2k_3\cdot k_4\right]}\Big)+\mathrm{Perm}\Big],
\end{aligned}
\tag{4.5.4}
$$

which has $30 = \frac{1}{3}\binom{6}{2}\binom{4}{2}$ (where $\frac{1}{3}$ mods out cyclic) terms under Perm, agrees with the loop integrand in (4.4) of [58] that has the same number of terms under $\mathcal{P}\,(2,3,4,5,6)$ permutation with a $\frac{1}{4}$ pre-factor. Again our result is in the linear propagator representation, but it is equivalent to that of [58] as shown in Appendix B. The six-point result after integration is given

$$
\begin{aligned}
A_{\mathrm{SD},\,6}^{(1)} =&\frac{1}{4}\Big[\frac{i}{2880\pi^2}[12]^2[34]^2[56]^2\left(s_{12}^2+s_{34}^2+s_{56}^2+s_{12}s_{34}+s_{12}s_{56}+s_{34}s_{56}\right) \\
&+\mathcal{P}\,(2,3,4,5,6)\Big]+\mathcal{O}(\epsilon).
\end{aligned}
\tag{4.5.5}
$$

We note that, at least for the cases we studied here, the one-loop integrands of amplitudes in the SD sector of non-supersymmetric D3-brane theory take a very similar form as those of the MHV amplitudes in the supersymmetric D3-brane theory. In fact, they are related to each other by exchanging the factor $(\mu^2)^2$ in amplitudes of the SD sector with $\delta^8(Q)$ in the supersymmetric amplitudes.

4.5.2 Next-to-Self-Dual sector

The computation for the one-loop amplitudes in the Next-to-Self-Dual (NSD) sector is very similar. They are the amplitudes with single-minus helicity configuration, so we only need to change the choice of Grassmann variables from all-plus to single-minus. Applying a similar construction as (4.5.1), we have

$$
A_{\mathrm{NSD},\,n}^{(1)} = \int\frac{d^D\tilde{\ell}}{(2\pi)^D}\frac{1}{\tilde{\ell}^2}\int d^2\eta_{n,1}(\prod_{i=1}^{n-1}d^2\eta_{i,2})\,d^4\eta_{n+1}\,\mathcal{A}_{\mathrm{M5},\,n+2}^{(0)}\big|_{\mathrm{F.L.}}.
\tag{4.5.6}
$$

We assign particle-n to be a minus-helicity photon and the rest of the external particles to be plus-helicity photons. The forward-limit particles $n+1$ and $n+2$ are again chosen to be scalars.

Let us consider explicitly the four- and six-point amplitudes in the NSD sector. In

the case of $n = 4$, we find that the result has the form

$$A_{\mathrm{NSD},\,4}^{(1)}$$

$$= \int \frac{d^D \tilde{\ell}}{(2\pi)^D} \left(\frac{\mu^2 \, [12]^2 \, \langle 4|\tilde{\ell}|3]^2}{\tilde{\ell}^2 [2\tilde{\ell} \cdot (k_1 + k_2) + 2k_1 \cdot k_2]} + \frac{\mu^2 \, [12]^2 \, \langle 4|\tilde{\ell} - (k_1 + k_2)|3]^2}{\tilde{\ell}^2 [-2\tilde{\ell} \cdot (k_1 + k_2) + 2k_1 \cdot k_2]} \right) + \mathrm{Perm}\,, \tag{4.5.7}$$

where we have defined $\langle i|k|j] = \lambda_i^\alpha \, k_{\alpha\dot\alpha} \, \tilde{\lambda}_j^{\dot\alpha}$. The result is in agreement with the one in (4.10) of [58], as shown in Appendix B. As explained in (4.2) and (C.24) in [58], the above tensor integral leads to a vanishing result as

$$A_{\mathrm{NSD},\,4}^{(1)} = 0 + \mathcal{O}(\epsilon). \tag{4.5.8}$$

For the six-point amplitude, we find the contributions contain triangle and bubble diagrams,

$$A_{\mathrm{NSD},\,6}^{(1)} = \int \frac{d^D \tilde{\ell}}{(2\pi)^D} \left(\mathcal{I}_{\mathrm{NSD},6}^{\mathrm{triangle}} + \mathcal{I}_{\mathrm{NSD},6}^{\mathrm{bubble}} \right). \tag{4.5.9}$$

The triangle contribution is given by

$$\mathcal{I}_{\mathrm{NSD},6}^{\mathrm{triangle}} = -(\mu^2)^2 \left[\frac{[12]^2 [34]^2 \langle 6|\tilde{\ell}|5]^2}{\tilde{\ell}^2 [2\tilde{\ell} \cdot (k_1 + k_2) + 2k_1 \cdot k_2] \, [-2\tilde{\ell} \cdot (k_5 + k_6) + 2k_5 \cdot k_6]} \right.$$

$$+ \frac{[12]^2 [34]^2 \langle 6|\tilde{\ell} - (k_1 + k_2)|5]^2}{\tilde{\ell}^2 [2\tilde{\ell} \cdot (k_3 + k_4) + 2k_3 \cdot k_4] \, [-2\tilde{\ell} \cdot (k_1 + k_2) + 2k_1 \cdot k_2]} \tag{4.5.10}$$

$$\left. + \frac{[12]^2 [34]^2 \langle 6|\tilde{\ell} + (k_5 + k_6)|5]^2}{\tilde{\ell}^2 [2\tilde{\ell} \cdot (k_5 + k_6) + 2k_5 \cdot k_6] \, [-2\tilde{\ell} \cdot (k_3 + k_4) + 2k_3 \cdot k_4]} + \mathrm{Perm} \right],$$

and the bubble integral takes the following form

$$\mathcal{I}_{\mathrm{NSD},6}^{\mathrm{bubble}} = -(\mu^2)^2 \left[\frac{[12]^2 [34]^2 \, \langle 6|(k_1 + k_2)|5]^2}{s_{125} \, \tilde{\ell}^2 \, [2\tilde{\ell} \cdot (k_1 + k_2) + 2k_1 \cdot k_2]} \right.$$

$$\left. + \frac{[12]^2 [34]^2 \, \langle 6|(k_1 + k_2)|5]^2}{s_{125} \, \tilde{\ell}^2 \, [-2\tilde{\ell} \cdot (k_1 + k_2) + 2k_1 \cdot k_2]} + \mathrm{Perm} \right]. \tag{4.5.11}$$

The results are in the agreement with (4.17) and (4.19) of [58], after translating the quadratic propagators into the linear ones as discussed in Appendix B.

Finally, we comment that the above supersymmetric reduction procedure is very general, and it can be applied to other non-supersymmetric theories. For instance, we have checked explicitly that the procedure reproduces well-known results of some rational terms in pure Yang-Mills theory [97, 111]. They are obtained from the super-

symmetric reduction of the amplitude in 6D SYM with the forward limit; in particular, the four-point all-plus result is given by

$$
\int d\mu^{6D} \, \frac{1}{\tilde{\ell}^2} \int (\prod_{i=1}^{4} d^2\eta_{i,2}) \, d^4\eta_{n+1} \, \mathcal{I}_L^{(1,1)} \mathcal{I}_R^{(\alpha)}|_{\text{F.L.}} \, , \tag{4.5.12}
$$

where the four external legs are assigned with positive helicities, and the internal loop is a complex scalar. The numerical result of (4.5.12) agrees with (16) in [97], which we reproduce below

$$
\frac{[12][34]}{\langle 12 \rangle \langle 34 \rangle} \, \frac{\mu^4}{\tilde{\ell}^2 \left(2\tilde{\ell} \cdot k_1 \right) \left(2\tilde{\ell} \cdot (k_1 + k_2) + 2k_1 \cdot k_2 \right) \left(-2\tilde{\ell} \cdot k_4 \right)} \, , \tag{4.5.13}
$$

where μ and $\tilde{\ell}$ are defined in (4.4.3) and (4.4.4).

4.6 Conclusion

We show how to compute the loop correction to scattering amplitudes from tree-level forward-limit amplitudes, which are expressed in the twistor formulae (4.3.4). Such procedure usually generates loop integrand with linear propagators; nevertheless, it can be shown that those linear propagators equivalent to the standard quadratic ones at the level of integral since the difference is simply shift of loop momentum. There are also some recent works that directly result in standard loop integrands with quadratic propagators based on the scattering equation formalism [98–101, 113].

Applying this procedure (4.3.4), we reproduce the one corrections of 4D super Yang-Mills and supergravity four-point amplitudes [15, 104], from considering 6D tree-level six-point $\mathcal{N} = (1, 1)$ super Yang-Mills, and $\mathcal{N} = (2, 2)$ supergravity, respectively. Similarly, the two loop corrections are obtained by considering and 6D eight-point amplitudes, which again reproduces the known results [17–19].

Having checked the formulation works for super Yang-Mills and supergravity theories, we furthere apply it to the one-loop D3-brane amplitude and show it can be obtain from the tree-level M5-brane amplitude via this forward limit procedure. The one-loop D3-brane amplitude is simply given by a rational term, which could potentially violates the $U(1)$ symmetry enjoyed by the D3-brane tree amplitudes, *e.g.* only helicity-conserved amplitude allowed. However, we argue that since such rational term is purely contact, it can be cancelled by adding a local counter term. This guarantees the $U(1)$ symmetry still holds for the D3-brane at the one-loop level.

Moreover, by performing supersymmtric reduction on the M5-brane amplitude, and again taking the forward limit, the one-loop amplitude of 4D non-supersymmetric Born-Infeld field can be obtained accordingly. We explicitly check the self-dual $(+ + \cdots +)$

and next-to-self-dual $(-+\cdots+)$ agree with known results by Elvang *et al* [58]. It will be very interesting to apply this loop-tree procedure to obtain loop amplitudes of more quantum field theories. Finally, the progress made by twistor formulae at loop level has inspired superstring computations; for instance, a formula for the three-loop four-point superstring integrand has been proposed recently [114].

Chapter 5

Amplituhedron for the ABJM Theory

5.1 Introduction

Scattering amplitudes in $\mathcal{N} = 6$ Chern-Simons matter theory (often termed ABJM) [51, 115], have long been an interesting close cousin of those in four-dimensional $\mathcal{N} = 4$ super Yang-Mills (sYM), mimicking its hidden structures with modifications tailored to the unique features of three-dimensional kinematics. For example the all multiplicity tree-amplitude worldsheet formula of Witten-RSV [8, 56], has a mirror image in ABJM theory [29]. Similarly the SU(4|4) dual-superconformal (and its full Yangian embedding) invariance of tree-level amplitude and loop-level integrand of $\mathcal{N} = 4$ sYM [116, 117], have their counterpart, the OSp(6|4) of the $\mathcal{N} = 6$ [118–120]. As a consequence, the Grassmannian geometry that yields individual Yangian blocks [121], once constrained to its orthogonal subspace yields the leading singularities of ABJM theory [28]. The stratification of the geometry admits a trivalent bi-partite graphical representation for the individual cells [26], can also be applied to ABJM theory with the simplification of using medial graphs with quadratic vertices [30, 52].

As is apparent in the above, this hand in hand development appears to have as its boundary the extension to momentum twistor [122]. Indeed the latter was instrumental in the realization of *amplituhedron* [27, 53], where the amplitude is identified as the canonical form on a positive geometry whose boundaries are given in momentum twistors. The difficulty lies in the nature of dual superconformal symmetry in three dimensions, which requires in addition to the introduction of dual variables for the conformal group Sp(4), but also the R-symmetry SO(6). This will appear to require a new set of twistor variables that do not have a kinematic origin.

An alternative amplituhedron definition for tree-level amplitudes of $\mathcal{N} = 4$ sYM was proposed directly in the spinor helicity kinematic space [54], motivated by [123]. This

opens the possibility for the existence of a tree-level amplituhedron for ABJM theory directly in the three-dimensional kinematic space. In this paper we will present precisely such a geometric object, which we call as the *orthogonal momentum amplituhedron*. Consider the image of the following map:

$$Y_a^A = \sum_{i=1}^{n} c_{ai} \Lambda_i^A \,, \tag{5.1.1}$$

where $a = 1, \cdots, k$, $A = 1, \cdots, k+2$ and $k = \frac{n}{2}$ (n is even here). Here Y_a^A lives in a subspace of the Grassmannian $G(k, k+2)$, that is the image of positive orthogonal Grassmannian $OG_+(k, 2k)$ (c_{ai} is an element of $OG_+(k, 2k)$) mapped through the bosonic kinematic variables Λ_i^A living on a moment curve. As we will show, the boundary of this space is given by odd-particle planar Mandelstam variables $S_{i,i+1,i+2,\cdots,i+p}$ (for odd number of particles, p is even), where

$$S_{i,i+1,\cdots,i+p} = \sum_{i \leq j < l \leq i+p} (-1)^{j+l+1} \langle Yjl \rangle^2,$$
$$\langle Yjl \rangle \equiv \epsilon_{A_1 A_2 \cdots A_{2+k}} Y_1^{A_1} Y_2^{A_2} \cdots Y_k^{A_k} \Lambda_j^{A_{1+k}} \Lambda_l^{A_{2+k}} \,. \tag{5.1.2}$$

Note that while all planar Mandelstam variables are non-negative, only the vanishing of each odd-particle Mandelstam variable is co-dimension one boundary. The vanishing of even-particle Mandelstam variables is higher co-dimensional. This reflects the fact that the non-vanishing amplitudes in ABJM theory have an even number of particles, therefore the amplitudes only have factorization poles of odd-particle Mandelstam variables. The space is $(n-3)$-dimensional, as Y_a^A given (5.1.1) satisfy the following conditions:

$$\sum_{i=1}^{n} (-1)^i (Y^\perp \cdot \Lambda^T)_i^\alpha (Y^\perp \cdot \Lambda^T)_i^\beta = 0 \,. \tag{5.1.3}$$

The amplitude is then identified with the volume function $\Omega_{2k,k}$ defined through

$$\mathbf{\Omega}_{2k,k}^{3d} \wedge d^3 P \, \delta^3(P) = \Omega_{2k,k} \left(\prod_{a=1}^{k} \langle Y_1 Y_2 \cdots Y_k d^2 Y_a \rangle \right) \delta^3(P) \,, \tag{5.1.4}$$

where $\mathbf{\Omega}_{2k,k}^{3d}$ is the $(n-3)$-dimensional canonical form on $OG_+(k, 2k)$ whose co-dimension one boundaries, via the map in (5.1.1) are the planar odd-particle Mandelstam variables. The subspace defined through the map in (5.1.1), can be carved out directly in Y space via the non-negativity of $\langle Yii+1 \rangle$, and a series of sign pattern as well as the

momentum conservation:

$$\{\langle Y12\rangle, \langle Y13\rangle, \cdots, \langle Y1n\rangle\}, \quad \text{having } k \text{ sign flips},$$

$$\sum_{i=1}^{n} (-1)^i \langle Yia\rangle \langle Yib\rangle = 0, \quad \text{for } a, b = 1, \cdots, n. \tag{5.1.5}$$

Note that this is identical to the sign flipping conditions associated with half of the momentum amplituthedron of $\mathcal{N} = 4$ sYM [54]. In particular, the amplituhedron geometry for the four-dimensional theory is given by $(Y, \tilde{Y}) \in (Gr(n-k, n-k+2), Gr(k, k+2))$, with $Y, \tilde{Y}$ satisfying $k-2$ and k sign-flip patterns respectively. Thus with $k = \frac{n}{2}$, we see that the orthogonal amplituhedron geometry for the ABJM theory can be identified with $\tilde{Y}$, with the additional constraint associated from momentum conservation. Thus *the orthogonal momentum amplituhedron is simply a kinematic projection of the momentum amplituhedron geometry for four-dimensional theories.*

We verify the above proposal through the BCFW construction, which identifies the tree-level amplitude as a particular combination of cells of the orthogonal Grassmannian [30,52]. We first confirm that the BCFW cells via the map in (5.1.1) tile the whole space. This is checked numerically at eight points, where each point in the image for the top cell lies only in one of the BCFW cells, vice versa. Next we identify the canonical form as

$$\mathbf{\Omega}_{2k,k}^{3d} = \sum_{\sigma} \int_{\mathcal{C}_\sigma} \frac{d^{k\times 2k}C}{\text{Vol}(GL(k))} \frac{M_{1,3,5,\cdots,n-1}}{M_1 M_2 \cdots M_k} \delta^{\frac{k(k+1)}{2}}(C^T C)\Big|_{Y=c\cdot\Lambda}, \tag{5.1.6}$$

where the contour $\mathcal{C}_\sigma$ localizes on the various BCFW cells labelled by σ, and $M_{1,3,5,\cdots,n-1}$ is a $k \times k$ involving columns $\{1, 3, 5, \cdots, n-1\}$, and similarly M_i is the minor involving consecutive columns $\{i, i+1, \cdots, i+k-1\}$. Note that the integrand is simply the original orthogonal integral introduced in [28], but reduced to $\mathcal{N} = 4$ SUSY, which leads to the numerator $M_{1,3,5,\cdots,n-1}$. The union of these forms then gives the BCFW triangulation of the amplituhedron. Since the BCFW cells tile the space for Y, with the contour $\mathcal{C}$ encircling these cells, (5.1.6) gives the correct canonical form that can be lifted to the volume form for the amplituhedron via the relation (5.1.4). It is intriguing that the canonical form on $OG_+(k, 2k)$ is more naturally derived using the $\mathcal{N} = 4$ formalism. Note that this is natural from the viewpoint of exchanging $\eta \to d\lambda$, similar to [123]. Indeed the n-point amplitude is degree n in η, and thus produces the n-form which can be matched to the volume form in kinematic space.

The rest of the paper is organised as follows. In the next section, we will briefly review basic properties of the momentum amplituhedron for four-dimensional $\mathcal{N} = 4$ sYM. In Section 5.3, we present the construction of the orthogonal momentum amplituhedron geometry and its definition through the sign flipping. In section 5.4, we

discuss in detail canonical forms of the orthogonal momentum amplituhedron, and their associated singularities and the boundary structures of the amplituhedron geometry. In section 5.5, we conclude and remark on future research directions.

5.2 Review of the momentum amplituhedron for $\mathcal{N} = 4$ sYM

In this section, we will review the construction of the momentum amplituhedron for four-dimensional $\mathcal{N} = 4$ sYM [54].* The momentum amplituhedron $\mathcal{M}_{n,k}$ is defined as the image of the positive Grassmannian $G_+(k,n)$ through the map depending on the positive kinematics. Here, positive kinematics is defined as two sets of moment curves on which the external data lives:

$$(\Lambda^\perp)_i^{\bar{A}} = x_i^{\bar{A}-1}, \quad \tilde{\Lambda}_i^{\dot{A}} = \tilde{x}_i^{\dot{A}-1}. \tag{5.2.1}$$

From this definition, we can see easily that all ordered minors of matrices $\tilde{\Lambda}, \Lambda^\perp$ are positive. When we extract the amplitudes, these matrices are identified as the bosonized kinematics:

$$\Lambda_i^A = \begin{pmatrix} \lambda_i^\alpha \\ \phi_I^1 \cdot \eta_i^I \\ \vdots \\ \phi_I^{n-k} \cdot \eta_i^I \end{pmatrix}, \quad A = 1, \ldots, n-k+2,$$

$$\tilde{\Lambda}_i^{\dot{A}} = \begin{pmatrix} \tilde{\lambda}_i^{\dot{\alpha}} \\ \tilde{\phi}_{\hat{I}}^1 \cdot \tilde{\eta}_i^{\hat{I}} \\ \vdots \\ \tilde{\phi}_{\hat{I}}^k \cdot \tilde{\eta}_i^{\hat{I}} \end{pmatrix}, \quad \dot{A} = 1, \ldots, k+2, \tag{5.2.2}$$

where $\eta, \tilde{\eta}, \phi, \tilde{\phi}$ are Grassmann-odd variables. Here we use the non-chiral SUSY for describing $\mathcal{N} = 4$ sYM superamplitudes, with a subgroup of R-symmetry $SU(2) \times SU(2)$ being manifest. Therefore $I = 1, 2, \quad \hat{I} = \hat{1}, \hat{2}$, and one may identify the R-symmetry index I with the little group index α (and $\hat{I}$ with $\dot{\alpha}$), and superamplitudes become differential forms after the identification $\eta \to d\lambda, \tilde{\eta} \to d\tilde{\lambda}$ [123].

The momentum amplituhedron $\mathcal{M}_{n,k}$ is defined as a pair of Grassmannian elements $(\tilde{Y}, Y) \in G(k, k+2) \times G(n-k, n-k+2)$:

$$\tilde{Y}_{\dot{a}}^{\dot{A}} = \sum_{i=1}^n c_{\dot{a}i} \tilde{\Lambda}_i^{\dot{A}} \qquad Y_a^A = \sum_{i=1}^n c_{ai}^\perp \Lambda_i^A, \tag{5.2.3}$$

---

*For further study on the momentum amplituhedron, see [124–126].

where $c_{\dot{a}i}$ are the elements of the positive Grassmannian $G_+(k,n)$ and $c_{\dot{a}i}^\perp$ are the element of its orthogonal complement. Although the dimension of the $(\tilde{Y}, Y)$ space is

$$\dim(G(k, k+2)) + \dim(G(n-k, n-k+2)) = 2(n-k) + 2k = 2n, \qquad (5.2.4)$$

the momentum amplituhedron $(\tilde{Y}, Y)$ is satisfying the following relation:

$$P^{\alpha\dot{\alpha}} = \sum_{i=1}^{n} \left(Y^\perp \cdot \Lambda^T\right)_i^\alpha \left(\tilde{Y}^\perp \cdot \tilde{\Lambda}^T\right)_i^{\dot{\alpha}} = 0. \qquad (5.2.5)$$

Then the momentum amplituhedron has dimension $2n - 4$.

The definition of the momentum amplituhedron implies particular sign patterns for Y and $\tilde{Y}$ brackets

$$\{\langle Y12\rangle, \langle Y13\rangle, \ldots, \langle Y1n\rangle\} \text{ has } k-2 \text{ sign flips}, \qquad (5.2.6)$$

$$\{[\tilde{Y}12], [\tilde{Y}13], \ldots, [\tilde{Y}1n]\} \text{ has } k \text{ sign flips}. \qquad (5.2.7)$$

Here we introduce the brackets

$$\langle Yij\rangle = \epsilon_{A_1 A_2 \ldots A_{n-k+2}} Y_{i_1}^{A_1} Y_{i_2}^{A_2} \ldots Y_{i_{n-k}}^{A_{n-k}} \Lambda_i^{A_{n-k+1}} \Lambda_j^{A_{n-k+2}},$$

$$[\tilde{Y}ij] = \epsilon_{\dot{A}_1 \dot{A}_2 \ldots \dot{A}_{k+2}} \tilde{Y}_{i_1}^{\dot{A}_1} \tilde{Y}_{i_2}^{\dot{A}_2} \ldots \tilde{Y}_{i_k}^{\dot{A}_k} \tilde{\Lambda}_i^{\dot{A}_{k+1}} \tilde{\Lambda}_j^{\dot{A}_{k+2}} . \qquad (5.2.8)$$

The co-dimension one boundaries are then simply given in [54] as follows

$$\langle Yii+1\rangle = [\tilde{Y}ii+1] = 0, \quad \text{and} \quad S_{i,i+1,\cdots,i+p} \equiv \sum_{i \leq j_1 < j_2 \leq i+p} \langle Yj_1j_2\rangle[\tilde{Y}j_1j_2] = 0 \,, \qquad (5.2.9)$$

where the first two are related to the collinear limits and the last corresponds to factorisation of the amplitudes. Note that as discussed in [54] it is crucial for the external kinematics to be ordered on the moment curve for the planar Mandelstams to be positive, and hence its zero being the boundaries.

In order to obtain scattering amplitudes from the momentum amplituhedron, we need to construct the canonical form $\boldsymbol{\Omega}_{n,k}$ with logarithmic singularities on all boundaries. The momentum amplituhedron $\mathcal{M}_{n,k}$ is $2n-4$ dimensional and therefore its canonical form $\boldsymbol{\Omega}_{n,k}$ has also the same degree. One then constructs the volume form

$$V_{vol} = \prod_{a=1}^{n-k} \langle Y_1 \ldots Y_{n-k} d^2 Y_a\rangle \prod_{\dot{a}=1}^{k} [\tilde{Y}_1 \ldots \tilde{Y}_k d^2 \tilde{Y}_{\dot{a}}] \Omega_{n,k} \,, \qquad (5.2.10)$$

through the relation

$$\mathbf{\Omega}_{n,k} \wedge d^4 P \delta^4(P) = \prod_{a=1}^{n-k} \langle Y_1 \dots Y_{n-k} d^2 Y_a \rangle \prod_{\dot{a}=1}^{k} [\tilde{Y}_1 \dots \tilde{Y}_k d^2 \tilde{Y}_{\dot{a}}] \Omega_{n,k} \delta^4(P) . \qquad (5.2.11)$$

The amplitude is obtained from the volume function $\Omega_{n,k}$, where we localize $(Y, \tilde{Y})$ to $(Y^*, \tilde{Y}^*)$:

$$Y^* = \begin{pmatrix} \mathbb{0}_{2 \times (n-k)} \\ \mathbb{1}_{(n-k) \times (n-k)} \end{pmatrix}, \quad \tilde{Y}^* = \begin{pmatrix} \mathbb{0}_{2 \times (k)} \\ \mathbb{1}_{(k) \times (k)} \end{pmatrix} . \qquad (5.2.12)$$

The amplitude can be obtained by integrating out the auxiliary fermionic variables ϕ and $\tilde{\phi}$ that we have introduced

$$\mathcal{A}_{n,k}^{\text{tree}} = \delta^4(p) \int d^2 \phi^1 \dots d^2 \phi^{n-k} \int d^2 \tilde{\phi}^1 \dots d^2 \tilde{\phi}^k \, \Omega_{n,k}(Y^*, \tilde{Y}^*, \Lambda, \tilde{\Lambda}) . \qquad (5.2.13)$$

In practice one can use the BCFW triangulation to construct the form for $\mathbf{\Omega}_{n,k}$. We write

$$\mathbf{\Omega}_{n,k} = \sum_{\sigma} \int_{\mathcal{C}_{\{M_\sigma\}}} \frac{d^{n \times k} c}{\text{Vol}(GL(k))} \frac{1}{M_1 M_2 \cdots M_n} \Bigg|_{Y = c^\perp \cdot \Lambda, \, \tilde{Y} = c \cdot \tilde{\Lambda}} , \qquad (5.2.14)$$

where σ labels the set of BCFW cells that constitute the tree amplitude, with each cell characterized by a set of vanishing minors $\{M_\sigma\}$ and hence the integration contour $\mathcal{C}_{\{M_\sigma\}}$. To obtain $\Omega_{n,k}$, one starts with the $G_+(k,n)$ top cell c, and solve for the set of vanishing minors associated with each cell $\{M_\sigma\}$. Next, momentum conservation in (5.2.5) is used to constrain the top cell c' of $G_+(n-k, k)$. We partially solve it so that $c' = c^\perp + \Delta$ where Δ would contain four unfixed parameters, which will be set to zero on the support of $\delta^4(P)$. Matching both sides of (5.2.11) allows us to fix $\Omega_{n,k}$.

5.3 The orthogonal momentum amplituhedron

In this section, we will introduce the orthogonal momentum amplituhedron geometry. We will define it in two ways. In the first way, we utilize the positive orthogonal Grassmannian OG_+ through the definition of $Y = C \cdot \Lambda$, with $C \in OG_+$. We will also define the geometry by understanding its sign flipping structures. The canonical forms of the orthogonal momentum amplituhedron and their relations to the amplitudes in the ABJM theory will be studied in the next section 5.4.

5.3.1 Definition of the orthogonal momentum amplituhedron

In this section, we define the Orthogonal momentum amplituhedron. Again, we first consider the positive external data, where Λ_i^A are $2k$ ordered points on an $k+2$-dimensional moment curve:

$$\Lambda_i^A = x_i^{A-1}, \tag{5.3.1}$$

where x_is are arbitrary ordered points $x_1 < x_2 < \cdots < x_n$. This arrangement will be necessary for the planar Mandelstams to be positive as we will soon see. For ABJM we will always have $2k = n$, thus from the get go the geometry is closely related to the middle sector (split helicity) of $\mathcal{N} = 4$ sYM. As a result the moment matrix $\Lambda_i^A \in G(k+2, 2k)$ will have all ordered minors being positive. This matrix will be identified as the bosonized kinematic variables

$$\Lambda_i^A = \begin{pmatrix} \lambda_i^\alpha \\ \phi_I^a \cdot \eta_i^I \end{pmatrix}, \quad A = (\alpha, a) = 1, 2, \ldots, k+2, \tag{5.3.2}$$

where we introduced k auxiliary Grassmann variables ϕ_I with $I = 1, 2$, which are contracted.[*] On the space of Λ's we define a kinematic bracket

$$\langle i_1 i_2 \ldots i_{k+2} \rangle = \epsilon_{A_1 A_2 \ldots A_{k+2}} \Lambda_{i_1}^{A_1} \Lambda_{i_2}^{A_2} \ldots \Lambda_{i_{k+2}}^{A_{k+2}}. \tag{5.3.3}$$

We define the Orthogonal momentum amplituhedron as a Grassmannian element Y given by:

$$Y_a^A = \sum_{i=1}^n c_{ai} \Lambda_i^A, \tag{5.3.4}$$

where $a = 1, \cdots, k$ and $A = 1, \cdots, k+2$. Here Λ_i^A is an element of the positive moment matrix, c_{ai} is an element of positive orthogonal Grassmannian $OG_+(k, 2k)$ in the positive branch. The definition of the positive orthogonal Grassmannian which is the moduli space of null planes, as discussed in [30, 52]. The important point is that the positive part of orthogonal Grassmannian is defined with respect to the split signature metric $\eta^{ij} = (+, -, +, \ldots, -)$, and the orthogonal constraints take the form:

$$\eta^{ij} C_{ai} C_{bj} = 0. \tag{5.3.5}$$

In this signature, the minors satisfy $M_I / M_{\bar{I}} = \pm 1$, where $\bar{I}$ is the ordered complement of I. For $M_I / M_{\bar{I}} = 1(-1)$, the $OG_+(k, 2k)$ is called "positive (negative)" branch.

---

[*]As we will discuss later in section 5.4, it is natural to work in the $\mathcal{N} = 4$ formalism for the construction of the orthogonal momentum amplituhedron, therefore $I = 1, 2$, instead of $I = 1, 2, 3$ in the case of the $\mathcal{N} = 6$ formalism. This is realized through a SUSY reduction as we will show in detail in section 5.4.

The dimension of the orthogonal momentum amplituhedron is $n - 3$. First, since $Y \in G(k, k + 2)$, we have:

$$\dim(G(k, k + 2)) = 2k = n. \tag{5.3.6}$$

Indeed, the orthogonal momentum amplituhedron lives on a co-dimension 3 surface inside $G(k, k + 2)$ satisfying:

$$0 = \sum_{i=1}^{n} P_i^{\alpha\beta} = \sum_{i=1}^{n} (-1)^i \left(Y^{\perp} \cdot \Lambda^T \right)_i^{\alpha} \left(Y^{\perp} \cdot \Lambda^T \right)_i^{\beta}. \tag{5.3.7}$$

We can see this from the definition (5.3.4). Let us start from the following equation:

$$0 = Y^{\perp} \cdot Y^T = Y^{\perp} \cdot \Lambda^T \cdot C^T. \tag{5.3.8}$$

Then the 2-dimensional space $Y^{\perp} \cdot \Lambda^T$ is a subspace of $(C^T)^{\perp}$. This means that the space $Y^{\perp} \cdot \Lambda^T$ is orthogonal. Since we take the odd legs as the outgoing and even legs as ingoing, there is a $(-1)^i$ factor. Therefore, combining (5.3.6) and (5.3.7), we deduce the orthogonal momentum amplituhedron has dimension $n - 3$.

Defining the planar Mandelstam variables as

$$S_{i,i+1,\ldots,i+p} = \sum_{i \leq j_1 < j_2 \leq i+p} (-1)^{j_1 + j_2 + 1} \langle Y j_1 j_2 \rangle^2, \tag{5.3.9}$$

where the (-1) factor reflects the fact that the odd (even) legs as outgoing (ingoing) momenta, the orthogonal momentum amplituhedron has two type of the boundaries:

$$\underbrace{S_{i,\, i+1,\, \ldots,\, i+p}}_{\text{odd}} = 0, \qquad p = 2, 4, 6, \ldots, \tag{5.3.10}$$

$$\underbrace{S_{i,\, i+1,\, \ldots,\, i+p}}_{\text{even}} = 0, \qquad p = 1, 3, 5, \ldots. \tag{5.3.11}$$

Note that since $\langle Y i\, i{+}1 \rangle^2 = S_{i,i+1}$, the boundary associated with $\langle Y i\, i{+}1 \rangle = 0$ is the same as $S_{i,i+1}$. As we will see later, only "odd-particle Mandelstam variables" (5.3.10) are the co-dimension one boundaries, the other "even-particle Mandelstam variables" (5.3.11) are higher co-dimension boundaries. To see that these are boundaries, we need to first check the positivity of the planar Mandelstam variables for all points in the orthogonal momentum amplituhedron. Although this positivity is not manifest from the definition (5.3.4), we can check this fact by using the explicit C-matrix parametrization.

Here we have used the "Veronese parametrization" of the C-matrix:[*]

$$
C = \begin{pmatrix}
t_1 & t_2 & t_3 & \cdots & t_n \\
t_1 z_1 & t_2 z_2 & t_3 z_3 & \cdots & t_n z_n \\
t_1 z_1^2 & t_2 z_2^2 & t_3 z_3^2 & \cdots & t_n z_n^2 \\
\vdots & \vdots & \vdots & \cdots & \vdots \\
t_1 z_1^{k-1} & t_2 z_2^{k-1} & t_3 z_3^{k-1} & \cdots & t_n z_n^{k-1}
\end{pmatrix}, \tag{5.3.12}
$$

where $t_2, \ldots, t_n$ are given as

$$
t_i = t_1 \frac{\sqrt{\prod_{j \geq 2, j \neq i}(z_j - z_1)}}{\sqrt{\prod_{j \geq 2, j \neq i}(z_j - z_i)}} . \tag{5.3.13}
$$

When these parameters satisfy $t_1 > 0, z_i > 0$ and $z_i - z_j > 0$ for $i > j$, all ordered minors of C are positive. By using this parametrization, we have checked numerically that $S_{i,i+1,\ldots,i+p}$ are indeed positive up to 10-points.

In the section 5.4, we will further show that the BCFW cells tile the space of Y, and hence the boundaries in (5.3.10) and (5.3.11) are simply a reflection of that for the collection of cells.

5.3.2 Sign flip definition

The orthogonal momentum amplituhedron defined in (5.3.4) can also be carved out by imposing constraints directly on Y through a set of sign flip conditions. First note that (5.3.4) is the same as the one of the ordinary amplituhedron with $m = 2$ [27] except the orthogonal condition in C-matrix. Following [127], the sign flip definition of the $m = 2$ amplituhedron

$$
\langle Y\,i\,i+1 \rangle > 0 \,,
$$
$$
\{\langle Y12 \rangle, \langle Y13 \rangle, \ldots, \langle Y1n \rangle\} \text{ has } k \text{ sign flips} \,, \tag{5.3.14}
$$

along with positive external data (in the sense of positive ordered minors) is conjectured to fix Y to (5.3.4). The additional condition is the orthogonality of the Grassmannian. We will show that the condition

$$
\sum_{j=1}^{n} (-1)^j \langle Y\,j\,a \rangle \langle Y\,j\,b \rangle = 0, \quad \text{for } a, b = 1, \cdots, n \,, \tag{5.3.15}
$$

---

[*]This is instrumental in connecting the geometry of the moduli space of punctured disk to the amplituhedron as explored recently in [31].

is equivalent to the orthogonal condition of the C-matrix. Therefore the sign flip conditions (5.3.14) and the condition (5.3.15) give the sign flip definition of the orthogonal momentum amplituhedron. This definition reveals the fact the geometry for Y is the same as $\tilde{Y}$ for $\mathcal{N} = 4$ sYM, with the extra orthogonal condition in (5.3.15). Thus the geometry for ABJM amplitude lives on a subspace of the geometry for the split-helicity sector of $\mathcal{N} = 4$ sYM!

To see the equivalence of (5.3.15) and the orthogonality of C-matrix, we rewrite the relation (5.3.15) as

$$\sum_{j=1}^{n}(-1)^j\langle Yja\rangle\langle Yjb\rangle = \sum_{j=1}^{n}\sum_{\substack{i_1<\cdots<i_k \\ j_1<\cdots<j_k}}(-1)^j M_{i_1i_2\ldots i_k}M_{j_1j_2\ldots j_k}\langle i_1i_2\ldots i_kja\rangle\langle j_1j_2\ldots j_kjb\rangle,$$

(5.3.16)

where $M_{i_1,\ldots,i_k}$ is the minor of the C-matrix. Let us consider only terms that are proportional to $\langle a_1a_2\ldots a_ka_{k+1}a\rangle\langle b_1b_2\ldots b_kb_{k+1}b\rangle$, where $j \in (a_1,\ldots,a_{k+1}),(b_1,\ldots,b_{k+1})$. These terms can be expressed as

$$\sum_{j=c_1}^{c_{k'}}(-1)^j M_{a_1\ldots\hat{j}\ldots a_{k+1}}M_{b_1\ldots\hat{j}\ldots b_{k+1}}\langle a_1\ldots\hat{j}\ldots a_{k+1}ja\rangle\langle b_1\ldots\hat{j}\ldots b_{k+1}jb\rangle, \quad (5.3.17)$$

where the sum of j runs only the common parts $(a_1,\ldots,a_{k+1}) \cap (b_1,\ldots,b_{k+1}) \equiv (c_1,\ldots,c_{k'})$ and $c_1 = \max\{a_1,b_1\}, c_{k'} = \min\{a_k,b_k\}$. Without loss of generality, we can fix $\max\{a_1,b_1\} = a_1 = b_m$ (for some integer m) and $\min\{a_k,b_k\} = a_k(= b_{k+m-1})$. Then all the kinematic brackets of the right side of (5.3.17) become $(-1)^m\langle a_1\ldots a_{k+1}a\rangle\langle b_1\ldots b_{k+1}b\rangle$. Therefore equation (5.3.17) reduces to

$$(-1)^m\left(\sum_{j=c_1}^{c_{k'}}(-1)^j M_{a_1\ldots\hat{j}\ldots a_{k+1}}M_{b_1\ldots\hat{j}\ldots b_{k+1}}\right)\langle a_1\ldots a_{k+1}a\rangle\langle b_1\ldots b_{k+1}b\rangle. \quad (5.3.18)$$

Since the minors of the positive orthogonal Grassmannian satisfy $M_I = M_{\bar{I}}$, where $\bar{I}$ is the complement of I, therefore,

$$\sum_{j=c_1}^{c_{k'}}(-1)^j M_{a_1\ldots\hat{j}\ldots a_{k+1}}M_{b_1\ldots\hat{j}\ldots b_{k+1}} = \sum_{j=c_1}^{c_{k'}}(-1)^j M_{a_1\ldots\hat{j}\ldots a_{k+1}}M_{\bar{b}_1\ldots j\ldots\bar{b}_{k-1}} = 0. \quad (5.3.19)$$

Here we used the Plücker relation

$$\sum_{l=1}^{k+1}(-1)^l M_{i_1\ldots i_{k-1},j_l}M_{j_1\ldots\hat{j}_l\ldots j_{k+1}} = 0. \quad (5.3.20)$$

We conclude that, since our choice of the $(i_1,\ldots,i_k,j),(j_1,\ldots,j_k,j)$ is general, the relation (5.3.15) holds for general kinematics when the C-matrix satisfies the orthogonal

conditions.

We further argue that (5.3.19) implies orthogonality in a similar manner as Appendix A of [30]. We gauge fix the $k \times 2k$ matrix to be

$$
C = (\mathbb{1}, c) = \begin{pmatrix} 1 & 0 & 0 & 0 & c_{1,k+1} & \cdots & c_{1,2k} \\ 0 & 1 & 0 & 0 & c_{2,k+1} & \cdots & c_{2,2k} \\ 0 & 0 & \cdots & 0 & \vdots & \vdots & \vdots \\ 0 & 0 & 0 & 1 & c_{k,k+1} & \cdots & c_{k,2k} \end{pmatrix} . \tag{5.3.21}
$$

The orthogonal condition $C \cdot C^T = 0$ is equivalent to

$$
c \cdot c^T = c^T \cdot c = -\mathbb{1} . \tag{5.3.22}
$$

While $c^T \cdot c = -\mathbb{1}$ gives

$$
1 + \sum_{j=1}^{k} c_{j,A}^2 = 0, \quad \text{and} \sum_{j=1}^{k} c_{j,A} c_{j,B} = 0, \quad A, B = k+1, \cdots, 2k, \tag{5.3.23}
$$

which we are going to show that it is equivalent to (5.3.19). Let us first choose $\{a_1, \cdots, a_{k+1}\} = \{b_1, \cdots, b_{k+1}\}$. Without loss of generality, if we choose $\{a_1, \cdots, a_{k+1}\}$ to be the first $k+1$ columns of (5.3.21), it is easy to see (5.3.19) gives the diagonal part of orthogonal constraints in (5.3.23). Next, we consider $\{a_1, \cdots, a_k\} = \{b_1, \cdots, b_k\}$ while $a_{k+1} \neq b_{k+1}$. With no loss of generality we set $\{a_1, \cdots, a_k\}$ to be the first k columns of (5.3.21), then one can see that in such choice, (5.3.19) produces the off-diagonal part of (5.3.23).

This finishes the proof that the conditions (5.3.15) are equivalent to the orthogonal conditions on the C-matrix.

5.4 Canonical forms from the Orthogonal Grassmannian

In the previous section we have defined the orthogonal momentum amplituhedron as a positive kinematic map from the positive orthogonal Grassmannian. In this section we will consider its boundaries in more detail, showing that it corresponds to the physical boundaries of ABJM amplitude. Note that since the four and six-point amplitude corresponds to the top cell of $OG_+(2,4)$ and $OG_+(3,6)$ respectively, the boundary of the amplitude trivially matches to the amplituhedron. For more than six points, the amplitude is associated with a sum over lower dimensional cells (BCFW cells). Thus if the BCFW cells tile the amplituhedron, and are non-overlapping, then the boundaries of the amplitude can be mapped to those of the amplituhedron.

Let us consider the first non-trivial example, the eight-point amplitude, which is

a sum of two BCFW cells. We begin by choosing the top-cell C-matrix and fixed positive kinematics Λ. This gives a point $Y = C \cdot \Lambda$ inside the orthogonal momentum amplituhedron. We can check whether or not only one of the BCFW cells contains this point. More precisely, if we represent this point by using the BCFW C-matrices of the BCFW cells and the same positive kinematics, only one of them can reproduce this point. By checking this holds for many points inside the eight-point space numerically, we have verified that the eight-point BCFW cells are non-overlapping and tilling the orthogonal momentum amplituhedron space.

After confirming that the BCFW cells indeed tile the space, we can then utilize this connection to construct the volume form. We will construct the canonical form derived from the Grassmannian integral with reduced SUSY. We begin by discussing the $\mathcal{N} = 4$ formalism of ABJM amplitudes and the corresponding orthogonal Grassmannian and on-shell diagram constructions. We find the volume form of each on-shell diagram in the $\mathcal{N} = 4$ formalism is naturally a canonical $d\log$ form. In contrast, for the case of $\mathcal{N} = 6$ formalism, one needs to introduce the so-called Jacobian factors to incorporate the mismatch of the bosonic and fermionic delta-functions. We will then study the canonical forms in the language of the orthogonal momentum amplituhedron.

5.4.1 ABJM amplitudes and the Orthogonal Grassmannian in $\mathcal{N} = 4$ formalism

The ABJM theory is a three-dimensional Chern-Simons matter theory with $\mathcal{N} = 6$ supersymmetry. The physical degrees of freedom consist of the 4 complex scalars X_A, 4 complex fermions $\psi^{A\alpha}$ and their complex conjugates $\bar{X}^A, \bar{\psi}_{A\alpha}$ with $A = 1, 2, 3, 4$ and $\alpha = 1, 2$. These fields transform in the fundamental or anti-fundamental of the R-symmetry $SU(4)$ and in the bi-fundamental representation under the gauge group $U(N) \times U(N)$. The index α denotes the spinor representation in the three-dimensional Lorentz group. Let us define super-fields of the ABJM

$$\Phi^{\mathcal{N}=6} = X_4 + \eta_A \psi^A - \frac{1}{2}\epsilon^{ABC}\eta_A\eta_B X_C - \eta_1\eta_2\eta_3\psi^4 \,, \tag{5.4.1}$$

$$\bar{\Psi}^{\mathcal{N}=6} = \bar{\psi}_4 + \eta_A \bar{X}^A - \frac{1}{2}\epsilon^{ABC}\eta_A\eta_B\bar{\psi}_C - \eta_1\eta_2\eta_3\bar{X}^4 \,, \tag{5.4.2}$$

here we have decomposed the fields as $X_A \to (X_4, X_A)$ and $\psi_A \to (\psi_4, \psi_A)$, and the index A runs from $A = 1, 2, 3$ from now on, for which we apologise the abuse of notation.

The tree-level super-amplitudes in ABJM theory can be written as:

$$\mathcal{A}_n^{\text{tree}} = \delta^3\left(\sum_{i=1}^n p_i\right)\delta^6\left(\sum_{i=1}^n q_i\right)F_n(\lambda_i, \eta_i) \,, \tag{5.4.3}$$

where p and q are the on-shell momentum and supermomentum

$$(p_i)^{\alpha\beta} = \lambda_i^\alpha \lambda_i^\beta, \quad q_i^{\alpha A} = \lambda_i^\alpha \eta_i^A. \tag{5.4.4}$$

The function F_n is a rational function of Lorentz invariants.

In three dimensions, the on-shell variables transform under the little group Z_2 as

$$\lambda_i^\alpha \to -\lambda_i^\alpha, \quad \eta_i^A \to -\eta_i^A. \tag{5.4.5}$$

There are only two states, the fermion state that obtains a minus sign under (5.4.5), and the scalar state that does not. Under little group transformations (5.4.5) if external leg i, the function F_n changes as

$$F_n \to \begin{cases} F_n & i \in \Phi \\ -F_n & i \in \Psi. \end{cases} \tag{5.4.6}$$

From this, there are only two classes of amplitudes

$$\mathcal{A}_n(\bar{1}2\bar{3}\ldots 2k), \quad \mathcal{A}_n(1\bar{2}3\ldots \bar{2k}), \tag{5.4.7}$$

here we denote $\bar{i}$ that leg i is $\bar{\Psi}$ and use the fact that only even-multiplicity scattering amplitudes can be non-vanishing for this ABJM theory.

As we remarked earlier, that it is vital to work in the $\mathcal{N} = 4$ formalism for the construction of the orthogonal momentum amplituhedron. One may obtain the $\mathcal{N} = 4$ superfields from the more familiar $\mathcal{N} = 6$ superfields through a SUSY reduction. They are defined as,

$$\Phi^{\mathcal{N}=4} := \Phi^{\mathcal{N}=6}\big|_{\eta^3 \to 0} = X_4 + \eta_I \psi^I + (\eta)^2 X_3\,,$$

$$\bar{\Phi}^{\mathcal{N}=4} := \int d\eta^3 \bar{\Psi}^{\mathcal{N}=6} = \bar{X}^3 + \eta_I \bar{\psi}^I - (\eta)^2 \bar{X}^4\,,$$

$$\Psi^{\mathcal{N}=4} := \int d\eta^3 \Phi^{\mathcal{N}=6} = \psi^3 + \eta_I X^I + (\eta)^2 \psi^4\,,$$

$$\bar{\Psi}^{\mathcal{N}=4} := \bar{\Psi}^{\mathcal{N}=6}\big|_{\eta^3 \to 0} = \bar{\psi}_4 + \eta_I \bar{X}^I + (\eta)^2 \bar{\Psi}_3\,, \tag{5.4.8}$$

here we have decomposed the fields as $X_A \to (X_4, X_3, X_I)$ and $\psi_A \to (\psi_4, \psi_3, \psi_I)$, with $I = 1, 2$. The superamplitudes in the $\mathcal{N} = 4$ formalism can again be obtained by the same SUSY reduction, namely setting k of $\eta^3 \to 0$ and integrating out the other k of η^3 for a $2k$-point superamplitude.

The orthogonal Grassmannian is defined as the space of k-planes in $\mathbb{C}^n$, such that $\eta^{ij} C_{ai} C_{bj} = 0$. A tree-level $(n = 2k)$-point scattering amplitudes of ABJM is given as a

sum of the residues of the integral over an orthogonal Grassmannian $C_{ai} \in OG(k, 2k)$

$$\mathcal{A}_{2k} = \int \frac{d^{2k \times k} C_{ai}}{\text{Vol}(\text{GL}(k))} \frac{M_{i_1, i_2, \ldots, i_k}}{M_1 M_2 \ldots M_k} \delta^{k(k+1)/2} (C \cdot C^T) \prod_{a=1}^{k} \delta^{2|2}(C_a \cdot \Lambda), \qquad (5.4.9)$$

where M_i are the i-th consecutive minor

$$M_i \equiv \sum_{a_1, a_2, \ldots, a_k} \epsilon_{a_1 a_2 \ldots a_k} c_{i a_1} c_{i+1 a_2} \ldots c_{i+k a_k} . \qquad (5.4.10)$$

The numerator $M_{i_1, i_2, \ldots, i_k}$ is given by

$$M_{i_1, i_2, \ldots, i_k} = \sum_{a_1, a_2, \ldots, a_k} \epsilon_{a_1 a_2 \ldots a_k} c_{i_1 a_1} c_{i_2 a_2} \ldots c_{i_k a_k} . \qquad (5.4.11)$$

It is due to the fact that we work in the $\mathcal{N} = 4$ formalism, arising from the SUSY reduction we discussed above, where $i_1, i_2, \ldots, i_k$ are superfields of either $\bar{\Phi}^{\mathcal{N}=4}$ or $\Psi^{\mathcal{N}=4}$ in (5.4.8). The integration over η^3 for each of these fields generates $M_{i_1, i_2, \ldots, i_k}$.

A few remarks are in order here. Firstly, in the $\mathcal{N} = 4$ formalism, as indicated in (5.4.9), the bosonic and fermionic delta-functions, $\delta^{2|2}(C_a \cdot \Lambda)$, match each other. One of the consequences of this is that, unlike $\mathcal{N} = 6$ formalism [30, 52], the so-called Jacobi are not required for the volume forms of the on-shell diagrams in the $\mathcal{N} = 4$ formalism. As we will see shortly, they are given by products of canonical $d \log$ forms for each on-shell diagram. Secondly, due to the fact that the geometry of orthogonal momentum amplituhedron has the cyclic invariance, we will consider the amplitudes

$$\mathcal{A}_{2k}(\bar{\Phi}_1^{\mathcal{N}=4}, \Phi_2^{\mathcal{N}=4}, \bar{\Phi}_3^{\mathcal{N}=4}, \Phi_4^{\mathcal{N}=4}, \ldots, \Phi_{2k}^{\mathcal{N}=4}), \qquad (5.4.12)$$

which implies the numerator in (5.4.9) is $M_{1,3,\ldots,2k-1}$[*]. With this choice, $\mathcal{A}_{2k}$ defined in (5.4.9) has the cyclic invariance. Thirdly, again thanks to the match of bosonic and fermionic variables in the $\mathcal{N} = 4$ formalism, one may identify η^I by $d\lambda^\alpha$. This will lead to a differential form representation of scattering amplitudes in ABJM theory in an analogous construction of scattering amplitudes in $\mathcal{N} = 4$ sYM in four dimensions [123].

The building blocks of on-shell diagrams for ABJM theory are the four-point am-

---

[*]One may also consider $\mathcal{A}_{2k}(\bar{\Psi}_1^{\mathcal{N}=4}, \Psi_2^{\mathcal{N}=4}, \bar{\Psi}_3^{\mathcal{N}=4}, \Psi_4^{\mathcal{N}=4}, \ldots, \Psi_{2k}^{\mathcal{N}=4})$, for which we have $M_{2,4,\ldots,2k}$ in the numerator.
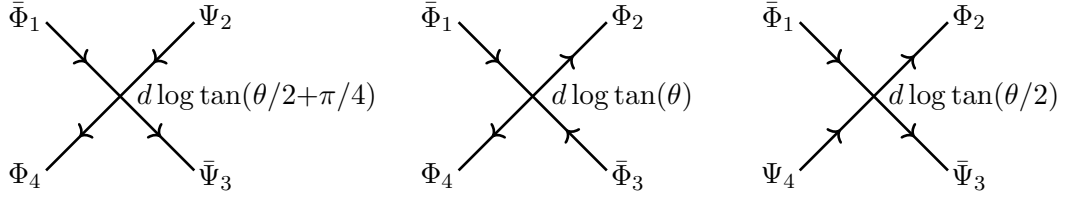
Figure 5.1: The three four-point vertices of $\mathcal{N} = 4$ formalism of on-shell diagram representation of scattering amplitudes in ABJM theory.

plitudes, which in the $\mathcal{N} = 4$ formalism are given by

$$\mathcal{A}_4(\bar{\Phi}_1^{\mathcal{N}=4}, \Psi_2^{\mathcal{N}=4}, \bar{\Psi}_3^{\mathcal{N}=4}, \Phi_4^{\mathcal{N}=4}) = \int dC \delta^3(CC^T)\delta^{2|2}(C \cdot \Lambda)\frac{1}{(23)} ,$$

$$\mathcal{A}_4(\bar{\Phi}_1^{\mathcal{N}=4}, \Phi_2^{\mathcal{N}=4}, \bar{\Phi}_3^{\mathcal{N}=4}, \Phi_4^{\mathcal{N}=4}) = \int dC \delta^3(CC^T)\delta^{2|2}(C \cdot \Lambda)\frac{(13)}{(12)(23)} ,$$

$$\mathcal{A}_4(\bar{\Phi}_1^{\mathcal{N}=4}, \Phi_2^{\mathcal{N}=4}, \bar{\Psi}_3^{\mathcal{N}=4}, \Psi_4^{\mathcal{N}=4}) = \int dC \delta^3(CC^T)\delta^{2|2}(C \cdot \Lambda)\frac{(14)}{(12)(23)} . \quad (5.4.13)$$

Using the $OG_+(2,4)$,

$$C = \begin{pmatrix} 1 & \cos\theta & 0 & -\sin\theta \\ 0 & \sin\theta & 1 & \cos\theta \end{pmatrix} , \quad (5.4.14)$$

we find the three types of four-point amplitudes can all be expressed in $d\log$ forms, as shown in Fig.5.1. The incoming arrows represent the superfields $\bar{\Phi}^{\mathcal{N}=4}$ or $\Psi^{\mathcal{N}=4}$, and they are obtained by integrating out η^3 as shown in (5.4.8); whereas the outgoing arrows represent the superfields $\Phi^{\mathcal{N}=4}$ or $\bar{\Psi}^{\mathcal{N}=4}$, which are obtained by setting $\eta^3 \to 0$.

These four-point vertices form building blocks for the on-shell diagrams of the amplitudes in ABJM theory, and one may glue them together to form more general diagrams. Generally, the n-point superamplitudes in the $\mathcal{N} = 4$ formalism can be expressed as

$$\mathcal{A}_{2k} = \int \prod_{a=1}^{k} \delta^{2|2}(C_a \cdot \Lambda)\,\omega_{2k} , \quad (5.4.15)$$

here $n = 2k$. The integrand ω_{2k} is obtained by gluing the four-point vertices given in Fig.5.1 in all possible ways following the BCFW construction of tree-level amplitudes. Each diagram is given by products of $d\log$'s, and ω_{2k} is a sum of these canonical $d\log$ forms. As we anticipated, when we express c_{ai} of $OG_+(k, 2k)$ in terms of Y under the support of $Y = C \cdot \Lambda$, ω_{2k} essentially becomes the canonical form of the orthogonal momentum amplituhedron, $\mathbf{\Omega}_{2k,k}^{3d}$, which we will study in details in the next section. It is therefore vital to construct ω_{2k}, as we will do below.

Let us begin with the six-point case as an example. There are two diagrams con-
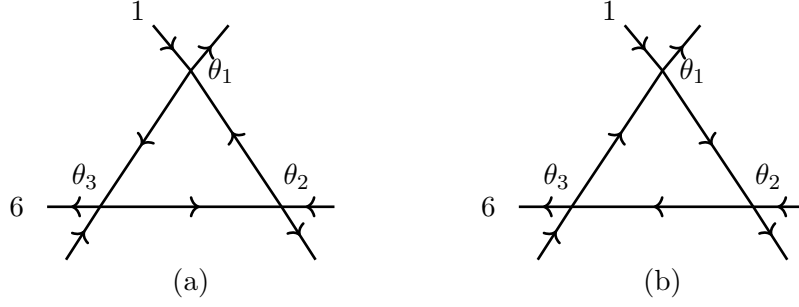
Figure 5.2: The two six-point diagrams correspond to different ways of arranging arrow flow of the internal lines. Here and throughout this paper we only label the first and last external legs.

tributing to six-point amplitude, as shown in Fig.5.2 that correspond to two different choices of internal arrow flows. Each diagram in this formalism takes a canonical $d\log$ form. The contribution from the diagram on the left, Fig.5.2 (a), is given by

$$\omega_{6,1} = \bigwedge_{i=1}^{3} d\log\tan(\theta_i)\,, \tag{5.4.16}$$

and the contribution from the right, Fig.5.2 (b), can be expressed as

$$\omega_{6,2} = \bigwedge_{i=1}^{3} d\log\tan(\theta_i/2) = c_1 c_2 c_3 \bigwedge_{i=1}^{3} d\log\tan(\theta_i)\,. \tag{5.4.17}$$

They are obtained by simply gluing the four-point amplitudes given in (5.4.13) and Fig. 5.1. One may combine these two contributions, which lead to

$$\omega_6 = \omega_{6,1} + \omega_{6,2} = (1 + c_1 c_2 c_3) \bigwedge_{i=1}^{3} d\log\tan\theta_i\,. \tag{5.4.18}$$

This is in agreement with the result in [30, 52] using the $\mathcal{N} = 6$ formalism. In the $\mathcal{N} = 6$ formalism, there is a single BCFW diagram, due to the mismatch of the bosonic and fermionic delta-functions, which leads to the prefactor $(1 + c_1 c_2 c_3)$ arising as a Jacobian.

The construction applies to on-shell diagram representation of higher-point amplitudes, both at tree and loop levels. We conclude this section by considering the eight-point BCFW diagrams, as shown in Fig.5.3. Here we only show explicitly one set of four BCFW diagrams, there are four more diagrams, which can be obtained from those in Fig.5.3 by a cyclic shift. The contribution from each diagram in Fig.5.3 again

is given by a canonical $d\log$ form,

$$\omega_{8,1} = \bigwedge_{i=1}^{5} d\log\tan(\theta_i)\,, \tag{5.4.19}$$

$$\omega_{8,2} = \bigwedge_{i=1}^{3} d\log\tan(\theta_i/2+\pi/4) \bigwedge_{i=4}^{5} d\log\tan(\theta_i) = s_1 s_2 s_3 \bigwedge_{i=1}^{5} d\log\tan(\theta_i)\,,$$

$$\omega_{8,3} = \bigwedge_{i=1}^{2} d\log\tan(\theta_i) \bigwedge_{i=3}^{5} d\log\tan(\theta_i/2+\pi/4) = s_3 s_4 s_5 \bigwedge_{i=1}^{5} d\log\tan(\theta_i)\,,$$

$$\omega_{8,4} = \bigwedge_{i=1}^{2} d\log\tan(\theta_i/2+\pi/4) \wedge d\log\tan(\theta_3) \bigwedge_{i=4}^{5} d\log\tan(\theta_i/2+\pi/4)$$

$$= s_1 s_2 s_4 s_5 \bigwedge_{i=1}^{5} d\log\tan(\theta_i)\,.$$

Combining the above four contributions, we have

$$\omega_8 = (1 + s_1 s_2 s_3 + s_3 s_4 s_5 + s_1 s_2 s_4 s_5) \bigwedge_{i=1}^{5} d\log\tan\theta_i\,. \tag{5.4.20}$$

The final expression agrees with the volume form of one of the BCFW diagrams (there are two BCFW diagrams in the $\mathcal{N}=6$ formalism) for the eight-point amplitude obtained originally in [52] using $\mathcal{N}=6$ formalism. In particular, the prefactor $(1 + s_1 s_2 s_3 + s_3 s_4 s_5 + s_1 s_2 s_4 s_5)$ arises as a Jacobian due to the mismatch of the bosonic and fermionic delta-functions.

5.4.2 The canonical forms and boundaries

In this section, we will construct the canonical forms in the Y space of the amplituhedron for tree-level amplitudes in ABJM theory. The dimension of the orthogonal momentum amplituhedron is $(n-3)$, and the canonical form $\mathbf{\Omega}^{3d}_{2k,k}$ is also $(n-3)$ dimensional. We define the independent expression of the volume function $\Omega^{3d}_{2k,k}$ by using $1 = \delta^3(P)d^3P$ as follows:

$$\mathbf{\Omega}^{3d}_{2k,k} \wedge d^3 P \delta^3(P) = \prod_{a=1}^{k} \langle Y_1 \ldots Y_k d^2 Y_a \rangle \delta^3(P) \Omega^{3d}_{2k,k}\,. \tag{5.4.21}$$

In the following, we demonstrate how to obtain volume function $\Omega^{3d}_{2k,k}$ from the canonical form $\mathbf{\Omega}^{3d}_{2k,k}$ through the definition (5.4.21) for $k = 2, 3$ (i.e. four- and six-point amplitudes). For $k = 2$, the canonical form associated with the amplitude (5.4.12) is given in (5.4.13) (or Fig.5.1), which is simply $d\log\tan(\theta)$. Using $Y_a^A = \sum_{i=1}^{4} c_{ai}\Lambda_i^A$,
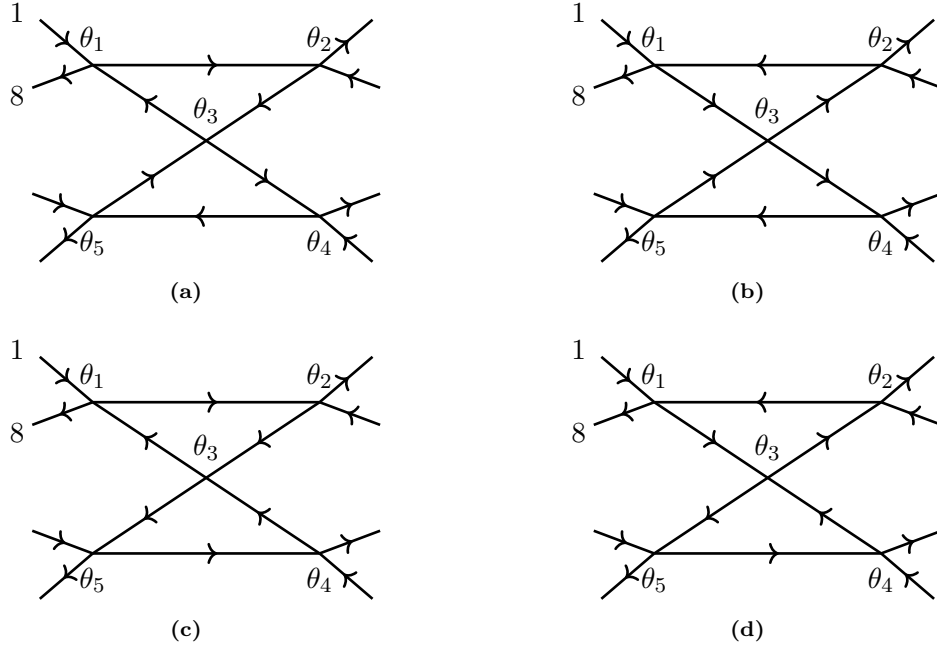
Figure 5.3: There are eight BCFW diagrams that contribute to the eight-point tree-level amplitudes. Here we have only listed four diagrams corresponding to different ways of arranging arrow flow of the internal lines, the other set of four diagrams can be obtained by a simple cyclic shift on the external particles.

we can recast the result in the Y space, which leads to

$$\mathbf{\Omega}_{4,2}^{3d} = d\log\frac{\langle Y12\rangle}{\langle Y23\rangle}\,. \tag{5.4.22}$$

Using the definition (5.4.21), we find that the volume function is given by[*]

$$\Omega_{4,2}^{3d}(Y,\Lambda) = \frac{\langle Y13\rangle}{\langle Y12\rangle\langle Y23\rangle}\,\langle 1234\rangle^2\,. \tag{5.4.23}$$

For the six-point case, the canonical form is given by (5.4.18). The relation between $\tan(\theta_i)$ and Y-bracket can be explicitly solved according to the parametrization of $OG_+(3,6)$, recasting in the Y space we have

$$\mathbf{\Omega}_{6,3}^{3d} = \frac{1}{8}\times d\log\left[\left(\frac{A_{54}^+}{A_{36}^+}\right)^2 - 1\right] \wedge d\log\left[\left(\frac{A_{16}^+}{A_{52}^+}\right)^2 - 1\right] \wedge d\log\left[\left(\frac{A_{32}^+}{A_{14}^+}\right)^2 - 1\right]$$

$$+\frac{1}{8}\times d\log\left[\frac{A_{54}^+ + A_{36}^+}{A_{54}^+ - A_{36}^+}\right] \wedge d\log\left[\frac{A_{16}^+ + A_{52}^+}{A_{16}^+ - A_{52}^+}\right] \wedge d\log\left[\frac{A_{32}^+ + A_{14}^+}{A_{32}^+ - A_{14}^+}\right]\,. \tag{5.4.24}$$

---

[*]Due to the orthogonal conditions (5.3.5), we can also write the 4-pt form as $\frac{\sqrt{\langle Y13\rangle\langle Y24\rangle}}{\sqrt{\langle Y12\rangle\langle Y23\rangle\langle Y34\rangle\langle Y14\rangle}}\langle 1234\rangle^2$, which makes the equal weight of each point explicitly seen.

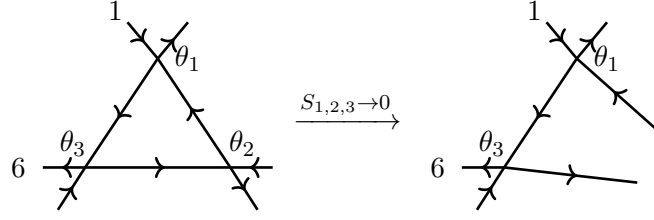**Figure 5.4:** The diagram shows the factorization limit of a six-point diagram, $S_{1,2,3} \to 0$, which corresponds to taking $\theta_2 \to \pi/2$ on the diagram (a) in Fig.5.2, and note that diagram (b) doesn't develop a singularity in this limit.

where $A_{ab}^{\pm}$ are defined as

$$A_{ab}^{\pm} = \sum_{i=1,3,5} \langle Yia \rangle \langle Yib \rangle \pm \langle Ya{+}2\, a{-}2 \rangle \langle Yb{-}2\, b{+}2 \rangle \,. \tag{5.4.25}$$

They are related to the three-particle planar Mandelstam variables as follows

$$A_{52}^+ A_{52}^- = -S_{1,2,3}\, S_{1,3,5}\,, \quad A_{36}^+ A_{36}^- = -S_{2,3,4}\, S_{1,3,5}\,, \quad A_{14}^+ A_{14}^- = -S_{3,4,5}\, S_{1,3,5}\,. \tag{5.4.26}$$

Plugging the above canonical form (5.4.24) in (5.4.21), we obtain the six-point volume function

$$\Omega_{6,3}^{3d}(Y,\Lambda) = \frac{\left(\sum_{i,j=1,3,5} \langle Yij \rangle \langle ij246 \rangle + (1,3,5) \leftrightarrow (2,4,6)\right)^2 S_{1,3,5}}{A_{52}^+ A_{36}^+ A_{14}^+}\,, \tag{5.4.27}$$

We conclude the discussions by studying the boundaries of the momentum amplituhedron. As we remarked previously that the planar Mandelstam variables are all positive for the positive Grassmannian and positive moment kinematics. The volume function at six points develops a singularity when A_{52} approaches to zero, according to (5.4.26) and note that A_{ab}^- never vanish in the positive region, $S_{1,2,3}$ also vanishes, which corresponds to $\theta_2 \to \pi/2$ in Fig.5.2. This opening up of θ_2 is a co-dimension one boundary, which corresponds to the factorization singularity of the amplitude as shown in Fig.5.4. While $\theta_1 \to 0$ corresponds to $S_{1,2} = \langle Y12 \rangle^2$ vanishing. This is associated with the soft singularity, where leg-1 and leg-2 decouple (connecting with the rest of the diagram through a soft a gluon), and the remaining particles form a reducible bubble as shown in Fig.5.5. Therefore, $\theta_1 \to 0$ or $S_{1,2} \to 0$ is a co-dimension two boundary. In a similar fashion, we find the vanishing of each $S_{i,i+1,i+2}$ leads to co-dimension one boundary, and the vanishing of $S_{i,i+1}$ corresponds to co-dimension two boundaries.

It is straightforward to generalize the analysis to the cases with arbitrary multiplicity. In general, we find that all odd planar Mandelstam variables correspond to co-dimension one boundaries, associated with the factorization poles of the amplitudes; whereas the two-particle planar Mandelstam variables correspond to co-dimension two
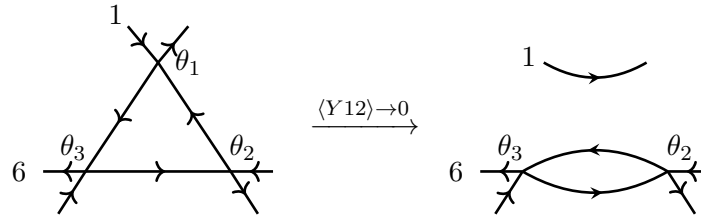
Figure 5.5: The diagram shows the soft limit of a six-point diagram, $\langle Y12 \rangle \to 0$, which corresponds to taking $\theta_1 \to \pi/2$ on the diagrams (a) or (b) in Fig.5.2, here we show the case for diagram (a).
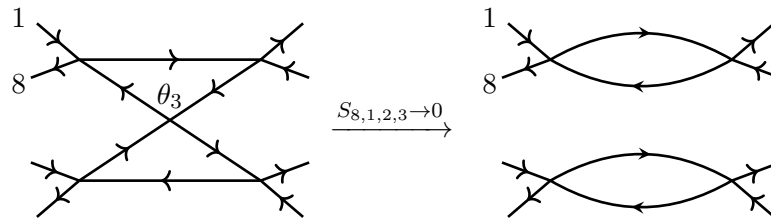
Figure 5.6: The diagram shows the $S_{8,1,2,3} \to 0$ limit for an eight-point diagram, where the diagram separates into two reducible bubbles, therefore it is a co-dimension three boundaries.

boundaries, as we have seen in the six-point case. Let us now focus on the higher even planar Mandelstam variables. This is easy to illustrate using the eight-point case as shown in Fig.5.3. For this particular case, $\theta_3 \to \pi/2$ exposes the singularity at $S_{8,1,2,3} \to 0$. In this limit, the diagrams separate into two parts, each containing a reducible bubble as shown in Fig.5.6. Therefore this is a co-dimension three boundary. In Fig. 5.7, we show the same structure in an example of twelve-point diagrams. In general, when an even planar Mandelstam variable vanishes, the diagram separates into two parts, and each of them contains a reducible bubble, which is a co-dimension three boundary.
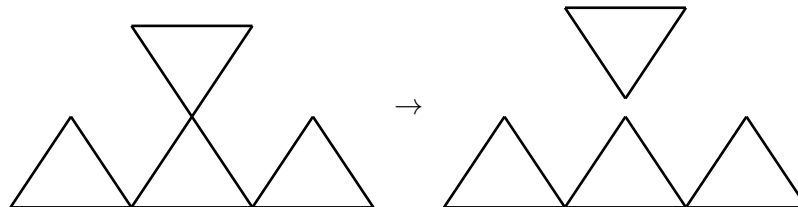
Figure 5.7: The diagrams show when an even planar Mandelstam variable vanishes, the diagram on the left separates into two parts as shown on the right, and each of them contains a reducible bubble. Note that here we omit the external legs in the diagram, which should be attached to external corners of triangles.

5.4.3 Amplitudes from the canonical form

Following [27], to extract the amplitude from the canonical form, we localize Y as follows,

$$Y^* = \begin{pmatrix} \mathbb{0}_{2\times k} \\ \mathbb{1}_{k\times k} \end{pmatrix}, \tag{5.4.28}$$

and the amplitude can be obtained from the volume function $\Omega_{n,k}^{3d}(Y,\Lambda)$ by setting $Y = Y^*$ and integrating out the bosonized variables:

$$\mathcal{A}_{2k}^{3d} = \delta^3(p) \int d^2\phi_1 \ldots d^2\phi_k \, \Omega_{n,k}^{3d}(Y^*,\Lambda). \tag{5.4.29}$$

Under this projection, the Y-brackets become usual three-dimensional spinor-helicity brackets, namely $\langle Y^*ij\rangle = \langle ij\rangle$. Furthermore, one can perform the integration over fermionic variables ϕ in (5.4.29) explicitly. In the four-point case, we have,

$$\int d^2\phi_1 d^2\phi_2 \langle 1234\rangle^2 = \delta^4(\sum_i q_i), \tag{5.4.30}$$

where $q_i = \lambda_i^\alpha \eta_i^I$ is the supercharge. We see that when set Y to be Y^*, $\Omega_{4,2}^{3d}(Y,\Lambda)$ becomes

$$\delta^4(\sum_i q_i)\frac{\langle 13\rangle}{\langle 12\rangle\langle 23\rangle}, \tag{5.4.31}$$

which is the four-point amplitude $\mathcal{A}_4(\bar{\Phi}_1^{\mathcal{N}=4}, \Phi_2^{\mathcal{N}=4}, \bar{\Phi}_3^{\mathcal{N}=4}, \Phi_4^{\mathcal{N}=4})$.

Similarly, we find that $\Omega_{6,3}^{3d}(Y^*,\Lambda)$ gives the six-point ABJM superamplitude. In particular, to perform the integration over the auxiliary fermionic variables ϕ, we the following integration relation,

$$\int d^2\phi_1 d^2\phi_2 d^2\phi_3 \Big(\sum_{i,j=1,3,5} \langle Y^*ij\rangle\langle ij246\rangle + (1,3,5) \leftrightarrow (2,4,6) \Big)^2$$

$$= \delta^4(\sum_i q_i)\, \delta^2\Big(\sum_{i,j,k=1,3,5} \epsilon_{ijk}\langle ij\rangle\eta_k + (1,3,5) \leftrightarrow (2,4,6) \Big). \tag{5.4.32}$$

The tree-level six-point superamplitude is then given by summing over the contributions

from both the positive and negative branches, which lead to

$$
\begin{aligned}
&\mathcal{A}_6(\bar{\Phi}_1^{\mathcal{N}=4}, \Phi_2^{\mathcal{N}=4}, \ldots, \bar{\Phi}_5^{\mathcal{N}=4}, \Phi_6^{\mathcal{N}=4}) \\
&= \frac{\delta^4(\sum_i q_i)\, \delta^2\Big(\sum_{i,j,k=1,3,5} \epsilon_{ijk}\langle ij\rangle\eta_k + (1,3,5) \leftrightarrow (2,4,6) \Big)^2 s_{1,3,5}}{A_{52}^{*+}\, A_{36}^{*+}\, A_{14}^{*+}} \\
&\quad + \frac{\delta^4(\sum_i q_i)\, \delta^2\Big(\sum_{i,j,k=1,3,5} \epsilon_{ijk}\langle ij\rangle\eta_k - (1,3,5) \leftrightarrow (2,4,6) \Big)^2 s_{1,3,5}}{A_{52}^{*-}\, A_{36}^{*-}\, A_{14}^{*-}} \,,
\end{aligned} \tag{5.4.33}
$$

where $s_{1,3,5} = (p_1+p_3+p_5)^2$ is the standard Mandelstam variable, and $A_{ab}^{*\pm}$ are defined as

$$
A_{ab}^{*\pm} = \sum_{i=1,3,5} \langle ia\rangle\langle ib\rangle \pm \langle a{+}2\, a{-}2\rangle\langle b{-}2\, b{+}2\rangle \,. \tag{5.4.34}
$$

The expression in (5.4.33) is in agreement with the known six-point superamplitude (see, e.g. [128]), after a SUSY reduction to $\mathcal{N}=4$ and translating into the normal signature.

Finally, we remark that since the BCFW forms of the positive orthogonal Grassmannian are known to produce tree-level amplitudes in ABJM theory [30, 52], we therefore expect that the volume forms of the orthogonal momentum amplituhedron should also lead to the correct tree-level amplitudes for general multiplicity since they are obtained directly from the BCFW forms.

5.5 Conclusion

In this paper, we have introduced the amplituhedron geometry associated with tree-level ABJM amplitudes. Note that through the sign flipping definition, we see that the geometry can be identified with half of the amplituhedron for four-dimensional $\mathcal{N}=4$ sYM, subject to additional momentum conservation constraint. Thus this in a sense constitutes an holographic relation, where the subspace of the four-dimension geometry lives the geometry for the three-dimensional theory. It is then natural to ask how the two forms can be related. Indeed as explored in [52] the cells of orthogonal Grassmannian, and hence the associated forms, can be identified as subspace of positive cells for the usual positive Grassmannian. The form for $\mathcal{N}=4$ sYM lives in the space Y and $\tilde{Y}$, it is tempting to simply identify Y and $\tilde{Y}$ for $k=\frac{n}{2}$, where their dimensions are the same. However, this naive prescription cannot be the whole story since their sign flipping conditions are different. We leave the correct map between the two forms to future work.

This suggests that a similar projection of viewing the geometry of the three-dimensional

theory as subspace of the four-dimensional one might be applicable to the momentum twistor amplituhedron of $\mathcal{N} = 4$ sYM. The momentum twistor Grassmannian for ABJM was studied in [129], where it was found that the orthogonal condition is defined on a kinematic dependent metric. Our analysis motivates us to take the $\mathcal{N} = 4$ amplituhedron, and require that the four-component variables

$$z_i^A \equiv (Y^\perp \cdot Z_i)^A \,, \qquad (5.5.1)$$

satisfy the additional Sp(4) null constraint

$$z_i^A z_i^B \Omega_{AB} = 0 \,, \qquad (5.5.2)$$

where Ω_{AB} is the Sp(4) invariant metric. We leave the exploration of this possibility to future work as well.

In a recent work [31], it was shown that the orthogonal momentum amplituhedron can be identified as the push forward of the canonical form on the moduli-space of n punctured disk $\mathcal{M}_{0,n}^+$, through the Veronese map. The image has the property that the zero of even-particle Mandelstams are higher co-dimensional boundaries. However, for the pre-image, these are all co-dimension one boundaries. Thus it would appear that while the push forward maps boundary to boundary, the co-dimensionality will change. It will be interesting to understand how the Veronese map systematically achieves this and what is the geometric mechanism behind it.

The positive orthogonal Grassmannian geometry has very intriguing connections with the correlation functions of planar Ising networks [130, 131], and the connections have led to efficient tools for the computations of the correlation functions. It will be of interest to study if the orthogonal amplituhedron geometry constructed in this paper offers new understanding. In this paper, we extended the original amplituhedron geometry [27] for the scatterings in three-dimensional ABJM theory. It was understood that the scattering amplitudes in six-dimensional theories should be associated with the Symplectic Grassmannian [1, 10, 32], a natural future research direction is to extend the amplituhedron geometry for the Symplectic Grassmannian and study its applications for the amplitudes in six-dimensional theories.

Chapter 6

Review on Correlation Functions

6.1 Correlation functions in CFT

In this section we briefly review conformal symmetry and correlation functions in conformal field theories.

6.1.1 Conformal symmetry

A conformal transformation is a coordinate transformation, $x \to \tilde{x}$, such that the form of the metric tensor is preserved up to a scale factor, $\Omega(x)$, as the following

$$g_{\mu\nu}(\tilde{x}) \frac{d\tilde{x}^\mu}{dx^\alpha} \frac{d\tilde{x}^\nu}{dx^\beta} = \Omega(x) g_{\alpha\beta}(x) \ . \tag{6.1.1}$$

There are two types of local operators: primary and descendant. The descendants can be obtained by acting derivatives on other local operators, while primaries can not. Also, primary operators are annihilated by the generators of special conformal transformation and are eigenvectors of the dilatation generator.

$$[K_\mu, \mathcal{O}(0)] = 0 \,, \qquad [D, \mathcal{O}(0)] = \Delta \, \mathcal{O}(0) \,. \tag{6.1.2}$$

The dilatation and special conformal transformation generators take the form

$$D = -x^\mu \partial_\mu \,, \qquad\qquad K_\mu = 2i x_\mu x^\nu \partial_\nu - i \, x^2 \partial_\mu \,, \tag{6.1.3}$$

along with the usual translation and Lorentz generators

$$P_\mu = -i\partial_\mu \,, \qquad M_{\mu\nu} = -i \left(x_\mu \partial_\nu - x_\nu \partial_\mu \right) \,, \tag{6.1.4}$$

form the conformal group, which satisfy the following commutation relations:

$$
\begin{aligned}
[D, P_\mu] &= P_\mu \,, \\
[D, K_\mu] &= -K_\mu \,, \\
[K_\mu, P_\nu] &= 2\delta_{\mu\nu} D - 2i\, M_{\mu\nu} \,, \\
[M_{\mu\nu}, P_\alpha] &= i\,(\delta_{\mu\alpha} P_\nu - \delta_{\nu\alpha} P_\mu) \,, \\
[M_{\mu\nu}, K_\alpha] &= i\,(\delta_{\mu\alpha} K_\nu - \delta_{\nu\alpha} K_\mu) \,, \\
[M_{\alpha\beta}, M_{\mu\nu}] &= i\,(\delta_{\alpha\mu} M_{\beta\nu} + \delta_{\beta\nu} M_{\alpha\mu} - \delta_{\beta\mu} M_{\alpha\nu} - \delta_{\alpha\nu} M_{\beta\mu}) \,.
\end{aligned}
\tag{6.1.5}
$$

Correlation functions of scalar primary operators, $\mathcal{O}_{\Delta_i}(x_i)$, satisfies

$$
\langle \mathcal{O}_1(\tilde{x}_1) \ldots \mathcal{O}_n(\tilde{x}_n) \rangle = \left| \frac{\partial \tilde{x}}{\partial x} \right|_{x_1}^{-\frac{\Delta_1}{d}} \ldots \left| \frac{\partial \tilde{x}}{\partial x} \right|_{x_n}^{-\frac{\Delta_n}{d}} \langle \mathcal{O}_{\Delta_1}(x_1) \ldots \mathcal{O}_{\Delta_n}(x_n) \rangle
\tag{6.1.6}
$$

Let us look at the 2-,3-, and 4-point correlation functions.

- Two-point function is completely fixed by conformal symmetry

$$
\langle \mathcal{O}_{\Delta_i}(x) \mathcal{O}_{\Delta_j}(y) \rangle = \frac{\delta_{\Delta_i, \Delta_j}}{(x - y)^{2\Delta_i}} \,.
\tag{6.1.7}
$$

- Three-point function is also fixed by conformal symmetry

$$
\langle \mathcal{O}_{\Delta_1}(x_1) \mathcal{O}_{\Delta_2}(x_2) \mathcal{O}_{\Delta_3}(x_3) \rangle = \frac{C_{123}}{|x_{12}|^{\Delta_1 + \Delta_2 - \Delta_3} \, |x_{13}|^{\Delta_1 + \Delta_3 - \Delta_2} \, |x_{23}|^{\Delta_2 + \Delta_3 - \Delta_1}} \,,
\tag{6.1.8}
$$

  up to an overall constant C_{123}.

- Four-point function is *not* completely fixed by conformal symmetry and takes the following generic form

$$
\langle \mathcal{O}_\Delta(x_1) \ldots \mathcal{O}_\Delta(x_4) \rangle = \frac{f(U, V)}{\left(x_{13}^2 x_{24}^2 \right)^\Delta} \,,
\tag{6.1.9}
$$

  where the cross ratios are given by

$$
U = \frac{x_{12}^2 x_{34}^2}{x_{13}^2 x_{24}^2} \,, \qquad V = \frac{x_{14}^2 x_{23}^2}{x_{13}^2 x_{24}^2} \,.
\tag{6.1.10}
$$

The four-point functions will be our main focus in the following sections. The traditional approach of computing it will be summing over Witten diagrams, while in the following discussion we will apply modern techniques such as bootstraps, Mellin space

approaches, or considering integrating over spacetime U, V to make connection with supersymmetric localisation and so on, to arrive at simple results.

6.2 Integrated correlators in $\mathcal{N} = 4$ SYM

Recently, the integrated correlators of 4D $\mathcal{N} = 4$ SYM have been extensively studied [37–39]. We first introduce a four-point correlator in the stress-tensor multiplet with a generic gauge group G_N,

$$\langle \mathcal{O}_2(x_1, Y_1) \dots \mathcal{O}_2(x_4, Y_4) \rangle = \frac{1}{x_{12}^4 x_{34}^4} \left[\mathcal{T}_{G_N, \text{free}}(U, V; Y_i) + \mathcal{I}_4(U, V; Y_i) \mathcal{T}_{G_N}(U, V) \right] , \tag{6.2.1}$$

where the superconformal primary operator is defined as

$$\mathcal{O}_2(x, Y) := \text{tr}(\Phi^I(x)\Phi^J(x)) Y_I Y_J . \tag{6.2.2}$$

We have introduced null vector Y_I's ($I = 1, 2, \cdots, 6$) taking care of the $SO(6)$ R-symmetry indices, and here again the conformal cross ratios, U, V are given by

$$U = \frac{x_{12}^2 x_{34}^2}{x_{13}^2 x_{24}^2}, \qquad V = \frac{x_{14}^2 x_{23}^2}{x_{13}^2 x_{24}^2} . \tag{6.2.3}$$

We will focus the non-trivial part of the correlator, $\mathcal{T}_{G_N}(U, V)$, (stripped off the SUSY pre-factor $\mathcal{I}_4(U, V; Y_i)$) , which will be integrated over the spacetime coordinate with some measures that preserve supersymmetry. For example, the first correlator is given by

$$\mathcal{C}_{G_N}(\tau, \bar{\tau}) := I_2 \left[\mathcal{T}_{G_N}(U, V) \right] = -\frac{8}{\pi} \int_0^\infty dr \int_0^\pi d\theta \frac{r^3 \sin^2(\theta)}{U^2} \mathcal{T}_{G_N}(U, V) , \tag{6.2.4}$$

where r, θ are functions of U, V. The correlator can be computed by supersymmetric localisation, which gives a exact result, that is, finite in N and the complex Yang-Mills coupling

$$\tau = \tau_1 + i\tau_2 := \frac{\theta}{2\pi} + i\frac{4\pi}{g_{YM}^2} . \tag{6.2.5}$$

We will mainly focus on the perturbative contribution of the integrated correlator, *i.e.* $\tau_1 = 0$, or equivalently the Yang-Mills θ angle vanishes, which is given by

$$\mathcal{C}_{G_N}^{pert}(\tau_2) = \frac{1}{4} \tau_2^2 \, \partial_{\tau_2}^2 \langle \partial_m^2 \hat{Z}_{G_N}^{pert}(m, a) \big|_{m=0} \rangle_{G_N} , \tag{6.2.6}$$

where $\hat{Z}_{G_N}^{pert}(m, a)$ is partition function for a classical gauge group G_N, and $\langle \cdots \rangle_{G_N}$ is the expectation value defined in a standard way. For example, in the $SU(N)$ case, the

partition function is

$$\hat{Z}_{SU(N)}^{pert}(m,a) = \frac{1}{H(m)^{N-1}} \prod_{i<j} \frac{a_{ij}^2 H^2(a_{ij})}{H(a_{ij}-m)H(a_{ij}+m)}\,, \tag{6.2.7}$$

with $a_{ij} = a_i - a_j$, and the expectation value of a function $F(a_i)$ is defined as

$$\langle F(a_i)\rangle_{SU(N)} = \frac{1}{\mathcal{N}_{SU(N)}} \int d^N a\,\delta\left(\sum_i a_i\right)\left(\prod_{i<j} a_{ij}^2\right) e^{-\frac{8\pi^2}{g_{YM}^2}\sum_i a_i^2} F(a_i)\,, \tag{6.2.8}$$

where $\mathcal{N}_{SU(N)}$ being the normalisation factor, and the function $H(m)$ is defined as

$$H(m) = e^{-(1+\gamma)m^2}\,G(1+im)\,G(1-im)\,, \tag{6.2.9}$$

where $G(m)$ is a Barnes G-function (and γ is the Euler constant). Here we give the simplest $SU(2)$ correlator (we define $y := \pi\tau_2$)

$$\begin{aligned} &\mathcal{C}_{SU(2)}^{pert}(y)\\ &\sim \frac{9\zeta(3)}{y} - \frac{225\zeta(5)}{2y^2} + \frac{2205\zeta(7)}{2y^3} - \frac{42525\zeta(9)}{4y^4} + \frac{1715175\zeta(11)}{16y^5} + \cdots\,, \end{aligned} \tag{6.2.10}$$

and the complete series is given by a closed form

$$\mathcal{C}_{SU(2)}^{pert}(y) \sim \sum_{s=2}^{\infty} \frac{(2s-1)\Gamma(2s+1)(-1)^s}{2^{2s-1}\Gamma(s-1)}\zeta(2s-1)y^{1-s}\,. \tag{6.2.11}$$

Moreover, the correlator satisfies a Laplace difference equation relating $SU(N-1)$, $SU(N)$, and $SU(N+1)$ correlators, which determines all the higher $SU(N)$ correlators once the $SU(2)$ one is given. The equation takes the following form for the $SU(N)$ case

$$\begin{aligned} (\Delta_\tau - 2)\,\mathcal{C}_{SU(N)}(\tau,\bar{\tau}) =\,& N^2\Big[\mathcal{C}_{SU(N+1)}(\tau,\bar{\tau}) - 2\mathcal{C}_{SU(N)}(\tau,\bar{\tau}) + \mathcal{C}_{SU(N-1)}(\tau,\bar{\tau})\Big]\\ &- N\Big[\mathcal{C}_{SU(N+1)}(\tau,\bar{\tau}) - \mathcal{C}_{SU(N-1)}(\tau,\bar{\tau})\Big]\,. \end{aligned}$$

The Laplace difference equation for $G_N = SO(2N)$, $SO(2N+1)$, and $USp(2N)$ has also been found [132].

Now we present the perturbative expansion of the first integrated correlator generalising the previous $SU(2)$ case in (6.2.10), which is valid for all the gauge groups G_N

with arbitrary N given as

$$\mathcal{C}_{G_N}^{pert}(\tau_2) = 4c_{G_N}\left[\frac{3\,\zeta(3)a_{G_N}}{2} - \frac{75\,\zeta(5)a_{G_N}^2}{8} + \frac{735\,\zeta(7)a_{G_N}^3}{16} - \frac{6615\,\zeta(9)\,(1+P_{G_N,1})\,a_{G_N}^4}{32}\right.$$
$$\left. + \frac{114345\,\zeta(11)\,(1+P_{G_N,2})\,a_{G_N}^5}{128} + \mathcal{O}(a_{G_N}^6)\right],$$

where $a_{G_N} = \lambda_{G_N}/(4\pi^2)$, and the 't Hooft coupling is

$$\lambda_{SU(N)} = g_{YM}^2\,N\,, \qquad \lambda_{SO(n)} = g_{YM}^2\,(n-2)\,, \qquad \lambda_{USp(n)} = \frac{g_{YM}^2\,(n+2)}{2}\,, \quad (6.2.12)$$

where for $n = 2N$ or $2N+1$ for $SO(n)$, and $n = 2N$ for $USp(n)$. Similarly, the The central charge for different gauge group is

$$c_{SU(N)} = \frac{N^2-1}{4}\,, \qquad c_{SO(n)} = \frac{n(n-1)}{8}\,, \qquad c_{USp(n)} = \frac{n(n+1)}{8}\,. \qquad (6.2.13)$$

We notice in (6.2.12) the non-planar structure first enters at the $a_{G_N}^4$ order (four-loop order in perturbation theory), which agrees with results in the literature [133]. The explicit non-planar factors, $P_{G_N,i}$ ($i = L - 3$ and L is the loop number), are given by (for instance the $SU(N)$ case)

$$P_{SU(N),1} = \frac{2}{7N^2}\,, \qquad P_{SU(N),2} = \frac{1}{N^2}\,, \qquad (6.2.14)$$

We also observe that in each loop order, the coefficient are rational functions times single zeta values, which is shown to be the (linear combination of) periods ($\mathcal{P}$) of certain conformal graphs [4] (see detailed derivation in Sec. 7.3.2),

$$I_2\left[\mathcal{T}_{G_N}(U,V)\right] = -4c_{G_N}\sum_{L\geq 1}\frac{a_{G_N}^L}{L!(-4)^L}\mathcal{P}_{f^{(L)}}\,. \qquad (6.2.15)$$

The symbol $\mathcal{P}_{f^{(L)}}$ denotes period of f-graphs as the following

$$\mathcal{P}_{f^{(L)}} = \frac{1}{\pi^{2(L+1)}}\int d^4x_4\int d^4x_5\cdots d^4x_{4+L}\,f^{(L)}(x_i)\Big|_{(x_1,x_2,x_3)=(\mathbf{0},\mathbf{1},\infty)}\,, \qquad (6.2.16)$$

where the choice of (x_1, x_2, x_3) are arbitrary due to the conformal symmetry of $f^{(L)}$. The function, $f^{(L)}$, as well as its graph representation, f-graphs, are used to construct 4-point L-loop integrands (up to 10 loops) in the YM perturbation theory [134–137].

One important feature of $f^{(L)}(x_i)$ is that it has total permutation symmetry under the exchange of the four external as well as all the internal points. It is due to the L-loop correction to the correlation function of 4 stress-tensor operators, $\mathcal{O}_2$, is given

by point Born-level correlation function with L Lagrangian insertions $\mathcal{O}_\tau$ [134] as the following

$$\langle \mathcal{O}_2(x_1, y_1) \cdots \mathcal{O}_2(x_4, y_4)\, \mathcal{O}_\tau(x_5) \ldots \mathcal{O}_\tau(x_4 + L)\rangle\,, \tag{6.2.17}$$

where $\mathcal{O}_2$ and $\mathcal{O}_\tau$ belong to the same stress tensor supermultiplet (in the chiral sector):

$$\mathcal{T}^C(x, \rho, y) \equiv \mathcal{T}(x, \rho, 0, y) = \mathcal{O}_2(x, y) + \cdots + \rho^4 \mathcal{O}_\tau(x)\,. \tag{6.2.18}$$

The complete structure of the stress tensor supermultiplet is given as

$$\mathcal{T}(x, \rho, \bar{\rho}, y) = \exp\left(\rho_\alpha^a Q_a^\alpha + \bar{\rho}_{a'}^{\dot{\alpha}} \bar{Q}_{\dot{\alpha}}^{a'}\right) \mathcal{O}_2(x, y)\,, \tag{6.2.19}$$

where ρ and $\bar{\rho}$ are Grassmann variables in the $\mathcal{N} = 4$ harmonic superspace formalism [138–140]

$$\theta_\alpha^A = (\rho_\alpha^a, \theta_\alpha^{a'})\,, \qquad \bar{\theta}_A^{\dot{\alpha}} = (\bar{\rho}_{a'}^{\dot{\alpha}}, \bar{\theta}_a^{\dot{\alpha}})\,, \tag{6.2.20}$$

where the $SU(4)$ index $A = 1, 2, 3, 4$ split into $(A = a, a')$ with $a, a' = 1, 2$, and

$$\rho_\alpha^a = \theta_\alpha^a + \theta_\alpha^{a'}\, y_{a'}^a\,, \qquad \bar{\rho}_{a'}^{\dot{\alpha}} = \bar{\theta}_{a'}^{\dot{\alpha}} + \bar{\theta}_a^{\dot{\alpha}}\, \bar{y}_{a'}^a\,. \tag{6.2.21}$$

The operator $\mathcal{O}_2$ is annihilated by half of the supersymmetric generators, which is take to be the eight supersymmetry components, $Q_\alpha^{a'}$ and $\bar{Q}_a^{\dot{\alpha}}$. In [134], the L-loop correction is related to the f-graph by

$$\langle \mathcal{O}_2(x_1, y_1) \cdots \mathcal{O}_2(x_4, y_4)\, \mathcal{O}_\tau(x_5) \ldots \mathcal{O}_\tau(x_{4+L})\rangle$$
$$= \frac{2\,(N_c^2 - 1)}{(-4\pi^2)^{4+\ell}} \times \mathcal{I}_{4+\ell} \times f^{(\ell)}(x_1, \ldots, x_{4+L})\,, \tag{6.2.22}$$

with $\mathcal{I}_{4+\ell}$ being some prefactor. Once again, $f(x_i)$ has total permutation symmetry, and it can be expressed in graph representation, so-called $f^{(L)}$-graph.

We note the period of $f^{(L)}$-graph (6.2.16) gives zeta value; for example, the first three terms in (6.2.12) are related to the periods of the three diagrams in Fig.(6.1), which gives $\zeta(3)$, $\zeta(5)$, $\zeta(7)$, with some rational numbers in front of them. Identifying integrated correlators with periods drastically simplifies the computation due to the following two features:

- The $f^{(L)}$-functions enjoy total S_{4+L} permutation symmetry.

- The period is invariant under the S_{4+L} permutation.

Combing above two points, we reduce the computation from S_{4+L} terms to one term.

$f^{(1)}, \mathcal{P}_{f^{(1)}} = 6\,\zeta(3)$ $f^{(2)}, \mathcal{P}_{f^{(2)}} = \frac{1}{48} \times 6! \times 20\,\zeta(5)$ $f^{(3)}, \mathcal{P}_{f^{(3)}} = \frac{1}{20} \times 7! \times 70\,\zeta(7)$
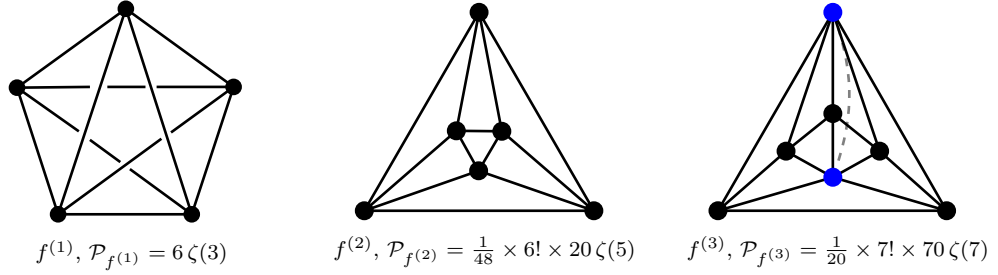
Figure 6.1: The planar f-graphs up to three loops, and their periods are $\mathcal{P}_{f^{(3)}}$ related to the first three terms in (6.2.12).

For example, the three loop order contribution ($L = 3$) in Fig.6.1 in general has 7! terms to consider. While the property of periods tells us all the 7! terms (graphs) has the same period value: $70\,\zeta(7)$, so the period of $f^{(3)}$ is simply $\mathcal{P}_{f^{(3)}} = \frac{1}{20} \times 7! \times 70\zeta(7)$, where $\frac{1}{20}$ is dividing the graph symmetric factor. This matches the rational function given in (6.2.12). At four loops, there are three planar $f_\alpha^{(4)}$-functions ($\alpha = 1, 2, 3$), again the property of period reduces the computation from $3 \times 8!$ terms down to 3×1 terms. In the section. 7, we will further discuss the five-loop case, where 7 planar topologies, $f_\alpha^{(5)}$-functions ($\alpha = 1, \cdots, 7$), need to be considered. We explicitly evaluate periods of 6 out of 7 $f_\alpha^{(5)}$-functions. In order to match the supersymmteric localisation result, *i.e* $a_{G_N}^5$ term is (6.2.12), the leftover period is predicted to be certain value of multi-zeta values.

6.3 Mellin amplitudes

The AdS/CFT correspondence states that the correlation function of a boundary (conformal) theory can be represented as scattering amplitudes in the bulk (AdS) space. A famous example is that the 4D $\mathcal{N} = 4$ SYM is dual to the type IIB string theory on $AdS_5 \times S^5$ background. It was shown in [21] that a tree-level AdS_5 correlator of four one-half BPS operator with arbitrary weights, $\langle O_{p_1} O_{p_2} O_{p_3} O_{p_4} \rangle$, takes a remarkable simple form when expressed in Mellin space. We consider the following BPS operator of weight p,

$$O_p(x, t) = Y_{I_1} \dots Y_{I_p} O_p^{I_1 \cdots I_p}(x), \quad Y \cdot Y = 0. \tag{6.3.1}$$

The four-point correlator, after pulling out some overall factors, is given by

$$\langle O_{p_1} O_{p_2} O_{p_3} O_{p_4} \rangle \sim \mathcal{G}(U, V; \sigma, \tau) = \mathcal{G}_{\text{free}}(U, V; \sigma, \tau) + R\,\mathcal{H}(U, V; \sigma, \tau), \tag{6.3.2}$$

where we only focus on the dynamic part $\mathcal{H}(U, V; \sigma, \tau)$ (with the SUSY factor R stripped off), which is a function of spacetime and R-symmetry cross ratios, *i.e.* U, V and σ, τ, respectivelty. The (reduced) Mellin amplitude is defined as the integral transform of

the $\mathcal{H}$ function,

$$
\begin{aligned}
&\widetilde{M}(s,t;\sigma,\tau) \\
&= \int_0^\infty dU\,dV\; U^{-\frac{s}{2}+\frac{p_3+p_4}{2}-L-1}\, V^{-\frac{t}{2}+\frac{\min\{p_1+p_4,p_2+p_3\}}{2}-1}\, \mathcal{H}(U,V;\sigma,\tau)\,.
\end{aligned}
\tag{6.3.3}
$$

The Mellin amplitude for $AdS_5 \times S^5$ has extremely compact form

$$
\widetilde{\mathcal{M}}(s,t;\sigma,\tau) = \sum \frac{a_{ijk}\,\sigma^i\tau^j}{(s-s_M+2k)(t-t_M+2j)(\tilde{u}-u_M+2i)}\,,
\tag{6.3.4}
$$

where s_M, t_M, u_M are associated with the simple poles of s, t, u. The factor a_{ijk} is a function of weights p_i's. From (6.3.3), the non-reduced Mellin amplitude can written as

$$
\mathcal{M}(s,t;\sigma,\tau) = \hat{R}\circ\widetilde{\mathcal{M}}(s,t;\sigma,\tau)\,,
\tag{6.3.5}
$$

with $\hat{R}$ being an shifting operator. The simple and neat result (6.3.4) was obtained by applying bootstrap approaches, *i.e.* imposing consistency conditions such as crossing symmetry,

$$
\begin{aligned}
\sigma^{p-2}\widetilde{\mathcal{M}}(\tilde{u},t;1/\sigma,\tau/\sigma) &= \widetilde{\mathcal{M}}(s,t,;\sigma,\tau) \\
\tau^{p-2}\widetilde{\mathcal{M}}(t,s;\sigma/\tau,1/\tau) &= \widetilde{\mathcal{M}}(s,t;\sigma,\tau)\,,
\end{aligned}
\tag{6.3.6}
$$

along with correct asymptotic behaviours,

$$
\mathcal{M}(\beta s,\beta t;\sigma,\tau) \sim O(\beta) \quad \text{for } \beta\to\infty\,.
\tag{6.3.7}
$$

and so on, that bypasses the complicated Witten diagram computations to arrive at a unique answer (6.3.4). It was later realised by the authors of [23] that the aforementioned four-point $AdS_5\times S^5$ with different weights can be packaged as a single four-point correlator of scalar operators in ten dimensions due to a hidden ten-dimensional conformal symmetry. Similar approach was applied to the four-point tree-level holographic correlators of type IIB supergravity in $AdS_3 \times S^3 \times M_4$, where the hidden symmetry is found to be the 6D conformal symmetry. Supergravity on $AdS_3 \times S^3$ background only has half supersymmetry, which means there exists two superfields: tensor multiplet and gravity multiplet. We consider the following types of four-point correlators, $\langle s_{k_1}s_{k_2}s_{k_3}s_{k_4}\rangle$, and $\langle s_{k_1}s_{k_2}\sigma_{k_3}\sigma_{k_4}\rangle$, where s_{k_i}/σ_{k_i} denotes operator in tensor/gravity multiplet. The first type can be obtained by considering a single correlator of four scalar operators in a six-dimensional CFT, and the second type by replacing 6D two scalars by two self-dual 3-forms. The Mellin amplitude of the first type correlator takes

a simple form

$$\widetilde{\mathcal{M}}_{s_{k_1}s_{k_2}s_{k_3}s_{k_4}}(s,t) = \sum_{m_1=0,m_2=0}^{\infty} \frac{\sigma^{m_2+\frac{k_{21}^-+k_{43}^-}{2}}\tau^{k_1-1-m_{12}}}{\prod_{i=1}^6 m_i!}$$
$$\times \left(\frac{\delta_{f_1f_2}\delta_{f_3f_4}}{s+2+2m_1-k_{12}^+} + \frac{\delta_{f_2f_3}\delta_{f_1f_4}}{t+2+2m_5-k_{23}^+} + \frac{\delta_{f_1f_3}\delta_{f_2f_4}}{\tilde{u}+2+2m_2-k_{13}^+}\right),$$
$$(6.3.8)$$

where f_i being the flavor indices of states in the tensor multiplet. One can take the flat-space limit $(s \to \infty,\ t \to \infty)$ of $\widetilde{\mathcal{M}}_{s_{k_1}s_{k_2}s_{k_3}s_{k_4}}(s,t)$ and arrive at

$$\mathcal{M}_{s_{k_1}s_{k_2}s_{k_3}s_{k_4}}(s,t)$$
$$\to P_{\{k_i\}}(\sigma,\tau)\,(u\,t + s\,t\,\sigma + s\,u\,\tau)\left(\frac{\delta_{f_1f_2}\delta_{f_3f_4}}{s} + \frac{\delta_{f_1f_4}\delta_{f_2f_3}}{t} + \frac{\delta_{f_1f_3}\delta_{f_2f_4}}{u}\right),$$

which resembles the flat-space amplitude of 6D (2, 0) supergravity with all four states in tensor multiplet that has been discussed in chapter 3, which has the following form

$$\mathcal{A}_4^{\text{tensor}} = G_6\,\delta^8\left(\sum_{i=1}^4 q_i\right)\delta^6\left(\sum_{i=1}^4 p_i\right)\left(\frac{\delta_{f_1f_2}\delta_{f_3f_4}}{\mathbf{s}} + \frac{\delta_{f_2f_3}\delta_{f_1f_4}}{\mathbf{t}} + \frac{\delta_{f_1f_3}\delta_{f_2f_4}}{\mathbf{u}}\right). \quad (6.3.9)$$

The second type correlator involving operators in gravity multiplet, $\langle s_{k_1}s_{k_2}\sigma_{k_3}\sigma_{k_4}\rangle$, will be discussed in chapter 8 in details. Many of these ideas above have also been applied to obtain correlators in other AdS backgrounds, such as $AdS_7 \times S^4$ and $AdS_4 \times S^7$ [141].

Having introduced the background materials of the correlation functions, we are ready to apply them to study many interesting topics in the chapter 7, and 8.

Chapter 7

Integrated correlators in $\mathcal{N} = 4$ SYM

7.1 Introduction

The correlation functions of superconformal primary operators in the stress tensor multiplet of $\mathcal{N} = 4$ super Yang-Mills theory (SYM) have received intensive study both at weak coupling and at strong coupling. Recently, the concept of the integrated correlators was introduced in [37], where it was found that, when integrated over spacetime coordinates with certain integration measures that preserve supersymmetry, the correlators of four superconformal primary operators in $\mathcal{N} = 4$ SYM with $SU(N)$ gauge group can be computed using supersymmetric localisation techniques.[*] This has led to many interesting developments. In particular, the integrated correlators were used as constraints for determining unfixed parameters in the perturbative computation of holographic correlators in $AdS_5 \times S^5$ at supergravity limit and beyond [37–39]. Exact results of the integrated correlators with finite complexified Yang-Mills coupling τ were also obtained, in the large-N expansion [142, 143] as well as for arbitrary values of N [144, 145]. These exact results of integrated correlators have important applications to the numerical bootstrap of understanding non-BPS operators in $\mathcal{N} = 4$ SYM [146] and to the study of ensemble average of $\mathcal{N} = 4$ SYM [147]. The integrated correlators have been generalised for $\mathcal{N} = 4$ SYM with general classical gauge groups, in the large-N expansion [148] and for gauge groups with arbitrary ranks and finite coupling τ [132]. One may further extend the integrated correlators for correlation functions with more than four operators; in [149, 150], the integrated n-point maximal $U(1)_Y$-violating correlators were introduced and their implications to the n-point maximal $U(1)$-violating superstring amplitudes [151, 152] in $AdS_5 \times S^5$ were studied.

---

[*]There were two such integrated correlators that have been studied in the literature, and we will refer them as the first integrated correlator and the second integrated correlator, respectively.

In this paper, we will study perturbative aspects of integrated correlators using standard Feynman diagram methods. We will compute the integrated correlators order by order in the perturbation expansion using the loop integrands constructed in [134, 135] (see also [136, 137] for higher-loop contributions) for the un-integrated correlator. It was observed in [134] that the integrands of the four-point correlator of superconformal primary operators of stress-tensor supermultiplets in $\mathcal{N} = 4$ SYM has a hidden complete permutation symmetry of external and integration points. This observation has led to very powerful graphical representation of the loop integrands. In particular, the integrands of the four-point correlator at L-loop order can be expressed as linear combination of particular graphs, with $(L + 4)$ degree-(-4) vertices – each propagator counts as degree minus one, and each numerator (or inverse propagator) counts as degree plus one. Some of these graphs are simple 4-regular graphs, but in general they contain numerators. These loop integrals have been computed explicitly up to three loops. At one loop [153–155] and two loops [156, 157], the resulting correlator is expressed in terms of polylogarithms with transcendental weight two and four, respectively. The three-loop integrals are much harder to evaluate. The correlator at three loops was computed analytically in [158], and the final result involves much more complicated multiple polylogarithms.

To obtain the integrated correlators, in principle one may take these analytical expressions for the un-integrated correlator and then integrate them over spacetime coordinates (more precisely the conformal cross ratios) with the integration measures in the definition of the integrated correlators, as given in (7.2.4) and (7.2.5). However, given the fact that the un-integrated correlator is given by complicated polylogarithms, and even multiple polylogarithms, it is rather challenging to integrate these functions directly with the non-trivial integration measures. Furthermore, there are no analytical results for the un-integrated correlator beyond three loops, which makes it impossible to study the integrated correlators using Feynman diagram methods at higher loops in this way.

The observation of this paper is that, instead of taking the analytical results of the un-integrated correlator, it is much more convenient to simply use the loop integrands of the correlator. When integrated with the integration measures that are used in the definition of the integrated correlators, the graphs representing the loop integrands of the un-integrated correlator become precisely the periods of certain Feynman graphs with vertices of degree-(-4), and such periods have been studied quite extensively in the literature, see for example [40, 159–165]. In particular, for the first integrated correlator at L loops, it involves the computation of $(L+1)$-loop periods; for the second integrated correlator at L loops, it is given by a sum of $(L + 2)$-loop periods. Special powerful techniques and packages (such as `HyperInt` [163] and `HyperlogProcedures` [49]) have been developed for computing these periods, which allow us to evaluate the

first integrated correlator up to four loops – it was computed up to two loops in [145] – and up to three loops for the second integrated correlator. We find these results from explicit loop integrals of periods match precisely with the results that are obtained using supersymmetric localisation.

It should be stressed that the construction of the loop integrands based on the methods of [134, 135], and hence the periods for the integrated correlators, are general and not specific to the $SU(N)$ gauge group. Especially for the planar sector, which we consider in this paper, the correlator takes a universal form for all classical gauge groups once we use appropriate 't Hooft couplings [132]. We therefore compare our Feynman diagram computations with the results obtained from supersymmetric localisation for the integrated correlators in $\mathcal{N} = 4$ SYM with general classical gauge groups. The perturbative contribution of the first integrated correlator has in fact been evaluated in [132, 148] using localisation. We will also compute the second integrated correlator for general classical groups using supersymmetric localisation in this paper, for the comparison with the Feynman diagram results.

On the one hand, the agreement between Feynman diagram results and the localisation computation provides important confirmation of the integrated correlators obtained from supersymmetric localisation. The analysis also provides interesting insights of the correlation function in the weak coupling region. In particular, it highlights the simplicity of the integrated correlators. On the other hand, since the integrated correlators can be computed using supersymmetric localisation to arbitrarily high orders, these results from localisation provide very interesting and new relations among the periods associated with these degree-(-4) Feynman graphs that are relevant for the correlator. In particular, when the periods cannot be computed using current techniques, the results of localisation give predictions. We will illustrate this idea by considering one of the integrated correlators at five loops in the planar limit, the results of localisation lead to a prediction for the analytical expression of a period of a certain six-loop integral.

The paper is organised as follows. In section 7.2, we will review the integrated four-point correlators in $\mathcal{N} = 4$ SYM with general classical gauge groups, and some of the perturbative results obtained from supersymmetric localisation. In section 7.3, we will review the construction of the loop integrands for the un-integrated four-point correlator. These integrands can be naturally represented in terms of degree-(-4) Feynman graphs. We will then show that once integrated over the integration measures introduced in section 7.2 for the definition of integrated correlators, they become periods of these degree-(-4) Feynman graphs. In section 7.4, we will evaluate all the relevant periods for the first integrated correlator up to four loops in the planar limit, and for the second integrated correlator up to three loops. In both cases, the computation involves periods that are up to five loops. We will also consider the first integrated

correlator at five loops in the planar limit. For this case, we are able to compute all the relevant periods except one (they are all six-loop integrals). The known result from localisation then allows us to predict this particular unknown six-loop period. We conclude in section 7.5, and some technical details of our calculation are described in the appendices.

7.2 Integrated correlators in $\mathcal{N} = 4$ SYM

In this section, we will review the definition of integrated four-point correlators in $\mathcal{N} = 4$ SYM, and their relations to the localised partition function of $\mathcal{N} = 2^*$ SYM on S^4. We are interested in the correlation function of four superconformal primary operators in the stress-tensor multiplet of $\mathcal{N} = 4$ SYM with a gauge group G_N, which can be expressed as

$$\langle \mathcal{O}_2(x_1, Y_1) \dots \mathcal{O}_2(x_4, Y_4) \rangle = \frac{1}{x_{12}^4 x_{34}^4} \left[\mathcal{T}_{G_N, \text{free}}(U, V; Y_i) + \mathcal{I}_4(U, V; Y_i) \mathcal{T}_{G_N}(U, V) \right] ,$$

$$(7.2.1)$$

where the superconformal primary operator is defined as

$$\mathcal{O}_2(x, Y) := \text{tr}(\Phi^I(x)\Phi^J(x))Y_I Y_J , \qquad (7.2.2)$$

which has conformal dimension 2. We have introduced null vector Y_I's ($I = 1, 2, \cdots, 6$) taking care of the $SO(6)$ R-symmetry indices, and the conformal cross ratios, U, V are given by

$$U = \frac{x_{12}^2 x_{34}^2}{x_{13}^2 x_{24}^2}, \qquad V = \frac{x_{14}^2 x_{23}^2}{x_{13}^2 x_{24}^2} . \qquad (7.2.3)$$

The quantity $\mathcal{T}_{G_N, \text{free}}(U, V; Y_i)$ represents the free theory part of the correlator. The non-trivial part of the correlator has been factorised into two pieces: the pre-factor $\mathcal{I}_4(U, V; Y_i)$ is fixed by the superconformal symmetry due to partial non-renormalisation theorem [166, 167] (the expression of $\mathcal{I}_4(U, V; Y_i)$ is given in (7.3.6)), and $\mathcal{T}_{G_N}(U, V)$ is the dynamic part of the correlator, which will be the focus of our study.

We will be interested in the perturbative aspects of the correlator. As we commented in the introduction, in perturbation theory, $\mathcal{T}_{G_N}(U, V)$ has been computed only up to three loops [158]. However the integrands in the planar limit have constructed up to ten loops using very efficient graphic tools [137]. The non-planar contributions first appear at four loops, and the corresponding integrand is also known [133].

It was shown in [37, 39] that when integrated over suitable integration measures, the correlator can be determined in terms of the partition function of $\mathcal{N} = 2^*$ SYM ($\mathcal{N} = 4$ SYM with certain mass deformation on the hypermultiplet) on S^4, which

can be computed using supersymmetric localisation [168]. There are two kinds of integrated correlators that have been studied in the literature due to different choices of the integration measures[*]. Concretely, they are defined as[†]

$$\mathcal{C}_{G_N,1}(\tau, \bar{\tau}) := I_2 \left[\mathcal{T}_{G_N}(U, V) \right] = -\frac{8}{\pi} \int_0^\infty dr \int_0^\pi d\theta \frac{r^3 \sin^2(\theta)}{U^2} \mathcal{T}_{G_N}(U, V), \qquad (7.2.4)$$

and

$$\begin{aligned} \mathcal{C}_{G_N,2}(\tau, \bar{\tau}) &:= I_4 \left[\mathcal{T}_{G_N}(U, V) \right] \\ &= -\frac{32}{\pi} \int_0^\infty dr \int_0^\pi d\theta \frac{r^3 \sin^2(\theta)}{U^2} (1 + U + V) \bar{D}_{1111}(U, V) \mathcal{T}_{G_N}(U, V), \quad (7.2.5) \end{aligned}$$

where r and θ are related to cross ratios by $U = 1 + r^2 - 2r\cos(\theta)$ and $V = r^2$. The function $\bar{D}_{1111}$ is the usual D-function that appears in the computation of contact Witten diagrams, which can be expressed as a one-loop box integral in four dimensions, given by

$$\bar{D}_{1111}(U, V) = -\frac{1}{\pi^2} x_{13}^2 x_{24}^2 \int \frac{d^4 x_5}{x_{15}^2 x_{25}^2 x_{35}^2 x_{45}^2}. \qquad (7.2.6)$$

In the notation for the integrated correlators, we have made clear that they are independent of the spacetime coordiantes, and they are functions of the (complexified) Yang-Mills coupling

$$\tau = \tau_1 + i\tau_2 := \frac{\theta}{2\pi} + i\frac{4\pi}{g_{YM}^2}. \qquad (7.2.7)$$

In this paper, we will be mostly concerned with the perturbative contributions, in which case, $\tau_1 = 0$ (or equivalently the θ angle vanishes), and the integrated correlators are functions of τ_2 (or g_{YM}^2) only. As we commented earlier, with the choices of the integration measures given in (7.2.4) and (7.2.5), the integrated correlators are known to be related to the partition function of $\mathcal{N} = 2^*$ SYM on S^4 through the following relations. For the first integrated correlator, the relation takes the following form,

$$\mathcal{C}_{G_N,1}(\tau, \bar{\tau}) = \frac{1}{4} \Delta_\tau \partial_m^2 \log Z_{G_N}(\tau, \bar{\tau}, m) \big|_{m=0}, \qquad (7.2.8)$$

where the hyperbolic Laplacian is given by $\Delta_\tau = 4\tau_2^2 \partial_\tau \partial_{\bar{\tau}} = \tau_2^2 \left(\partial_{\tau_1}^2 + \partial_{\tau_2}^2 \right)$, and $Z_{G_N}(m, \tau, \bar{\tau})$ is the partition function of $\mathcal{N} = 2^*$ SYM on S^4 with G_N gauge group and m is the mass of the hypermultiplet. The second integrated correlator is then

---

[*]Some possible generalisation of these two integrated correlators was suggested in [169].

[†]The normalisation of $\mathcal{T}_{G_N}(U, V)$ follows the convention of [145] and differs from that in [37,39] by a factor of $c_{G_N}^2$, and c_{G_N} is the central charge given in (7.2.10).

given by

$$\mathcal{C}_{G_N,2}(\tau, \bar{\tau}) = -48\,\zeta(3)\,c_{G_N} + \partial_m^4 \log Z_{G_N}(m, \tau, \bar{\tau})\big|_{m=0}\,, \qquad (7.2.9)$$

where c_{G_N} is the central charge,

$$c_{SU(N)} = \frac{N^2 - 1}{4}\,, \qquad c_{SO(n)} = \frac{n(n-1)}{8}\,, \qquad c_{USp(n)} = \frac{n(n+1)}{8}\,. \qquad (7.2.10)$$

The partition function $Z_{G_N}(m, \tau, \bar{\tau})$ can be expressed as a matrix model integral due to supersymmetric localisation [168]. Explicitly, it can be expressed as

$$Z_{G_N}(m, \tau, \bar{\tau}) = \langle\, \hat{Z}_{G_N}^{pert}(m, a)\, |\hat{Z}_{G_N}^{inst}(m, \tau, a)|^2 \,\rangle_{G_N}\,, \qquad (7.2.11)$$

where we have separated the partition function into the perturbative term $\hat{Z}_{G_N}^{pert}(m, a)$ and the non-perturbative instanton contribution $\hat{Z}_{G_N}^{inst}(m, \tau, a)$. We will omit the instanton contribution, therefore in our consideration $\hat{Z}_{G_N}^{inst}(m, \tau, a) = 1$. The explicit form of $\hat{Z}_{G_N}^{pert}(m, a)$ for each classical gauge group G_N and the definition of the expectation value $\langle \cdots \rangle_{G_N}$ can be found in appendix A.1. Focusing on the perturbative terms, the localisation expressions for integrated correlators reduce to

$$\mathcal{C}_{G_N,1}^{pert}(\tau_2) = \frac{1}{4}\tau_2^2\,\partial_{\tau_2}^2\langle\, \partial_m^2\,\hat{Z}_{G_N}^{pert}(m, a)\big|_{m=0}\,\rangle_{G_N}\,,$$
$$\mathcal{C}_{G_N,2}^{pert}(\tau_2) = -48\,\zeta(3)\,c_{G_N} + \langle\, \partial_m^4\,\hat{Z}_{G_N}^{pert}(m, a)\big|_{m=0}\,\rangle_{G_N} - 3\left(\langle\, \partial_m^2\,\hat{Z}_{G_N}^{pert}(m, a)\big|_{m=0}\,\rangle_{G_N}\right)^2.$$
$$(7.2.12)$$

In the following we will compute the perturbative terms of integrated correlators $\mathcal{C}_{G_N,1}^{pert}(\tau_2)$ and $\mathcal{C}_{G_N,2}^{pert}(\tau_2)$ using the matrix model integrals given in the appendix A.1. As was found in [132], it is convenient to express the perturbation series in terms of central charge, as given in (7.2.10), and the 't Hooft coupling

$$\lambda_{SU(N)} = g_{YM}^2\,N\,, \qquad \lambda_{SO(n)} = g_{YM}^2\,(n-2)\,, \qquad \lambda_{USp(n)} = \frac{g_{YM}^2\,(n+2)}{2}\,, \qquad (7.2.13)$$

where $\lambda_{SU(N)}$ is the standard 't Hooft coupling for $SU(N)$ gauge group, and the others are the generalisations for other gauge groups [132] (see also [170]).

The perturbative expansion for the first integrated correlator was already computed in [132]. It was found that $\mathcal{C}_{G_N,1}^{pert}(\tau_2)$ takes the following universal form for all the gauge

groups G_N,

$$\mathcal{C}^{pert}_{G_N,1}(\tau_2) = 4\, c_{G_N} \left[\frac{3\,\zeta(3) a_{G_N}}{2} - \frac{75\,\zeta(5) a_{G_N}^2}{8} + \frac{735\,\zeta(7) a_{G_N}^3}{16} - \frac{6615\,\zeta(9)\,(1 + P_{G_N,1})\, a_{G_N}^4}{32} \right. $$
$$\left. + \frac{114345\,\zeta(11)\,(1 + P_{G_N,2})\, a_{G_N}^5}{128} + \mathcal{O}(a_{G_N}^6) \right] ,$$

(7.2.14)

where $a_{G_N} = \lambda_{G_N}/(4\pi^2)$. We see that the first three perturbative contributions are universal and their dependence on N is contained entirely within c_{G_N} and a_{G_N}, therefore the first three loops are all planar, and the non-planar terms only start to enter at four loops. Furthermore, the planar contribution is universal for all gauge groups. Explicit non-planar factors, $P_{G_N,i}$ (where $i = L - 3$ and L is the loop number), first enter at four loops and the first two orders for all classical groups are listed below:

$$P_{SU(N),1} = \frac{2}{7N^2}\,, \qquad\qquad P_{SU(N),2} = \frac{1}{N^2}\,,$$
$$P_{SO(n),1} = -\frac{n^2 - 14n + 32}{14(n-2)^3}\,, \qquad\qquad P_{SO(n),2} = -\frac{n^2 - 14n + 32}{8(n-2)^3}\,, \qquad (7.2.15)$$
$$P_{USp(n),1} = \frac{n^2 + 14n + 32}{14(n+2)^3}\,, \qquad\qquad P_{USp(n),2} = \frac{n^2 + 14n + 32}{8(n+2)^3}\,,$$

where for $n = 2N$ or $2N + 1$ for $SO(n)$, and $n = 2N$ for $USp(n)$. It was observed in [132] that the expression manifests the relations between the correlators of $SU(N)$ theory and $SU(-N)$ theory, as well as the correlators of $SO(n)$ theory and $USp(-n)$ theory [171, 172]:

$$\mathcal{C}^{pert}_{SU(N),1}(\tau_2) = \mathcal{C}^{pert}_{SU(-N),1}(-\tau_2)\,,$$
$$\mathcal{C}^{pert}_{SO(n),1}(\tau_2) = \mathcal{C}^{pert}_{USp(-n),1}(-\tau_2/2)\,.$$

(7.2.16)

It is straightforward to evaluate higher-order terms in perturbative expansion, where one finds similar structures for the integrated correlator, and the relations given in (7.2.16) also hold at higher orders.

Similarly, using (7.2.12) and the matrix model description of the partition function given in appendix A.1, we have also evaluated the perturbative contributions to the

second integrated correlator $\mathcal{C}_{G_N,2}^{pert}(\tau_2)$, which is given by,

$$
\mathcal{C}_{G_N,2}^{pert}(\tau_2)
$$
$$
= 4\, c_{G_N} \Bigg[-60 a_{G_N} \zeta(5) + \frac{3 a_{G_N}^2}{2} \Big(36 \zeta(3)^2 + 175 \zeta(7) \Big) - \frac{45 a_{G_N}^3}{2} \Big(20 \zeta(3)\zeta(5) + 49 \zeta(9) \Big)
$$
$$
+ \frac{45 a_{G_N}^4}{2} \Big(340 \zeta(5)^2 + 588 \zeta(3)\zeta(7) + 1617 \zeta(11) + P_{G_N,1} \big(840 \zeta(5)^2 + 1617 \zeta(11) \big) \Big)
$$
$$
- \frac{63 a_{G_N}^5}{16} \Big(1820 \zeta(5)\zeta(7) + 1512 \zeta(3)\zeta(9) + 4719 \zeta(13)
$$
$$
+ \frac{21 P_{G_N,1}}{2} \big(840 \zeta(5)\zeta(7) + 144 \zeta(3)\zeta(9) + 1573 \zeta(13) \big) \Big) + \mathcal{O}(a_{G_N}^6) \Bigg],
$$
$$(7.2.17)$$

where the non-planar contribution $P_{G_N,1}$ is given in (7.2.15). We see that $\mathcal{C}_{G_N,2}^{pert}(\tau_2)$ is considerably more complicated compared to $\mathcal{C}_{G_N,1}^{pert}(\tau_2)$ (that is also the reason that we do not show the higher-order terms). However, some important features of $\mathcal{C}_{G_N,1}^{pert}(\tau_2)$ that we commented earlier remain to be true for $\mathcal{C}_{G_N,2}^{pert}(\tau_2)$. In particular, once again, the planar contribution is universal for gauge groups and the non-planar contributions only start to enter at four loops. The expression given in (7.2.17) (as well as for the higher-order terms which we did not show explicitly) makes it clear that the relationships (7.2.16) also hold for $\mathcal{C}_{G_N,2}^{pert}(\tau_2)$.

In the following section, we will study these two integrated correlators using Feynman diagram methods. In particular, by using the definitions given in (7.2.4) and (7.2.5), we will argue that applying the loop integrands constructed in [134, 135] using graphical tools, the integrated correlators are given by linear combinations of periods associated with the graphs that represent the loop integrands (and their simple generalisations). By computing these higher-loop periods explicitly, we will show that, up to four loops in the planar limit for the first integrated correlator and up to three loops for the second integrated correlator, the numerical coefficients of the perturbation expansion given in (7.2.14) and (7.2.17) agree precisely with the direct loop computations from Feynman diagrams.

7.3 Integrated correlators and Feynman graph periods

In this section, following [134, 135], we will review the construction of perturbative loop integrands for the four-point correlation function of superconformal primary operators in the stress tensor multiplet of $\mathcal{N} = 4$ SYM. It was shown in [134, 135] that due to conformal symmetry and certain hidden permutation symmetry, the Feynman integrals relevant for the correlation function are of very particular forms. At L loops, they are

given by the so-called $f^{(L)}$-functions, which can be represented by the so-called f-graphs [137]. We will then argue that these $f^{(L)}$-functions, when integrated the measures given in (7.2.4) and (7.2.5) for the definition of the integrated correlators, are precisely periods of $(L + 1)$ loops and $(L + 2)$ loops, respectively. Furthermore, these types of Feynman integral periods have been studied in the literature (see e.g. [40, 159–165]), and special techniques, especially computer packages, have been developed for their computations. Therefore this observation allows us to compute the integrated correlators to high-loop orders, as we will do in the next section.

7.3.1 Four-point correlator in $\mathcal{N} = 4$ SYM and its loop integrands

The Feynman integrals that are relevant for the L-loop contribution to the four-point correlator of the superconformal primary operators $\mathcal{O}_2$ operators are the so-called $f^{(L)}$-functions [135]. In general, $f^{(L)}$-function is given by a linear combination of $f_\alpha^{(L)}(x_1, x_2, \ldots, x_{4+L})$ with coefficients that are determined by physical requirements,

$$f^{(L)}(x_i) = \sum_{\alpha=1}^{n_L} c_\alpha^{(L)} f_\alpha^{(L)}(x_1, x_2, \ldots, x_{4+L}). \tag{7.3.1}$$

and $f_\alpha^{(L)}$ may contain both planar and non-planar topologies. We will only consider the planar ones in this paper. Each function $f_\alpha^{(L)}$ is given by

$$f_\alpha^{(L)}(x_1, x_2, \ldots, x_{4+L}) = \frac{P_\alpha^{(L)}(x_1, x_2, \ldots, x_{4+L})}{\prod_{1 \leq i < j \leq 4+L} x_{ij}^2}, \tag{7.3.2}$$

where the subscript α denotes different planar topologies, and we sum over all n_L number of them, see Table.1 in [135] for n_L at lower loops. The function $f^{(L)}$ without the subscript α simply means it has only one planar topology, i.e. $n_L = 1$. The numerator $P_\alpha^{(L)}$ is a polynomial that is determined by the so-called P-graphs. The P-graphs are loop-less multigraph with $(4 + L)$ vertices of degree $(L - 1)$. A line that connects vertices i, j represents a factor x_{ij}^2 – a loop (i.e. a line that connects to the same vertex) is therefore not allowed, it would otherwise lead to a vanishing result, $x_{ii}^2 = 0$. The function $P_\alpha^{(L)}$ is then given by the product of these factors x_{ij}^2 associated with a given P-graph. For example see Fig.7.1, where we give P-graphs for $L = 1, 2, 3$. It is easy to see that $f_\alpha^{(L)}(x_1, x_2, \ldots, x_{4+L})$ has degree-(-4) at each point x_i. Furthermore, $f_\alpha^{(L)}(x_1, x_2, \ldots, x_{4+L})$ is permutation symmetric due to the hidden permutation symmetry found in [134]. The $f_\alpha^{(L)}$-functions can also be represented as graphs: where the solid straight lines denote propagators in (7.3.2) and dashed lines denote the numerators, and each vertex has weight (-4) if we count a solid straight line as (-1) and a dashed line $(+1)$. Such graphs are called f-graphs [137]. Examples of such $f^{(L)}$-graphs for $L = 4$ is shown in Fig.7.2 – they are the loop integrands that
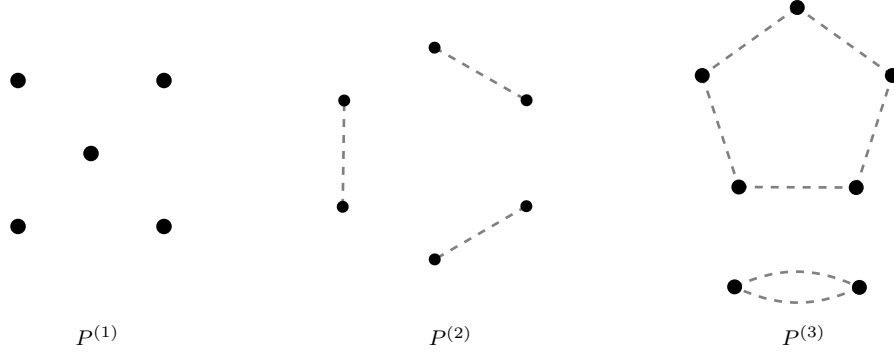
Figure 7.1: Here we draw examples of the P-graphs for the numerator polynomials $P^{(L)}$ with $L = 1, 2, 3$, they are taken from Fig.1 in [135]. As one can see that each $P^{(L)}$-graph has $(L + 4)$ vertices, and each vertex has degree $(L - 1)$.

contribute to the correlator at four loop in the planar limit, and for the first three loops, they are shown in Fig.7.4.

As shown in [134, 135], these $f^{(L)}$-functions are the building blocks for constructing the L-loop integrands for the four-point correlator. In particular, we may write the perturbative expansion of the correlator as

$$\langle \mathcal{O}_2(x_1, Y_1) \dots \mathcal{O}_2(x_4, Y_4) \rangle_{pert} = 2\, c_{G_N} \sum_{L=1}^{\infty} a_{G_N}^L \mathcal{G}_4^{(L)}(1, 2, 3, 4)\,, \tag{7.3.3}$$

where c_{G_N} is the central charge of gauge group G_N given in (7.2.10), and $a_{G_N} = \lambda_{G_N}/(4\pi^2)$ with the 't Hooft coupling λ_{G_N} defined in (7.2.13). The L-loop contribution to the correlation function, denoted by $\mathcal{G}_4^{(L)}(1, 2, 3, 4)$, is given by

$$\mathcal{G}_4^{(L)}(1, 2, 3, 4) = R(1, 2, 3, 4) \times F^{(L)}(x_i)\,, \tag{7.3.4}$$

where the prefactor $R(1, 2, 3, 4)$ is completely fixed by superconformal symmetries [166, 167], and is defined as

$$\begin{aligned}
R(1, 2, 3, 4) = {} & \frac{Y_{12}Y_{23}Y_{34}Y_{14}}{x_{12}^2 x_{23}^2 x_{34}^2 x_{14}^2}(x_{13}^2 x_{24}^2 - x_{12}^2 x_{34}^2 - x_{14}^2 x_{23}^2) \\
& + \frac{Y_{12}Y_{13}Y_{24}Y_{34}}{x_{12}^2 x_{13}^2 x_{24}^2 x_{34}^2}(x_{14}^2 x_{23}^2 - x_{12}^2 x_{34}^2 - x_{13}^2 x_{24}^2) \\
& + \frac{Y_{13}Y_{14}Y_{23}Y_{24}}{x_{13}^2 x_{14}^2 x_{23}^2 x_{24}^2}(x_{12}^2 x_{34}^2 - x_{14}^2 x_{23}^2 - x_{13}^2 x_{24}^2) \\
& + \frac{Y_{12}^2 Y_{34}^2}{x_{12}^2 x_{34}^2} + \frac{Y_{13}^2 Y_{24}^2}{x_{13}^2 x_{24}^2} + \frac{Y_{14}^2 Y_{23}^2}{x_{14}^2 x_{23}^2}\,, \tag{7.3.5}
\end{aligned}$$

where $Y_{ij} = Y_i \cdot Y_j$, and it is proportional to $\mathcal{I}_4(U, V, Y_i)$ in (7.2.1) as,

$$\mathcal{I}_4(U, V, Y_i) = x_{13}^2 x_{24}^2 \, UV\, R(1, 2, 3, 4)\,. \tag{7.3.6}$$
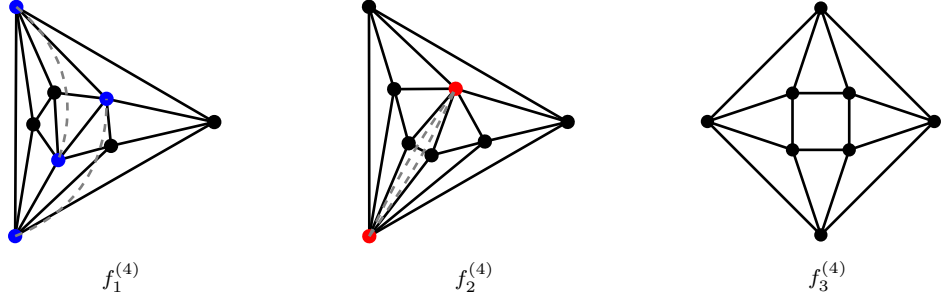
Figure 7.2: Here we draw f-graphs that contribute the correlator at four loops in the planar limit. They are also given in Fig.8 in [135]. The solid straight lines denote propagators and the dashed lines are the numerators (or inverse propagators). The blue or red vertex means it has one or two numerator(s) attached, respectively. This ensures that each vertex has degree (-4), if we count each solid straight line as (-1) and dashed line as $(+1)$.

The function $F^{(L)}(x_i)$ is related to $f^{(L)}(x_i)$, as the following

$$F^{(L)}(x_i) = \frac{x_{12}^2 x_{13}^2 x_{14}^2 x_{23}^2 x_{24}^2 x_{34}^2}{L!(-4\pi^2)^L} \int d^4 x_5 \cdots d^4 x_{4+L} \, f^{(L)}(x_i) \,. \tag{7.3.7}$$

The loop integrands $f^{(L)}(x_i)$ have been computed up to ten loops in the planar limit [134–137], and up to four loops for the non-planar contribution [133]. Finally, comparing (7.3.3) with (7.2.1) and using (7.3.6), we find the perturbative contribution to the correlator can be expressed as

$$\mathcal{T}_{G_N}(U,V) = 2 \, c_{G_N} \frac{U}{V} \sum_{L=1}^{\infty} a_{G_N}^L \, x_{13}^2 x_{24}^2 \, F^{(L)}(x_i) \,. \tag{7.3.8}$$

This is the formula that we will be using for the computation of integrated correlators in the next subsection.

7.3.2 Integrated correlators as Feynman graph periods

A period [173] is defined to be the absolutely convergent integral of a rational differential form over a domain given by polynomial inequalities:

$$\pi^{-2n} \int_{\Delta} dx_1 \ldots dx_n \frac{P(x_1, \ldots, x_n)}{Q(x_1, \ldots, x_n)} \,, \tag{7.3.9}$$

where the integration domain Δ is defined by $\{h_i(x_1, \ldots, x_n) \geq 0\}$, and P, Q, h_i are polynomials with rational coefficients. The construction of periods has many fascinating applications to number theory as well as to the computations of Feynman diagrams in quantum field theory. In this subsection, we will argue that the integrated correlators defined in (7.2.4) and (7.2.5) using the loop integrands reviewed in subsection 7.3.1 are precisely periods of Feynman graphs associated with the $f^{(L)}$-functions. In particular,

we find the first integrated correlator can be expressed in terms of the periods of f-graphs, whereas for the second integrated correlator, it is given by the periods of $\widetilde{f}$-graphs. A $\widetilde{f}$-graph is the generalisation of the f-graph by attaching it with an additional one-loop box integral, which will define later with more details.

First integrated correlator

We begin with the first correlator given in (7.2.4),

$$\mathcal{C}_{G_N, 1}(\tau_2) = I_2\left[\mathcal{T}_{G_N}(U, V)\right] = -\frac{8}{\pi} \int_0^\infty dr \int_0^\pi d\theta \frac{r^3 \sin^2(\theta)}{U^2} \mathcal{T}_{G_N}(U, V) , \qquad (7.3.10)$$

then plug in the perturbative contribution of $\mathcal{T}_{G_N}(U, V)$ in (7.3.8) to arrive the following expression

$$I_2\left[\mathcal{T}_{G_N}(U, V)\right] = -\frac{8}{\pi}(2c_{G_N}) \int_0^\infty dr \int_0^\pi d\theta \, r^3 \sin^2(\theta) \frac{1}{UV} x_{13}^2 x_{24}^2 \sum_{L \geq 1} a_{G_N}^L F^{(L)}(x_i) . \tag{7.3.11}$$

For the later convenience and comparison with the localisation result (7.2.14), we will consider the integration acting on $F^{(L)}$ at each loop order, and pull out an overall factor $(4 c_{G_N})$ as follows

$$I_2\left[\mathcal{T}_{G_N}(U, V)\right] = 4 c_{G_N} \sum_{L \geq 1} a_{G_N}^L I_2'\left[F^{(L)}(x_i)\right] , \tag{7.3.12}$$

and define the I_2' integral as

$$I_2'\left[F^{(L)}(x_i)\right] = -\frac{4}{\pi} \int_0^\infty dr \int_0^\pi d\theta \, r^3 \sin^2(\theta) \frac{1}{UV} x_{13}^2 x_{24}^2 F^{(L)}(x_i) . \tag{7.3.13}$$

As observed in [145], the above integral (7.3.13) can be viewed as an integration over a four-dimensional vector, P_V, with $P_V^2 = V$. Using the relations $U = 1 + r^2 - 2r \cos(\theta)$ and $V = r^2$, we have

$$\int d^4 P_V = 4\pi \int_0^\infty dr \, r^3 \int_0^\pi d\theta \sin^2(\theta) . \tag{7.3.14}$$

In this form, the integrated correlator can be expressed as

$$I_2'\left[F^{(L)}(x_i)\right] = -\frac{1}{\pi^2} \int d^4 P_V \frac{1}{UV} x_{13}^2 x_{24}^2 F^{(L)}(x_i) . \tag{7.3.15}$$

Substituting the definition for the cross ratios U, V given in (7.2.3) in terms of x_i's, we find,

$$
\begin{aligned}
I_2' \left[F^{(L)}(x_i) \right] &= -\frac{1}{\pi^2} \int d^4 P_V \frac{x_{13}^6 x_{24}^6}{x_{12}^2 x_{34}^2 x_{14}^2 x_{23}^2} F^{(L)}(x_i) \\
&= -\frac{1}{\pi^2 L! (-4\pi^2)^L} \int d^4 P_V x_{13}^8 x_{24}^8 \int d^4 x_5 \cdots d^4 x_{4+L} \, f^{(L)}(x_i), \quad (7.3.16)
\end{aligned}
$$

where we have used the relation (7.3.7) to arrive at the final expression.

The integrated correlator is given by finite conformal integrals, which allow us to fix three points, for the convenience, we choose them to be $(\mathbf{0}, \mathbf{1}, \infty)$. Firstly, we set x_4 to be infinity, and the integration (7.3.16) reduces to the following expression,

$$
I_2' \left[F^{(L)}(x_i) \right] = -\frac{1}{\pi^2 L! (-4\pi^2)^L} \int d^4 P_V x_{13}^8 \int d^4 x_5 \cdots d^4 x_{4+L} \, f^{(L)}(x_i), \quad (7.3.17)
$$

and we also observe under the $x_4 \to \infty$ limit, the cross ratios become

$$
U = \frac{x_{12}^2}{x_{13}^2}, \qquad V = \frac{x_{23}^2}{x_{13}^2}. \quad (7.3.18)
$$

We further choose $x_3 = \mathbf{0}$, $x_1 = \mathbf{1}$, then x_2 is identified with P_V. Finally, putting everything together, we find the integrated correlator is given by

$$
I_2' \left[F^{(L)}(x_i) \right] = -\frac{1}{\pi^2 L! (-4\pi^2)^L} \int d^4 x_2 \int d^4 x_5 \cdots d^4 x_{4+L} \, f^{(L)}(x_i) \Big|_{(x_3, x_1, x_4) = (\mathbf{0}, \mathbf{1}, \infty)}, \quad (7.3.19)
$$

which is exactly the definition of a period with $(x_3, x_1, x_4) = (\mathbf{0}, \mathbf{1}, \infty)$ in (7.3.9). Therefore, we conclude[*]

$$
I_2' \left[F^{(L)}(x_i) \right] = -\frac{1}{L! (-4)^L} \mathcal{P}_{f^{(L)}}. \quad (7.3.20)
$$

Importantly, since $f^{(L)}(x_i)$ is permutation invariant, the result is independent of choosing which three points to take special values.

Because these graphs are finite and conformal, we may 'complete' the graph by putting back x_1, x_3, x_4 in (7.3.19), in terminology of [162]. The periods defined above are then associated with f-graphs, such as those in Fig.7.2. In the simplest case when the numerator cancels completely some of the denominators, $\mathcal{P}_{f_\alpha^{(L)}}$ reduces to the period associated with certain Feynman diagram of the ϕ^4 theory, and it is then a 4-regular graph. While for the integrated correlators we consider here, the graphs generally involve numerators, but all the graphs are still restricted to be Feynman graphs with

---

[*]Note the factor $1/(\pi^2)^L$ has been absorbed in the definition of periods in (7.3.9).

each vertex of degree-(-4).

In summary, we conclude that the first integrated correlator can be expressed as a sum of periods at every loop order,

$$
\begin{aligned}
I_2\left[\mathcal{T}_{G_N}(U,V)\right] &= 4\,c_{G_N}\sum_{L\geq 1} a_{G_N}^L I_2'\left[F^{(L)}(x_i)\right] = -4\,c_{G_N}\sum_{L\geq 1}\frac{a_{G_N}^L}{L!(-4)^L}\mathcal{P}_{f^{(L)}}\\
&= -4\,c_{G_N}\sum_{L\geq 1}\frac{a_{G_N}^L}{L!(-4)^L}\sum_{\alpha=1}^{n_L} c_\alpha^{(L)}\,\mathcal{P}_{f_\alpha^{(L)}}\,,
\end{aligned}
\tag{7.3.21}
$$

where we have used (7.3.1) to arrive at the final expression.

Second integrated correlator

Let us now consider the second integrated correlator as defined in (7.2.5). We will see that, at L loops, the integrated correlator is expressed as a sum of periods of $(L+2)$ loops. Compared to the first integrated correlator, there is an additional loop integral, this is because of the one-loop box integral $\bar{D}_{1111}(U,V)$ in the integration measure.

The second integrated correlator is given in (7.2.5), which we quote below,

$$
\begin{aligned}
\mathcal{C}_{G_N,2}(\tau_2) &= I_4\left[\mathcal{T}_{G_N}(U,V)\right]\\
&= -\frac{32}{\pi}\int_0^\infty dr \int_0^\pi d\theta \frac{r^3\sin^2(\theta)}{U^2}\,(1+U+V)\bar{D}_{1111}(U,V)\,\mathcal{T}_{G_N}(U,V)\,.
\end{aligned}
\tag{7.3.22}
$$

Using the definition of $\mathcal{T}_{G_N}(U,V)$ in terms of $F^{(L)}(x_i)$ in (7.3.8), and we arrive at the following expression

$$
\begin{aligned}
&I_4\left[\mathcal{T}_{G_N}(U,V)\right]\\
&= -\frac{32}{\pi}\,(2c_{G_N})\int_0^\infty dr\int_0^\pi d\theta\frac{r^3\sin^2(\theta)}{UV}(1+U+V)\bar{D}_{1111}(U,V)\,x_{13}^2 x_{24}^2\sum_{L\geq 1} a_{G_N}^L F^{(L)}(x_i)\,.
\end{aligned}
\tag{7.3.23}
$$

Similarly to (7.3.12) and (7.3.13), we define the integral that acts on $F^{(L)}(x_i)$ at each loop order,

$$
I_4\left[\mathcal{T}_{G_N}(U,V)\right] = 4\,c_{G_N}\sum_{L\geq 1} a_{G_N}^L I_4'\left[F^{(L)}(x_i)\right]\,.
\tag{7.3.24}
$$

The I_4' integral is defined as

$$
\begin{aligned}
I_4'\left[F^{(L)}(x_i)\right] &= -\frac{16}{\pi} \int_0^\infty dr \int_0^\pi d\theta \frac{r^3 \sin^2(\theta)}{UV} x_{13}^2 x_{24}^2 (1 + U + V)\bar{D}_{1111}(U,V) F^{(L)}(x_i) \\
&= 4\, I_2'\left[\widetilde{F}^{(L)}(x_i)\right],
\end{aligned}
\tag{7.3.25}
$$

where in the last step we have used (7.3.13) to express the I_4' integral as the I_2' integral with a different function in the argument, called $\widetilde{F}^{(L)}(x_i)$, which is defined as

$$
\widetilde{F}^{(L)}(x_i) = (1 + U + V)\bar{D}_{1111}(U,V)F^{(L)}(x_i)\,.
\tag{7.3.26}
$$

Furthermore, using the definition of the one-loop box integral $\bar{D}_{1111}(U,V)$ given in (7.2.6), we can express $\widetilde{F}^{(L)}(x_i)$ as

$$
\widetilde{F}^{(L)}(x_i) = 4\,\frac{x_{12}^2 x_{13}^2 x_{14}^2 x_{23}^2 x_{24}^2 x_{34}^2}{L!\,(-4\pi^2)^{L+1}} \int d^4x_5 \cdots d^4x_{4+L} d^4x_{5+L}\,\widetilde{f}^{(L)}(x_i)\,,
\tag{7.3.27}
$$

with

$$
\widetilde{f}^{(L)}(x_i) = \sum_{\blacksquare = 1, U, V} \widetilde{f}_{\blacksquare}^{(L)}(x_i) = \frac{x_{13}^2 x_{24}^2 (1 + U + V)}{x_{1,5+L}^2 x_{2,5+L}^2 x_{3,5+L}^2 x_{4,5+L}^2}\,f^{(L)}(x_i)\,,
\tag{7.3.28}
$$

where $\blacksquare$ specifies the three terms, 1, U, and V, and we sum over all these terms to ensure S_4 permutation symmetry.[*] Since the $I_2'\left[\widetilde{F}^{(L)}(x_i)\right]$ integral gives the period of $\widetilde{f}^{(L)}$ as in (7.3.20), we therefore conclude

$$
I_4'\left[F^{(L)}(x_i)\right] = 4\,I_2'\left[\widetilde{F}^{(L)}(x_i)\right] = 4 \times \frac{1}{L!(-4)^L}\mathcal{P}_{\widetilde{f}^{(L)}}\,.
\tag{7.3.29}
$$

Due to the extra one-loop box integral, $\widetilde{f}^{(L)}$ only respects $S_4 \times S_L$ permutation symmetry instead of full S_{4+L} symmetry. The isometry of a graph will then depend on which four vertices are attached to the extra x_{5+L} point, hence may result in different period values. We will call the graphs associated with $\widetilde{f}$-functions as $\widetilde{f}$-graphs, which are f-graphs attached with an additional one-loop box (see Fig.7.3 for some examples). Using the fact that f-graphs have degree-(-4) at each point x_i, (7.3.28) implies that $\widetilde{f}$-graphs also have degree-(-4) at each point x_i.

The period of $\widetilde{f}^{(L)}$ needs to be summed over all different isometries, $\widetilde{f}^{(L,k)}$, explicitly

$$
\widetilde{f}^{(L)}(x_i) = \sum_{k=1}^{\widetilde{n}_L} \widetilde{f}^{(L,k)}(x_i)\,,
\tag{7.3.30}
$$

---

[*]In general, $\widetilde{f}_{\blacksquare}^{(L)}$ could have another subscript α, but since we only consider up to three loops for the second correlator, where $f^{(L)}$ only has one planar topology, we will drop the subscript α.
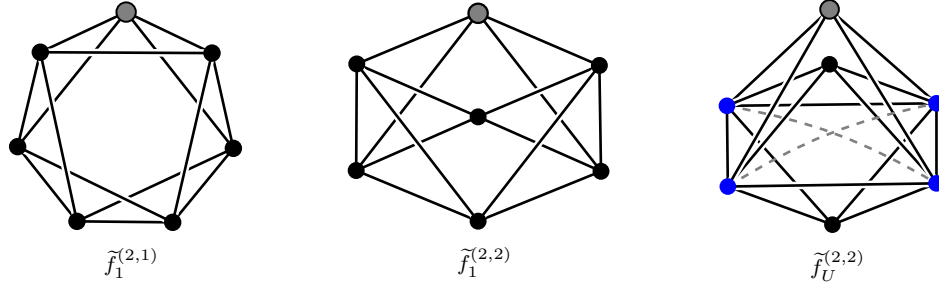
Figure 7.3: Here we draw some examples of $\widetilde{f}$-graphs, $\widetilde{f}_1^{(2,1)}, \widetilde{f}_1^{(2,2)}, \widetilde{f}_U^{(2,2)}$, which are isomorphic to $f_1^{(3)}, f_3^{(3)}, f_4^{(3)}$ in Fig.2 in [135], respectively. Other $\widetilde{f}_\blacksquare^{(2,k)}$'s are isomorphic to the graphs shown above or to the three loop planar graph $f^{(3)}$ in Fig.7.4. The grey vertices in the graphs denote the point x_{5+L} arising from inserting the one-loop box $\bar{D}_{1111}$ in the definition of the second integrated correlator.

where each $\widetilde{f}^{(L,k)}$ respects $S_4 \times S_L$ permutation symmetry, and $\widetilde{n}_L$ denotes the number of graphs that have distinguished isometries. Within each $\widetilde{f}^{(L,k)}$, it contains three terms with different prefactor, 1, U and V. We denote these three terms by $\widetilde{f}_1^{(L,k)}$, $\widetilde{f}_U^{(L,k)}$, and $\widetilde{f}_V^{(L,k)}$ (some examples are given in Fig.7.3), therefore,

$$\widetilde{f}^{(L,k)}(x_i) = \sum_{\blacksquare=1,U,V} \widetilde{f}_\blacksquare^{(L,k)}(x_i). \qquad (7.3.31)$$

To conclude, $\mathcal{P}_{\widetilde{f}^{(L)}}$ can be expressed as,

$$\mathcal{P}_{\widetilde{f}^{(L)}} = \sum_{k=1}^{\widetilde{n}_L} \sum_{\blacksquare=1,U,V} \mathcal{P}_{\widetilde{f}_\blacksquare^{(L,k)}}. \qquad (7.3.32)$$

Here again $\widetilde{n}_L$ is the number of the non-isomorphic graphs. For example, at two loops, we have two terms (i.e. $\widetilde{n}_2 = 2$), $g \times h(1,2;3,4) + S_4 \times S_2$ and $g \times [g(1,2,3,4)]^2 + S_4 \times S_2$, which are a one-loop box times a two-loop ladder, and a one-loop box times a square of one-loop boxes, respectively. At three loops, we find $\widetilde{n}_3 = 5$, as we will use later.

7.4 Integrated correlators from Feynman graph periods

In this section, we will apply the relation between the integrated correlators and periods that we discussed in the previous section to concretely compute the integrated correlators order by order in the perturbative expansion. We will use the Maple package `HyperlogProcedures` developed by Schnetz [49] for the evaluations of the periods associated with f-graphs and $\widetilde{f}$-graphs to high-loop orders, and find agreement with the perturbation expansion of the integrated correlators obtained using supersymmetric localisation, as given in (7.2.14) and (7.2.17).

The identification between the integrated correlators and periods of certain degree-

(-4) Feynman graphs also implies interesting relations among these periods. In particular, the sum of these particular periods should produce the results of the integrated correlators that are given by supersymmetric localisation. We will consider the first integrated correlator at five loops in the planar limit, for which, we have computed all the relevant periods, except one. In this case, using the result from supersymmetric localisation, one can predict an analytical expression for the period of a six-loop Feynman graph.

7.4.1 First integrated correlator up to four loops

We begin by considering the first integrated correlator at one and two loops. This was already done in [145], and was shown that the results from explicit loop integrals agree with what was obtained from localisation. Here we will reproduce these results using the technique of periods (7.3.20). We will then present new results of the integrated correlator at three and four loops.

Recall that in general the first integrated correlator can be expressed as a sum of periods,

$$
I_2\left[\mathcal{T}_{G_N}(U, V)\right] = 4\, c_{G_N} \sum_{L \geq 1} a_{G_N}^L\, I_2'\left[F^{(L)}(x_i)\right] = -4\, c_{G_N} \sum_{L \geq 1} \frac{a_{G_N}^L}{L!(-4)^L} \sum_{\alpha=1}^{n_L} c_\alpha^{(L)}\, \mathcal{P}_{f_\alpha^{(L)}}\,.
$$
(7.4.1)

At one and two loops, as shown in Fig.7.1, the $P^{(L)}$-graphs with $L = 1, 2$, are unique. Therefore, the associated loop integrands $f^{(1)}, f^{(2)}$ are also unique, as we show in Fig.7.4. Using (7.4.1), we have

$$
I_2'\left[F^{(1)}(x_i)\right] = -\frac{1}{1!(-4)^1} \times \mathcal{P}_{f^{(1)}}\,,
$$
(7.4.2)

where the $f^{(1)}$-function, see Fig.7.4, is given by

$$
f^{(1)}(x_i) = c^{(1)}\, \frac{P^{(1)}(x_1, \ldots, x_5)}{\prod_{1 \leq i < j \leq 5} x_{ij}^2}\,, \qquad \text{with} \qquad c^{(1)} = 1\,, \qquad P^{(1)}(x_1, \ldots, x_5) = 1\,,
$$
(7.4.3)

Using the period of $f^{(1)}(x_i)$, which is well-known,

$$
\mathcal{P}_{f^{(1)}} = 6\zeta(3)\,,
$$
(7.4.4)

we arrive at

$$
I_2'\left[F^{(1)}(x_i)\right] = \frac{3\zeta(3)}{2}\,.
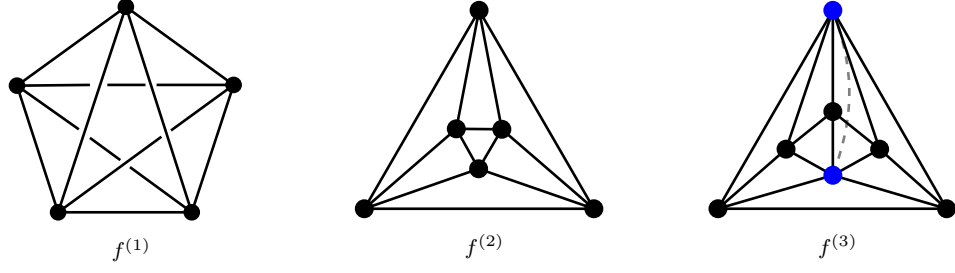$$
(7.4.5)

Figure 7.4: Here we draw the planar f-graphs up to three loops. (They have been given in Fig.2 in [135]).

Similarly, at two loops (i.e. $L = 2$), the $f^{(2)}$-function, see Fig.7.4, is given by

$$f^{(2)}(x_i) = c^{(2)} \frac{P^{(2)}(x_1, \ldots, x_6)}{\prod_{1 \leq i < j \leq 6} x_{ij}^2} , \qquad (7.4.6)$$

where the coefficient $c^{(2)} = 1$ and the numerator $P^{(2)}$ is given by

$$P^{(2)}(x_1, \ldots, x_6) = \left(\frac{1}{48} x_{12}^2 x_{34}^2 x_{56}^2 \right) + S_6 . \qquad (7.4.7)$$

A few comments are in order regarding the numerator $P^{(2)}$, which will also be useful for higher-loop computations. Here S_{4+L} (in this case $L = 2$) denotes total permutations of $(x_1, \cdots, x_{4+L})$ labels. The factor 48 ensures the each term in the sum appears with a unit weight, i.e. it mods out the over-counting of S_{4+L} permutations. There are 6! terms in S_6 permutations, while they all have the same value when taking periods. So the $\mathcal{P}_{f^{(2)}}$ is simply given by 6! (and divided by 48) times the period of a single term. For example, we take the first term in $P^{(2)}$, which is $x_{12}^2 x_{34}^2 x_{56}^2$, divided by numerator $\prod_{1 \leq i < j \leq 6} x_{ij}^2$, and this single term gives a period with value of $20\zeta(5)$. So the period of $f^{(2)}$ is given by

$$\mathcal{P}_{f^{(2)}} = 6! \times \frac{1}{48} \times 20\zeta(5) . \qquad (7.4.8)$$

Put all the factors together, we finally obtain,

$$I_2' \left[F^{(2)}(x_i) \right] = -\frac{1}{2! \, (-4)^2} c^{(2)} \mathcal{P}_{f^{(2)}} = -\frac{75\zeta(5)}{8} . \qquad (7.4.9)$$

We see that the results of $L = 1, 2$ cases given in (7.4.5) and (7.4.9) reproduce the computation of [145] and match precisely with the first two orders of the localisation result given in (7.2.14). The same methods apply to higher-loop terms, and below we will consider three- and four-loop cases.

At three loops, it was shown in [134] that even though one may be able to draw graphs with non-planar topologies at this order, only the planar diagram (and there is a single such planar diagram) can contribute to the four-point correlator. Therefore,

just as the one- and two-loop cases, there is a unique integrand at this order, as shown in Fig.7.4, and it is given by

$$f^{(3)}(x_i) = c^{(3)} \frac{P^{(3)}(x_1, \ldots, x_7)}{\prod_{1 \leq i < j \leq 7} x_{ij}^2}, \tag{7.4.10}$$

with coefficient $c^{(3)} = 1$ and the numerator given by

$$P^{(3)}(x_1, \ldots, x_7) = \left(\frac{1}{20} x_{12}^4 x_{34}^2 x_{45}^2 x_{56}^2 x_{67}^2 x_{37}^2 \right) + S_7. \tag{7.4.11}$$

There are 7! terms in S_7 permutations (the factor 20 again ensures the unit weight of each term in S_7 permutations), while they all have the same value when taking periods. So the $\mathcal{P}_{f^{(3)}}$ is simply given by 7! (and divided by 20) times the period of a single term, which is given by

$$\mathcal{P}_{f^{(3)}} = 7! \times \frac{1}{20} \times 70\zeta(7), \tag{7.4.12}$$

where we have used the Maple program `HyperLogProcedures` to the evaluate this period[*]. Together, we find

$$I_2' \left[F^{(3)}(x_i) \right] = -\frac{1}{3!\,(-4)^3} \times c^{(3)}\, \mathcal{P}_{f^{(3)}} = \frac{735\zeta(7)}{16}, \tag{7.4.13}$$

which agrees with the localisation result (7.2.14).

We would like to remark that the three-loop integration over points x_5, x_6, x_7 of $f^{(3)}$ leads to the three-loop contribution to the correlator [158], where the answer was found to be expressed in terms of rather complicated multiple polylogarithms. As we showed above, with one additional integral with the measure given in (7.3.10), the result actually simplifies dramatically and reduces to simply some rational number times $\zeta(7)$, as given in (7.4.13). This example shows clearly the simplicity of the integrated correlator.

Starting at $L = 4$, there are non-trivial non-planar contributions [133, 135]. We will only focus on the planar contribution here. At this order, there are three planar f-graphs (see Fig.7.2), explicitly they are expressed as

$$f^{(4)}(x_i) = \sum_{\alpha=1}^{3} c_\alpha^{(4)} f_\alpha^{(4)}(x_1, \cdots, x_8) = \sum_{\alpha=1}^{3} c_\alpha^{(4)} \frac{P_\alpha^{(4)}(x_1, \ldots, x_8)}{\prod_{1 \leq i < j \leq 8} x_{ij}^2}, \tag{7.4.14}$$

---

[*]Recall that the periods associated with the L-loop contributions to the first integrated correlator are $(L+1)$-loop integrals. So in this case with $L = 3$, the period is a four-loop integral.

where $c_1^{(4)} = c_2^{(4)} = -c_3^{(4)} = 1$, and the numerator $P_\alpha^{(4)}$'s are given by

$$P_1^{(4)}(x_1, \ldots, x_8) = \left(\frac{1}{8} x_{12}^2 x_{13}^2 x_{16}^2 x_{24}^2 x_{27}^2 x_{34}^2 x_{38}^2 x_{45}^2 x_{56}^4 x_{78}^4 \right) + S_8 \,,$$

$$P_2^{(4)}(x_1, \ldots, x_8) = \left(\frac{1}{24} x_{12}^2 x_{13}^2 x_{16}^2 x_{23}^2 x_{25}^2 x_{34}^2 x_{45}^2 x_{46}^2 x_{56}^2 x_{78}^6 \right) + S_8 \,,$$

$$P_3^{(4)}(x_1, \ldots, x_8) = \left(\frac{1}{16} x_{12}^2 x_{15}^2 x_{18}^2 x_{23}^2 x_{26}^2 x_{34}^2 x_{37}^2 x_{45}^2 x_{48}^2 x_{56}^2 x_{67}^2 x_{78}^2 \right) + S_8 \,. \qquad (7.4.15)$$

The first integrated correlator at four loops (the planar sector) is then given by

$$I_2' \left[F^{(4)}(x_i) \right] = -\frac{1}{4! \, (-4)^4} \times \left(\mathcal{P}_{f_1^{(4)}} + \mathcal{P}_{f_2^{(4)}} - \mathcal{P}_{f_3^{(4)}} \right) = -\frac{6615 \zeta(9)}{32} \,, \qquad (7.4.16)$$

where we have used the results of each period of $f_\alpha^{(4)}$

$$\mathcal{P}_{f_1^{(4)}} = 8! \times \frac{1}{8} \times 252 \zeta(9) \,,$$

$$\mathcal{P}_{f_2^{(4)}} = 8! \times \frac{1}{24} \times 252 \zeta(9) \,,$$

$$\mathcal{P}_{f_3^{(4)}} = 8! \times \frac{1}{16} \times 168 \zeta(9) \,.$$

We have again utilised Maple package `HyperLogProcedures` and the S_8 permutation symmetry of $f^{(4)}$-graph periods for the computation. The Feynman diagram result (7.4.16) once again agrees with the localisation computation given in (7.2.14) for the planar part at the order $a_{G_N}^4$.

7.4.2 First integrated correlator at five loops and relations of periods

As we anticipated, beyond four loops, we have not computed all the periods that are relevant for the first integrated correlator and cannot compare with the supersymmetric localisation results. We will however take a different point of view by considering the localisation results as constraints on these higher-loop Feynman periods. This then leads to non-trivial relations among these periods. In the four-loop example we considered in the previous subsection, one may consider (7.4.16) as the required relationship of the five-loop periods for the graphs in Fig.7.2. We will now apply this consideration to the five-loop integrated correlator, which will lead to prediction for a particular six-loop period.

At five loops, there are seven planar f-graphs that contribute to the four-point correlator in the planar limit [135], which can be written as

$$f^{(5)}(x_i) = \sum_{\alpha=1}^{7} c_\alpha^{(5)} f_\alpha^{(5)}(x_1, \cdots, x_9) \,, \qquad (7.4.17)$$
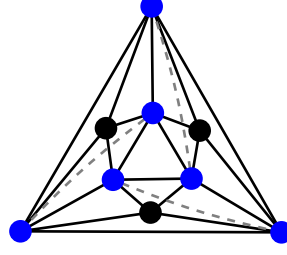
Figure 7.5: The graph for $f_4^{(5)}$, whose period is predicted by supersymmetric localisation in (7.4.26).

with the coefficients determined in [135], $c_2^{(5)} = c_3^{(5)} = c_4^{(5)} = c_6^{(5)} = c_7^{(5)} = 1$ and $c_1^{(5)} = c_5^{(5)} = -1$. The explicit forms of $f_\alpha^{(5)}$ are given in equations (6.2) and (6.5) of the paper [135] in terms of P-polynomials. They are also shown in Figure 9 in [135].

Using `HyperlogProcedures`, we have evaluated all the periods for $f_\alpha^{(5)}$, except for $f_4^{(5)}$, which is shown in Fig.7.5. The results of these periods that we have evaluated are listed below:

$$\mathcal{P}_{f_1^{(5)}} = 9! \times \frac{1}{2} \times \Big[- 40\zeta(3)^2\zeta(5) + 4240\zeta(11) + \frac{8\pi^6}{63}\zeta(5) - \frac{8\pi^4}{5}\zeta(7) - 360\pi^2\zeta(9)$$
$$- 48\zeta(5,3,3) \Big] \,, \tag{7.4.18}$$

$$\mathcal{P}_{f_2^{(5)}} = 9! \times \frac{1}{4} \times 924\zeta(11) \,, \tag{7.4.19}$$

$$\mathcal{P}_{f_3^{(5)}} = 9! \times \frac{1}{4} \times 924\zeta(11) \,, \tag{7.4.20}$$

$$\mathcal{P}_{f_5^{(5)}} = 9! \times \frac{1}{8} \times \Big[320\zeta(3)^2\zeta(5) + 800\zeta(5)^2 - 29300\zeta(11) - \frac{64\pi^6}{63}\zeta(5) + \frac{64\pi^4}{5}\zeta(7)$$
$$+ 2880\pi^2\zeta(9) + 384\zeta(5,3,3) \Big] \,, \tag{7.4.21}$$

$$\mathcal{P}_{f_6^{(5)}} = 9! \times \frac{1}{28} \times 924\zeta(11) \,, \tag{7.4.22}$$

$$\mathcal{P}_{f_7^{(5)}} = 9! \times \frac{1}{12} \times 400\zeta(5)^2 \,. \tag{7.4.23}$$

The multiple zeta value is defined as

$$\zeta(n_d, \cdots, n_1) = \sum_{k_d > \cdots > k_1 \geq 1} \frac{1}{k_d^{n_d} \cdots k_1^{n_1}} \,, \qquad n_d \geq 2 \,. \tag{7.4.24}$$

In order to match with the localisation result given in (7.2.14) at order $a_{G_N}^5$, it requires the following relations among the periods of $f_\alpha^{(5)}$ to hold

$$I_2'\Big[F^{(5)}\Big] = -\frac{1}{5!\,(-4)^5} \times \Big(-\mathcal{P}_{f_1^{(5)}} + \mathcal{P}_{f_2^{(5)}} + \mathcal{P}_{f_3^{(5)}} + \mathcal{P}_{f_4^{(5)}} - \mathcal{P}_{f_5^{(5)}} + \mathcal{P}_{f_6^{(5)}} + \mathcal{P}_{f_7^{(5)}} \Big)$$
$$= \frac{114345}{128}\zeta(11) \,. \tag{7.4.25}$$

Knowing $\mathcal{P}_{f_\alpha^{(5)}}$ for all the α's except $\alpha = 4$ (as given in Fig.7.5), the above relation allows us to determine the period $\mathcal{P}_{f_4^{(5)}}$, which we find to be

$$
\begin{aligned}
\mathcal{P}_{f_4^{(5)}} = 9! \times \frac{1}{6} \times \Big[& 120\zeta(3)^2\zeta(5) + 400\zeta(5)^2 - 10410\zeta(11) \\
& - \frac{8\pi^6}{21}\zeta(5) + \frac{24\pi^4}{5}\zeta(7) + 1080\pi^2\zeta(9) + 144\zeta(5,3,3) \Big] , \quad (7.4.26)
\end{aligned}
$$

where the prefactor $9! \times \frac{1}{6}$ is some combinatorics factors associated with the permutation symmetry of the integrand, and the numerical value of $\mathcal{P}_{f_4^{(5)}}$ is $9! \times \frac{1}{6} \times (967.13267 \cdots)$.

7.4.3 Second integrated correlator up to three loops

In this subsection, we will consider the second integrated correlator. As we argued in the section 7.3.2, the L-loop contribution of the second integrated correlator can be expressed in terms of periods of $(L + 2)$ loops. We will compute all the second integrated correlators up to three loops.

Let us begin by considering the integrated correlator at one loop. Using (7.3.29) and (7.3.32), we have

$$
I_4' \left[F^{(1)}(x_i) \right] = 4 \times \frac{1}{(-4)^1} \times \mathcal{P}_{\widetilde{f}^{(1,1)}} , \quad (7.4.27)
$$

where

$$
\widetilde{f}^{(1,1)}(x_i) = \sum_{\blacksquare=1,U,V} \widetilde{f}_\blacksquare^{(1,1)}(x_i) = \frac{x_{13}^2 x_{24}^2 (1 + U + V)}{\prod_{1 \leq i < j \leq 4} x_{ij}^2} \, g \times g_{(1,2,3,4)}^{(5)} . \quad (7.4.28)
$$

The function $g_{(1,2,3,4)}^{(5)}$ is the integrand of the one-loop box

$$
g_{(1,2,3,4)}^{(5)} = \frac{1}{x_{1,5}^2 x_{2,5}^2 x_{3,5}^2 x_{4,5}^2} , \quad (7.4.29)
$$

and we define a short-hand notation, $g \times [\cdots]$, which is the product of a one-loop box g and an L-loop integrand,

$$
g \times [\cdots] := \frac{1}{x_{1,5+L}^2 x_{2,5+L}^2 x_{3,5+L}^2 x_{4,5+L}^2} \times [\cdots] , \quad (7.4.30)
$$

where $[\cdots]$ is the integrand of any L-loop integral. The period of $\widetilde{f}^{(1,1)}$ can be evaluated straightforwardly, and it is given by

$$
\mathcal{P}_{\widetilde{f}^{(1,1)}} = \sum_{\blacksquare=1,U,V} \mathcal{P}_{\widetilde{f}_\blacksquare^{(1,1)}} = 20\zeta(5) + 20\zeta(5) + 20\zeta(5) = 60\zeta(5) . \quad (7.4.31)
$$

In conclusion, we find

$$I'_4 \left[F^{(1)}(x_i) \right] = -60\zeta(5) , \tag{7.4.32}$$

which agrees with the localisation result given in (7.2.17).

At two loops, we have

$$I'_4 \left[F^{(2)}(x_i) \right] = 4 \times \frac{1}{2!(-4)^2} \times \left(\mathcal{P}_{\widetilde{f}^{(2,1)}} + \mathcal{P}_{\widetilde{f}^{(2,2)}} \right) , \tag{7.4.33}$$

where $\widetilde{f}^{(2,1)}$ and $\widetilde{f}^{(2,2)}$ are give by

$$\widetilde{f}^{(2,1)}(x_i) = \sum_{\blacksquare = 1, U, V} \widetilde{f}^{(2,1)}_{\blacksquare}(x_i) = \left(\frac{x_{13}^2 x_{24}^2 \left(1 + U + V \right)}{\prod_{1 \leq i < j \leq 4} x_{ij}^2} \, g \times h^{(5,6)}_{(1,2;3,4)} \right) + \mathcal{S}_4 \times \mathcal{S}_2$$

$$\widetilde{f}^{(2,2)}(x_i) = \sum_{\blacksquare = 1, U, V} \widetilde{f}^{(2,2)}_{\blacksquare}(x_i)$$

$$= \left(\frac{x_{13}^2 x_{24}^2 \left(1 + U + V \right)}{\prod_{1 \leq i < j \leq 4} x_{ij}^2} \, g \times \left[g^{(5)}_{(1,2,3,4)} \times g^{(6)}_{(1,2,3,4)} \right] \right) + \mathcal{S}_4 \times \mathcal{S}_2 , \tag{7.4.34}$$

and $h^{(5,6)}_{(1,2;3,4)}$ is the integrand of a two loop ladder

$$h^{(5,6)}_{(1,2;3,4)} = \frac{x_{34}^2}{(x_{15}^2 x_{35}^2 x_{45}^2) x_{56}^2 (x_{26}^2 x_{36}^2 x_{46}^2)} . \tag{7.4.35}$$

Here $\mathcal{S}_4 \times \mathcal{S}_L$ (for the case we are considering, $L = 2$) means that we first sum over distinct permutation of $\mathcal{S}_4$ of the four external points (x_1, x_2, x_3, x_4), and then sum over distinct permutations of $\mathcal{S}_L$ for the L vertices that we integrate over. In practice, this implies

$$(\cdots) + \mathcal{S}_4 \times \mathcal{S}_L = ((\cdots) + \mathcal{S}_4) + \mathcal{S}_L = ((\cdots) + \mathcal{S}_L) + \mathcal{S}_4 . \tag{7.4.36}$$

By 'distinct permutation' we mean, for example, $h^{(5,6)}_{(1,2;3,4)}$ and $h^{(5,6)}_{(1,3;2,4)}$ are distinct under $\mathcal{S}_4$ permutation, while $h^{(5,6)}_{(1,2;3,4)}$ and $h^{(5,6)}_{(2,1;3,4)}$ are not. Following such counting rules, we deduce $\widetilde{f}^{(2,1)}$ and $\widetilde{f}^{(2,2)}$ have 12 and 3 terms, respectively. We will again utilise the fact that the period for each term inside $\mathcal{S}_4 \times \mathcal{S}_2$ permutations has the same value.

Their periods are explicitly given by

$$\mathcal{P}_{\widetilde{f}^{(2,1)}} = \sum_{\blacksquare=1,U,V} \mathcal{P}_{\widetilde{f}^{(2,1)}_{\blacksquare}} = 12 \times \left(\frac{441}{8}\zeta(7) + 70\zeta(7) + \frac{441}{8}\zeta(7) \right) = 12 \times \frac{721}{4}\zeta(7) \,,$$

$$\tag{7.4.37}$$

$$\mathcal{P}_{\widetilde{f}^{(2,2)}} = \sum_{\blacksquare=1,U,V} \mathcal{P}_{\widetilde{f}^{(2,2)}_{\blacksquare}} = 3 \times \left[36\zeta(3)^2 + \left(72\zeta(3)^2 - 21\zeta(7) \right) + 36\zeta(3)^2 \right]$$

$$= 3 \times \left(144\zeta(3)^2 - 21\zeta(7) \right) \,.$$

Using these results, we find

$$I_4' \left[F^{(2)}(x_i) \right] = 4 \times \frac{1}{2!(-4)^2} \times \left(12 \times \frac{721}{4}\zeta(7) + 3 \times (144\zeta(3)^2 - 21\zeta(7)) \right)$$

$$= \frac{3}{2} \times \left(36\zeta(3)^2 + 175\zeta(7) \right) \,, \tag{7.4.38}$$

which is in agreement with the result of supersymmetric localisation computation, as given in (7.2.17).

At three loops, summing over $\widetilde{n}_3 = 5$ structures, we have

$$I_4' \left[F^{(3)}(x_i) \right] = 4 \times \frac{1}{3!(-4)^3} \times \left(\sum_{k=1}^{5} \mathcal{P}_{\widetilde{f}^{(3,k)}} \right) \,, \tag{7.4.39}$$

where the $\widetilde{f}^{(3,k)}$ terms are give by (according to (4.16) of [135], see also Fig.7.6 for some examples of the graphs,

$$\widetilde{f}^{(3,1)}(x_i) = \left(\frac{x_{13}^2 x_{24}^2 \left(1 + U + V \right)}{\prod_{1 \le i < j \le 4} x_{ij}^2} g \times T^{(5,6,7)}_{(1,3;2,4)} \right) + \mathcal{S}_4 \times \mathcal{S}_3 \tag{7.4.40}$$

$$\widetilde{f}^{(3,2)}(x_i) = \left(\frac{x_{13}^2 x_{24}^2 \left(1 + U + V \right)}{\prod_{1 \le i < j \le 4} x_{ij}^2} g \times E^{(5,6,7)}_{(1,3;2,4)} \right) + \mathcal{S}_4 \times \mathcal{S}_3 \tag{7.4.41}$$

$$\widetilde{f}^{(3,3)}(x_i) = \left(\frac{x_{13}^2 x_{24}^2 \left(1 + U + V \right)}{\prod_{1 \le i < j \le 4} x_{ij}^2} g \times L^{(5,6,7)}_{(1,3;2,4)} \right) + \mathcal{S}_4 \times \mathcal{S}_3 \tag{7.4.42}$$

$$\widetilde{f}^{(3,4)}(x_i) = \left(\frac{x_{13}^2 x_{24}^2 \left(1 + U + V \right)}{\prod_{1 \le i < j \le 4} x_{ij}^2} g \times (g \times h)^{(5,6,7)}_{(1,3;2,4)} \right) + \mathcal{S}_4 \times \mathcal{S}_3 \tag{7.4.43}$$

$$\widetilde{f}^{(3,5)}(x_i) = \left(\frac{x_{13}^2 x_{24}^2 \left(1 + U + V \right)}{\prod_{1 \le i < j \le 4} x_{ij}^2} g \times H^{(5,6,7)}_{(1,3;2,4)} \right) + \mathcal{S}_4 \times \mathcal{S}_3 \,. \tag{7.4.44}$$

The explicit expressions of these integrands and their corresponding periods $\mathcal{P}_{\widetilde{f}^{(3,k)}}$ are given in appendix A.2. Using the results that are given in appendix A.2 and after
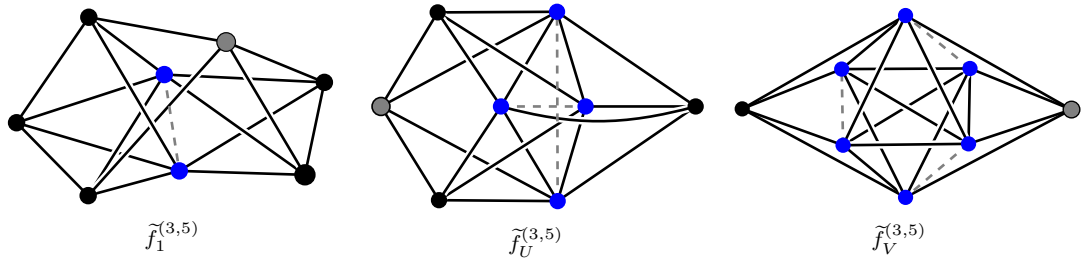
Figure 7.6: Here we draw some examples of $\widetilde{f}$-graphs, $\widetilde{f}_1^{(3,5)}, \widetilde{f}_U^{(3,5)}, \widetilde{f}_V^{(3,5)}$, which are relevant for the three-loop computation.

summing over all the periods $\mathcal{P}_{\widetilde{f}^{(3,k)}}$'s (in particular (A.2.2)), we obtain,

$$
\begin{aligned}
I_4' \left[F^{(3)}(x_i) \right] &= 4 \times \frac{1}{3!(-4)^3} \times \left(\sum_{k=1}^{5} \mathcal{P}_{\widetilde{f}^{(3,k)}} \right) \\
&= -\frac{45}{2} \times (20\zeta(3)\zeta(5) + 49\zeta(9)) \,,
\end{aligned} \tag{7.4.45}
$$

which again agrees with the localisation result (7.2.17) for the $a_{G_N}^3$ term. As we know the first and second integrated correlators are periods of $(L+1)$ loops and $(L+2)$ loops, respectively, due to the extra box in the measure (7.2.5). At $L = 5$, the first correlator has one term that can cannot be directly computed, which is a 6-loop integral; similarly, several (more than one) 6-loop integrals appear in the second correlator at $L = 4$, which will be interesting to see if they can be evaluated by other techniques.

7.5 Conclusion

In this paper, we studied the perturbative aspects of recently introduced integrated correlators in $\mathcal{N} = 4$ SYM with general classical gauge groups. We identified interesting relations between the integrated correlators and periods of so-called f-graphs and their generalisation $\widetilde{f}$-graphs. f-graphs were used for constructing loop integrands of the un-integrated correlators. This identification paves the way of systematically computing integrated correlators to higher loops. In this paper, we applied the idea and computed all the relevant periods for the first integrated correlator up to four loops and for the second integrated correlator up to three loops, and we found the results perfectly agree with the expressions obtained from supersymmetric localisation. Our results extend the earlier computation of [145], where the first integrated correlator was computed for the first two loops.

These explicit perturbative results verify the prediction of supersymmetrical localisation. Furthermore, the results also show explicitly the simplicity of the integrated correlators. A nice example of this is that even though the three-loop un-integrated correlator takes rather complicated form, the additional integration arising from the

definition of integrated correlators simplify the structures drastically. It would be interesting to extend the computation of this paper to higher loops and the non-planar sectors, and systematically understand the simplicity of integrated correlators from Feynman diagram point of view, which may help to find new integration measures different from those considered in this paper that can also simply the un-integrated correlator. It will also be interesting to consider correlators involving higher-weight operators. In particular, the perturbative contribution of integrated four-point correlator of $\langle \mathcal{O}_2 \mathcal{O}_2 \mathcal{O}_p \mathcal{O}_p \rangle$ can also be computed using supersymmetric localisation [37]. It would be interesting to analyse these integrated correlators with higher-weight operators using our methods and the corresponding integrands constructed in [174, 175] and more recently [176].

Our observation that relates the integrated correlators and periods also provides new non-trivial relations for the periods, given the fact that the integrated correlators can be computed using supersymmetric localisation exactly to any orders in the perturbation theory. This idea was illustrated and used to predict an analytical expression for a six-loop period, by using the localisation result of the first integrated correlator at five loops. It is of interest to verify our prediction by a direct computation of this particular six-loop period. It is also very interesting to understand these relations from mathematical viewpoints, and such an understanding will help to lead to systematic evaluation of the integrated correlators in the perturbation theory. In particular, each period may contain multiple zeta values, and their particular combinations to form integrated correlators, from the results of supersymmetric localisation, we know that these multiple zeta values should actually all cancel out when we add the periods together to form the integrated correlators[*].

---

[*]The fact that only single zeta value appear in all order for the first correlator can be seen from (5.3) in [145], where $\alpha_s(N)$ is determined recursively by (5.4) in [145] and therefore it is proportional (up to some rational function of N) to $\alpha_s(2)$, the latter contains only single zeta $\zeta(2s + 1)$ to all order as shown in (3.6) in [145].

Chapter 8

Holographic Correlators in $AdS_3 \times S^3$

8.1 Introduction

Over past several years, many powerful methods have been developed to study the correlation functions of local operators in holographic CFTs when it is possible to exploit the dual description in terms of a weakly coupled gravity theory. A beautiful example is the study of holographic correlators in type IIB string theory on $AdS_5 \times S^5$. In particular, in supergravity limit, a very compact formula in Mellin space was obtained for the tree-level correlation functions of four one-half BPS single-trace operators with arbitrary conformal weights [21, 177]. These results, combining with other powerful techniques and ideas, such as analytical bootstrap program, supersymmetric localisation, have led to many further developments in understanding the holographic correlation functions in $AdS_5 \times S^5$. For instance, the methodology allows constructing loop corrections to these correlators as well as determining higher-derivative contributions arising from α'-expansion of superstring theory [37–39, 142–145, 149, 178–192].

One of the remarkable properties of these holographic correlators in $AdS_5 \times S^5$ supergravity, which will be mostly relevant for our study, is that the correlators of operators with different conformal weights are in fact all related to each other due to a hidden ten-dimensional conformal symmetry [23]. This hidden conformal symmetry allows packaging the four-point holographic correlators of operators with different conformal weights into a single four-point correlator of scalar operators in ten dimensions. This observation leads to a recursion relation that relates holographic correlators of operators with higher weights to the lowest-weight one, and the solution of the recursion relation yields precisely the formula originally given in [21]. This observation has been further explored for the holographic correlators in $AdS_5 \times S^5$ beyond the tree-level approximation [186], and the fate of the hidden symmetry, when higher-derivative stringy

effects are included, has been studied in [193–195].

Analogous hidden conformal symmetries have been found for other holographic theories. In particular, it was found that four-point tree-level holographic correlators of type IIB supergravity in $AdS_3 \times S^3 \times M_4$ (the internal space M_4 can be T^4 or $K3$ surface) also exhibit a hidden symmetry [24, 25] *. In the case of $AdS_3 \times S^3$, the hidden symmetry was found to be a six-dimensional conformal symmetry. Supergravity in $AdS_3 \times S^3$ has half maximal supersymmetry, and contains two super multiplets: gravity multiplet and tensor multiplet. It was found that for the correlators in tensor multiplet, just as in the case of $AdS_5 \times S^5$, the tree-level holographic correlators of four chiral primary operators (CPOs) in tensor multiplet can again be packaged into a single correlator of scalar operators in a six-dimensional CFT. This six-dimensional correlator serves as a generating function, which generates holographic correlators of operators with arbitrary weights. Equivalently, the hidden symmetry leads to a recursion relation which can be solved explicitly and gives rise to a compact formula for all tree-level four-point holographic correlators in $AdS_3 \times S^3$ for CPOs in tensor multiplet, which puts our understanding of these correlators at the same level of the holographic correlators in $AdS_5 \times S^5$.

The hidden six-dimensional conformal symmetry for holographic correlators in $AdS_3 \times S^3$ has recently been extended to more general four-point correlators in [25], including those with CPOs in gravity multiplet. It was found that the correlators of operators in gravity multiplet are described by a single correlator involving self-dual 3-forms (instead of simple scalars as in the case of tensor multiplet) in a six-dimensional CFT. This paper aims at a better understanding of holographic correlators in $AdS_3 \times S^3$, especially with operators in gravity multiplet. We will be mainly concerned with the mixed correlators, with two operators in gravity multiplet and the other two in tensor multiplet.

With this new understanding of the hidden conformal symmetry, again a recursion relation was obtained for the mixed correlators of operators in both tensor and gravity multiplets [25]. The main focus of this paper is to solve the recursion relation, and to obtain a compact formula for the mixed correlators of operators with arbitrary conformal weights. The results arising directly from solving the recursion relation are in fact rather lengthy and complex for the correlators involving operators in gravity multiplet. They are greatly simplified by a better understanding of their analytic structures in Mellin space. We will also make contact with the known flat-space scattering amplitudes by taking flat-space limit on the Mellin amplitudes, and find a perfect match.

The paper is organised as follows. In section 8.2, we will begin by reviewing the hidden 6D conformal symmetry for the holographic correlators in $AdS_3 \times S^3$ of operators

---

*See recent work [196] for the study of hidden symmetries of correlation functions in other holographic theories.

in tensor multiplet as well as the recursion relation arsing from the hidden conformal symmetry. We will solve the recursion relation and obtain a compact formula for the correlators in Mellin space. The study of correlators in tensor multiplet serves a warm-up for understanding the correlators with operators in gravity multiplet. In this section 8.3, we will review the main results [25], where a recursion relation was obtained from the hidden 6D conformal symmetry for mixed correlators involving operators in both tensor and gravity multiplets. However, we find that the solution arising from solving directly the recursion relation is rather lengthy and it is obscured to any simple structures in the formula. The result can be greatly simplified by carefully analysing the analytic structures of the correlators in Mellin space, and a much more compact expression is obtained. We verify the final expression is local, in the sense that all the multiple poles cancel out non-trivially. We further study various limits (including flat-space limit and maximally R-symmetry violating limit) of the results. We conclude and comment on future research directions in section 8.4.

8.2 Hidden 6D conformal symmetry in $AdS_3 \times S^3$

It was observed in [23] that tree-level holographic correlation functions of four BPS scalar operators in $AdS_5 \times S^5$ obeys a remarkable 10D hidden conformal symmetry, which allows packaging the correlators of operators with different conformal weights into a single correlator of four scalars in a 10D CFT. This 10D hidden conformal symmetry leads to a powerful recursion relation that relates correlators of operators with higher weights to those with lowest weights. Solving the recursion relation explicitly gives rise to a compact expression for all tree-level correlators of four BPS operators, in agreement with the results of [21].

This observation has been extended to four-point correlation functions in $AdS_3 \times S^3 \times M_4$, where the internal manifold M_4 can either be four torus T^4 or the $K3$ surface. Compared to the case of $AdS_5 \times S^5$, due to the fact that the $AdS_3 \times S^3$ background has only half maximal supersymmetry, the structure of hidden symmetry is more involved. In particular, the 6D $(2,0)$ supergravity contains tensor and gravity multiplets, for the correlators of operators in tensor multiplet, the situation is very similar to the case of $AdS_5 \times S^5$, where the four-point tree-level correlators of BPS operators with different conformal weights are packaged into a single four-point correlation function of scalars in a 6D CFT [24]. However, when the operators in gravity multiplet are involved, the structures become much richer. It was understood in [25] that the tree-level four-point holographic correlators with two operators in tensor multiplet and two in gravity multiplet are, again, described by a single CFT_6 correlator, but now with two scalars and two self-dual 3-forms in six dimensions.

Below we will review the hidden 6D conformal symmetry, especially its implications

on the recursion relation for the four-point holographic correlators in $AdS_3 \times S^3$. As a warm-up, we will begin with the simpler case where all the operators are in tensor multiplet. In next section, we will study the more involved case, where the correlators contain operators with two of them in tensor multiplet and the other two in gravity multiplet.

8.2.1 Four-point correlators of operators in tensor multiplet

Flat space superamplitudes

In flat-space, the four-point superamplitude in 6D $(2,0)$ supergravity of states in tensor multiplet takes a simple form, given as [*]

$$\mathcal{A}_4^{\text{tensor}} = G_6\, \delta^8 \left(\sum_{i=1}^4 q_i \right) \delta^6 \left(\sum_{i=1}^4 p_i \right) \left(\frac{\delta_{f_1 f_2} \delta_{f_3 f_4}}{\mathbf{s}} + \frac{\delta_{f_2 f_3} \delta_{f_1 f_4}}{\mathbf{t}} + \frac{\delta_{f_1 f_3} \delta_{f_2 f_4}}{\mathbf{u}} \right), \quad (8.2.1)$$

where $\mathbf{s}, \mathbf{t}, \mathbf{u}$ are Mandelstam variables defined as $\mathbf{s} = (p_1 + p_2)^2, \mathbf{t} = (p_2 + p_3)^2, \mathbf{u} = (p_1 + p_3)^2$, obeying $\mathbf{s} + \mathbf{t} + \mathbf{u} = 0$. And G_6 is the Newton constant in 6D and $\delta^8(\sum_{i=1}^4 q_i)$ is due to the conservation of the supercharge, which reflects 6D $(2,0)$ supersymmetry. Explicitly, the supercharge is defined as $q_i^{A,I} = \lambda_{i,a}^A \eta_i^{a,I}$, with $I = 1, 2$. Here we have used the spinor-helicity formalism for 6D massless momentum

$$p_{i\,\mu}(\Gamma^\mu)^{AB} = \lambda_{i\,a}^A \lambda_i^{B,a} = \frac{1}{2} \epsilon^{ABCD} \tilde{\lambda}_{i,C\,\hat{a}} \tilde{\lambda}_{i\,D}^{\hat{a}}. \quad (8.2.2)$$

The index i indicates the external particle, μ is a vector index and $A, B, \ldots$, are spinor indices of 6D Lorentz group, and a and $\hat{a}$ are $SU(2) \times SU(2)$ indices labelling the 6D little group $SO(4)$ for massless particles. To describe the 6D $(2,0)$ supersymmetry we have introduced Grassmann variables $\eta_i^{a,I}$, which can be used to package all the on-shell states into a on-shell superfield [1]. Finally, f_i are flavour indices of the states in tensor multiplet.

After stripping off the supercharge conservation factor $\delta^8(\sum_{i=1}^4 q_i)$, the amplitude is identical to the four-point tree-level amplitude of ϕ^3 theory (with a flavour symmetry), which is conformal invariant in 6D. This property (and the results of $AdS_5 \times S^5$) has led to the conjecture of hidden 6D conformal symmetry for four-point tree-level holographic correlators in $AdS_3 \times S^3$ of operators in tensor multiplet.

---

[*]More details regarding all tree-level superamplitudes in 6D $(2,0)$ supergravity in flat-space can be found in [1,32].

Hidden 6D conformal symmetry and recursion relation in tensor multiplet

In general, four-point correlators of CPOs in the 2D CFT that is dual to type IIB string theory on $AdS_3 \times S^3$ that we will consider take the following form,

$$\langle O_{k_1} O_{k_2} O_{k_3} O_{k_4} \rangle = \left(\frac{|\zeta_{13}|^{k_{21}^- + k_{43}^-} |\zeta_{23}|^{-k_{21}^- + k_{43}^-}}{|\zeta_{12}|^{k_{12}^+ + k_{43}^-} |\zeta_{34}|^{2k_4}} \right) \left[\mathcal{G}_{\{k_i\}}^{(0)} + \left| \frac{1 - \alpha_c z}{1 - \alpha_c} \right|^2 \widetilde{\mathcal{G}}_{\{k_i\}}(z, \bar{z}; \alpha_c, \bar{\alpha}_c) \right] , \tag{8.2.3}$$

where k_i's are the conformal dimensions of the operators, and $k_{ij}^- = k_i - k_j$ and $k_{ij\ldots l}^+ = k_i + k_j + \ldots + k_l$. The cross ratios are defined as

$$|\xi_{ij}|^2 = \frac{|z_{ij}|^2}{t_{ij}^2} , \qquad \alpha_c = \frac{A_1 \cdot A_3 A_2 \cdot A_4}{A_1 \cdot A_4 A_2 \cdot A_3} , \qquad z = \frac{z_{14} z_{23}}{z_{13} z_{24}} , \tag{8.2.4}$$

and $z_{ij} = z_i - z_j$ and $t_{ij} = t_i - t_j$. To describe the R-symmetry group $SU(2)_L \times SU(2)_R$ of the CFT (or equivalently the isometry of S^3), we have associated each operator with spinors $A_i^\alpha, \bar{A}_i^{\dot{\alpha}}$, or equivalently a $SO(4)$ null vector $t_i^\mu = (\sigma_{\alpha\dot{\alpha}})^\mu A_i^\alpha \bar{A}_i^{\dot{\alpha}}$. The role of these R-symmetry factors will become more explicit when we consider concrete examples.

The separation of the full correlator into $\mathcal{G}_{\{k_i\}}^{(0)}$ and $\widetilde{\mathcal{G}}_{\{k_i\}}$ such that $\mathcal{G}_{\{k_i\}}^{(0)}$ is a simple rational function of cross ratios, whereas $\widetilde{\mathcal{G}}_{\{k_i\}}$ is the "dynamical part", which contains the so-called D-functions and contributes non-trivially to Mellin amplitudes, which will be our main focus. Finally, the prefactor $\left| \frac{1-\alpha_c z}{1-\alpha_c} \right|^2$ is fixed by the half maximal supersymmetry and super conformal symmetry of the theory [24, 197]. We will call $\widetilde{\mathcal{G}}_{\{k_i\}}$ as the reduced correlator, whereas the full result including the prefactor $\left| \frac{1-\alpha_c z}{1-\alpha_c} \right|^2$ as the non-reduced correlator.

To study holographic correlators, it is convenient to express them in Mellin space when it is possible. The Mellin amplitude of the connected part of a correlation function is defined through a Mellin transform [22, 198],

$$\widetilde{\mathcal{G}}_{\{k_i\}}(U, V) = \int \frac{ds}{4\pi i} \frac{dt}{4\pi i} U^{\frac{s - k_{34}^+}{2} + L} V^{\frac{t - \min\{k_{23}^+, k_{14}^+\}}{2}} \widetilde{\Gamma}_{\{k_i\}}(s, t) \widetilde{\mathcal{M}}_{\{k_i\}}(s, t) , \tag{8.2.5}$$

where $\widetilde{\mathcal{M}}_{\{k_i\}}(s, t)$ is the reduced Mellin amplitude, $\tilde{u} = \sum_{i=1}^4 k_i - s - t - 2$, the cross ratios U, V are defined as

$$U = (1 - z)(1 - \bar{z}) , \qquad V = z\bar{z} . \tag{8.2.6}$$

and $\widetilde{\Gamma}_{\{k_i\}}(s, t)$ is a product of Γ-functions

$$\widetilde{\Gamma}_{\{k_i\}}(s, t)$$
$$= \Gamma\left(\frac{k_{12}^+ - s}{2} \right) \Gamma\left(\frac{k_{34}^+ - s}{2} \right) \Gamma\left(\frac{k_{14}^+ - t}{2} \right) \Gamma\left(\frac{k_{23}^+ - t}{2} \right) \Gamma\left(\frac{k_{13}^+ - \tilde{u}}{2} \right) \Gamma\left(\frac{k_{24}^+ - \tilde{u}}{2} \right) .$$

Finally, $L = k_4$ if $k_{14}^+ \leq k_{23}^+$, and $L = \frac{k_{234}^+ - k_1}{2}$ if $k_{14}^+ > k_{23}^+$. Without losing generality, we will only focus on the first case, namely $k_{14}^+ \leq k_{23}^+$.

One may put back the factor $\left| \frac{1 - \alpha_c z}{1 - \alpha_c} \right|^2$ in (8.2.3) to obtain the non-reduced correlator. To study the Mellin amplitude, we express his factor in terms of cross ratios U and V,

$$\left| \frac{1 - \alpha_c z}{1 - \alpha_c} \right|^2 = \frac{1}{2}(\tau - \sigma + 1) + \frac{U}{2}(\sigma + \tau - 1) + \frac{V}{2}(\sigma - \tau + 1) - \frac{\tau}{2}(\alpha_c - \bar{\alpha}_c)(z - \bar{z}),$$

(8.2.7)

where

$$\sigma = \frac{\alpha_c \bar{\alpha}_c}{(1 - \alpha_c)(1 - \bar{\alpha}_c)}, \qquad \tau = \frac{1}{(1 - \alpha_c)(1 - \bar{\alpha}_c)}.$$

(8.2.8)

The factor $(\alpha_c - \bar{\alpha}_c)(z - \bar{z})$ (which we will encounter again later) contains square roots in terms of cross ratios U, V, and it is incompatible with the definition of Mellin amplitudes we used in (8.2.5). So we will have to drop this piece when we consider the Mellin amplitude for non-reduced correlator.* The same consideration was also used in [24]. In general, the non-reduced Mellin amplitude $\mathcal{M}_{\{k_i\}}(s, t)$ is defined as

$$\mathcal{G}_{\{k_i\}}(U, V) = \int \frac{ds}{4\pi i} \frac{dt}{4\pi i} U^{\frac{s - k_{34}^+}{2} + L} V^{\frac{t - \min\{k_{23}^+, k_{14}^+\}}{2}} \Gamma_{\{k_i\}}(s, t) \mathcal{M}_{\{k_i\}}(s, t),$$

(8.2.9)

with $u = \sum_i k_i - s - t$ and

$$\Gamma_{\{k_i\}}(s, t)$$
$$= \Gamma\left(\frac{k_{12}^+ - s}{2}\right) \Gamma\left(\frac{k_{34}^+ - s}{2}\right) \Gamma\left(\frac{k_{14}^+ - t}{2}\right) \Gamma\left(\frac{k_{23}^+ - t}{2}\right) \Gamma\left(\frac{k_{13}^+ - u}{2}\right) \Gamma\left(\frac{k_{24}^+ - u}{2}\right).$$

From the definition of Mellin amplitudes in (8.2.5) and (8.2.9), it is straightforward to see the translation between the reduced Mellin amplitude and the non-reduced Mellin amplitude takes the following form,

$$U^m V^n \widetilde{\mathcal{M}}_{\{k_i\}}(s, t) \rightarrow \frac{\widetilde{\Gamma}_{\{k_i\}}(s - 2m, t - 2n)}{\Gamma_{\{k_i\}}(s, t)} \mathcal{M}_{\{k_i\}}(s - 2m, t - 2n).$$

(8.2.10)

Use the result of the above relation and (8.2.7) (after dropping the term $(\alpha_c - \bar{\alpha}_c)(z - \bar{z})$), we see that, for holographic correlators in $AdS_3 \times S^3$, the non-reduced Mellin amplitude $\mathcal{M}_{\{k_i\}}(s, t)$ is related to the reduced amplitude $\widetilde{\mathcal{M}}_{\{k_i\}}(s, t)$ through the following

---

*This can be achieved by summing over the correlator and its conjugate, namely $\alpha_c \leftrightarrow \bar{\alpha}_c$.

relation,

$$
\begin{aligned}
\mathcal{M}_{\{k_i\}}(s,t) = {} & \frac{1}{8}(\tau - \sigma + 1)(k_{13}^+ - u)(k_{24}^+ - u)\, \widetilde{\mathcal{M}}_{\{k_i\}}(s,t) \\
& + \frac{1}{8}(\sigma + \tau - 1)(k_{12}^+ - s)(k_{34}^+ - s)\, \widetilde{\mathcal{M}}_{\{k_i\}}(s-2,t) \\
& + \frac{1}{8}(\sigma - \tau + 1)(k_{14}^+ - t)(k_{23}^+ - t)\, \widetilde{\mathcal{M}}_{\{k_i\}}(s,t-2)\,.
\end{aligned}
\tag{8.2.11}
$$

Let us now be concrete by considering the holographic correlators of CPOs in tensor multiplet. In tensor multiplet, there is a family of CPOs, s_k, with holomorphic and antihomorphic conformal dimensions $(h, \bar{h}) = (k/2, k/2)$ with $k = 1, 2, \cdots$, so that it has dimension $h + \bar{h} = k$. They are in the $(j, \bar{j}) = (h, \bar{h})$ representation of R-symmetry group $SU(2)_L \times SU(2)_R$. The operator s_k, after encoding the R-symmetry group factor, is then defined as

$$
s_k(z_i, \bar{z}_i, t_i) = t_{i\mu_1} \ldots t_{i\mu_k} s_k^{\mu_1 \ldots \mu_k}(z_i, \bar{z}_i)\,,
\tag{8.2.12}
$$

where $t_{i\mu}$ is the $SO(4)$ null vector associated with R-symmetry of the theory, as we introduced earlier. The hidden conformal symmetry that we discussed earlier implies that the four-point correlator of $\langle s_{k_1} s_{k_2} s_{k_3} s_{k_4} \rangle$ is described by a 6D correlator of scalar operators [24, 25]

$$
\widetilde{\mathcal{G}}_{s_{k_1} s_{k_2} s_{k_3} s_{k_4}} = t_{12}^2 t_{34}^2 |z_{13}^2||z_{24}^2| \frac{|\xi_{12}|^{k_{12}^+ + k_{43}^-}|\xi_{34}|^{2k_4}}{|\xi_{13}|^{k_{21}^- + k_{43}^-}|\xi_{23}|^{k_{43}^- - k_{21}^-}} \frac{g(Z_i)}{|Z_{12}|^4 |Z_{34}|^4} \bigg|_{t_1^{k_1} t_2^{k_2} t_3^{k_3} t_4^{k_4}}\,.
\tag{8.2.13}
$$

Importantly, Z_i is a 6D coordinate by combining the AdS_3 and S^3 coordinates,

$$
Z_i = (z_i, \bar{z}_i, t_i^\mu)\,,
\tag{8.2.14}
$$

therefore $|Z_{ij}|^2 = |Z_i - Z_j|^2 = |z_{ij}|^2 + t_{ij}^2$. To obtain the correlator $\langle s_{k_1} s_{k_2} s_{k_3} s_{k_4} \rangle$, we simply Taylor expand $\widetilde{\mathcal{G}}_{s_{k_1} s_{k_2} s_{k_3} s_{k_4}}$ and collect all the terms of the order $t_1^{k_1} t_2^{k_2} t_3^{k_3} t_4^{k_4}$, as indicated in the subscript in (8.2.13). Finally, $g(Z_i)$ is a function of cross ratios built out of 6D coordinates Z_i, which is the consequence of the hidden conformal symmetry.

8.2.2 Solution to the recursion relation

To extract the coefficient of $t_1^{k_1} t_2^{k_2} t_3^{k_3} t_4^{k_4}$ efficiently, we rescale $t_{ij}^2 \to a_i a_j t_{ij}^2$, and express the $\widetilde{\mathcal{G}}_{s_{k_1} s_{k_2} s_{k_3} s_{k_4}}$ as a contour integral following the ideas of [23],

$$
\begin{aligned}
& \widetilde{\mathcal{G}}_{s_{k_1} s_{k_2} s_{k_3} s_{k_4}} \\
& = \oint_{a_i = 0} da_i\, a_i^{-k_i} t_{12}^2 t_{34}^2 |z_{13}^2||z_{24}^2| \frac{|\xi_{12}|^{k_{12}^+ + k_{43}^-}|\xi_{34}|^{2k_4}}{|\xi_{13}|^{k_{21}^- + k_{43}^-}|\xi_{23}|^{k_{43}^- - k_{21}^-}} \frac{g(Z_i(a_i))}{|z_{12}^2 + a_1 a_2 t_{12}^2|^2 |z_{34}^2 + a_3 a_4 t_{34}^2|^2}\,.
\end{aligned}
\tag{8.2.15}
$$

After a suitable rescaling on the integration variables, we can further simplify the result and express it in terms of cross ratios,

$$\widetilde{\mathcal{G}}_{s_{k_1} s_{k_2} s_{k_3} s_{k_4}} = \sigma^{k_2-1} \tau^{\frac{k_{12}^- - k_{34}^-}{2}} U^{\frac{k_{12}^+ + k_{43}^- - 4}{2}} V^{\frac{k_{21}^- + k_{34}^-}{2}} \oint_{a_i=0} da_i a_i^{-k_i} \frac{g\left(U', V'\right)}{(1 + \frac{a_1 a_2}{U\sigma})^2 (1 + a_3 a_4)^2}\,, \tag{8.2.16}$$

where we have introduced the rescaled cross ratios U', V', which are defined as

$$U' = U\frac{(1 + \frac{1}{\sigma U} a_1 a_2)(1 + a_3 a_4)}{(1 + a_1 a_3)(1 + a_2 a_4)}\,, \qquad V' = V\frac{(1 + \frac{\tau}{\sigma V} a_2 a_3)(1 + a_1 a_4)}{(1 + a_1 a_3)(1 + a_2 a_4)}\,. \tag{8.2.17}$$

The function $g\left(U, V\right)$ that serves as initial data of the recursion relation is determined by the correlator of lowest-weight operators with $k_i = 1$, and is given by [*]

$$g\left(U, V\right) = U \int \frac{ds\,dt}{(4\pi i)^2} U^{\frac{s}{2}} V^{\frac{t}{2}-1}\,\Gamma^2(1 - \frac{s}{2})\Gamma^2(1 - \frac{t}{2})\Gamma^2(1 - \frac{\tilde{u}}{2})$$
$$\times \left(\frac{\delta_{f_1 f_2}\delta_{f_3 f_4}}{s} + \frac{\delta_{f_2 f_3}\delta_{f_1 f_4}}{t} + \frac{\delta_{f_1 f_3}\delta_{f_2 f_4}}{\tilde{u}}\right)\,, \tag{8.2.18}$$

with $\tilde{u} = 2 - s - t$. Here we have expressed the function in Mellin space, which can be straightforwardly re-expressed in the coordinate space in terms of D-functions [197].

Perform the contour integral using $(1 + x)^n = \sum_{i=0}^{\infty} \frac{\Gamma(i-n)}{\Gamma(-n)} \frac{(-x)^i}{i!}$, and shift the integration variables by $s \to s + 2 + 2m_1 - k_{12}^+$ and $t \to t + 2 + 2m_5 - k_{23}^+$, we arrive at

$$\widetilde{\mathcal{G}}_{s_{k_1} s_{k_2} s_{k_3} s_{k_4}}$$
$$= \int \frac{ds\,dt}{(4\pi i)^2} \sum_{m_1=0, m_2=0}^{\infty} \sigma^{m_2 + \frac{k_{21}^- + k_{43}^-}{2}} \tau^{k_1-1-m_{12}} U^{\frac{s+k_{43}^-}{2}} V^{\frac{t-k_{14}^+}{2}} \widetilde{\Gamma}_{\{k_i\}}(s, t)$$
$$\times \frac{1}{\prod_{i=1}^{6} m_i!} \left(\frac{\delta_{f_1 f_2}\delta_{f_3 f_4}}{s + 2 + 2m_1 - k_{12}^+} + \frac{\delta_{f_2 f_3}\delta_{f_1 f_4}}{t + 2 + 2m_5 - k_{23}^+} + \frac{\delta_{f_1 f_3}\delta_{f_2 f_4}}{\tilde{u} + 2 + 2m_2 - k_{13}^+}\right)\,,$$

where $\widetilde{\Gamma}_{\{k_i\}}(s, t)$ is given in (8.2.7), and m_i for $i > 2$ are determined in terms of m_1, m_2,

$$m_3 = k_1 - m_{12} - 1\,, \qquad m_4 = \frac{k_{31}^- + k_{42}^-}{2} + m_1\,, \tag{8.2.19}$$
$$m_5 = \frac{k_{12}^+ + k_{34}^-}{2} - m_{12} - 1\,, \qquad m_6 = \frac{k_{21}^- + k_{43}^-}{2} + m_2\,,$$

with $m_{ij} = m_i + m_j$. Note, the summation on m_1, m_2 is truncated due to the factorials $m_i!$ in the denominator. According to the definition of Mellin amplitudes given in

---

[*]This correlator was first obtained in [197] by taking a limit on the heavy-heavy-light-light correlators computed in [199, 200].

(8.2.5), we conclude that the reduced Mellin amplitude of $\langle s_{k_1} s_{k_2} s_{k_3} s_{k_4} \rangle$ is given by

$$\widetilde{\mathcal{M}}_{s_{k_1} s_{k_2} s_{k_3} s_{k_4}}(s,t) = \sum_{m_1=0,m_2=0}^{\infty} \frac{\sigma^{m_2 + \frac{k_{21}^- + k_{43}^-}{2}} \tau^{k_1 - 1 - m_{12}}}{\prod_{i=1}^{6} m_i!}$$

$$\times \left(\frac{\delta_{f_1 f_2} \delta_{f_3 f_4}}{s + 2 + 2m_1 - k_{12}^+} + \frac{\delta_{f_2 f_3} \delta_{f_1 f_4}}{t + 2 + 2m_5 - k_{23}^+} + \frac{\delta_{f_1 f_3} \delta_{f_2 f_4}}{\tilde{u} + 2 + 2m_2 - k_{13}^+} \right).$$
(8.2.20)

For the special case $k_1 = k_2 = k$ and $k_3 = k_4 = \ell$, we find the formula is in agreement with the result given in [201] (up to an overall factor of $-2k\ell$ due to a different convention we use here).

We conclude this section by taking two interesting limits of the Mellin amplitudes: flat-space limit and maximally R-symmetry violating (MRV) limit. We will consider the limits on the full non-reduced Mellin amplitudes using (8.2.11). Flat-space limit is achieved by setting $s \to \infty, t \to \infty$, which yields

$$\mathcal{M}_{s_{k_1} s_{k_2} s_{k_3} s_{k_4}}(s,t)$$
$$\to P_{\{k_i\}}(\sigma, \tau) (u\,t + s\,t\,\sigma + s\,u\,\tau) \left(\frac{\delta_{f_1 f_2} \delta_{f_3 f_4}}{s} + \frac{\delta_{f_1 f_4} \delta_{f_2 f_3}}{t} + \frac{\delta_{f_1 f_3} \delta_{f_2 f_4}}{u} \right),$$

where $u \to -s - t$ in the flat-space limit, and the overall factor $P_{\{k_i\}}(\sigma, \tau)$ is given by

$$P_{\{k_i\}}(\sigma, \tau) = -\frac{1}{4} \sum_{m_1=0,m_2=0}^{\infty} \frac{\sigma^{m_2 + \frac{k_{21}^- + k_{43}^-}{2}} \tau^{k_1 - 1 - m_{12}}}{\prod_{i=1}^{6} m_i!} .$$
(8.2.21)

One may perform one of the summations in $P_{\{k_i\}}(\sigma, \tau)$ and express the result in terms of a Hypergeometric function. We see that (8.2.21) is in agreement with the flat-space amplitude given in (8.2.1). The factor $(u\,t + s\,t\,\sigma + s\,u\,\tau)$, arising from $\left| \frac{1-\alpha_c z}{1-\alpha_c} \right|^2$ as can be seen from (8.2.11), represents the fact that the theory has half maximal supersymmetry factor. In the case of maximal supersymmetric theories, it is $(u\,t + s\,t\,\sigma + s\,u\,\tau)^2$ that associates with the supersymmetry [202, 203].

We now consider the MRV limit. This was first introduced in [141, 203] for the study of holographic correlators in maximal supersymmetric theories. The limit chooses to align the R-symmetry directions A_i^α such that the u-channel contribution vanishes, namely we set $A_1 \cdot A_3 = A_2 \cdot A_4 = 0$ and $\bar{A}_1 \cdot \bar{A}_3 = \bar{A}_2 \cdot \bar{A}_4 = 0$, which implies $\alpha_c = \bar{\alpha}_c = 0$. In terms of σ and τ, we have $\sigma \to 0$, $\tau \to 1$ in the MRV limit. So in this limit, the factor $(\alpha_c - \bar{\alpha}_c)(z - \bar{z})$ in (8.2.7) drops out, and the non-reduced Mellin amplitude is always well-defined.

For the correlator given in (8.2.20), we see that in the MRV limit only $m_2 = -\frac{k_{21}^- + k_{43}^-}{2}$

term of the m_2 sum in (8.2.20) contributes, therefore we have

$$
\begin{aligned}
&\mathcal{M}_{\mathrm{MRV}, s_{k_1} s_{k_2} s_{k_3} s_{k_4}}(s,t) \\
&= \frac{1}{4} (s+t-k_{13}^+)(s+t-k_{24}^+) \\
&\times \sum_{m_1=0}^{\infty} \left(\frac{\delta_{f_1 f_2} \delta_{f_3 f_4}}{s+2+2m_1-k_{12}^+} + \frac{\delta_{f_2 f_3}\delta_{f_1 f_4}}{t-2m_1+k_{23}^-} + \frac{\delta_{f_1 f_3}\delta_{f_2 f_4}}{-s-t+k_{13}^+} \right) \\
&\times \frac{1}{\Gamma(m_1+1)\Gamma(k_2-m_1)\Gamma(\frac{k_{12}^-+k_{34}^-}{2}+1)\Gamma(\frac{k_{12}^+-k_{34}^-}{2}-m_1)\Gamma(m_1+\frac{k_{34}^+-k_{12}^+}{2}+1)} \,.
\end{aligned}
\tag{8.2.22}
$$

We note that the u-channel poles are cancelled by the prefactor $(s+t-k_{13}^+)$, and there is a zero in u-channel when $s+t-k_{24}^+ = 0$. These are the properties of holographic correlators in the MRV limit that played key roles for constructing tree-level holographic correlators in other AdS backgrounds with maximal supersymmetry, which include $AdS_5 \times S^5$, $AdS_4 \times S^7$, and $AdS_7 \times S^4$ [141, 203].

8.3 Four-point correlators of operators in tensor and gravity multiplets

8.3.1 Flat space superamplitudes

We will now consider the correlators involving operators in gravity multiplet. As we commented, compared to the correlators of operators in tensor multiplet, these correlators are more involved. Let us begin with the amplitudes in flat-space. The four-point superamplitude in 6D $(2,0)$ supergravity of general external states is given by [1]

$$
\mathcal{A}_4 = G_6 \delta^8 (\sum_{i=1}^4 q_i) \delta^6 (\sum_{i=1}^4 p_i) \frac{[1_{\hat{a}_1} 2_{\hat{a}_2} 3_{\hat{a}_3} 4_{\hat{a}_4}][1_{\hat{b}_1} 2_{\hat{b}_2} 3_{\hat{b}_3} 4_{\hat{b}_4}]}{\mathbf{s}\,\mathbf{t}\,\mathbf{u}} \,.
\tag{8.3.1}
$$

To simplify the discussion, we have assumed that the tensors have the same flavour, and more general cases can be found in [1], which are constructed using twistor formulation. The square parenthesis is defined as $[i_{\hat{a}_1} j_{\hat{a}_2} k_{\hat{a}_3} l_{\hat{a}_4}] := \epsilon^{ABCD} \tilde{\lambda}_{i\,A\,\hat{a}_1} \tilde{\lambda}_{j\,B\,\hat{a}_2} \tilde{\lambda}_{k\,C\,\hat{a}_3} \tilde{\lambda}_{l\,D\,\hat{a}_4}$. Importantly, as pointed out in [25], after stripping of the delta-function prefactors $G_6 \delta^8 (\sum_{i=1}^4 q_i) \delta^6 (\sum_{i=1}^4 p_i)$, this general four-point superamplitude in 6D $(2,0)$ supergravity is again invariant under 6D conformal transformation, which hints on hidden conformal symmetry for all four-point tree-level holographic correlators (instead of just those in tensor multiplet).

The superamplitude of given states can be obtained from (8.3.1) by appropriately choosing the little group indices. For the states in tensor multiplet (they are the states without free little group indices), we contract all the little group indices, the numerator

simplifies:

$$[1_{\hat{a}_1} 2_{\hat{a}_2} 3_{\hat{a}_3} 4_{\hat{a}_4}][1^{\hat{a}_1} 2^{\hat{a}_2} 3^{\hat{a}_3} 4^{\hat{a}_4}] = \mathbf{s}^2 + \mathbf{t}^2 + \mathbf{u}^2 \,, \tag{8.3.2}$$

we then find (8.3.1) reproduces (8.2.1) when the tensors have the same flavour, which is the case we consider here. We are interested in the amplitudes with two states in tensor multiplet and two in gravity multiplet (the states with free little group indices), for which we have

$$\mathcal{A}_4 = G_6 \delta^8 (\sum_{i=1}^4 q_i) \delta^6 (\sum_{i=1}^4 p_i) \frac{[1_{\hat{a}_1} 2_{\hat{a}_2} 3_{\hat{a}_3} 4_{\hat{a}_4}][1^{\hat{a}_1} 2^{\hat{a}_2} 3_{\hat{b}_3} 4_{\hat{b}_4}]}{\mathbf{s}\,\mathbf{t}\,\mathbf{u}} \,, \tag{8.3.3}$$

where we contact the little-group indices for the first two states (they are in tensor multiplet) and leave the indices free for the last two states (they are in gravity multiplet). Here we have also assumed two tensors have the same flavour, otherwise the amplitude vanishes, said in another way, we have suppressed a flavour factor $\delta_{f_1 f_2}$ in (8.3.3), with f_1, f_2 being the flavours of the tensors.

For the comparison of holographic correlators in AdS_3, we compactify the above amplitude to three dimensions. This is done by reducing the 6D spinors to 3D spinor, which effectively sets $[1_- 2_- 3_+ 4_+] = -\langle 12 \rangle \langle 34 \rangle$, where in 3D, the massless momentum can be expressed as $p_i^{\alpha\beta} = \lambda_i^\alpha \lambda_i^\beta$, and the angle braket is defined as $\langle ij \rangle = \lambda_i^\alpha \lambda_j^\beta \epsilon_{\alpha\beta}$, which relates to Mandelstam variables by $\langle ij \rangle^2 = (p_i + p_j)^2$. We then obtain the dimension reduced amplitude of four three-dimensional scalars from (8.3.3), given as

$$\mathcal{A}_4 = G_6 \delta^8 (\sum_{i=1}^4 q_i) \delta^6 (\sum_{i=1}^4 p_i) \frac{\mathbf{s}^2 - \mathbf{t}^2 - \mathbf{u}^2}{\mathbf{s}\,\mathbf{t}\,\mathbf{u}} = G_6 \delta^8 (\sum_{i=1}^4 q_i) \delta^6 (\sum_{i=1}^4 p_i) \frac{2}{\mathbf{s}} \,. \tag{8.3.4}$$

The structure of this result is expected. When compactified to 4D, the $(2,0)$ supergravity becomes supersymmetric multiple-$U(1)$ Einstein-Maxwell theory. Both the scalar arising from the 6D graviton multiplet and the scalar from the 6D tensor multiplet are matters of Einstein-Maxwell theory [1], but they belong to different $U(1)$'s of Maxwell theory, therefore they do not couple to a 4D graviton. This fact implies only the s-channel pole is allowed, and a further reduction to 3D does not change the structure.

8.3.2 Correlators with gravity multiplet operators and hidden conformal symmetry

A family of CPOs in gravity multiplet that we will consider here are scalar operators which have left-right symmetry $(h, \bar{h}) = (k/2, k/2)$, with $k = 2, 3, \ldots$, we will denote them as σ_k. As we see, they have similar structures as the operators s_k that we studied in the previous section. However, these operators arise from the Kaluza-Klein reduction

of the supergravitons in 6D $(2,0)$ supergravity over the S^3,[*] therefore the interaction couplings involving σ_k operators are rather different from those of operators s_k. For instance, a coupling of three σ's is allowed but not for three s's [204]. As already indicated in the flat-space amplitudes (8.3.1), these properties make the correlators in gravity multiplet much more complicated comparing to those in tensor multiplet. As in the case of s_k, to incorporate the R-symmetry we introduce the $SO(4)$ null vector $t_{i\,\mu}$ in the definition of the operators, which are given by

$$\sigma_k(z_i, \bar{z}_i; t_i) = t_{i\,\mu_1} \ldots t_{i\,\mu_k} \sigma_k^{\mu_1 \ldots \mu_k}(z_i, \bar{z}_i). \tag{8.3.5}$$

As we will see that, unlike the correlators of s_k that we studied in the previous section, even for the reduced correlators, when the operators σ_k are involved, the correlators cannot be expressed in terms of σ, τ and U, V only. To describe these correlators, it is necessary to use $\alpha_c, \bar{\alpha}_c$ and $z, \bar{z}$. This should be closely related to the fact that the flat-space superamplitude involving graviton states, as given in (8.3.3), cannot be expressed in terms of Mandelstam variables only.

As we already anticipated earlier when we discussed the flat-space amplitudes, and as understood in [25], the holographic correlators $\langle s_{k_1} s_{k_2} \sigma_{k_3} \sigma_{k_4} \rangle$ also exhibit a hidden conformal symmetry, just as for the correlators in tensor multiplet. In particular, the holographic correlators for arbitrary conformal weights k_i can be described by a single 6D CFT correlator with two scalar operators (corresponding to s_{k_1} and s_{k_2}) and two 3-forms (corresponding to σ_{k_3} and σ_{k_4}). In practice, this leads to a recursion relation that determines $\langle s_{k_1} s_{k_2} \sigma_{k_3} \sigma_{k_4} \rangle$ for any k_i in terms of initial datas which can be obtained from four-point correlators of operators with low conformal weights.

---

[*]See the Tables 1, 2, 3 in [24] for more details of the spectrum in $AdS_3 \times S^3$ supergravity.

Explicitly, the correlator $\langle s_{k_1} s_{k_2} \sigma_{k_3} \sigma_{k_4} \rangle$ is described by [25]

$$
\begin{aligned}
\widetilde{\mathcal{G}}_{s_{k_1} s_{k_2} \sigma_{k_3} \sigma_{k_4}} = {}& t_{12}^2 t_{34}^2 |z_{13}^2| |z_{24}^2| \frac{|\xi_{12}|^{k_{12}^+ + k_{43}^-} |\xi_{34}|^{2k_4}}{|\xi_{13}|^{k_{21}^- + k_{43}^-} |\xi_{23}|^{k_{43}^- - k_{21}^-}} \frac{1}{|Z_{12}|^4 |Z_{34}|^8} \Big\{ g_1(Z)\, t_{34}^2 |z_{34}|^2 \\
& + g_2(Z) \Big[\big(t_{14}^2 t_{23}^2 - t_{13}^2 t_{24}^2 \big) \frac{|z_{34}|^2}{|Z_{12}|^2} + t_{34}^2 \frac{|z_{14}|^2 |z_{23}|^2 - |z_{13}|^2 |z_{24}|^2}{|Z_{12}|^2} \Big] \\
& + g_3(Z) \Big[\frac{(t_{13}^2 t_{24}^2 + t_{14}^2 t_{23}^2)|z_{34}|^2 + t_{34}^2 (|z_{14}|^2 |z_{23}|^2 + |z_{13}|^2 |z_{24}|^2)}{2|Z_{12}|^2}
\end{aligned}
$$

(8.3.6)

$$
\begin{aligned}
& - \frac{t_{12}^2 t_{34}^2 |z_{13}|^2 |z_{24}|^2 (z + \bar{z})}{|Z_{12}|^4} - \frac{t_{13}^2 t_{14}^2 |z_{23}|^2 |z_{24}|^2 + t_{23}^2 t_{24}^2 |z_{13}|^2 |z_{14}|^2}{|Z_{12}|^4} \\
& - \frac{t_{13}^2 t_{24}^2 (|z_{12}|^2 |z_{34}|^2 - |z_{13}|^2 |z_{24}|^2) + t_{14}^2 t_{23}^2 (|z_{12}|^2 |z_{34}|^2 - |z_{14}|^2 |z_{23}|^2)}{|Z_{12}|^4} \\
& - 4\, \epsilon_{\mu_1 \mu_2 \mu_3 \mu_4} t_1^{\mu_1} t_2^{\mu_2} t_3^{\mu_3} t_4^{\mu_4} (z - \bar{z}) \frac{|z_{13}|^2 |z_{24}|^2}{|Z_{12}|^4} \Big] \Big\} \Big|_{t_1^{k_1} t_2^{k_2} t_3^{k_3} t_4^{k_4}},
\end{aligned}
$$

where, again, the correlator $\langle s_{k_1} s_{k_2} \sigma_{k_3} \sigma_{k_4} \rangle$ is obtained by Taylor expanding the above expression to the order $t_1^{k_1} t_2^{k_2} t_3^{k_3} t_4^{k_4}$. We have suppressed the flavour factor $\delta_{f_1 f_2}$ of the tensors in the above expression.

Compare to the correlators of operators in tensor multiplet, we now have more unknown functions that is because, unlike the scalars, the self-dual 3-forms in 6D allow for more independent structures. In particular, it was found there are three of them [25], which are associated with the unknown functions g_1, g_2 and g_3 in (8.3.6). These functions that serve as initial data of the recursion relation are determined by comparing with the known results of correlators $\langle s_1 s_1 \sigma_2 \sigma_2 \rangle$ and $\langle s_2 s_2 \sigma_2 \sigma_2 \rangle$, and they are given by [25]

$$
g_1(U,V) = \int \frac{ds\, dt}{(4\pi i)^2} U^{\frac{s}{2}} V^{\frac{t}{2}-2} \frac{(s-6)(s-4)}{6(s-2)} \Gamma^2\big(2 - \frac{s}{2}\big) \Gamma^2\big(2 - \frac{t}{2}\big) \Gamma^2\big(\frac{s+t}{2} - 2\big), \quad (8.3.7)
$$

$$
g_2(U,V) = \int \frac{ds\, dt}{(4\pi i)^2} U^{\frac{s}{2}} V^{\frac{t}{2}-2} \frac{(s-6)(s-4)(s+2t-8)}{12(t-2)(s+t-6)} \Gamma^2\big(2 - \frac{s}{2}\big) \Gamma^2\big(2 - \frac{t}{2}\big) \Gamma^2\big(\frac{s+t}{2} - 2\big),
$$

$$
g_3(U,V) = \int \frac{ds\, dt}{(4\pi i)^2} U^{\frac{s}{2}} V^{\frac{t}{2}-2} \frac{(s-6)(s-4)^2}{6(t-2)(s+t-6)} \Gamma^2\big(2 - \frac{s}{2}\big) \Gamma^2\big(2 - \frac{t}{2}\big) \Gamma^2\big(\frac{s+t}{2} - 2\big).
$$

It is worth noting that not any initial data (namely g_1, g_2, g_3 given in (8.3.7)) would generate sensible correlation functions of operators with higher conformal weights. Therefore, we expect the recursion relation can even constrain the initial data. Surprisingly, we find that the initial data is in fact uniquely fixed by simple consistency conditions of correlators generated from the recursion relation. Concretely, we begin

by assuming the following ansatzs for the initial data,

$$g_1(U,V) = \int \frac{dsdt}{(4\pi i)^2} U^{\frac{s}{2}} V^{\frac{t}{2}-2} \frac{\sum a_{i,j} s^i t^j}{s-2} \Gamma^2(2-\frac{s}{2})\Gamma^2(2-\frac{t}{2})\Gamma^2(\frac{s+t}{2}-2), \qquad (8.3.8)$$

$$g_2(U,V) = \int \frac{dsdt}{(4\pi i)^2} U^{\frac{s}{2}} V^{\frac{t}{2}-2} \left(\frac{\sum b_{i,j} s^i t^j}{t-2} + \frac{\sum c_{i,j} s^i t^j}{s+t-6} \right) \Gamma^2(2-\frac{s}{2})\Gamma^2(2-\frac{t}{2})\Gamma^2(\frac{s+t}{2}-2),$$

$$g_3(U,V) = \int \frac{dsdt}{(4\pi i)^2} U^{\frac{s}{2}} V^{\frac{t}{2}-2} \left(\frac{\sum d_{i,j} s^i t^j}{t-2} + \frac{\sum e_{i,j} s^i t^j}{s+t-6} \right) \Gamma^2(2-\frac{s}{2})\Gamma^2(2-\frac{t}{2})\Gamma^2(\frac{s+t}{2}-2).$$

Here the summations on i,j are restricted by $i+j \leq 2$ due to the two-derivative power counting of supergravity. We have also used the fact that the functions should have correct pole structures, which are dictated by the exchanged states. The ansatzs contain 30 free parameters, namely the coefficients $a_{ij}, b_{ij}, c_{ij}, d_{ij}$, and e_{ij} in (8.3.8). We then require the full correlators of higher weights that are generated from the recursion relation by plugging the ansatzs (8.3.8) into (8.3.6) to have right pole structures and the correct power counting. In particular, we know that the correlator $M_{s_1 s_1 \sigma_k \sigma_k}(s,t)$ has and only has simple pole at $s=0$, since only the identity operator is allowed to be exchanged in this type of correlators. For as a two-derivative theory, we also know that $M_{s_1 s_1 \sigma_k \sigma_k}(\beta s, \beta t) \sim \beta$ in the limit $\beta \to \infty$. By imposing such conditions for $k=2,3$, we find that the anstazs of g_1, g_2 and g_3 given in (8.3.8) are uniquely fixed up to an overall factor, and agree precisely with what are given in (8.3.7) which were determined from explicit known results.

8.3.3 Solution to the recursion relation

We will now solve the recursion relation following the same strategy of section 8.2.1 for the simpler correlators of tensor multiplet. In particular, we express the recursion relation as contour integrals. We also note that, due to the last term in (8.3.6) proportional to $\epsilon_{\mu_1\mu_2\mu_3\mu_4}$, it is not possible to express the correlator in terms of cross ratios U,V and σ,τ only, instead it is necessary to use $z,\bar{z}$ and $\alpha_c, \bar{\alpha}_c$. Therefore it is natural to separate the correlator into two parts where one of them contains $z,\bar{z}$ and $\alpha_c, \bar{\alpha}_c$ (namely the term proportional to $\epsilon_{\mu_1\mu_2\mu_3\mu_4}$ in (8.3.6)), which we will denote as the chiral sector $\widetilde{\mathcal{G}}^{(c)}_{s_{k_1} s_{k_2} \sigma_{k_3} \sigma_{k_4}}$, and the remaining part only depends on U,V and σ,τ, which is the non-chiral sector $\widetilde{\mathcal{G}}^{(nc)}_{s_{k_1} s_{k_2} \sigma_{k_3} \sigma_{k_4}}$. Therefore, we will express the full correlator as

$$\widetilde{\mathcal{G}}_{s_{k_1} s_{k_2} \sigma_{k_3} \sigma_{k_4}} = \widetilde{\mathcal{G}}^{(c)}_{s_{k_1} s_{k_2} \sigma_{k_3} \sigma_{k_4}} + \widetilde{\mathcal{G}}^{(nc)}_{s_{k_1} s_{k_2} \sigma_{k_3} \sigma_{k_4}}, \qquad (8.3.9)$$

where $\widetilde{\mathcal{G}}^{(c)}_{s_{k_1}s_{k_2}\sigma_{k_3}\sigma_{k_4}}$ and $\widetilde{\mathcal{G}}^{(nc)}_{s_{k_1}s_{k_2}\sigma_{k_3}\sigma_{k_4}}$ are given in terms of contour integrals,

$$\widetilde{\mathcal{G}}^{(c)}_{s_{k_1}s_{k_2}\sigma_{k_3}\sigma_{k_4}} = (\alpha_c - \bar{\alpha}_c)(z - \bar{z})\sigma^{k_2-2}\tau^{\frac{k_{12}^- - k_{34}^-}{2}+1}U^{\frac{k_{12}^+ + k_{43}^- - 8}{2}}V^{\frac{k_{21}^- + k_{34}^-}{2}}$$

$$\times \oint_{a_i=0} da_i\, a_1^{1-k_1}a_2^{1-k_2}a_3^{1-k_3}a_4^{1-k_4}\frac{g_3(U',V')}{(1+\frac{a_1a_2}{U\sigma})^4(1+a_3a_4)^4}\,, \qquad (8.3.10)$$

and

$$\widetilde{\mathcal{G}}^{(nc)}_{s_{k_1}s_{k_2}\sigma_{k_3}\sigma_{k_4}}$$
$$=\sigma^{k_2-1}\tau^{\frac{k_{12}^- - k_{34}^-}{2}}U^{\frac{k_{12}^+ + k_{43}^- - 4}{2}}V^{\frac{k_{21}^- + k_{34}^-}{2}}\oint_{a_i=0} da_i\, a_1^{-k_1}a_2^{-k_2}a_3^{1-k_3}a_4^{1-k_4}\frac{1}{(1+\frac{a_1a_2}{U\sigma})^2(1+a_3a_4)^4}$$
$$\qquad\qquad\qquad\qquad\qquad\qquad\qquad\qquad\qquad\qquad\qquad\qquad\qquad\qquad\qquad (8.3.11)$$

$$\times\Big\{ g_1(U',V') + \frac{a_1a_2\tau}{(1+\frac{a_1a_2}{U\sigma})U\sigma}F_2^{(s)}(U',V') + \frac{a_1a_2}{(1+\frac{a_1a_2}{U\sigma})U}F_2^{(a)}(U',V')$$

$$+ \frac{V}{(1+\frac{a_1a_2}{U\sigma})U}F_2^{(s)}(U',V') + \frac{F_2^{(a)}(U',V')}{(1+\frac{a_1a_2}{U\sigma})U}$$

$$+ g_3(U',V')\Big[-\frac{a_1a_2(1-U+V)}{(1+\frac{a_1a_2}{U\sigma})^2U^2\sigma} - \frac{a_1^2v+a_2^2\tau/\sigma}{(1+\frac{a_1a_2}{U\sigma})^2U^2} - a_1a_2\frac{(U-1)+\tau/\sigma(U-V)}{(1+\frac{a_1a_2}{U\sigma})^2U^2}\Big]\Big\}\,,$$
$$\qquad\qquad\qquad\qquad\qquad\qquad\qquad\qquad\qquad\qquad\qquad\qquad\qquad\qquad\qquad (8.3.12)$$

with U',V' given in (8.2.17). Here we have expressed the results in the form of contour integrals, as we did in the previous section. Finally, $F_2^{(s)}$ and $F_2^{(a)}$ are linear combinations of g_2 and g_3. In Mellin space, they are given by

$$F_2^{(s)} = g_3/2 + g_2 = \int \frac{dsdt}{(4\pi i)^2}U^{\frac{s}{2}}V^{\frac{t}{2}-2}\frac{(s-6)(s-4)}{6(t-2)}\Gamma^2(2-\frac{s}{2})\Gamma^2(2-\frac{t}{2})\Gamma^2(\frac{s+t}{2}-2)\,,$$
$$F_2^{(a)} = g_3/2 - g_2 = -\int \frac{dsdt}{(4\pi i)^2}U^{\frac{s}{2}}V^{\frac{t}{2}-2}\frac{(s-6)(s-4)}{6(s+t-6)}\Gamma^2(2-\frac{s}{2})\Gamma^2(2-\frac{t}{2})\Gamma^2(\frac{s+t}{2}-2)\,.$$
$$\qquad\qquad\qquad\qquad\qquad\qquad\qquad\qquad\qquad\qquad\qquad\qquad\qquad\qquad\qquad (8.3.13)$$

In next subsections, we will solve the recursion relation for $\widetilde{\mathcal{G}}^{(c)}_{s_{k_1}s_{k_2}\sigma_{k_3}\sigma_{k_4}}$ and $\widetilde{\mathcal{G}}^{(nc)}_{s_{k_1}s_{k_2}\sigma_{k_3}\sigma_{k_4}}$, respectively.

The chiral sector

The recursion relation for the chiral sector $\widetilde{\mathcal{G}}^{(c)}_{s_{k_1}s_{k_2}\sigma_{k_3}\sigma_{k_4}}$ as given in (8.3.10) is relatively simple. It has an analogous structure as the correlators of tensor multiplet. After factoring out $(\alpha_c - \bar{\alpha}_c)(z - \bar{z})$, we can then formally express $\widetilde{\mathcal{G}}^{(c)}_{s_{k_1}s_{k_2}\sigma_{k_3}\sigma_{k_4}}$ in Mellin space using the standard definition in (8.2.5), and the recursion relation can be solved in a similar manner as for the correlators of tensor multiplet that we studied in the previous section. Since the computation is very similar to that has been done for the correlators of tensor multiplet, we will not repeat the steps here. Instead we will simply

present the final result of this particular part of the correlator, which is given by

$$
\begin{aligned}
\widetilde{\mathcal{G}}^{(c)}_{s_{k_1} s_{k_2} \sigma_{k_3} \sigma_{k_4}} & \\
= (\alpha_c - \bar{\alpha}_c)(z - \bar{z}) & \int \frac{ds\,dt}{(4\pi i)^2} U^{\frac{s+k^-_{43}}{2}} V^{\frac{t-k^+_{14}}{2}} \widetilde{\Gamma}_{\{k_i\}}(s,t) \sum_{m_1,m_2=0}^{\infty} \sigma^{m_2 + \frac{k^-_{21} + k^-_{43}}{2}} \tau^{k_1 - 1 - m_{12}} \\
\times & \frac{1}{\prod_{i=1}^{6} m_i!} \frac{2(k^+_{24} - \tilde{u})(k^+_{13} - \tilde{u})}{3(s + 2m_1 - k^+_{12} + 2)(t + k^-_{14} - 2m_{12} - 2)(-\tilde{u} + k^+_{13} - 2m_2)} \,,
\end{aligned}
$$
(8.3.14)

where

$$
\begin{aligned}
m_3 &= k_1 - m_{12} - 2 \,, & m_4 &= \frac{k^-_{31} + k^-_{42}}{2} + m_1 \,, \\
m_5 &= \frac{k^+_{12} + k^-_{34}}{2} - m_{12} - 2 \,, & m_6 &= \frac{k^-_{21} + k^-_{43}}{2} + m_2 \,.
\end{aligned}
$$
(8.3.15)

The full non-reduced correlator is obtained by putting back the factor given in (8.2.7). To have a well-defined non-reduced Mellin amplitude accoding to (8.2.9), one may combine the factor $(\alpha_c - \bar{\alpha}_c)(z - \bar{z})$ in (8.3.14) with the same factor in (8.2.7), so that $(\alpha_c - \bar{\alpha}_c)^2(z - \bar{z})^2$ is a simple polynomial in U, V and σ, τ, given as

$$
(\alpha_c - \bar{\alpha}_c)^2(z - \bar{z})^2 = \tau^{-2} \left[(\sigma - \tau)^2 - 2(\sigma + \tau) + 1 \right] \left[(U - V)^2 - 2(U + V) + 1 \right] \,.
$$
(8.3.16)

So for this particular part of the chiral sector contribution, the non-reduced Mellin amplitude is well-defined, and can be obtained explicitly from (8.3.16) and using the relation (8.2.10). We find that, interestingly, this term vanishes in the flat-space limit. More precisely, the leading two-derivative contribution arising from each term in (8.3.16) cancels out. We also note $\widetilde{\mathcal{G}}^{(c)}_{s_{k_1} s_{k_2} \sigma_{k_3} \sigma_{k_4}}$ vanishes in the MRV limit, due to $(\alpha_c - \bar{\alpha}_c) = 0$ in the limit.

Another important feature is that the multiple poles in (8.3.14) do not cancel out even after converted into non-reduced Mellin amplitude using (8.3.16), as described above. As we will come back to this in the next section, these multiple poles precisely cancel with the same multiple poles arising from the non-chiral sector $\widetilde{\mathcal{G}}^{(nc)}_{s_{k_1} s_{k_2} \sigma_{k_3} \sigma_{k_4}}$, such that the full non-reduced Mellin amplitude only contains single poles, as it should be for a local theory.

The non-chiral sector

As shown in (8.3.11), the recursion relation for the non-chiral sector $\widetilde{\mathcal{G}}^{(nc)}_{s_{k_1} s_{k_2} \sigma_{k_3} \sigma_{k_4}}$ is clearly more complicated, which however is a function of U, V only and has a well-defined Mellin representation. We have performed the contour integrals following the

same methods, however the answer obtained in this way turns out to be rather lengthy, and it is not illuminating to present the expression here. Roughly, each term in (8.3.11) gives an expression that is similar to that of the correlators in tensor multiplet as given in (8.2.20) or those of the chiral sector as given in (8.3.14), and it is not clear how to combine these terms together and simplify them. However, we find that an equivalent but much more compact expression can be obtained by exploring the analytic structures of the correlators in Mellin space. That is what we will present in the following.

In particular, we express the result to manifest the pole structures of the Mellin amplitude,

$$\widetilde{\mathcal{M}}^{(nc)}_{s_{k_1} s_{k_2} \sigma_{k_3} \sigma_{k_4}}(s,t) = \widetilde{\mathcal{M}}^{(nc)}_s(s,t) + \widetilde{\mathcal{M}}^{(nc)}_{s,t}(s,t) + \widetilde{\mathcal{M}}^{(nc)}_{s,u}(s,t), \qquad (8.3.17)$$

where $\widetilde{\mathcal{M}}^{(nc)}_s(s,t)$ represents terms with single poles, $\widetilde{\mathcal{M}}^{(nc)}_{s,t}(s,t)$ is the contribution that has simultaneous poles in both s and t channels and similarly $\widetilde{\mathcal{M}}^{(nc)}_{s,u}(s,t)$ contains s- and u-channel poles. Furthermore, $\widetilde{\mathcal{M}}^{(nc)}_{s,t}(s,t)$ and $\widetilde{\mathcal{M}}^{(nc)}_{s,u}(s,t)$ are related to each other by a simple permutation,

$$\widetilde{\mathcal{M}}^{(nc)}_{s,u}(s,t) = \widetilde{\mathcal{M}}^{(nc)}_{s,t}(s,\tilde{u}) \,|_{k_1 \leftrightarrow k_2, \, \sigma \leftrightarrow \tau} \,. \qquad (8.3.18)$$

Therefore, we will focus on $\widetilde{\mathcal{M}}^{(nc)}_{s,t}(s,t)$ only.

Let us begin with the single-pole term, $\widetilde{\mathcal{M}}^{(nc)}_s(s,t)$. We find this term only contains s-channel poles, and according to its behaviour as polynomials in σ and τ, we find it is convenient to write $\widetilde{\mathcal{M}}^{(nc)}_s(s,t)$ as,

$$\widetilde{\mathcal{M}}^{(nc)}_s(s,t) = \sum_{s_p=0}^{s_{\max}} \sum_{j=j_{\min}}^{j_{\max}} \frac{\mathcal{R}^j_{s_p,1}\tau + \mathcal{R}^j_{s_p,0}}{s - s_p} \sigma^j \tau^{\frac{s_p + k_{43}^-}{2} - j - 1}, \qquad (8.3.19)$$

where $s_{\max} = \min\{k_{12}^+, k_{34}^+\} - 2$, and the j-sum runs from $j_{\min} = \max\{0, \frac{k_{12}^- + k_{34}^-}{2}\}$ to $j_{\max} = \min\{\frac{s_p - k_{12}^-}{2}, \frac{s_p - k_{34}^-}{2}\}$. The residues $\mathcal{R}^j_{s_p,1}, \mathcal{R}^j_{s_p,0}$ are independent of σ and τ, and they are given by

$$
\begin{aligned}
\mathcal{R}^j_{s_p,1} &= -\frac{(-1)^{\frac{k_{1234}^+}{2} + k_{34}^-} \left(k_3^2 + k_4^2 - s_p(s_p + 2) - 2\right)}{3\,\Gamma^j_\otimes}, \\[2mm]
\mathcal{R}^j_{s_p,0} &= -\frac{(-1)^{\frac{k_{1234}^+}{2} + k_{34}^-} \left(s_p - k_{12}^- - 2j\right)\left(s_p - k_{34}^- - 2j\right)}{3\,\Gamma^j_\otimes},
\end{aligned}
\qquad (8.3.20)
$$

where $\Gamma_\otimes^j$ is a product of Γ functions

$$\Gamma_\otimes^j = \Gamma(j+1)\,\Gamma\left(\frac{k_{12}^- + k_{34}^-}{2} + j + 1\right)\Gamma\left(\frac{k_{12}^+ - s_p}{2}\right)\Gamma\left(\frac{k_{34}^+ - s_p}{2}\right)$$
$$\times \Gamma\left(\frac{k_{21}^- + s_p}{2} + 1 - j\right)\Gamma\left(\frac{k_{43}^- + s_p}{2} + 1 - j\right). \tag{8.3.21}$$

The term $\widetilde{\mathcal{M}}_{s,t}^{(nc)}(s,t)$, that contains poles in both s and t channels, has similar structures and takes the following form,

$$\widetilde{\mathcal{M}}_{s,t}^{(nc)}(s,t) = \sum_{s_p=0}^{s_{\max}} \sum_{j=j_{\min}}^{j_{\max}} \frac{\mathcal{R}_{s_p,t_p}^j}{(s-s_p)(t-t_p)}\,\sigma^j \tau^{\frac{s_p+k_{43}^-}{2}-j-1}, \tag{8.3.22}$$

where $t_p = k_{13}^+ - s_p$, and we find the residue is given by

$$\mathcal{R}_{s_p,t_p}^j = \frac{(-1)^{\frac{k_{1234}^+}{2}}}{3\,\Gamma_\otimes^j}\left(s_p + k_{21}^- - 2j\right)\left(s_p + k_{43}^- - 2j\right)\left[j\left(j - \frac{k_{21}^- + k_{43}^-}{2}\right)\frac{x^2}{\sigma}\right. \tag{8.3.23}$$
$$+ \left(j(k_{21}^- + k_{43}^- - 2) + k_{24}^+ - s_p - 2 - 2j^2\right)x + (2j+1)(k_{21}^- + k_{43}^- - 2) - 4j^2$$
$$+ \left(s_p(3 - k_{1234}^+ + s_p) + (k_{12}^+ k_{34}^+ - k_{13}^+ - 2k_{24}^+ + 4) - \frac{j}{2}(k_{21}^- + k_{43}^- - 4 - 2j)\right)\sigma$$
$$\left. - \frac{1}{4}(k_{12}^+ - s_p - 2)(k_{34}^+ - s_p - 2)(\sigma - x)^2\right],$$

with $x = \tau - 1$. Together with the result of $\widetilde{\mathcal{G}}_{s_{k_1}s_{k_2}\sigma_{k_3}\sigma_{k_4}}^{(c)}$ in (8.3.14), we obtain the complete solution for the holographic correlator $\langle s_{k_1}s_{k_2}\sigma_{k_3}\sigma_{k_4}\rangle$.

A few comments are in order. Firstly, we have verified that the simplified expression (8.3.17) agrees with the result obtained directly from solving recursion relation using the methods similar to that in the previous section for studying the correlators of operators in tensor multiplet. Secondly, the compact expression we obtained here suggests that the holographic correlators in $AdS_3 \times S^3$ exhibit new structures that cannot be seen from hidden conformal symmetries, especially when operators in gravity multiplets are involved. Finally, use the relation (8.2.11), we can again obtain the non-reduced Mellin amplitude for the contribution of the non-chiral sector, $\mathcal{M}_{s_{k_1}s_{k_2}\sigma_{k_3}\sigma_{k_4}}^{(nc)}(s,t)$. Importantly, as we commented earlier, we find $\mathcal{M}_{s_{k_1}s_{k_2}\sigma_{k_3}\sigma_{k_4}}^{(nc)}(s,t)$ contains multiple poles (arising from $\widetilde{\mathcal{M}}_{s,t}^{(nc)}(s,t)$ and $\widetilde{\mathcal{M}}_{s,u}^{(nc)}(s,t)$), however, these poles cancel precisely with those from the chiral sector. This cancellation provides a very non-trivial check on our results.

8.3.4 The flat-space and MRV limits

We will now study the flat-space and MRV limits of the non-reduced Mellin amplitude $\mathcal{M}_{s_{k_1} s_{k_2} \sigma_{k_3} \sigma_{k_4}}(s,t)$. As we commented in the section 8.3.3, the chiral sector contribution $\mathcal{G}^{(c)}_{s_{k_1} s_{k_2} \sigma_{k_3} \sigma_{k_4}}$ does not contribute in these limits. So we will focus on the contribution from the non-chiral sector.

Let us begin with flat-space limit. It is easy to see that the Mellin amplitude is dominated by the single pole term $\widetilde{\mathcal{M}}^{(nc)}_s(s,t)$ in this limit. The explicit form of the correlator in flat-space limit is given by

$$\mathcal{M}^{(nc)}_{s_{k_1} s_{k_2} \sigma_{k_3} \sigma_{k_4}}(s,t)|_{s,t\to\infty} \to \frac{u\,t + s\,t\,\sigma + s\,u\,\tau}{s} P^{(nc)}_{\{k_i\}}(\sigma,\tau)\,, \qquad (8.3.24)$$

where the overall factor $P^{(nc)}_{\{k_i\}}(\sigma,\tau)$ is a polynomial in σ,τ,

$$P^{(nc)}_{\{k_i\}}(\sigma,\tau) = -\frac{1}{4} \sum_{s_p=0}^{s_{\max}} \sum_{j=j_{\min}}^{j_{\max}} (\mathcal{R}^j_{s_p,1}\tau + \mathcal{R}^j_{s_p,0})\,\sigma^j \tau^{\frac{s_p+k_{43}^-}{2}-j-1}\,, \qquad (8.3.25)$$

with $\mathcal{R}^j_{s_p,1}$ and $\mathcal{R}^j_{s_p,0}$ given in (8.3.20). We note, as required, the flat-space limit of the Mellin amplitude has a two-derivative power counting and has precisely the same structure as the flat-space superamplitude when compactified to 3D, as given in (8.3.4). In particular, they both only contain a single pole in s-channel. As in the case of tensor multiplet, we see again the appearance of the factor $(u\,t + s\,t\,\sigma + s\,u\,\tau)$, which represents the fact that the theory has half maximal supersymmetry.

The MRV limit of the non-reduced Mellin amplitude is defined as

$$\mathcal{M}_{\mathrm{MRV},s_{k_1} s_{k_2} \sigma_{k_3} \sigma_{k_4}}(s,t) = \mathcal{M}^{(nc)}_{s_{k_1} s_{k_2} \sigma_{k_3} \sigma_{k_4}}(s,t)\big|_{\alpha_c\to 0,\bar\alpha_c\to 0}\,. \qquad (8.3.26)$$

We find that the term with s,u-channel poles, $\widetilde{\mathcal{M}}^{(nc)}_{s,u}(s,t)$, vanishes identically in the MRV limit, and the single-pole term, $\widetilde{\mathcal{M}}^{(nc)}_s(s,t)$, and the term with poles in s,t-channels, $\widetilde{\mathcal{M}}^{(nc)}_{s,t}(s,t)$, reduce to,

$$\mathcal{M}_{\mathrm{MRV},s_{k_1} s_{k_2} \sigma_{k_3} \sigma_{k_4}}(s,t) = \mathcal{M}^{(nc)}_{\mathrm{MRV},s}(s,t) + \mathcal{M}^{(nc)}_{\mathrm{MRV},s,t}(s,t)\,, \qquad (8.3.27)$$

where

$$\mathcal{M}^{(nc)}_{\mathrm{MRV},s}(s,t) = (s+t-k_{13}^+)(s+t-k_{24}^+)$$
$$\times \sum_{s_p=0}^{s_{\max}} \frac{1}{(s-s_p)} \frac{(-1)^{\frac{k_{1234}^+}{2}+k_{43}^-}\left(2 - k_{21}^-\,k_{43}^- - k_3^2 - k_4^2 - (k_{21}^- + k_{43}^- - 2)s_p\right)}{12\,\Gamma_\otimes^{j=0}}\,, \qquad (8.3.28)$$

and

$$
\mathcal{M}^{(nc)}_{\mathrm{MRV},s,t}(s,t) = (s+t-k^+_{13})(s+t-k^+_{24})
$$
$$
\times \sum_{s_p=0}^{s_{\max}} \frac{1}{(s-s_p)\,(t-t_p)} \frac{(-1)^{\frac{k^+_{1234}}{2}+k^-_{43}}(k^-_{21}+k^-_{43}-2)(k^-_{21}+s_p)(k^-_{43}+s_p)}{12\,\Gamma_\otimes^{j=0}}\,,
$$
$$(8.3.29)$$

and $\Gamma_\otimes^{j=0}$ is given in (8.3.21) with j being set to 0. Importantly, the apparent double poles in $\mathcal{M}^{(nc)}_{\mathrm{MRV},s,t}(s,t)$ in fact cancel out after the sum. This can be understood by the fact that the residues at the double poles are all proportional to $(\alpha - \bar{\alpha})^2$ (so that they cancel with the contributions from chiral sector), which vanishes identically in the MRV limit.

We note that, there are no u-channel singularities since $\mathcal{M}^{(nc)}_{\mathrm{MRV},s,u}(s,t)$ vanishes identically in the MRV limit as we commented earlier. Furthermore, the prefactor $(s+t-k^+_{13})(s+t-k^+_{24})$ in (8.3.28) and (8.3.29) gives arise zeros in u-channel. As we have already emphasised in the previous section when we studied the correlators of operators in tensor multiplet, these properties of the correlators in the MRV limit are crucial in the study of holographic correlators in other AdS backgrounds.

Finally, let us remark that one may consider the other MRV limit with $\alpha_c = \bar{\alpha}_c = 1$, for which, we find that the chiral sector contribution $\mathcal{G}^{(c)}_{s_{k_1} s_{k_2} \sigma_{k_3} \sigma_{k_4}}$ also vanishes due to the fact it is proportional to $\alpha_c - \bar{\alpha}_c$. The non-trivial contribution arising from the non-chiral sector is given by the terms that have leading order term in σ, τ. Explicitly, we find

$$
\mathcal{M}_{\mathrm{MRV}',s_{k_1} s_{k_2} \sigma_{k_3} \sigma_{k_4}}(s,t) = \mathcal{M}^{(nc)}_{\mathrm{MRV}',s}(s,t) + \mathcal{M}^{(nc)}_{\mathrm{MRV}',s,t}(s,t) + \mathcal{M}^{(nc)}_{\mathrm{MRV}',s,u}(s,t)\,,
$$
$$(8.3.30)$$

where

$$
\mathcal{M}^{(nc)}_{\mathrm{MRV}',s}(s,t) = (k^+_{12}-s)(k^+_{34}-s)\,\sigma^{\frac{s_{\max}+k^-_{43}}{2}+1}
$$
$$
\times \sum_{j=j_{\min}}^{j_{\max}} \frac{1}{(s-s_p-2)} \left.\frac{\mathcal{R}^j_{s_p,1}}{4\,\Gamma_\otimes}\right|_{s_p=s_{\max}}\,,
$$
$$(8.3.31)$$

and

$$
\mathcal{M}^{(nc)}_{\mathrm{MRV}',s,t}(s,t) = (k^+_{12}-s)(k^+_{34}-s)\,\sigma^{\frac{s_{\max}+k^-_{43}}{2}+1}
$$
$$
\times \sum_{j=j_{\min}}^{j_{\max}} \frac{1}{(s-s_p-2)(t-t_p)} \left.\frac{\mathcal{R}^j_{s_p,t_p}}{4\,\Gamma_\otimes}\right|_{s_p=s_{\max}}\,,
$$
$$(8.3.32)$$

and $\mathcal{M}^{(nc)}_{\mathrm{MRV}',s,u}(s,t) = \mathcal{M}^{(nc)}_{\mathrm{MRV}',s,t}(s,u)|_{k_1 \leftrightarrow k_2}$. The apparent s-channel poles in (8.3.31) and (8.3.32) are always cancelled by the pre-factor $(k_{12}^+ - s)(k_{34}^+ - s)$, so there are no singularities in the s-channel.

8.4 Conclusion

In this paper, we present compact formulas for all four-point tree-level holographic correlators in $AdS_3 \times S^3$ in supergravity limit, with all the operators in tensor multiplet, as well as for the mixed correlators where we have two operators in tensor multiplet and the other two in gravity multiplet. The formulas are obtained by assuming the hidden 6D conformal symmetry of the theory [25] that leads to recursion relations that relates correlators of operators with higher weights to correlators of operators with lower weights. The recursion relation for the mixed correlators involving operators in gravity multiplet is relatively more complex compared to the one for the correlators involving only tensors. As we emphasised that the expression of the mixed correlators obtained directly from the recursion relation is rather lengthy, and a compact formula was found only after we carefully analyse the analytical properties of the correlators and re-express the result in a form that manifests the pole structures. The simple expression suggests new properties beyond the hidden conformal symmetry. It is therefore of interest to investigate if the expression can be obtained by other means. We also studied the structures of the correlators by taking various limits (that include flat-space limit and MRV limit) of the results, and interesting properties were found in these limits. We have further verified that the multiple poles cancel out non-trivially for the non-reduced Mellin amplitude.

It will be of interest to extend the analysis to the correlators of four operators all in gravity multiplet, namely $\langle \sigma_{k_1} \sigma_{k_2} \sigma_{k_3} \sigma_{k_4} \rangle$. With the result of all these correlators, we will in principle complete the computation of all the four-point tree-level holographic correlators in $AdS_3 \times S^3$ in supergravity limit. It is expected that the correlators $\langle \sigma_{k_1} \sigma_{k_2} \sigma_{k_3} \sigma_{k_4} \rangle$ are described by a single 6D CFT correlator of four self-dual 3-forms [25], due to the conjectured hidden 6D conformal symmetry. The tree-level four-point correlators would allow the computation of CFT datas such as anomalous dimensions of non-BPS operators, some of which has been studied recently utilising the results of correlators in tensor multiplet [205, 206]. The complete tree-level results would also allow the construction of loop corrections using analytical conformal bootstrap and unitarity methods. The loop corrections for amplitudes in 6D $(2,0)$ supergravity are of particular interest, since the theory is anomalous only if we have the right matter content. The study of the anomaly in flat-space amplitudes in 6D $(2,0)$ supergravity was explored in [65]. It will be very interesting to extend these ideas to the holographic correlators in $AdS_3 \times S^3$. Finally, four-point correlators with special

multiple particle operators in tensor multiplet have been recently studied in [206], and interesting structures were found, it is interesting to study analogous correlators but now involving operators in gravity multiplet.

Chapter 9

Conclusion

In this thesis, we have introduced several on-shell techniques that have been applied to the high energy physics research. In chapter 3 we study the twistor formulations of scattering amplitudes in 6D supersymmetric theories, and some of them are known to be difficult to have a Lagrangian description, *e.g.* the (2,0) M5-brane theory. The twistor formula expresses 6D amplitudes as an worldsheet integral localised on the solutions of scattering equation following the idea of CHY formulation [55]. The information of theories, such as colour factor, supersymmetry, and so on are encoded in the half integrands. There are two major twistor formulations, one is the rational map [1, 9, 10],and the other is the polarised scattering equation [11]. Both formulations can be written as matrix forms. We first arrange variables of rational maps or polarised scattering equation into matrices, called symplectic Grassmannian S, which satisfies the symplectic conditions

$$\delta^{4 \times n}(S \cdot \Omega \cdot \Lambda^A) \quad \text{with} \quad S \cdot \Omega \cdot S^T = 0 \,, \tag{9.0.1}$$

where $S = C$ (C being the matrix constructed from rational maps variables), or $S = V$ (S is constructed from the variables in polarised scattering equation). The two different looking twistor formulations are actually equivalent since they can be viewed as different gauge fixing of the symplectic Grassmannian [32]. Given the measure has the symplectic Grassmannian form, it will be very interesting to find epressions of those half integrands in terms of Plücker coordinates, *i.e.* the minors of S. Furthermore, once the tree-level formula is obtained in the CHY or twistor-like formulation, it is straightforward to apply the forward limit procedure to arrive at one- or higher-loop amplitudes [13]. Such procedure usually generates a loop integrand with a linear propagator, which is equivalent to the standard quadratic one at the level of integral since the difference is simply shift of loop momentum. In chapter 4, we show the one-loop D3-brane amplitude can be obtained from the tree-level M5-brane amplitude via this forward limit procedure. The one-loop D3-brane amplitude is simply a rational term,

which could potentially violate the $U(1)$ symmetry enjoyed by the D3-brane tree amplitudes, *e.g.* only helicity-conserved amplitude allowed. Such rational term is purely contact so it can be cancelled by adding a local counter term. By performing supersymmtric reduction on the M5-brane amplitude and then taking the forward limit procedure, the one-loop amplitude of 4D non-supersymmetric Born-Infeld field can be obtained accordingly. We check the self-dual $(++\cdots+)$ and next-to-self-dual $(-+\cdots+)$ agree with known results by Elvang *et al* [58]. It will be very interesting to apply this loop-tree procedure to obtain loop amplitudes of more quantum field theories.

In chapter 5 we discuss a new direction of formulating scattering amplitudes using positive geometry. The construction was first proposed by Arkani-Hamed and Trnka [27] to describe amplitudes in the $\mathcal{N} = 4$ SYM theory in terms of a geometric object, called amplituhedron. The idea is to view the amplitude as the "canonical form" of its associated "positive geometry". The original amplituhedron was defined in the momentum twistor space, and later on the momentum amplituhedron directly defined in the spinor helicity space was proposed [54], which makes it more straightforward to extend the construction to the 3D ABJM theory [3]. The orthogonal momentum amplituhedron was defined in the space of product of positive orthogonal Grassmannian and the moment curve. The co-dimension one boundaries of this space are given by the odd-particle planar Mandelstam variables:

$$\underbrace{S_{i,\,i+1,\ldots,i+p}}_{\text{odd}} = 0, \qquad p = 2, 4, 6, \ldots. \tag{9.0.2}$$

The even-particle counterparts are hidden as higher co-dimension boundaries, and the full boundary stratification was studied in [207]. We verify the canonical form derived using the Grassmannian formula gives scattering amplitudes of ABJM theory in the $\mathcal{N} = 4$ formalism. Also, it is well-known in the 4D amplituhedron story that the BCFW triangulation tiles the amplituhedron space, which has been checked for the 8-pt case for 3D momentum amplituhedron. The geometric description also extends to other physical observables, such as bi-adjoint ϕ^3 theory, effective field theories, correlation function [35], and the "squared amplitude" [36]. Below we list several examples where such connection between amplitudes and geometries has been built.

Theory	Positive geometry	Refs
$\mathcal{N} = 4$ SYM	Amplituhedron/Momentum amplituhedron	[27, 54]
Bi-adjoint ϕ^3	ABHY associahedron	[33]
EFTs	EFT-Hedron	[34]
Correlation function	Correlahedron	[35]
Squared amplitude	Amplituhedron-like geometries	[36]
ABJM	Orthogonal momentum amplituhedron	[3, 31, 208]
⋮	⋮	⋮

It will be a lot more interesting to explore more possibility of the existing positive geometry for the physical observables that we concern.

In chapter 7, we study the four-point integrated correlators in the $\mathcal{N} = 4$ SYM theory. When focusing its perturbative part, we identify the integrated correlator as periods of f-graph (and $\widetilde{f}$-graph as a generalisation). This identification allows us to systematically computing the integrated correlator up to higher loops. With the computer programs `HyperInt` and `HyperlogProcedure`, the planar four loop result for the first correlator, and the three-loop result for the second can be analytically computed. They perfectly agree with the expressions obtained from the supersymmetric localisation. This matching with supersymmetric localisation can conversely constrain or predict certain period when the evaluation if period is not plausible at higher loop order. The case starts at 5 loop, where 6 out of 7 periods are evaluated while the leftover one is predicted to be certain order to agree with the localisation. It will be interesting to extend the analysis to higher loop orders as well as the non-planar sector.

In chapter 8, the four-point holographic correlator of 6D (2,0) supergravity on $AdS_3 \times S^3$ was studied. The purpose to push our understanding of $AdS_3 \times S^3$ correlator to the same level to that of $AdS_5 \times S^5$. Following the idea of 10D hidden conformal symmetry for $AdS_5 \times S^5$ correlator [23], with the 6D hidden conformal symmetry we discover compact formulae of correlator with four operators in tensor multiplet, $\langle s_{k_1} s_{k_2} s_{k_3} s_{k_4} \rangle$, and correlator with two operators in tensor multiplet and the other two in gravity mulitplet, $\langle s_{k_1} s_{k_2} \sigma_{k_3} \sigma_{k_4} \rangle$. The formulae has the correct behaviours at certain limits, such as flat-space limit and the MRV limit. The explicit tree-level four-point correlators would allow the computation of CFT datas such as anomalous dimensions of non-BPS operators [179, 180, 183, 190], some of which has been recently studied utilising the results of AdS_3 correlators in tensor multiplet [205]. It would be very interesting to extend the analysis to the correlators of four operators all in gravity multiplet,

namely $\langle \sigma_{k_1} \sigma_{k_2} \sigma_{k_3} \sigma_{k_4} \rangle$. Having the complete tree-level results would also allow the construction of loop corrections using analytical conformal bootstrap and unitarity methods. [178, 181, 184–188, 191–193]

Appendix A

Matrix model computations

This appendix derives the form of the global conformal blocks in two different ways, firstly by explicit resummation of a quasi-primary's global descendants and secondly by use of the quadratic Casimir of the global conformal group.

A.1 Matrix model computations

In this appendix we review the perturbative contribution of the $\mathcal{N} = 2^*$ SYM partition function on S^4, $\hat{Z}_{G_N}^{pert}(m, a)$, for all classical gauge groups G_N, and the corresponding matrix model expectation values.[*] The perturbative contribution for the first integrated correlator has been computed in [132, 148]. Therefore, we use these expressions of $\hat{Z}_{G_N}^{pert}(m, a)$ mainly for the computations of the perturbative contribution of the second integrated correlators in the main text. The expressions of $\hat{Z}_{G_N}^{pert}(m, a)$ for $G_N = SU(N), SO(2N), SO(2N+1), USp(2N)$ are listed below.

- For $SU(N)$, we have

$$\hat{Z}_{SU(N)}^{pert}(m, a) = \frac{1}{H(m)^{N-1}} \prod_{i<j} \frac{H^2(a_{ij})}{H(a_{ij} - m)H(a_{ij} + m)} \,, \qquad (A.1.1)$$

with $a_{ij} = a_i - a_j$, and the expectation value of a function $F(a_i)$ is defined as

$$\langle F(a_i) \rangle_{SU(N)} = \frac{1}{\mathcal{N}_{SU(N)}} \int d^N a \, \delta \left(\sum_i a_i \right) \left(\prod_{i<j} a_{ij}^2 \right) e^{-\frac{8\pi^2}{g_{YM}^2} \sum_i a_i^2} F(a_i) \,, \qquad (A.1.2)$$

---

[*]The non-perturbative instanton contributions to the partition function, the Nekrasov partition function [209, 210], with general gauge groups can be found in [211–213], and their contributions to the first integrated correlator were studied in [132].

where $\mathcal{N}_{SU(N)}$ is a normalisation factor such that $\langle 1 \rangle_{SU(N)} = 1$. The function $H(m)$ is defined as

$$H(m) = e^{-(1+\gamma)m^2} \, G(1+im) \, G(1-im) \,, \qquad (A.1.3)$$

where $G(m)$ is a Barnes G-function (and γ is the Euler constant).

- For $SO(2N)$, we have

$$\hat{Z}^{pert}_{SO(2N)}(m,a) = \frac{1}{H(m)^N} \prod_{i<j} \frac{H^2(a_{ij})H^2(a_{ij}^+)}{H(a_{ij}-m)H(a_{ij}+m)H(a_{ij}^+-m)H(a_{ij}^++m)} \,,$$
$$(A.1.4)$$

where $a_{ij}^+ = a_i + a_j$, and the expectation value is defined as

$$\langle F(a_i) \rangle_{SO(2N)} = \frac{1}{\mathcal{N}_{SO(2N)}} \int d^N a \left(\prod_{i<j} a_{ij}^2 (a_{ij}^+)^2 \right) e^{-\frac{8\pi^2}{g_{YM}^2} \sum_i a_i^2} F(a_i) \,. \quad (A.1.5)$$

- For $SO(2N+1)$, we have

$$\hat{Z}^{pert}_{SO(2N+1)}(m,a) = \frac{1}{H(m)^N} \prod_i \frac{H^2(a_i)}{H(a_i+m)H(a_i-m)}$$
$$\times \prod_{i<j} \frac{H^2(a_{ij})H^2(a_{ij}^+)}{H(a_{ij}-m)H(a_{ij}+m)H(a_{ij}^+-m)H(a_{ij}^++m)} \,, \quad (A.1.6)$$

and the expectation value is defined as

$$\langle F(a_i) \rangle_{SO(2N+1)} = \frac{1}{\mathcal{N}_{SO(2N+1)}} \int d^N a \left(\prod_i a_i^2 \right) \left(\prod_{i<j} a_{ij}^2 (a_{ij}^+)^2 \right) e^{-\frac{8\pi^2}{g_{YM}^2} \sum_i a_i^2} F(a_i) \,.$$
$$(A.1.7)$$

When $N=1$ (i.e. for the correlator of $SO(3)$), one needs to rescale $g_{YM}^2 \to 2 \, g_{YM}^2$ in the above formula, as discussed in [148].

- For $USp(2N)$, we have

$$\hat{Z}^{pert}_{USp(2N)}(m,a) = \frac{1}{H(m)^N} \prod_i \frac{H^2(2a_i)}{H(2a_i+m)H(2a_i-m)}$$
$$\times \prod_{i<j} \frac{H^2(a_{ij})H^2(a_{ij}^+)}{H(a_{ij}-m)H(a_{ij}+m)H(a_{ij}^+-m)H(a_{ij}^++m)} \,, \quad (A.1.8)$$

and the expectation value is defined below

$$\langle F(a_i)\rangle_{USp(2N)} = \frac{1}{\mathcal{N}_{USp(2N)}} \int d^N a \left(\prod_i a_i^2\right) \left(\prod_{i<j} a_{ij}^2 (a_{ij}^+)^2\right) e^{-\frac{16\pi^2}{g_{YM}^2}\sum_i a_i^2} F(a_i)\,.$$

$$(A.1.9)$$

A.2 Periods for the second integrated correlator at three loops

We list the relevant f-graphs and their periods for the three loop computations. The functions associated with $\widetilde{f}^{(3,k)}$'s in (7.4.40) are given by

$$T^{(5,6,7)}_{(1,2;3,4)} = \frac{x_{34}^2 x_{17}^2}{(x_{15}^2 x_{35}^2)(x_{16}^2 x_{46}^2)(x_{27}^2 x_{37}^2 x_{47}^2)(x_{56}^2 x_{57}^2 x_{67}^2)}\,,$$

$$E^{(5,6,7)}_{(1,2;3,4)} = \frac{x_{23}^2 x_{24}^2 x_{16}^2}{(x_{15}^2 x_{25}^2 x_{35}^2)x_{56}^2(x_{26}^2 x_{36}^2 x_{46}^2)x_{67}^2(x_{17}^2 x_{27}^2 x_{47}^2)}\,,$$

$$L^{(5,6,7)}_{(1,2;3,4)} = \frac{x_{34}^4}{(x_{15}^2 x_{35}^2 x_{45}^2)x_{56}^2(x_{36}^2 x_{46}^2)x_{67}^2(x_{27}^2 x_{37}^2 x_{47}^2)}\,,$$

$$(g\times h)^{(5,6,7)}_{(1,2;3,4)} = \frac{x_{12}^2 x_{34}^4}{(x_{15}^2 x_{25}^2 x_{35}^2 x_{45}^2)(x_{16}^2 x_{36}^2 x_{46}^2)(x_{27}^2 x_{37}^2 x_{47}^2)x_{67}^2}\,,$$

$$H^{(5,6,7)}_{(1,2;3,4)} = \frac{x_{14}^2 x_{23}^2 x_{34}^2 x_{57}^2}{(x_{15}^2 x_{25}^2 x_{35}^2 x_{45}^2)x_{56}^2(x_{36}^2 x_{46}^2)x_{67}^2(x_{17}^2 x_{27}^2 x_{37}^2 x_{47}^2)}\,.$$

$$(A.2.1)$$

The periods of $\widetilde{f}^{(3,k)}$'s are given by

$$\sum_{k=1}^5 \mathcal{P}_{\widetilde{f}^{(3,k)}} = 2160\times\left[20\zeta(3)\zeta(5) + 49\zeta(9)\right]\,,$$

$$(A.2.2)$$

where each term in the sum above is given by

$$\mathcal{P}_{\widetilde{f}^{(3,1)}} = 72\times\left(16\zeta(3)^3 + \frac{5402}{9}\zeta(9)\right)\,,$$

$$\mathcal{P}_{\widetilde{f}^{(3,2)}} = 72\times\left(-48\zeta(3)^3 + 240\zeta(5)\zeta(3) + \frac{1231\zeta(9)}{3}\right)\,,$$

$$\mathcal{P}_{\widetilde{f}^{(3,3)}} = 36\times\left(16\zeta(3)^3 + \frac{5402}{9}\zeta(9)\right)\,,$$

$$\mathcal{P}_{\widetilde{f}^{(3,4)}} = 36\times\left(48\zeta(3)^3 - 144\zeta(3)^2 + 432\zeta(5)\zeta(3) + 378\zeta(7) - \frac{388\zeta(9)}{3}\right)\,,$$

$$\mathcal{P}_{\widetilde{f}^{(3,5)}} = 36\times\left(144\zeta(3)^2 + 288\zeta(5)\zeta(3) - 378\zeta(7) + 448\zeta(9)\right)\,.$$

$$(A.2.3)$$

The factor 72 and 36 above are numbers of terms inside the $\mathcal{S}_4 \times \mathcal{S}_3$ permutations, and they have the same period value. We note that $\zeta(3)^3$ terms cancel out in the sum

(A.2.2), and each $\mathcal{P}_{\widetilde{f}^{(3,k)}}$ in (A.2.3) consists of three periods $\mathcal{P}_{\widetilde{f}_{\blacksquare}^{(3,k)}}$'s with $\blacksquare = 1, U, V$, therefore

$$\mathcal{P}_{\widetilde{f}^{(3,k)}} = \sum_{\blacksquare = 1, U, V} \mathcal{P}_{\widetilde{f}_{\blacksquare}^{(3,k)}}, \tag{A.2.4}$$

and each $\mathcal{P}_{\widetilde{f}_{\blacksquare}^{(3,k)}}$ is listed below

$$\mathcal{P}_{\widetilde{f}_1^{(3,1)}} = 72 \times \left(\frac{1567}{9} \zeta(9) + 8\zeta(3)^3 \right)$$

$$\mathcal{P}_{\widetilde{f}_U^{(3,1)}} = 72 \times (252\zeta(9))$$

$$\mathcal{P}_{\widetilde{f}_V^{(3,1)}} = 72 \times \left(\frac{1567}{9} \zeta(9) + 8\zeta(3)^3 \right), \tag{A.2.5}$$

and

$$\mathcal{P}_{\widetilde{f}_1^{(3,2)}} = 72 \times \left(120\zeta(3)\zeta(5) + \frac{727}{6}\zeta(9) - 24\zeta(3)^3 \right)$$

$$\mathcal{P}_{\widetilde{f}_U^{(3,2)}} = 72 \times (168\zeta(9))$$

$$\mathcal{P}_{\widetilde{f}_V^{(3,2)}} = 72 \times \left(120\zeta(3)\zeta(5) + \frac{727}{6}\zeta(9) - 24\zeta(3)^3 \right), \tag{A.2.6}$$

and

$$\mathcal{P}_{\widetilde{f}_1^{(3,3)}} = 36 \times \left(\frac{1567}{9} \zeta(9) + 8\zeta(3)^3 \right)$$

$$\mathcal{P}_{\widetilde{f}_U^{(3,3)}} = 36 \times (252\zeta(9))$$

$$\mathcal{P}_{\widetilde{f}_V^{(3,3)}} = 36 \times \left(\frac{1567}{9} \zeta(9) + 8\zeta(3)^3 \right), \tag{A.2.7}$$

and

$$\mathcal{P}_{\widetilde{f}_1^{(3,4)}} = 36 \times \left(-36\zeta(3)^2 + \frac{189}{2} \zeta(7) + 108\zeta(3)\zeta(5) \right)$$

$$\mathcal{P}_{\widetilde{f}_U^{(3,4)}} = 36 \times \left(-72\zeta(3)^2 + 189\zeta(7) + 216\zeta(3)\,\zeta(5) + 48\zeta(3)^3 - \frac{388}{3}\zeta(9) \right)$$

$$\mathcal{P}_{\widetilde{f}_V^{(3,4)}} = 36 \times \left(-36\zeta(3)^2 + \frac{189}{2} \zeta(7) + 108\zeta(3)\zeta(5) \right), \tag{A.2.8}$$

and

$$\mathcal{P}_{\widetilde{f}_1^{(3,5)}} = 36 \times \left(120\zeta(3)\zeta(5) \right)$$

$$\mathcal{P}_{\widetilde{f}_U^{(3,5)}} = 36 \times \left(24\zeta(3)\zeta(5) + \frac{2126}{9}\zeta(9) + 72\zeta(3)^2 - 189\zeta(7) + 16\zeta(3)^3 \right)$$

$$\mathcal{P}_{\widetilde{f}_V^{(3,5)}} = 36 \times \left(144\zeta(3)\zeta(5) + \frac{1906}{9}\zeta(9) + 72\zeta(3)^2 - 189\zeta(7) - 16\zeta(3)^3 \right). \quad \text{(A.2.9)}$$

Using these results and (A.2.4), one finds the expressions given in (A.2.3).

Appendix B

Linear and quadratic propagators

B.1 Linear and quadratic propagators

In this appendix, we review the equivalence of the linear-propagator and quadratic-propagator of the m-gon integral following mostly [214]. The main idea is that we shift the loop momentum in the quadratic m-gon as the following

$$\tilde{\ell} \to \tilde{\ell} + \beta \,, \tag{B.1.1}$$

where β is in extra dimension other than $\tilde{\ell}$; that is, $\tilde{\ell} \cdot \beta = 0$ and $k_i \cdot \beta = 0$ for an external momentum k_i. So the propagator is deformed as

$$\tilde{\ell}^2 \to (\tilde{\ell} + \beta)^2 = \tilde{\ell}^2 + \beta^2 = \tilde{\ell}^2 + z \,, \tag{B.1.2}$$

where we define $z := \beta^2$. With such shift, we can write a loop integral as a Cauchy integral surrounding the $z = 0$ pole in the same spirit of BCFW recursion relation [7]

$$\mathcal{I}(\tilde{\ell}) = \oint_{z=0} \frac{dz}{z} \, \mathcal{I}(\hat{\ell}) \,, \tag{B.1.3}$$

where $\mathcal{I}(\tilde{\ell})$ is the one-loop integrand in quadratic form, and shifted loop momentum $\hat{\ell}$ is defined as $\hat{\ell} = \tilde{\ell} + \beta$. We then apply Cauchy's theorem to deform the contour and pick up (minus) the residues except for that at the pole of $z = 0$,

$$\oint_{z=0} \frac{dz}{z} \, \mathcal{I}(\hat{\ell}) = (-1) \sum \text{Res} \Big[\frac{\mathcal{I}(\hat{\ell})}{z} \Big] \,, \tag{B.1.4}$$

Each of the residues contains the following factor

$$\frac{1}{(\tilde{\ell} + K_0)^2} \,, \tag{B.1.5}$$

with K_0 being some 4D momentum. Since we need to perform loop integration $\int \frac{d^D \tilde{\ell}}{(2\pi)^D}$ at the end using dimensional regularisation, we are free to shift the loop momentum to obtain another integral which is equivalent to the original one upon loop integration. So we can do the following change of variable

$$\tilde{\ell} \to \tilde{\ell} - K_0 \,, \tag{B.1.6}$$

which sets $\frac{1}{(\tilde{\ell}+K_0)^2} \to \frac{1}{\tilde{\ell}^2}$. Recall $\tilde{\ell} = \ell + \mu$, where ℓ is the 4D loop momentum, therefore the above shift only affects ℓ but not μ. The result is an expression that only $\frac{1}{\tilde{\ell}^2}$ is quadratic, while the other propagators are linearised.

Let us use the bubble diagram as an explicit example to illustrate the above procedure, in the quadratic form it is given by

$$\tilde{I}_{\text{bubble}}(k_1, k_2) = \int \frac{d^D \tilde{\ell}}{(2\pi)^D} \left[\frac{\mu^m}{\tilde{\ell}^2 \, (\tilde{\ell} + k_1 + k_2)^2} \right]. \tag{B.1.7}$$

Using the shift (B.1.2) and dividing by z, the above bubble integral can be expressed as an contour integral surrounding $z = 0$ pole

$$\tilde{I}_{\text{bubble}}(k_1, k_2) = \int \frac{d^D \tilde{\ell}}{(2\pi)^D} \oint_{z=0} dz \left[\frac{\mu^m}{z \, (\tilde{\ell}^2 + z) \, (\tilde{\ell}^2 + z + 2\tilde{\ell} \cdot k_{1,2} + k_{1,2}^2)} \right], \tag{B.1.8}$$

where $k_{i,j} = k_i + k_j$. Applying Cauchy's theorem, we find that two residues contribute as

$$\int \frac{d^D \tilde{\ell}}{(2\pi)^D} \left[\frac{\mu^m}{\tilde{\ell}^2(2\tilde{\ell} \cdot k_{1,2} + k_{1,2}^2)} + \frac{\mu^m}{(\tilde{\ell} + k_{12})^2(-2\tilde{\ell} \cdot k_{1,2} - k_{1,2}^2)} \right]. \tag{B.1.9}$$

The shift of the loop momentum in the second term results into the linear-propagator representation of the bubble integral

$$\tilde{I}_{\text{bubble}}(k_1, k_2) \simeq \int \frac{d^D \tilde{\ell}}{(2\pi)^D} \left[\frac{\mu^m}{\tilde{\ell}^2(2\tilde{\ell} \cdot k_{1,2} + k_{1,2}^2)} + \frac{\mu^m}{\tilde{\ell}^2(-2\tilde{\ell} \cdot k_{1,2} + k_{1,2}^2)} \right], \tag{B.1.10}$$

where $\simeq$ denotes equivalence upon integration.

The linearised triangle can be obtained by similar manners, we first write the quadratic one as an Cauchy integral

$$\oint_{z=0} dz \int \frac{d^D \tilde{\ell}}{(2\pi)^D} \left[\frac{\mu^m}{z \, (\tilde{\ell}^2 + z)(\tilde{\ell}^2 + z + 2\tilde{\ell} \cdot k_{1,2} + k_{1,2}^2) \, (\tilde{\ell}^2 + z - 2\tilde{\ell} \cdot k_{5,6} + k_{5,6}^2)} \right] \tag{B.1.11}$$

We again apply the Cauchy theorem and shift loop momentum to obtain the following

expression

$$\int \frac{d^D\tilde{\ell}}{(2\pi)^D} \Bigg[\frac{\mu^m}{\tilde{\ell}^2 \left(2\tilde{\ell} \cdot k_{1,2} + k_{1,2}^2\right) \left(-2\tilde{\ell} \cdot k_{5,6} + k_{5,6}^2\right)}$$
$$+ \frac{\mu^m}{\tilde{\ell}^2 \left(2\tilde{\ell} \cdot k_{3,4} + k_{3,4}^2\right) \left(-2\tilde{\ell} \cdot k_{1,2} + k_{1,2}^2\right)} \tag{B.1.12}$$
$$+ \frac{\mu^m}{\tilde{\ell}^2 \left(2\tilde{\ell} \cdot k_{5,6} + k_{5,6}^2\right) \left(-2\tilde{\ell} \cdot k_{3,4} + k_{3,4}^2\right)} \Bigg] .$$

Similar computation applies to the integrals with non-trivial numerators such as those given in (4.5.7) and (4.5.10). In particular, one can show that (4.5.7) is equivalent to

$$\tilde{\mathcal{A}}_{\mathrm{NSD},\,4}^{(1)} = \int \frac{d^D\tilde{\ell}}{(2\pi)^D} \frac{\mu^2\,[12]^2\,\langle 4|\tilde{\ell}|3]^2}{\tilde{\ell}^2(\tilde{\ell} + k_1 + k_2)^2} + \mathrm{Perm}\,, \tag{B.1.13}$$

and under the loop integration, (4.5.10) is equivalent to

$$\tilde{\mathcal{I}}_{\mathrm{NSD},6}^{\mathrm{triangle}} = \frac{(\mu^2)^2[12]^2[34]^2\langle 6|\tilde{\ell}|5]^2}{\tilde{\ell}^2\,(\tilde{\ell} + k_1 + k_2)^2\,(\tilde{\ell} - k_5 - k_6)^2} + \mathrm{Perm}\,. \tag{B.1.14}$$

Bibliography

[1] M. Heydeman, J. H. Schwarz, C. Wen and S.-Q. Zhang, *All Tree Amplitudes of 6D* $(2, 0)$ *Supergravity: Interacting Tensor Multiplets and the K3 Moduli Space*, *Phys. Rev. Lett.* **122** (2019) 111604 [`1812.06111`].

[2] C. Wen and S.-Q. Zhang, *D3-Brane Loop Amplitudes from M5-Brane Tree Amplitudes*, *JHEP* **07** (2020) 098 [`2004.02735`].

[3] Y.-t. Huang, R. Kojima, C. Wen and S.-Q. Zhang, *The orthogonal momentum amplituhedron and ABJM amplitudes*, *JHEP* **01** (2022) 141 [`2111.03037`].

[4] C. Wen and S.-Q. Zhang, *Integrated correlators in* $\mathcal{N} = 4$ *super Yang-Mills and periods*, *JHEP* **05** (2022) 126 [`2203.01890`].

[5] C. Wen and S.-Q. Zhang, *Notes on gravity multiplet correlators in* $AdS_3 \times S^3$, *JHEP* **07** (2021) 125 [`2106.03499`].

[6] S. J. Parke and T. R. Taylor, *An Amplitude for n Gluon Scattering*, *Phys. Rev. Lett.* **56** (1986) 2459.

[7] R. Britto, F. Cachazo, B. Feng and E. Witten, *Direct proof of tree-level recursion relation in Yang-Mills theory*, *Phys. Rev. Lett.* **94** (2005) 181602 [`hep-th/0501052`].

[8] E. Witten, *Perturbative gauge theory as a string theory in twistor space*, *Commun. Math. Phys.* **252** (2004) 189 [`hep-th/0312171`].

[9] M. Heydeman, J. H. Schwarz and C. Wen, *M5-Brane and D-Brane Scattering Amplitudes*, *JHEP* **12** (2017) 003 [`1710.02170`].

[10] F. Cachazo, A. Guevara, M. Heydeman, S. Mizera, J. H. Schwarz and C. Wen, *The S Matrix of 6D Super Yang-Mills and Maximal Supergravity from Rational Maps*, *JHEP* **09** (2018) 125 [`1805.11111`].

[11] Y. Geyer and L. Mason, *Polarized Scattering Equations for 6D Superamplitudes*, *Phys. Rev. Lett.* **122** (2019) 101601 [`1812.05548`].

[12] Y. Geyer and L. Mason, *Supersymmetric S-matrices from the worldsheet in 10 \& 11d*, *Phys. Lett. B* **804** (2020) 135361 [1901.00134].

[13] S. He and E. Y. Yuan, *One-loop Scattering Equations and Amplitudes from Forward Limit*, *Phys. Rev. D* **92** (2015) 105004 [1508.06027].

[14] F. Cachazo, S. He and E. Y. Yuan, *One-Loop Corrections from Higher Dimensional Tree Amplitudes*, *JHEP* **08** (2016) 008 [1512.05001].

[15] Y. Geyer, L. Mason, R. Monteiro and P. Tourkine, *Loop Integrands for Scattering Amplitudes from the Riemann Sphere*, *Phys. Rev. Lett.* **115** (2015) 121603 [1507.00321].

[16] Y. Geyer, L. Mason, R. Monteiro and P. Tourkine, *One-loop amplitudes on the Riemann sphere*, *JHEP* **03** (2016) 114 [1511.06315].

[17] Y. Geyer, L. Mason, R. Monteiro and P. Tourkine, *Two-Loop Scattering Amplitudes from the Riemann Sphere*, *Phys. Rev. D* **94** (2016) 125029 [1607.08887].

[18] Y. Geyer and R. Monteiro, *Two-Loop Scattering Amplitudes from Ambitwistor Strings: from Genus Two to the Nodal Riemann Sphere*, *JHEP* **11** (2018) 008 [1805.05344].

[19] Y. Geyer, R. Monteiro and R. Stark-Muchão, *Two-Loop Scattering Amplitudes: Double-Forward Limit and Colour-Kinematics Duality*, *JHEP* **12** (2019) 049 [1908.05221].

[20] J. M. Maldacena, *The Large N limit of superconformal field theories and supergravity*, *Int. J. Theor. Phys.* **38** (1999) 1113 [hep-th/9711200].

[21] L. Rastelli and X. Zhou, *Mellin amplitudes for $AdS_5 \times S^5$*, *Phys. Rev. Lett.* **118** (2017) 091602 [1608.06624].

[22] J. Penedones, *Writing CFT correlation functions as AdS scattering amplitudes*, *JHEP* **03** (2011) 025 [1011.1485].

[23] S. Caron-Huot and A.-K. Trinh, *All tree-level correlators in $AdS_5 \times S^5$ supergravity: hidden ten-dimensional conformal symmetry*, *JHEP* **01** (2019) 196 [1809.09173].

[24] L. Rastelli, K. Roumpedakis and X. Zhou, **$AdS_3 \times S^3$** *Tree-Level Correlators: Hidden Six-Dimensional Conformal Symmetry*, *JHEP* **10** (2019) 140 [1905.11983].

[25] S. Giusto, R. Russo, A. Tyukov and C. Wen, *The CFT_6 origin of all tree-level 4-point correlators in $AdS_3 \times S^3$*, 2005.08560.

[26] N. Arkani-Hamed, J. L. Bourjaily, F. Cachazo, A. B. Goncharov, A. Postnikov and J. Trnka, *Grassmannian Geometry of Scattering Amplitudes*. Cambridge University Press, 4, 2016, 10.1017/CBO9781316091548, [1212.5605].

[27] N. Arkani-Hamed and J. Trnka, *The Amplituhedron*, *JHEP* **10** (2014) 030 [1312.2007].

[28] S. Lee, *Yangian Invariant Scattering Amplitudes in Supersymmetric Chern-Simons Theory*, *Phys. Rev. Lett.* **105** (2010) 151603 [1007.4772].

[29] Y.-t. Huang and S. Lee, *A new integral formula for supersymmetric scattering amplitudes in three dimensions*, *Phys. Rev. Lett.* **109** (2012) 191601 [1207.4851].

[30] Y.-T. Huang and C. Wen, *ABJM amplitudes and the positive orthogonal grassmannian*, *JHEP* **02** (2014) 104 [1309.3252].

[31] S. He, C.-K. Kuo and Y.-Q. Zhang, *The momentum amplituhedron of SYM and ABJM from twistor-string maps*, *JHEP* **02** (2022) 148 [2111.02576].

[32] J. H. Schwarz and C. Wen, *Unified Formalism for 6D Superamplitudes Based on a Symplectic Grassmannian*, *JHEP* **08** (2019) 125 [1907.03485].

[33] N. Arkani-Hamed, Y. Bai, S. He and G. Yan, *Scattering Forms and the Positive Geometry of Kinematics, Color and the Worldsheet*, *JHEP* **05** (2018) 096 [1711.09102].

[34] N. Arkani-Hamed, T.-C. Huang and Y.-T. Huang, *The EFT-Hedron*, *JHEP* **05** (2021) 259 [2012.15849].

[35] B. Eden, P. Heslop and L. Mason, *The Correlahedron*, *JHEP* **09** (2017) 156 [1701.00453].

[36] G. Dian and P. Heslop, *Amplituhedron-like geometries*, *JHEP* **11** (2021) 074 [2106.09372].

[37] D. J. Binder, S. M. Chester, S. S. Pufu and Y. Wang, *$\mathcal{N} = 4$ Super-Yang-Mills correlators at strong coupling from string theory and localization*, *JHEP* **12** (2019) 119 [1902.06263].

[38] S. M. Chester, *Genus-2 holographic correlator on $AdS_5 \times S^5$ from localization*, *JHEP* **04** (2020) 193 [1908.05247].

[39] S. M. Chester and S. S. Pufu, *Far beyond the planar limit in strongly-coupled $\mathcal{N}$ = 4 SYM*, *JHEP* **01** (2021) 103 [2003.08412].

[40] O. Schnetz, *Numbers and Functions in Quantum Field Theory*, *Phys. Rev. D* **97** (2018) 085018 [1606.08598].

[41] H. Elvang and Y.-t. Huang, *Scattering Amplitudes in Gauge Theory and Gravity*. Cambridge University Press, 4, 2015.

[42] J. M. Henn and J. C. Plefka, *Scattering Amplitudes in Gauge Theories*, vol. 883. Springer, Berlin, 2014, 10.1007/978-3-642-54022-6.

[43] A. Brandhuber, J. Plefka and G. Travaglini, *The SAGEX Review on Scattering Amplitudes, Chapter 1: Modern Fundamentals of Amplitudes*, 2203.13012.

[44] Y. Geyer and L. Mason, *The SAGEX Review on Scattering Amplitudes, Chapter 6: Ambitwistor Strings and Amplitudes from the Worldsheet*, 2203.13017.

[45] P. Heslop, *The SAGEX Review on Scattering Amplitudes, Chapter 8: Half BPS correlators*, 2203.13019.

[46] D. Dorigoni, M. B. Green and C. Wen, *The SAGEX Review on Scattering Amplitudes, Chapter 10: Modular covariance of type IIB string amplitudes and their $\mathcal{N} = 4$ supersymmetric Yang-Mills duals*, 2203.13021.

[47] T. McLoughlin, A. Puhm and A.-M. Raclariu, *The SAGEX Review on Scattering Amplitudes, Chapter 11: Soft Theorems and Celestial Amplitudes*, 2203.13022.

[48] E. Panzer, *Feynman integrals and hyperlogarithms*, Ph.D. thesis, Humboldt U., 2015. 1506.07243. 10.18452/17157.

[49] O. Schnetz. HYPERLOGPROCEDURES, https://www.math.fau.de/person/oliver-schnetz/.

[50] C. Cheung and D. O'Connell, *Amplitudes and Spinor-Helicity in Six Dimensions*, *JHEP* **07** (2009) 075 [0902.0981].

[51] O. Aharony, O. Bergman, D. L. Jafferis and J. Maldacena, *N=6 superconformal Chern-Simons-matter theories, M2-branes and their gravity duals*, *JHEP* **10** (2008) 091 [0806.1218].

[52] Y.-t. Huang, C. Wen and D. Xie, *The Positive orthogonal Grassmannian and loop amplitudes of ABJM*, *J. Phys. A* **47** (2014) 474008 [1402.1479].

[53] N. Arkani-Hamed and J. Trnka, *Into the Amplituhedron*, *JHEP* **12** (2014) 182 [`1312.7878`].

[54] D. Damgaard, L. Ferro, T. Lukowski and M. Parisi, *The Momentum Amplituhedron*, *JHEP* **08** (2019) 042 [`1905.04216`].

[55] F. Cachazo, S. He and E. Y. Yuan, *Scattering of Massless Particles in Arbitrary Dimensions*, *Phys. Rev. Lett.* **113** (2014) 171601 [`1307.2199`].

[56] R. Roiban, M. Spradlin and A. Volovich, *On the tree level S matrix of Yang-Mills theory*, *Phys. Rev. D* **70** (2004) 026009 [`hep-th/0403190`].

[57] F. Cachazo, S. He and E. Y. Yuan, *Scattering Equations and Matrices: From Einstein To Yang-Mills, DBI and NLSM*, *JHEP* **07** (2015) 149 [`1412.3479`].

[58] H. Elvang, M. Hadjiantonis, C. R. T. Jones and S. Paranjape, *All-Multiplicity One-Loop Amplitudes in Born-Infeld Electrodynamics from Generalized Unitarity*, *JHEP* **03** (2020) 009 [`1906.05321`].

[59] S. L. Adler, *Consistency conditions on the strong interactions implied by a partially conserved axial vector current*, *Phys. Rev.* **137** (1965) B1022.

[60] N. Arkani-Hamed, F. Cachazo and J. Kaplan, *What is the Simplest Quantum Field Theory?*, *JHEP* **09** (2010) 016 [`0808.1446`].

[61] P. S. Aspinwall, *K3 surfaces and string duality*, in *Theoretical Advanced Study Institute in Elementary Particle Physics (TASI 96): Fields, Strings, and Duality*, pp. 421–540, 11, 1996, `hep-th/9611137`.

[62] W.-M. Chen, Y.-t. Huang and C. Wen, *From U(1) to E8: soft theorems in supergravity amplitudes*, *JHEP* **03** (2015) 150 [`1412.1811`].

[63] F. Cachazo, S. He and E. Y. Yuan, *Scattering in Three Dimensions from Rational Maps*, *JHEP* **10** (2013) 141 [`1306.2962`].

[64] E. Witten, *Some comments on string dynamics*, in *STRINGS 95: Future Perspectives in String Theory*, pp. 501–523, 7, 1995, `hep-th/9507121`.

[65] W.-M. Chen, Y.-t. Huang and D. A. McGady, *Anomalies without an action*, `1402.7062`.

[66] H. Elvang, Y.-t. Huang and C. Peng, *On-shell superamplitudes in N<4 SYM*, *JHEP* **09** (2011) 031 [`1102.4843`].

[67] Y.-H. Lin, S.-H. Shao, Y. Wang and X. Yin, *Supersymmetry Constraints and String Theory on K3*, *JHEP* **12** (2015) 142 [`1508.07305`].

[68] A. Volovich, C. Wen and M. Zlotnikov, *Double Soft Theorems in Gauge and String Theories*, *JHEP* **07** (2015) 095 [`1504.05559`].

[69] Y.-t. Huang, *Non-Chiral S-Matrix of N=4 Super Yang-Mills*, `1104.2021`.

[70] S. Mizera and G. Zhang, *A String Deformation of the Parke-Taylor Factor*, *Phys. Rev. D* **96** (2017) 066016 [`1705.10323`].

[71] M. Aganagic, C. Popescu and J. H. Schwarz, *Gauge invariant and gauge fixed D-brane actions*, *Nucl. Phys. B* **495** (1997) 99 [`hep-th/9612080`].

[72] M. Cederwall, A. von Gussich, B. E. W. Nilsson and A. Westerberg, *The Dirichlet super three-brane in ten-dimensional type IIB supergravity*, *Nucl. Phys. B* **490** (1997) 163 [`hep-th/9610148`].

[73] M. Aganagic, C. Popescu and J. H. Schwarz, *D-brane actions with local kappa symmetry*, *Phys. Lett. B* **393** (1997) 311 [`hep-th/9610249`].

[74] M. Cederwall, A. von Gussich, B. E. W. Nilsson, P. Sundell and A. Westerberg, *The Dirichlet super p-branes in ten-dimensional type IIA and IIB supergravity*, *Nucl. Phys. B* **490** (1997) 179 [`hep-th/9611159`].

[75] E. Bergshoeff and P. K. Townsend, *Super D-branes*, *Nucl. Phys. B* **490** (1997) 145 [`hep-th/9611173`].

[76] E. Bergshoeff, F. Coomans, R. Kallosh, C. S. Shahbazi and A. Van Proeyen, *Dirac-Born-Infeld-Volkov-Akulov and Deformation of Supersymmetry*, *JHEP* **08** (2013) 100 [`1303.5662`].

[77] G. Albonico, Y. Geyer and L. Mason, *Recursion and worldsheet formulae for 6d superamplitudes*, *JHEP* **08** (2020) 066 [`2001.05928`].

[78] J. H. Schwarz, *M5-Brane Amplitudes*, `2001.03793`.

[79] A. A. Rosly and K. G. Selivanov, *Helicity conservation in Born-Infeld theory*, in *Workshop on String Theory and Complex Geometry*, 4, 2002, `hep-th/0204229`.

[80] C. Cheung, K. Kampf, J. Novotny and J. Trnka, *Effective Field Theories from Soft Limits of Scattering Amplitudes*, *Phys. Rev. Lett.* **114** (2015) 221602 [`1412.4095`].

[81] C. Cheung, K. Kampf, J. Novotny, C.-H. Shen and J. Trnka, *On-Shell Recursion Relations for Effective Field Theories*, *Phys. Rev. Lett.* **116** (2016) 041601 [`1509.03309`].

[82] H. Luo and C. Wen, *Recursion relations from soft theorems*, *JHEP* **03** (2016) 088 [`1512.06801`].

[83] C. Cheung, K. Kampf, J. Novotny, C.-H. Shen and J. Trnka, *A Periodic Table of Effective Field Theories*, *JHEP* **02** (2017) 020 [`1611.03137`].

[84] C. Cheung, K. Kampf, J. Novotny, C.-H. Shen, J. Trnka and C. Wen, *Vector Effective Field Theories from Soft Limits*, *Phys. Rev. Lett.* **120** (2018) 261602 [`1801.01496`].

[85] L. Rodina, *Scattering Amplitudes from Soft Theorems and Infrared Behavior*, *Phys. Rev. Lett.* **122** (2019) 071601 [`1807.09738`].

[86] C. Cheung, C.-H. Shen and C. Wen, *Unifying Relations for Scattering Amplitudes*, *JHEP* **02** (2018) 095 [`1705.03025`].

[87] S. He, Z. Liu and J.-B. Wu, *Scattering Equations, Twistor-string Formulas and Double-soft Limits in Four Dimensions*, *JHEP* **07** (2016) 060 [`1604.02834`].

[88] F. Cachazo, S. He and E. Y. Yuan, *Scattering of Massless Particles: Scalars, Gluons and Gravitons*, *JHEP* **07** (2014) 033 [`1309.0885`].

[89] L. Mason and D. Skinner, *Ambitwistor strings and the scattering equations*, *JHEP* **07** (2014) 048 [`1311.2564`].

[90] T. Adamo, E. Casali and D. Skinner, *Ambitwistor strings and the scattering equations at one loop*, *JHEP* **04** (2014) 104 [`1312.3828`].

[91] S. Caron-Huot, *Loops and trees*, *JHEP* **05** (2011) 080 [`1007.3224`].

[92] L. J. Dixon, *Calculating scattering amplitudes efficiently*, in *Theoretical Advanced Study Institute in Elementary Particle Physics (TASI 95): QCD and Beyond*, pp. 539–584, 1, 1996, `hep-ph/9601359`.

[93] H. Elvang and Y.-t. Huang, *Scattering Amplitudes*, `1308.1697`.

[94] R. Karpman and Y. Su, *Combinatorics of symmetric plabic graphs*, `1510.02122`.

[95] R. Karpman, *Total positivity for the lagrangian grassmannian*, 2015. 10.48550/ARXIV.1510.04386.

[96] W.-M. Chen, Y.-t. Huang and C. Wen, *Exact coefficients for higher dimensional operators with sixteen supersymmetries*, *JHEP* **09** (2015) 098 [`1505.07093`].

[97] C. Baadsgaard, N. E. J. Bjerrum-Bohr, J. L. Bourjaily, S. Caron-Huot, P. H. Damgaard and B. Feng, *New Representations of the Perturbative S-Matrix*, *Phys. Rev. Lett.* **116** (2016) 061601 [`1509.02169`].

[98] H. Gomez, *Quadratic Feynman Loop Integrands From Massless Scattering Equations*, *Phys. Rev. D* **95** (2017) 106006 [`1703.04714`].

[99] H. Gomez, C. Lopez-Arcos and P. Talavera, *One-loop Parke-Taylor factors for quadratic propagators from massless scattering equations*, *JHEP* **10** (2017) 175 [`1707.08584`].

[100] N. Ahmadiniaz, H. Gomez and C. Lopez-Arcos, *Non-planar one-loop Parke-Taylor factors in the CHY approach for quadratic propagators*, *JHEP* **05** (2018) 055 [`1802.00015`].

[101] J. Agerskov, N. E. J. Bjerrum-Bohr, H. Gomez and C. Lopez-Arcos, *One-Loop Yang-Mills Integrands from Scattering Equations*, *Phys. Rev. D* **102** (2020) 045023 [`1910.03602`].

[102] L. Brink, J. H. Schwarz and J. Scherk, *Supersymmetric Yang-Mills Theories*, *Nucl. Phys. B* **121** (1977) 77.

[103] Z. Bern, J. J. M. Carrasco, L. J. Dixon, H. Johansson and R. Roiban, *The Complete Four-Loop Four-Point Amplitude in N=4 Super-Yang-Mills Theory*, *Phys. Rev. D* **82** (2010) 125040 [`1008.3327`].

[104] M. B. Green, J. H. Schwarz and L. Brink, *N=4 Yang-Mills and N=8 Supergravity as Limits of String Theories*, *Nucl. Phys. B* **198** (1982) 474.

[105] Z. Bern, J. S. Rozowsky and B. Yan, *Two loop four gluon amplitudes in N=4 superYang-Mills*, *Phys. Lett. B* **401** (1997) 273 [`hep-ph/9702424`].

[106] Z. Bern, L. J. Dixon, D. C. Dunbar, M. Perelstein and J. S. Rozowsky, *On the relationship between Yang-Mills theory and gravity and its implication for ultraviolet divergences*, *Nucl. Phys. B* **530** (1998) 401 [`hep-th/9802162`].

[107] M. Shmakova, *One loop corrections to the D3-brane action*, *Phys. Rev. D* **62** (2000) 104009 [`hep-th/9906239`].

[108] Z. Bern, L. J. Dixon, D. C. Dunbar and D. A. Kosower, *One loop n point gauge theory amplitudes, unitarity and collinear limits*, *Nucl. Phys. B* **425** (1994) 217 [`hep-ph/9403226`].

[109] Z. Bern, L. J. Dixon, D. C. Dunbar and D. A. Kosower, *Fusing gauge theory tree amplitudes into loop amplitudes*, *Nucl. Phys. B* **435** (1995) 59 [`hep-ph/9409265`].

[110] C. Anastasiou, R. Britto, B. Feng, Z. Kunszt and P. Mastrolia, *D-dimensional unitarity cut method*, *Phys. Lett. B* **645** (2007) 213 [`hep-ph/0609191`].

[111] Z. Bern and A. G. Morgan, *Massive loop amplitudes from unitarity*, *Nucl. Phys. B* **467** (1996) 479 [`hep-ph/9511336`].

[112] A. L. Guerrieri, Y.-t. Huang, Z. Li and C. Wen, *On the exactness of soft theorems*, *JHEP* **12** (2017) 052 [`1705.10078`].

[113] J. A. Farrow, Y. Geyer, A. E. Lipstein, R. Monteiro and R. Stark-Muchão, *Propagators, BCFW recursion and new scattering equations at one loop*, *JHEP* **10** (2020) 074 [`2007.00623`].

[114] Y. Geyer, R. Monteiro and R. Stark-Muchão, *Superstring Loop Amplitudes from the Field Theory Limit*, *Phys. Rev. Lett.* **127** (2021) 211603 [`2106.03968`].

[115] K. Hosomichi, K.-M. Lee, S. Lee, S. Lee and J. Park, *N=5,6 Superconformal Chern-Simons Theories and M2-branes on Orbifolds*, *JHEP* **09** (2008) 002 [`0806.4977`].

[116] J. M. Drummond, J. Henn, G. P. Korchemsky and E. Sokatchev, *Dual superconformal symmetry of scattering amplitudes in N=4 super-Yang-Mills theory*, *Nucl. Phys. B* **828** (2010) 317 [`0807.1095`].

[117] J. M. Drummond, J. M. Henn and J. Plefka, *Yangian symmetry of scattering amplitudes in N=4 super Yang-Mills theory*, *JHEP* **05** (2009) 046 [`0902.2987`].

[118] T. Bargheer, F. Loebbert and C. Meneghelli, *Symmetries of Tree-level Scattering Amplitudes in N=6 Superconformal Chern-Simons Theory*, *Phys. Rev. D* **82** (2010) 045016 [`1003.6120`].

[119] Y.-t. Huang and A. E. Lipstein, *Dual Superconformal Symmetry of N=6 Chern-Simons Theory*, *JHEP* **11** (2010) 076 [`1008.0041`].

[120] D. Gang, Y.-t. Huang, E. Koh, S. Lee and A. E. Lipstein, *Tree-level Recursion Relation and Dual Superconformal Symmetry of the ABJM Theory*, *JHEP* **03** (2011) 116 [`1012.5032`].

[121] N. Arkani-Hamed, F. Cachazo, C. Cheung and J. Kaplan, *A Duality For The S Matrix*, *JHEP* **03** (2010) 020 [`0907.5418`].

[122] A. Hodges, *Eliminating spurious poles from gauge-theoretic amplitudes*, *JHEP* **05** (2013) 135 [`0905.1473`].

[123] S. He and C. Zhang, *Notes on Scattering Amplitudes as Differential Forms*, *JHEP* **10** (2018) 054 [`1807.11051`].

[124] L. Ferro, T. Łukowski and R. Moerman, *From momentum amplituhedron boundaries toamplitude singularities and back*, *JHEP* **07** (2020) 201 [2003.13704].

[125] D. Damgaard, L. Ferro, T. Lukowski and R. Moerman, *Momentum amplituhedron meets kinematic associahedron*, *JHEP* **02** (2021) 041 [2010.15858].

[126] D. Damgaard, L. Ferro, T. Lukowski and R. Moerman, *Kleiss-Kuijf relations from momentum amplituhedron geometry*, *JHEP* **07** (2021) 111 [2103.13908].

[127] N. Arkani-Hamed, H. Thomas and J. Trnka, *Unwinding the Amplituhedron in Binary*, *JHEP* **01** (2018) 016 [1704.05069].

[128] A. Brandhuber, G. Travaglini and C. Wen, *A note on amplitudes in N=6 superconformal Chern-Simons theory*, *JHEP* **07** (2012) 160 [1205.6705].

[129] H. Elvang, Y.-t. Huang, C. Keeler, T. Lam, T. M. Olson, S. B. Roland et al., *Grassmannians for scattering amplitudes in 4d $\mathcal{N} = 4$ SYM and 3d ABJM*, *JHEP* **12** (2014) 181 [1410.0621].

[130] P. Galashin and P. Pylyavskyy, *Ising model and the positive orthogonal Grassmannian*, *Duke Math. J.* **169** (2020) 1877.

[131] Y.-T. Huang, C.-K. Kuo and C. Wen, *Dualities for Ising networks*, *Phys. Rev. Lett.* **121** (2018) 251604 [1809.01231].

[132] D. Dorigoni, M. B. Green and C. Wen, *Exact results for duality-covariant integrated correlators in $\mathcal{N} = 4$ SYM with general classical gauge groups*, 2202.05784.

[133] T. Fleury and R. Pereira, *Non-planar data of $\mathcal{N} = 4$ SYM*, *JHEP* **03** (2020) 003 [1910.09428].

[134] B. Eden, P. Heslop, G. P. Korchemsky and E. Sokatchev, *Hidden symmetry of four-point correlation functions and amplitudes in N=4 SYM*, *Nucl. Phys. B* **862** (2012) 193 [1108.3557].

[135] B. Eden, P. Heslop, G. P. Korchemsky and E. Sokatchev, *Constructing the correlation function of four stress-tensor multiplets and the four-particle amplitude in N=4 SYM*, *Nucl. Phys. B* **862** (2012) 450 [1201.5329].

[136] J. L. Bourjaily, P. Heslop and V.-V. Tran, *Perturbation Theory at Eight Loops: Novel Structures and the Breakdown of Manifest Conformality in N=4*

Supersymmetric Yang-Mills Theory, *Phys. Rev. Lett.* **116** (2016) 191602 [1512.07912].

[137] J. L. Bourjaily, P. Heslop and V.-V. Tran, *Amplitudes and Correlators to Ten Loops Using Simple, Graphical Bootstraps*, *JHEP* **11** (2016) 125 [1609.00007].

[138] A. Galperin, E. Ivanov, S. Kalitsyn, V. Ogievetsky and E. Sokatchev, *Unconstrained Off-Shell N=3 Supersymmetric Yang-Mills Theory*, *Class. Quant. Grav.* **2** (1985) 155.

[139] G. Hartwell and P. S. Howe, *(N, p, q) harmonic superspace*, *Int. J. Mod. Phys. A* **10** (1995) 3901 [hep-th/9412147].

[140] L. Andrianopoli, S. Ferrara, E. Sokatchev and B. Zupnik, *Shortening of primary operators in N extended SCFT(4) and harmonic superspace analyticity*, *Adv. Theor. Math. Phys.* **4** (2000) 1149 [hep-th/9912007].

[141] L. F. Alday and X. Zhou, *All Holographic Four-Point Functions in All Maximally Supersymmetric CFTs*, 2006.12505.

[142] S. M. Chester, M. B. Green, S. S. Pufu, Y. Wang and C. Wen, *Modular invariance in superstring theory from $\mathcal{N} = 4$ super-Yang-Mills*, *JHEP* **11** (2020) 016 [1912.13365].

[143] S. M. Chester, M. B. Green, S. S. Pufu, Y. Wang and C. Wen, *New modular invariants in $\mathcal{N} = 4$ Super-Yang-Mills theory*, *JHEP* **04** (2021) 212 [2008.02713].

[144] D. Dorigoni, M. B. Green and C. Wen, *Novel Representation of an Integrated Correlator in $\mathcal{N} = 4$ Supersymmetric Yang-Mills Theory*, *Phys. Rev. Lett.* **126** (2021) 161601 [2102.08305].

[145] D. Dorigoni, M. B. Green and C. Wen, *Exact properties of an integrated correlator in $\mathcal{N} = 4$ SU(N) SYM*, *JHEP* **05** (2021) 089 [2102.09537].

[146] S. M. Chester, R. Dempsey and S. S. Pufu, *Bootstrapping $\mathcal{N} = 4$ super-Yang-Mills on the conformal manifold*, 2111.07989.

[147] S. Collier and E. Perlmutter, *Harnessing S-Duality in $\mathcal{N} = 4$ SYM & Supergravity as $SL(2, \mathbb{Z})$-Averaged Strings*, 2201.05093.

[148] L. F. Alday, S. M. Chester and T. Hansen, *Modular invariant holographic correlators for $\mathcal{N} = 4$ SYM with general gauge group*, *JHEP* **12** (2021) 159 [2110.13106].

[149] M. B. Green and C. Wen, *Maximal $U(1)_Y$-violating n-point correlators in $\mathcal{N} = 4$ super-Yang-Mills theory*, 2009.01211.

[150] D. Dorigoni, M. B. Green and C. Wen, *Exact expressions for n-point maximal $U(1)_Y$-violating integrated correlators in $SU(N)$ $\mathcal{N} = 4$ SYM*, *JHEP* **11** (2021) 132 [2109.08086].

[151] R. H. Boels, *Maximal R-symmetry violating amplitudes in type IIB superstring theory*, *Phys. Rev. Lett.* **109** (2012) 081602 [1204.4208].

[152] M. B. Green and C. Wen, *Modular Forms and $SL(2, \mathbb{Z})$-covariance of type IIB superstring theory*, *JHEP* **06** (2019) 087 [1904.13394].

[153] F. Gonzalez-Rey, I. Y. Park and K. Schalm, *A Note on four point functions of conformal operators in N=4 superYang-Mills*, *Phys. Lett. B* **448** (1999) 37 [hep-th/9811155].

[154] B. Eden, P. S. Howe, C. Schubert, E. Sokatchev and P. C. West, *Four point functions in N=4 supersymmetric Yang-Mills theory at two loops*, *Nucl. Phys. B* **557** (1999) 355 [hep-th/9811172].

[155] B. Eden, P. S. Howe, C. Schubert, E. Sokatchev and P. C. West, *Simplifications of four point functions in N=4 supersymmetric Yang-Mills theory at two loops*, *Phys. Lett. B* **466** (1999) 20 [hep-th/9906051].

[156] B. Eden, C. Schubert and E. Sokatchev, *Three loop four point correlator in N=4 SYM*, *Phys. Lett. B* **482** (2000) 309 [hep-th/0003096].

[157] M. Bianchi, S. Kovacs, G. Rossi and Y. S. Stanev, *Anomalous dimensions in N=4 SYM theory at order g**4*, *Nucl. Phys. B* **584** (2000) 216 [hep-th/0003203].

[158] J. Drummond, C. Duhr, B. Eden, P. Heslop, J. Pennington and V. A. Smirnov, *Leading singularities and off-shell conformal integrals*, *JHEP* **08** (2013) 133 [1303.6909].

[159] D. J. Broadhurst and D. Kreimer, *Knots and numbers in Phi**4 theory to 7 loops and beyond*, *Int. J. Mod. Phys. C* **6** (1995) 519 [hep-ph/9504352].

[160] O. Schnetz, *Quantum periods: A Census of phi**4-transcendentals*, *Commun. Num. Theor. Phys.* **4** (2010) 1 [0801.2856].

[161] F. C. S. Brown, *On the periods of some Feynman integrals*, 0910.0114.

[162] O. Schnetz, *Graphical functions and single-valued multiple polylogarithms*, *Commun. Num. Theor. Phys.* **08** (2014) 589 [1302.6445].

[163] E. Panzer, *Algorithms for the symbolic integration of hyperlogarithms with applications to Feynman integrals*, *Comput. Phys. Commun.* **188** (2015) 148 [1403.3385].

[164] E. Panzer and O. Schnetz, *The Galois coaction on ϕ^4 periods*, *Commun. Num. Theor. Phys.* **11** (2017) 657 [1603.04289].

[165] A. Georgoudis, V. Gonçalves, E. Panzer, R. Pereira, A. V. Smirnov and V. A. Smirnov, *Glue-and-cut at five loops*, *JHEP* **09** (2021) 098 [2104.08272].

[166] B. Eden, A. C. Petkou, C. Schubert and E. Sokatchev, *Partial nonrenormalization of the stress tensor four point function in N=4 SYM and AdS / CFT*, *Nucl. Phys. B* **607** (2001) 191 [hep-th/0009106].

[167] M. Nirschl and H. Osborn, *Superconformal Ward identities and their solution*, *Nucl. Phys. B* **711** (2005) 409 [hep-th/0407060].

[168] V. Pestun, *Localization of gauge theory on a four-sphere and supersymmetric Wilson loops*, *Commun. Math. Phys.* **313** (2012) 71 [0712.2824].

[169] U. Naseer and C. Thull, *Flavor deformations and supersymmetry enhancement in $4d\,\mathcal{N}=2$ theories*, 2110.09329.

[170] P. Cvitanovic, *Group theory: Birdtracks, Lie's and exceptional groups.* Princeton University Press, 2008.

[171] R. L. Mkrtchian, *The Equivalence of Sp(2N) and SO(-2N) Gauge Theories*, *Phys. Lett. B* **105** (1981) 174.

[172] P. Cvitanovic and A. D. Kennedy, *Spinors in Negative Dimensions*, *Phys. Scripta* **26** (1982) 5.

[173] M. Kontsevich and D. Zagier, *Periods*, *Mathematics Unlimited — 2001 And Beyond* (2001) 771 [].

[174] D. Chicherin, J. Drummond, P. Heslop and E. Sokatchev, *All three-loop four-point correlators of half-BPS operators in planar $\mathcal{N}=4$ SYM*, *JHEP* **08** (2016) 053 [1512.02926].

[175] D. Chicherin, A. Georgoudis, V. Gonçalves and R. Pereira, *All five-loop planar four-point functions of half-BPS operators in $\mathcal{N}=4$ SYM*, *JHEP* **11** (2018) 069 [1809.00551].

[176] S. Caron-Huot and F. Coronado, *Ten dimensional symmetry of N = 4 SYM correlators*, 2106.03892.

[177] L. Rastelli and X. Zhou, *How to Succeed at Holographic Correlators Without Really Trying*, *JHEP* **04** (2018) 014 [1710.05923].

[178] L. F. Alday and A. Bissi, *Loop Corrections to Supergravity on $AdS_5 \times S^5$*, *Phys. Rev. Lett.* **119** (2017) 171601 [1706.02388].

[179] F. Aprile, J. Drummond, P. Heslop and H. Paul, *Quantum Gravity from Conformal Field Theory*, *JHEP* **01** (2018) 035 [1706.02822].

[180] F. Aprile, J. M. Drummond, P. Heslop and H. Paul, *Unmixing Supergravity*, *JHEP* **02** (2018) 133 [1706.08456].

[181] F. Aprile, J. Drummond, P. Heslop and H. Paul, *Loop corrections for Kaluza-Klein AdS amplitudes*, *JHEP* **05** (2018) 056 [1711.03903].

[182] L. F. Alday and S. Caron-Huot, *Gravitational S-matrix from CFT dispersion relations*, *JHEP* **12** (2018) 017 [1711.02031].

[183] F. Aprile, J. Drummond, P. Heslop and H. Paul, *Double-trace spectrum of $N = 4$ supersymmetric Yang-Mills theory at strong coupling*, *Phys. Rev. D* **98** (2018) 126008 [1802.06889].

[184] L. F. Alday, A. Bissi and E. Perlmutter, *Genus-One String Amplitudes from Conformal Field Theory*, *JHEP* **06** (2019) 010 [1809.10670].

[185] F. Aprile, J. Drummond, P. Heslop and H. Paul, *One-loop amplitudes in $AdS_5 \times S^5$ supergravity from $\mathcal{N} = 4$ SYM at strong coupling*, *JHEP* **03** (2020) 190 [1912.01047].

[186] L. F. Alday and X. Zhou, *Simplicity of AdS Supergravity at One Loop*, *JHEP* **09** (2020) 008 [1912.02663].

[187] J. Drummond and H. Paul, *One-loop string corrections to AdS amplitudes from CFT*, 1912.07632.

[188] J. Drummond, R. Glew and H. Paul, *One-loop string corrections for AdS Kaluza-Klein amplitudes*, 2008.01109.

[189] F. Aprile and P. Vieira, *Large p explorations. From SUGRA to big STRINGS in Mellin space*, *JHEP* **12** (2020) 206 [2007.09176].

[190] J. M. Drummond, H. Paul and M. Santagata, *Bootstrapping string theory on $AdS_5 \times S^5$*, 2004.07282.

[191] A. Bissi, G. Fardelli and A. Georgoudis, *Towards all loop supergravity amplitudes on AdS5×S5*, *Phys. Rev. D* **104** (2021) L041901 [2002.04604].

[192] A. Bissi, G. Fardelli and A. Georgoudis, *All loop structures in supergravity amplitudes on AdS5 × S5 from CFT*, *J. Phys. A* **54** (2021) 324002 [2010.12557].

[193] J. Drummond, D. Nandan, H. Paul and K. Rigatos, *String corrections to AdS amplitudes and the double-trace spectrum of $\mathcal{N} = 4$ SYM*, *JHEP* **12** (2019) 173 [1907.00992].

[194] T. Abl, P. Heslop and A. E. Lipstein, *Towards the Virasoro-Shapiro amplitude in $AdS_5 \times S^5$*, *JHEP* **04** (2021) 237 [2012.12091].

[195] F. Aprile, J. M. Drummond, H. Paul and M. Santagata, *The Virasoro-Shapiro amplitude in $AdS_5 \times S^5$ and level splitting of 10d conformal symmetry*, *JHEP* **11** (2021) 109 [2012.12092].

[196] L. F. Alday, C. Behan, P. Ferrero and X. Zhou, *Gluon Scattering in AdS from CFT*, *JHEP* **06** (2021) 020 [2103.15830].

[197] S. Giusto, R. Russo and C. Wen, *Holographic correlators in AdS_3*, *JHEP* **03** (2019) 096 [1812.06479].

[198] G. Mack, *D-independent representation of Conformal Field Theories in D dimensions via transformation to auxiliary Dual Resonance Models. Scalar amplitudes*, 0907.2407.

[199] A. Galliani, S. Giusto and R. Russo, *Holographic 4-point correlators with heavy states*, *JHEP* **10** (2017) 040 [1705.09250].

[200] A. Bombini, A. Galliani, S. Giusto, E. Moscato and R. Russo, *Unitary 4-point correlators from classical geometries*, *Eur. Phys. J. C* **78** (2018) 8 [1710.06820].

[201] S. Giusto, R. Russo, A. Tyukov and C. Wen, *Holographic correlators in AdS_3 without Witten diagrams*, *JHEP* **09** (2019) 030 [1905.12314].

[202] S. M. Chester and E. Perlmutter, *M-Theory Reconstruction from (2,0) CFT and the Chiral Algebra Conjecture*, *JHEP* **08** (2018) 116 [1805.00892].

[203] L. F. Alday and X. Zhou, *All Tree-Level Correlators for M-theory on $AdS_7 \times S^4$*, *Phys. Rev. Lett.* **125** (2020) 131604 [2006.06653].

[204] G. Arutyunov, A. Pankiewicz and S. Theisen, *Cubic couplings in D = 6 N=4b supergravity on AdS(3) x S**3*, *Phys. Rev. D* **63** (2001) 044024 [hep-th/0007061].

[205] F. Aprile and M. Santagata, *Two particle spectrum of tensor multiplets coupled to AdS3×S3 gravity*, *Phys. Rev. D* **104** (2021) 126022 [2104.00036].

[206] N. Ceplak, S. Giusto, M. R. R. Hughes and R. Russo, *Holographic correlators with multi-particle states*, *JHEP* **09** (2021) 204 [`2105.04670`].

[207] T. Lukowski, R. Moerman and J. Stalknecht, *On the geometry of the orthogonal momentum amplituhedron*, `2112.03294`.

[208] S. He, C.-K. Kuo, Z. Li and Y.-Q. Zhang, *All-loop ABJM amplitudes from projected, bipartite amplituhedron*, `2204.08297`.

[209] N. A. Nekrasov, *Seiberg-Witten prepotential from instanton counting*, *Adv. Theor. Math. Phys.* **7** (2003) 831 [`hep-th/0206161`].

[210] N. Nekrasov and A. Okounkov, *Seiberg-Witten theory and random partitions*, *Prog. Math.* **244** (2006) 525 [`hep-th/0306238`].

[211] M. Billó, M. Frau, F. Fucito, A. Lerda and J. F. Morales, *S-duality and the prepotential in $\mathcal{N} = 2^\star$ theories (I): the ADE algebras*, *JHEP* **11** (2015) 024 [`1507.07709`].

[212] M. Billó, M. Frau, F. Fucito, A. Lerda and J. F. Morales, *S-duality and the prepotential of $\mathcal{N} = 2^\star$ theories (II): the non-simply laced algebras*, *JHEP* **11** (2015) 026 [`1507.08027`].

[213] M. Billò, M. Frau, F. Fucito, J. F. Morales and A. Lerda, *Resumming instantons in N = 2* theories with arbitrary gauge groups*, in *14th Marcel Grossmann Meeting on Recent Developments in Theoretical and Experimental General Relativity, Astrophysics, and Relativistic Field Theories*, vol. 4, pp. 4139–4150, 2017, DOI [`1602.00273`].

[214] R. Huang, Q. Jin, J. Rao, K. Zhou and B. Feng, *The Q-cut Representation of One-loop Integrands and Unitarity Cut Method*, *JHEP* **03** (2016) 057 [`1512.02860`].